

# **DRILL CONTROL AND AUTONOMOUS SURFACE ROTARY BLASTHOLE DRILLING**

Daniel J. Lucifora, B.Sc. (Queen's), M.A.Sc. (Queen's)



Department of Mining and Materials Engineering  
McGill University, Montreal

A thesis submitted to McGill University in partial fulfilment  
of the requirements of the degree of  
Doctor of Philosophy (Ph.D.)

(August, 2019)

Copyright © Daniel Joseph Lucifora, 2019

---

## Abstract

As the mining industry continues to embrace technology to become more efficient and more environmentally conscious, automated solutions and processes will become more common. This is true for all types of mining independent of commodity or type of operation (surface or underground). Due to the specifics of its application a production drill used in surface mining is an attractive use case for automation – either full or of operator assist variety.

The full operational cycle of a production drill rig is explored in detail; challenges and constraints regarding the implementation of automation are identified. The operational impacts of utilizing an automated production drill rig are commented upon.

The research details the design, development and testing of a novel and advanced drill control system that incorporates advanced exceptions handling concepts thereby allowing the solution to be more appropriate for use during long periods of unsupervised drilling which represents the majority of a production drill's operational cycle. Testing of the developed drill control system at a working mine site on a production drill was conducting and the results are presented and discussed. In addition, the influence of drill bit design on drill performance (and control) is explored and the influence of bit wear is commented upon.

A drill propel and positioning solution that incorporates HPGPS sensor information and crawler track motor speed sensor information is proposed. Required positioning accuracy is defined. The propel and positioning solution was tested at a working mine site on a production drill and the results are presented and discussed. The requirements of an automatic levelling system are defined, and an improved solution is proposed.

---

The research concludes with a proposal for a new intelligent drilling concept that includes better incorporation of the mine model and mine planning tools, automatic blast pattern generation, and on-the-fly pattern adjustment based upon monitoring-while-drilling signals. An overall, conceptual integration of the various proposed solutions is also presented.

---

## Sommaire

Étant donné que l'industrie minière poursuit son utilisation de la technologie pour essayer d'augmenter son efficacité et plus éco-responsable, l'automatisation de ses opérations et processus vas devenir de plus en plus commun. Cela est vraie pour tous les types de mines, quel que soit la matière exploiter ou le type opération (à ciel ouvert ou sous terrain). Les foreuses de production dans les mines à ciel ouvert sont particulièrement bien positionnées pour l'automatisation – que ce soit de l'automatisation complète, ou en mode d'assistance a l'opérateur.

Le cycle opérationnel d'une foreuse de production dans une mine à ciel ouvert est exploré en détail. Les défis et les contraintes qui relatent de la mise en place de l'automatisation sont identifiés. Les impacts opérationnels qui découlent de l'utilisation d'une foreuse automatisée sont aussi discuter.

Ce projet de recherche couvre les détails sur la conception, le développement et la mise aux essaies d'un système novateur et avancé de contrôle d'une foreuse de production. Ce système incorpore des éléments avancés de gestion des exceptions qui permettent à la solution d'effectuer des forages pour des longues périodes de temps, ce qui représente la majorité du cycle opérationnel d'une foreuse de production. Le system de control développer a été mis à l'essai sur une foreuse dans une mine à ciel ouvert dans un contexte opérationnel. Les résultats de ces essaies sont présenté et discuté. De plus, l'influence de la conception des forets sur la performance (et le contrôle) d'une foreuse est explorer. Des commentaires sont émis sur l'influence de l'usure des forets.

---

Une solution pour le contrôle du déplacement et le positionnement de la foreuse qui incorpore des receveurs GPS a haute précision ainsi que des capteurs de vitesse dans les moteurs est proposer. La précision requise pour le positionnement est déterminée. Les exigences pour un système de mise au niveau automatique sont définies et une solution améliorer est proposer.

Le projet de recherche se termine avec une proposition pour un nouveau système de forage intelligent qui permettrai de fusionner le modèle 3D du gisement et les outils de planification, la définition de plan de forages automatiques et l'ajustement des plans de forages à la volée baser sur les signaux de forage en temps réel. Une intégration conceptuelle des solutions proposés est aussi présenter.

---

## Acknowledgements

I would like to extend my deepest gratitude and thanks to McGill University and, specifically, the Faculty of Engineering. I must also express my appreciation for the receipt of a McGill Engineering Doctoral Award without which this research would not have been possible. Being a doctoral student at a school with the history and quality of McGill University has been a great privilege and one which I always considered an honor.

I am grateful for the mentorship, guidance and “weekly” phone calls of encouragement from my supervisor Dr. Ferri Hassani, Professor and Webster Chair in Mining Engineering. In addition, I would like to thank my fellow graduate students and researchers with whom creative ideas always seemed to flow so freely. I must also thank my various colleagues, professors and mentors in academia as well as industry that have inspired me both in my chosen profession and beyond.

I send a special thanks to Deborah and Logan Lucifora for their inspiration and support. You are truly “who I am coming home for”.

I dedicate this work to the memory of Michael Lucifora – he did not have the same opportunities as I, however, if he had I believe he would have excelled effortlessly.

Vancouver, B.C.,  
January 3<sup>rd</sup>, 2019

---

## Table of Contents

Abstract.....	ii
Sommaire.....	iv
Acknowledgements.....	vi
List of Figures.....	xi
List of Tables.....	xvii
List of Abbreviations.....	xviii
Chapter 1 Introduction.....	1
1.1 Autonomous Surface Blasthole Drilling.....	8
1.2 Purpose, Goals, and Objectives.....	11
1.3 Methodology.....	13
1.4 Overview.....	13
Chapter 2 Literature Review.....	17
2.1 Large Electric Rotary Blasthole Drills.....	18
2.1.1 Power Unit Assembly.....	21
2.1.2 Track Assembly.....	22
2.1.3 Rotary Carriage and Pulldown Mechanism.....	23
2.1.4 Mast and Back Brace Assembly.....	24
2.2 Drilling and Drill Control.....	25
2.2.1 Drill Bit Design.....	31
2.2.2 Bit-Rock Interaction.....	35
2.2.3 Optimal Rotary Drill Bit Performance and Depth of Cut.....	36
2.3 Bit Wear.....	39

---

2.3.1 Total Drilling Cost Curve and Bit Wear .....	39
2.3.2 Drill Bit Wear Monitoring .....	41
2.3.3 Vibration in Drilling.....	44
2.3.4 Vibration and Wear as Controllable Variables .....	48
2.4 Industry State of the Art Drill Control.....	50
2.5 Propel Control.....	53
2.6 Extraterrestrial Drilling.....	57
2.6.1 Drilling Automation and Intelligence for Extraterrestrial Applications .....	60
Chapter 3 Advanced Drill Control.....	64
3.1 Exceptional Drilling Conditions .....	69
3.2 Controller Hierarchy .....	74
3.2.1 Closed Loop Control of the Drill-Plant Model/System .....	76
3.3 Various Drill Control Modes .....	79
3.3.1 Collaring & Adaptive Collar Feature.....	79
3.3.2 Primary Control: Depth of Cut.....	83
3.3.3 Rotary Speed Feedback.....	86
3.3.4 Secondary Control: Rotary Torque .....	88
3.3.5 Alternate Control: Non-Critical, Predictive Bit Plugging.....	92
3.3.6 Alternate Control: Critical, Bit Plugging .....	94
3.3.7 Alternate Control: Vibration .....	96
3.3.7.1 Dynamic, dual-axis vibration control.....	98
3.3.8 Alternate Control: Retract.....	100
3.3.9 Alternate Control: Operational Limits .....	104
Chapter 4 Drill Control Field Testing.....	106
4.1 Drill Rig Instrumentation and Interfacing.....	106

---

4.2 Experimental Testing .....	113
4.2.1 Collaring & Adaptive Collar Feature .....	115
4.2.2 Primary Control: Depth of Cut.....	119
4.2.3 Rotary Speed Feedback.....	124
4.2.4 Secondary Control: Rotary Torque .....	126
4.2.5 Alternate Control: Non-Critical, Predictive Bit Plugging.....	129
4.2.6 Alternate Control: Critical, Bit Plugging .....	136
4.2.7 Alternate Control: Vibration .....	140
4.2.8 Alternate Control: Retract.....	142
4.2.9 Alternate Control: Operational Limits .....	145
4.2.10 Exception Handling: Drilling Through a Void .....	145
4.3 Advanced Drill Control Results & Discussion .....	148
4.3.1 North American Copper Test Results .....	149
4.3.2 Australian Iron Ore Test Results.....	150
4.3.3 Discussion.....	150
4.4 Influence of Drill Bit Design (and Wear) on Drill Control.....	152
Chapter 5 Considerations for Automation – Additional Drill Cycle Components .....	159
5.1 Hole to Hole Movement (Propel).....	159
5.1.1 Propel Motor Response Testing and Modelling.....	159
5.1.2 Propel and Positioning Control .....	179
5.1.3 Auto-Propel Field Test Results and Discussion.....	185
5.2 Auto-Level .....	187
5.2.1 Ground Contact.....	190
5.2.2 Levelling .....	191
5.2.3 Lowering .....	195

---

Chapter 6 Smart Pattern Layout.....	197
6.1 Blast Pattern Geometry.....	198
6.2 Blasthole Diameter.....	200
6.3 Blasthole Length.....	202
6.4 Burden.....	202
6.5 Spacing.....	203
6.6 Subdrilling.....	203
6.7 Desired Fragmentation.....	204
6.7.1 Kuz-Ram Model for Prediction of Fragmentation.....	205
6.8 Methodology of Proposed Smart Pattern Layout Tool.....	207
6.9 On-The-Fly Pattern Adjustments.....	209
Chapter 7 Conclusion.....	214
7.1 Original Contributions of the Research.....	217
7.2 Research Scope.....	218
7.3 Recommendations for Future Work.....	219
Bibliography.....	224
Appendix A : Feed Motor and Rotary Motor Response Testing, Modelling.....	228

---

## List of Figures

Figure 1-1: In-situ ore bodies (Gokhale, 2011).....	2
Figure 1-2: Creation of mine benches for access to ore and overburden (Gokhale, 2011).....	3
Figure 1-3: Mine bench with nomenclature (Gokhale, 2011).....	3
Figure 1-4: Mine bench and drill and blast specific nomenclature (Drilltech Mission, LLC, 2005).....	4
Figure 1-5: Diagram of a blasthole drill with nomenclature (Bucyrus International, Inc., 2005) .....	6
Figure 1-6: Simplified drilling cycle by relative time (Drilltech Mission, LLC, 2005) .....	9
Figure 2-1: P&H 120A Large Electric Rotary Blasthole Drill (Harnischfeger Corporation, 2006).....	20
Figure 2-2: P&H 120A Drill Deck Plan (Harnischfeger Corporation, 2006).....	21
Figure 2-3: Rotary Carriage and Pulldown Mechanism (Harnischfeger Corporation, 2006).....	24
Figure 2-4: Tri-cone rotary drilling method (Atlas Copco Drilling Solutions LLC, 2012).....	26
Figure 2-5: Simple overview of the drilling process (Aboujaoude, 1991).....	27
Figure 2-6: Block diagram representation of a PIV controller (Lucifora, 2012) .....	31
Figure 2-7: Hughes Two-Cone drill bit (Baker Hughes Inc., 2009).....	32
Figure 2-8: Assembled components of a tri-cone rotary drill bit (Atlas Copco Drilling Solutions LLC, 2012) .....	33
Figure 2-9: Bit-rock interaction between a single insert and the drilled rock mass (Maurer, The Perfect Cleaning Theory of Rotary Drilling, 1962) .....	36
Figure 2-10: Illustration of over penetration (Zink, Optimizing Drilling Productivity and Bit Life with "Depth of Cut" Studies, 2005) .....	38
Figure 2-11: Drill bit performance given by penetration rate with respect to weight on bit (Zink, Optimizing Drilling Productivity and Bit Life with "Depth of Cut" Studies, 2005).....	38
Figure 2-12: Total Drilling Cost curve .....	40

---

Figure 2-13: IADC Tooth Wear Grading System.....	41
Figure 2-14: Behaviour of weight on bit vibration spectra for tri-cone rotary drill bit with different tooth wear grades in a constant rock type (Naganawa, 2012).....	47
Figure 2-15: State of the art OEM drill control system .....	51
Figure 2-16: Differential drive kinematics.....	54
Figure 2-17: Robot kinematics for Astolfi’s problem (Astolfi, 1999).....	56
Figure 2-18: Idealized vehicle path using Astolfi’s controller (Astolfi, 1999).....	57
Figure 2-19: Various drill bits used on the DAME drill (Bar-Cohen, 2009).....	58
Figure 3-1: Hierarchy of various control modes.....	75
Figure 3-2: Advanced drill control interface to drill-plant model.....	77
Figure 3-3: Various control modules within the advanced drill control solution .....	78
Figure 3-4: Adaptive Collar Module.....	82
Figure 3-5: Depth of cut control module .....	85
Figure 3-6: Rotary speed control loop .....	87
Figure 3-7: Influence of rotary speed on rotary torque.....	89
Figure 3-8: Rotary torque control mode .....	91
Figure 3-9: Non-critical, predictive bit plugging control mode.....	93
Figure 3-10: Critical, bit plugging control mode .....	95
Figure 3-11: Vibration control mode .....	97
Figure 3-12: Logic diagram of dynamic, dual-axis vibration control scheme .....	99
Figure 3-13: End of hole retraction zones and corresponding logic .....	101
Figure 3-14: Retraction jamming control mode.....	103
Figure 4-1: Caterpillar MD6640 control system.....	107
Figure 4-2: Atlas Copco PV351 control system .....	108
Figure 4-3: DATAQ 718-Bx input channels with signal detail .....	110

---

Figure 4-4: CAT MD6640 drill rig interfacing for autonomous drill control testing .....	112
Figure 4-5: Hole Depth – collar scenario .....	117
Figure 4-6: Rotary Speed – collar scenario .....	117
Figure 4-7: Weight on Bit – collar scenario .....	119
Figure 4-8: DOC example hole – depth .....	120
Figure 4-9: DOC example hole – rotary speed .....	121
Figure 4-10: DOC example hole – weight on bit .....	122
Figure 4-11: DOC example hole – depth of cut .....	123
Figure 4-12: PIV control of rotary speed .....	124
Figure 4-13: Rotary speed response testing – no feedback control .....	125
Figure 4-14: Rotary Speed Request of 55 rpm – no feedback control .....	126
Figure 4-15: RT example hole – rotary torque .....	127
Figure 4-16: RT example hole – weight on bit .....	128
Figure 4-17: RT example hole – depth .....	129
Figure 4-18: Industry Standard Controller – Bit Plugging example hole, depth .....	130
Figure 4-19: Industry Standard Controller – Bit Plugging example hole, air pressure .....	131
Figure 4-20: Industry Standard Controller – Bit Plugging example hole, weight on bit .....	132
Figure 4-21: Industry Standard Controller – Bit Plugging example hole, rotary speed .....	132
Figure 4-22: Predictive Bit Plugging example hole – air pressure rate of change .....	134
Figure 4-23: Predictive Bit Plugging example hole – weight-on-bit .....	135
Figure 4-24: Predictive Bit Plugging example hole – air pressure .....	135
Figure 4-25: Predictive Bit Plugging example hole – depth .....	136
Figure 4-26: Critical Bit Plugging example hole – water flow .....	137
Figure 4-27: Critical Bit Plugging example hole – air flow command .....	137
Figure 4-28: Critical Bit Plugging example hole – plant air pressure .....	138

---

Figure 4-29: Critical Bit Plugging example hole – plant weight-on-bit .....	138
Figure 4-30: Vibration example hole – plant vibration.....	140
Figure 4-31: Vibration example hole – plant rotary speed .....	141
Figure 4-32: Vibration example hole – plant weight-on-bit .....	142
Figure 4-33: Retract example hole – bit position.....	143
Figure 4-34: Retract example hole – rotary torque.....	144
Figure 4-35: Retract example hole – penetration rate.....	144
Figure 4-36: Hole depth through void zone .....	146
Figure 4-37: Feed force through void zone.....	147
Figure 4-38: Rotary speed through void zone.....	148
Figure 4-39:IADC bit class and corresponding rock type (Atlas Copco Drilling Solutions LLC, 2012). 153	
Figure 4-40: Operational rate of penetration range by observed bit class .....	155
Figure 4-41: Operational rate of penetration range by bit height (observed and projected).....	156
Figure 4-42: Comparison of new and completely worn drill bit.....	158
Figure 5-1: Propel motor response data .....	160
Figure 5-2: Left propel motor input-output (unscaled).....	162
Figure 5-3: Right propel motor input-output (unscaled).....	163
Figure 5-4: Left propel motor input-output (scaled).....	164
Figure 5-5: Right propel motor input-output (scaled).....	165
Figure 5-6: Normal propel speed track response testing (scaled).....	166
Figure 5-7: Slow propel speed track response testing (scaled).....	168
Figure 5-8: Left propel motor, measured and simulated model output – normal propel speed .....	170
Figure 5-9: Bode magnitude plot – left propel motor, normal speed.....	171
Figure 5-10: Right propel motor, measured and simulated model output – normal propel speed.....	173
Figure 5-11: Bode magnitude plot – right propel motor, normal speed.....	174

---

Figure 5-12: Left propel motor, measured and simulated model output – slow propel speed.....	175
Figure 5-13: Bode magnitude plot – left propel motor, slow speed.....	176
Figure 5-14: Right propel motor, measured and simulated model output – slow propel speed.....	177
Figure 5-15: Bode magnitude plot – right propel motor, slow speed .....	178
Figure 5-16: Two-tiered propel and positioning controller.....	180
Figure 5-17: Propel motor speed control solution .....	182
Figure 5-18: Drill rig position control philosophy.....	183
Figure 5-19: Levelling jacks – location and naming convention.....	189
Figure 5-20: Auto-Level – ground contact .....	190
Figure 5-21: Level sequence – drill rig roll axis.....	192
Figure 5-22: Level sequence – drill rig pitch axis .....	193
Figure 5-23: Auto-Level – levelling .....	194
Figure 5-24: Auto-Level – lowering.....	196
Figure 6-1: Nomenclature of a blast pattern (Gokhale, 2011) .....	198
Figure 6-2: Zones of fragmentation with respect to pattern geometry (Gokhale, 2011).....	199
Figure 6-3: Influence of in-situ material properties on burden.....	212
Figure 6-4: Influence of in-situ material properties on spacing.....	212
Figure 6-5: Influence of in-situ material properties on subdrilling.....	213
Figure A-1: Rotary motor input-output data (unscaled) .....	230
Figure A-2: Feed motor input-output data (unscaled).....	231
Figure A-3: Rotary motor input-output data (scaled) .....	232
Figure A-4: Feed motor input-output data (scaled).....	233
Figure A-5: Drill model .....	234
Figure A-6: Rotary motor, measured and simulated model output.....	237
Figure A-7: Bode magnitude plot – rotary motor .....	238

---

Figure A-8: Step response plot – rotary motor .....	238
Figure A-9: Feed motor, measured and simulated model output.....	240
Figure A-10: Bode magnitude plot – feed motor .....	241
Figure A-11: Step response plot – feed motor .....	241

---

## List of Tables

Table 2-1: Autonomy rating system (Mukherjee, 2006).....	62
Table 3-1: Drill audit, equipment distribution by site.....	64
Table 3-2: List of exceptional drilling conditions with typical outcome, adjustment and applicable advanced drill controller mode .....	73
Table 3-3: Rotation speed in air step test inputs .....	89
Table 4-1: Technical specifications of interest for the Copper Machine .....	114
Table 4-2: Technical specifications of interest for the Iron Ore Machine .....	115
Table 4-3: Field test results, North American copper mine .....	149
Table 4-4: Field test results, Australian iron ore mine.....	150
Table 4-5: OEM operational guidelines for various tri-cone bit classes (Atlas Copco Drilling Solutions LLC, 2012).....	153
Table 4-6: Measured insert height by observed bit class .....	153
Table 4-7: Depth of cut and range of penetration rates for observed bit classes .....	154
Table 5-1: Results of auto-propel field test.....	187
Table 6-1: Blasthole diameter by dig tool capacity (Gokhale, 2011) .....	201
Table 6-2: Height of cut for commonly used electric rope shovels .....	202
Table 6-3: Definition of subdrilling by material type and fracture level .....	203

---

## List of Abbreviations

<b>AC</b>	Alternating Current
<b>BCL</b>	Bottom Charge Length
<b>BHA</b>	Bottom Hole Assembly
<b>CAT</b>	Caterpillar Mining Equipment & Solutions
<b>CCL</b>	Column Charge Length
<b>DC</b>	Direct Current
<b>DOC</b>	Depth of Cut
<b>GPS</b>	Global Positioning System
<b>HF</b>	Hardness Factor
<b>HPGPS</b>	High Precision Global Positioning System
<b>IADC</b>	International Association of Drilling Contractors
<b>MWD</b>	Monitoring-While-Drilling
<b>OEM</b>	Original Equipment Manufacturer
<b>P&amp;H</b>	Pawling and Harnischfeger Mining Equipment
<b>PDC</b>	Programmable Drilling Control
<b>PDT</b>	Pump Drive Transmission
<b>PID</b>	Proportional, Integral, and Derivative
<b>PIV</b>	Proportional, Integral and Velocity
<b>PLC</b>	Programmable Logic Controller
<b>PV</b>	Pit Viper
<b>RDI</b>	Rock Density Influence

<b>RMD</b>	Rock Mass Description
<b>RMS</b>	Root Mean Square
<b>ROI</b>	Return on Investment
<b>ROP</b>	Rate of Penetration
<b>RWS</b>	Relative Weight Strength
<b>TDC</b>	Total Drilling Cost
<b>TNT</b>	Trinitrotoluene
<b>UCS</b>	Unconfirmed Compressive Strength
<b>WOB</b>	Weight on Bit

## **Chapter 1**

### **Introduction**

The first production related task of the surface mining process is the drill component of the drill and blast process step. This process step allows the liberation of an intact rock mass for excavation. Drill and blast is a required process step for any formation that has a compressive strength greater than approximately 70 MPa (Gokhale, 2011). This encompasses the mining of any formation of material that has a qualitative hardness of moderate or greater. If a formation has a hardness of less than moderate it can be mined through methods that do not require a drill and blast step.

Through the efforts of mineral exploration ore bodies of interest are identified within in situ host rock. The ore bodies are composed of valuable minerals whose liberation and processing would be of a net economic gain for the mining company. The non-valuable host rock is commonly known as overburden.

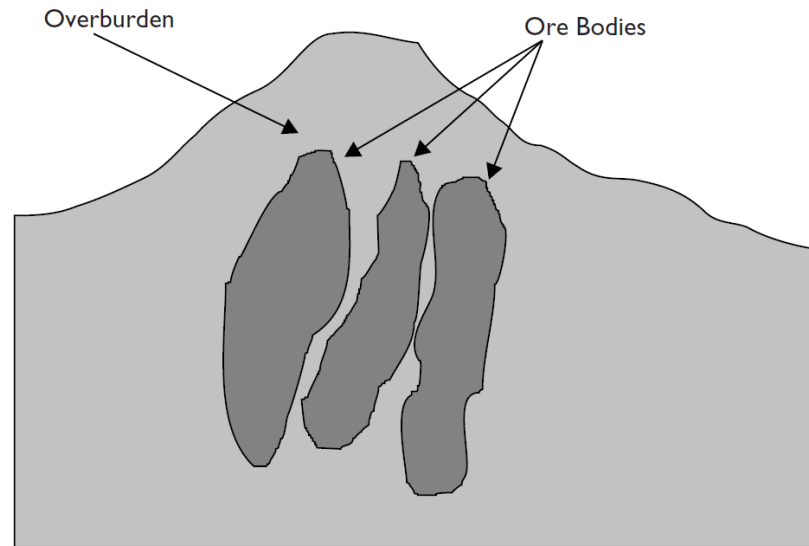


**Figure 1-1: In-situ ore bodies (Gokhale, 2011)**

The exploration phase yields a model of the in-situ ore body or ore bodies known as the mine model. This mine model is continually updated through the life of the mine using a combination of subsequent exploration and production related drill holes.

To access the ore bodies, unobstructed space must be created through the removal of the overburden material. This is accomplished via the mining process of which drill and blast is a core component. Drill and blast is utilized in the creation of mine benches from which both the ore and overburden material can be accessed and removed for mineral processing and relocation, respectively. A representation of mine benches in relation to in situ ore bodies is shown in Figure 1-2.

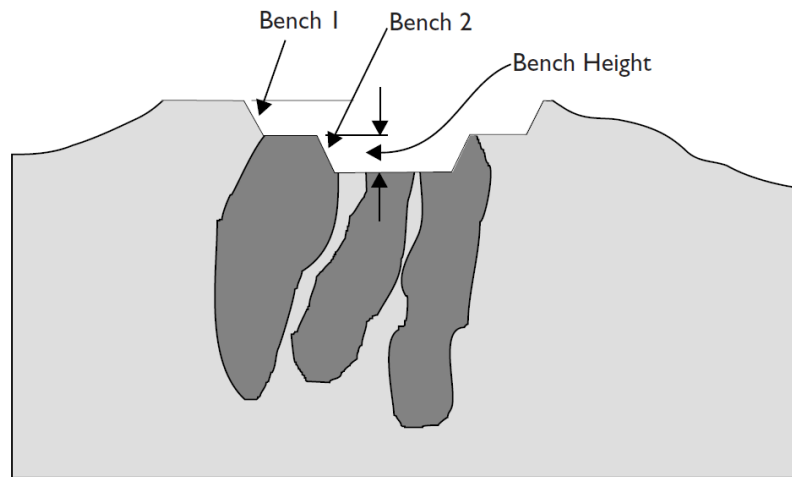


**Figure 1-2: Creation of mine benches for access to ore and overburden (Gokhale, 2011)**

A more detailed view of a mine bench with important nomenclature is provided in Figure 1-3. Additional bench and drill and blast specific terminology is provided in Figure 1-4.

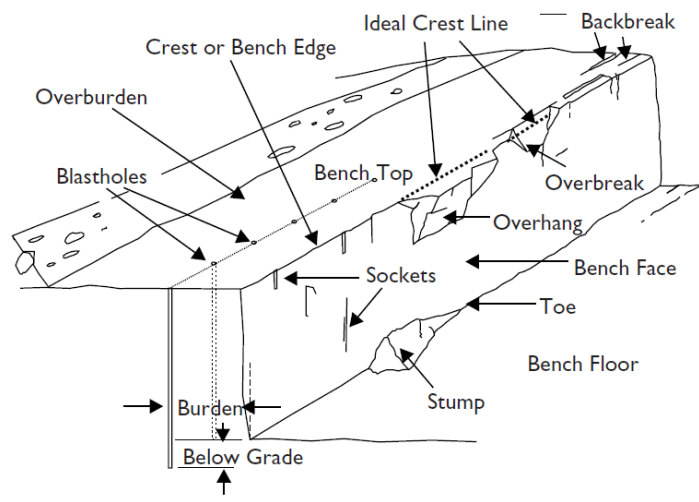
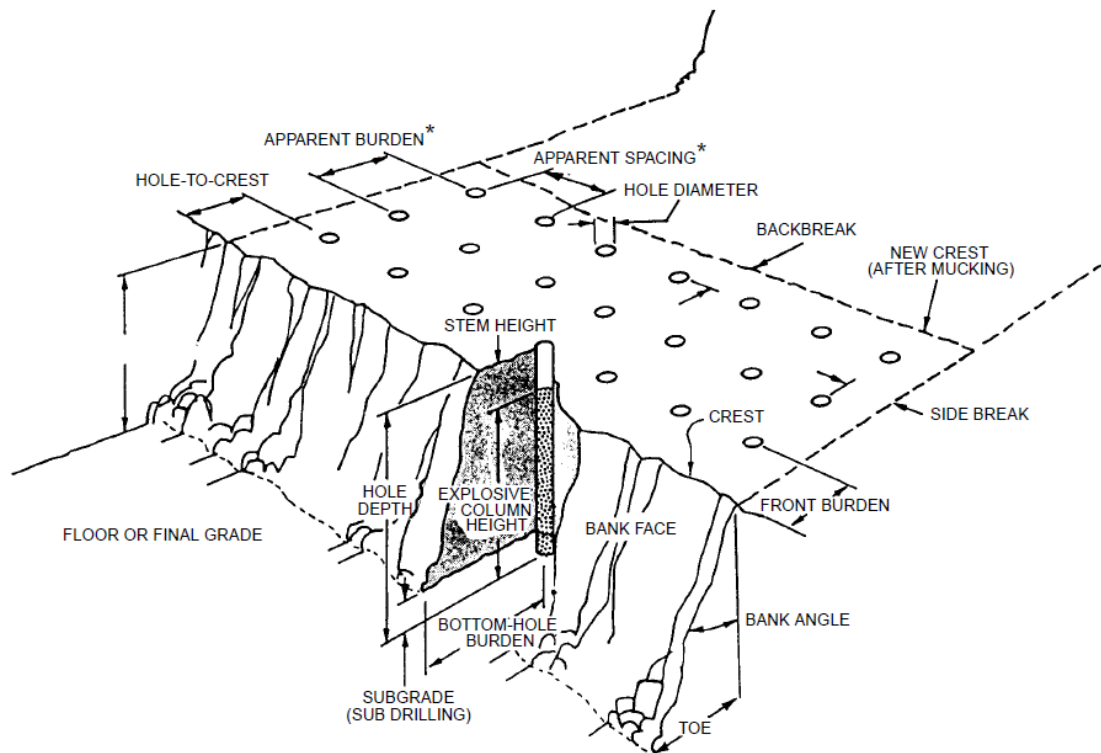


**Figure 1-3: Mine bench with nomenclature (Gokhale, 2011)**



*\*NOTE! TRUE burden and spacing may differ from APPARENT burden and spacing due to the delay between firing adjacent lines.*

**Figure 1-4: Mine bench and drill and blast specific nomenclature (Drilltech Mission, LLC, 2005)**

An array of blastholes (known as a pattern) is drilled through the in situ material from bench top to blasthole bottom level. These empty blastholes are then filled with explosives which, when detonated, transfer a large amount of energy through the in situ rock mass causing it to weaken. The now weakened rock mass can then be removed through excavation by an excavator and transported via haulage by a fleet of mining trucks. Some of the variables associated with the blast pattern such as burden, spacing and blasthole diameter are configurable based upon the strength and features of the rock mass. The difference between the blasthole bottom level and the bench floor is known as over drill. Sub drilling ensures that the bench floor is comprised of broken material (subgrade) for a depth of 0.5 – 2 metres. Subgrade is designed into the blast pattern to

protect the excavator from contact with intact, un-blasted below grade material. This contact can damage the excavator tool and increase associated maintenance costs and equipment downtime. However, too much sub drilling can result in unwanted costs for the mine operation. A typical blast pattern can consist of anywhere from dozens to hundreds of blastholes.

Once the rock mass has been blasted the excavator is positioned on the bench floor in front of the bench edge. The excavator will remove the blasted material by making dig passes from toe to crest through the now fragmented bank face. Each dig pass is loaded into a haul truck for transport to either the processing plant for ore or a dump location for overburden waste material. The bench height is dictated by the excavator size and, more precisely, the corresponding height of the dig passes. Generally, the larger the excavator the larger the bench height.

All the elements associated with the blast design, as well as the resulting mine bench design, are defined by the mine site engineer responsible for drill and blast and the engineer responsible for short range planning.

The actual drilling of the blast pattern is accomplished by the blasthole drill. The blasthole drill, under the control of a drill operator, will drill blastholes according to the predefined drill plan for the associated blast pattern. The drill plan includes the GPS coordinates of each planned blasthole (design hole)  $[x, y, z]$  as well as the corresponding hole depth [metres].

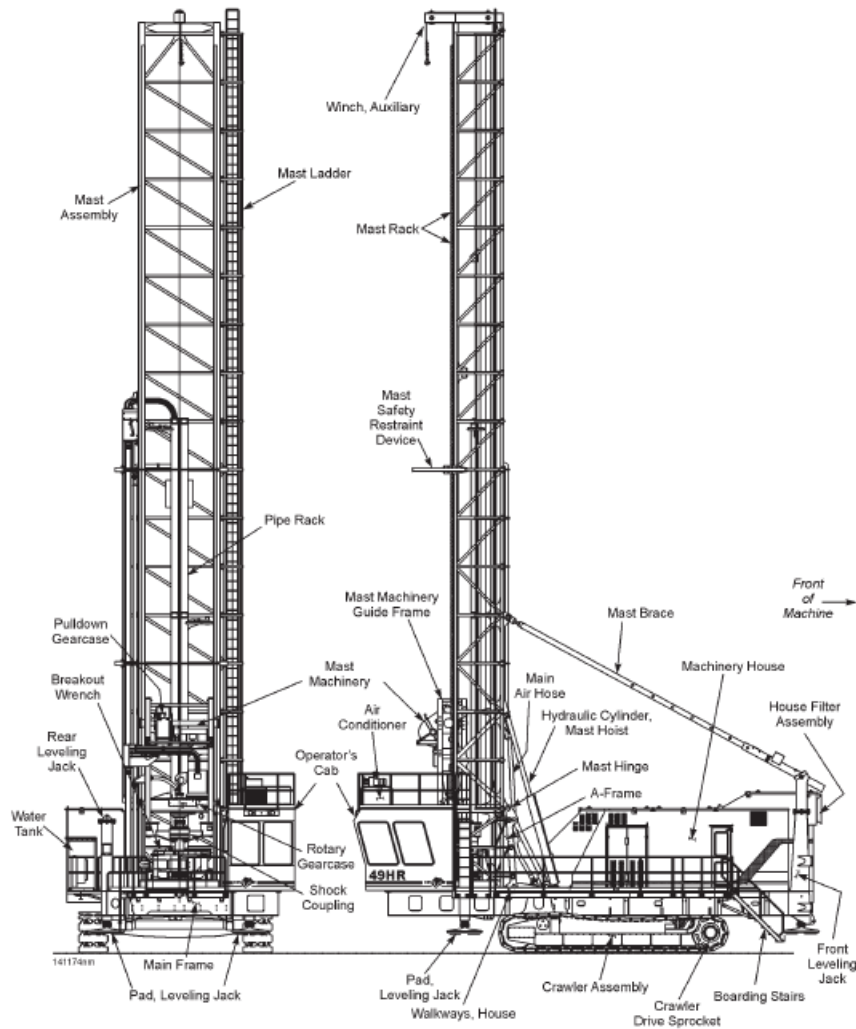


**Figure 1-5: Diagram of a blasthole drill with nomenclature (Bucyrus International, Inc., 2005)**

The drilling cycle commences once the blasthole drill is positioned on the bench containing the blast pattern (working bench). The drilling cycle is repeated until all design holes in the blast pattern are drilled to completion.

The drilling cycle consists of:

- **Machine movement (propel)** from start position to the target design hole.
- **Raising and levelling** of the machine using the levelling jacks. The purpose of this step is to align the drill string with the design hole, provide a stable drilling

---

platform and to relieve weight from the crawler components to protect them from drilling related vibration and premature wear.

- Downward movement of the drill string until **contact between the drill bit and the surface** of the working bench occurs. The purpose of this step is to tare the drill head position at the point of ground contact to accurately measure the drilled depth.
- **Commence drilling parameters** of air flushing, rotation, feed force, water flow, and air percussion (if applicable).
- Drill to a shallow depth at reduced drilling set-points until the drill bit has passed the subgrade and has entered the intact rock mass below. This step is known as **collaring** and is necessary to ensure that bit wobble in the broken subgrade is kept to a minimum thus ensuring the blasthole will stay true to the designed angle and depth.
- Drill using **normal drilling** set-points until the designed hole depth is reached.  
Note that a single pass operation refers to one in which design holes do not exceed the length of the drill pipe (steel) whereas a multi-pass operation is one in which design holes may require multiple drill steels be used.
- Drill string retraction to near hole start, followed by **hole cleaning (reaming)**.  
The function of the reaming step is twofold – to ensure that no material has fallen back into the hole lessening its final depth and to ensure the hole wall is stable so that the hole will stand until it is filled with explosives. Ensuring hole wall stability is commonly called forming a mud wall which is done by coating the hole wall with water ejected from the drill bit as it passes through the drilled hole.

---

This is an important step as sometimes the holes will not be ‘loaded’ with explosive material for several days. If a hole fails before being loaded it must be re-drilled from scratch which is time consuming and costly for the mine operation.

- **Un-levelling and lowering** of the machine using the levelling jacks. This step puts the crawler tracks back into contact with the surface of the working bench and returns the machine to a state suitable for propel.

Prior to the drilling cycle commencing and upon the arrival of the blasthole drill to the working bench the drill mast must be raised to the desired drilling position (either vertical or angled depending on pattern design and drill technical constraints) and locked into position. For stability the mast must be lowered for machine movement over longer distances (from one working bench to the next); this minimizes the risk of rollover. If the drill is to be transported through the mine site using a flatbed truck the mast will also be lowered.

### **1.1 Autonomous Surface Blasthole Drilling**

Due to the rigid, structured nature of the drilling cycle and the isolated, contained environment of the working bench; surface blasthole drilling is a logical application for automation. Figure 1-6 below shows the breakdown of a drilling cycle by relative time; note that the drill cycle is simplified but the four bins illustrated encompass all the required elements.

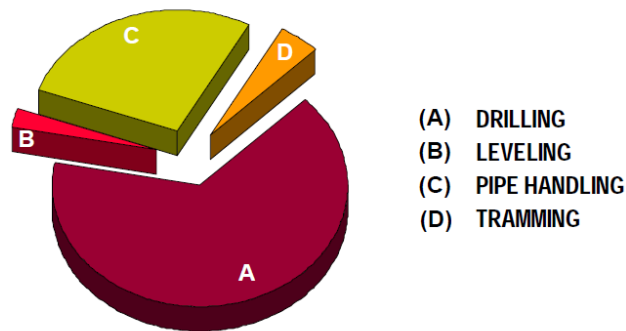


**Figure 1-6: Simplified drilling cycle by relative time (Drilltech Mission, LLC, 2005)**

While the Drilltech publication does not provide the actual time for each element of the drilling cycle it does clearly illustrate that the vast majority of the drilling cycle is spent drilling (collaring + normal drilling + hole cleaning/reaming) thus emphasising the importance of controlling drilling as a key for automation. Work done by Aboujaoude at McGill University did assign durations of time for the simplified drilling cycle. It was found that for normal operation 2-3 minutes was spent in propel/positioning, 1 minute in levelling, 20-40 minutes spent in drilling (depending on ground condition), 2-3 minutes for every steel pipe addition or removal (five pipe holes were drilled during that research work), and 1 minute for un-levelling (Aboujaoude, Feedback Control of Vibrations in Surface Rotary Blasthole Drilling, 1997). These results are dependant on the type of formation drilled (limestone quarry for that research work) and drill machine model utilized however the findings are consistent between the two referenced publications. It should be noted that for single pass operations the pipe handling element of the drill cycle can be neglected from the time distribution provided above.

The benefits of drill automation include: more productive and energy effective drills, reduced instances of severe vibration, less wear and tear on the drill, improved bit life, more consistent drill performance, more drill availability, and less requirement for an on-

drill human operator (Aboujaoude, Feedback Control of Vibrations in Surface Rotary Blasthole Drilling, 1997).

Additional benefits<sup>1</sup> are thought to include enhanced production from an autonomous drill due to higher utilization from the machine operating during periods when a human operator would not typically be available (shift change, break, meeting, etc.). This enhanced production from each autonomous drill should allow a mine operation to decrease their overall drill fleet size while maintaining or even increasing drill production levels. This would represent a significant savings in both capital costs for the drill and the operational costs for associated ongoing required maintenance. In addition, the role of drill operator could likely be expanded from one machine to include the supervision of multiple machines and therefore provide an overall reduction in field personnel.

However, some of these savings would be offset by the cost of the new autonomous systems and their ongoing maintenance and support requirements as well as the process changes introduced in the maintenance, operations, and infrastructure activities.

Design efforts toward blasthole drill autonomy range from semi-autonomous to fully autonomous. Semi-autonomous operation is an approach that has an operator still onboard the machine supervising the solution but with an automated drill cycle provided. Fully autonomous operation is an approach that no longer has an operator onboard the machine and has the majority of the machine's duty cycle carried out autonomously. This solution would have the machine supported by a shared field resource and a human operator supervising multiple drills via a remote operations centre. The human operator

---

<sup>1</sup> While these benefits are referred to as additional because they are not as immediate in their impact as say higher productivity and less energy usage, depending on the site they could even be more impactful and may form the primary business case to pursue automation.

could take control for exceptional situations beyond the capability of the autonomous system and the field resource could visit the drill for tasks outside the autonomous systems capabilities.

## **1.2 Purpose, Goals, and Objectives**

It is the purpose of this research to understand the theoretical requirements for an autonomous blasthole drill solution with specific focus on single pass rotary operation.

The research goal is to provide a practical design proposal for an autonomous blasthole drill solution with emphasis on conformation with established surface mining operational constraints. This will be accomplished through forming an understanding of the existing baseline drill and blast process. Automated solutions for each piece of the drilling and blast process will be proposed, analyzed and discussed. However, emphasis will be placed on automating the drilling component of the duty cycle as it represents the vast majority of operational time for the drill rigs.

The objectives of the research are:

- Document and analyze the duty cycle of a blasthole drill used for production drilling in a surface mining environment and note any exceptional scenarios that must be accommodated.
- Based upon the above, define the requirements and propose a design for an autonomous blasthole drill solution for surface mining.
- Discuss in detail the requirements for the drill control module, propose a drill control solution, and review results of field testing of the drill control solution.

- 
- Discuss the importance of bit wear for drilling in general but with particular emphasis on autonomous drilling and drill control.
  - Discuss in detail the requirements for the drill propel and positioning module, propose a drill propel and positioning solution, and review results of field testing of the proposed drill propel and positioning solution.
  - Review and discuss the requirements for blasthole drill levelling.
  - Examine the fundamentals of blast pattern design and comment on the potential for cooperation or improvements through the deployment of autonomous drilling systems.
  - Make recommendations for a new, drill-based drill and blast planning and design system.

This thesis explores the challenge of automating the full drill cycle in surface mining production drilling which is currently absent from academic and industry literature. A control systems engineering and design approach is utilized with an emphasis on practical mining engineering restrictions and requirements. This hybrid approach is considered particularly important and novel but also, in the author's opinion, faithful to the practical and applied tradition of the engineering profession.

The continued increase in reliance and utilization of electronics and software algorithms in all industries, combined with the mining industry's demands to minimize production costs will only further result in more autonomous-assist and fully autonomous solutions deployed in operational contexts at mine sites throughout the globe. It is expected that portions of this thesis will be relevant to those efforts.

### **1.3 Methodology**

The research examines and defines an autonomous drilling solution for production drilling in surface mining. The autonomous solution is formed through the combination of several modules, together encompassing the full drill cycle and additional, related autonomy applications: drill control, propel and positioning, bit wear, levelling and unlevelling, and intelligent blast pattern design and modification. Where appropriate, the modules are created and tested in MATLAB's Simulink.

MATLAB is a software tool developed by the company MathWorks that is widely used by engineers and scientists in industry and academia. Simulink is a graphical programming environment module within the MATLAB software package which is used for the design, modelling, simulation, and analysis of multi domain dynamic systems. Drill control, propel and positioning, and levelling / unlevelling are particularly well suited for Simulink.

All aforementioned research tasks are reviewed and modelled based upon a review of the available literature, mine site field experimentation and data collection, the author's experience and input from experienced professionals.

Where possible and feasible the discussed autonomous modules have been tested at working surface mine operations at various locations in Canada and the United States of America.

### **1.4 Overview**

The following structure is used to organize the research contained in this doctoral dissertation: Chapter Two introduces the concepts and theories used for the design of the

autonomous solution developed. Chapter Three presents a review of the requirements around a control system for drilling and presents a drill control solution for such an application that is both advanced and novel compared to the state of the art available in industry. The drill control system is field tested in Chapter Four, and the results discussed. The influence of bit design (and accumulated wear) is examined and explained in detail with reference to conducted field testing. Chapter Five examines the remainder of the drill cycle and provides algorithms for autonomous propel and positioning and autonomous levelling / un-levelling. The algorithms provided match the complexity of the application; the propel algorithm is a multi-tiered design and the level algorithm is a relatively simple design. An automatic pattern layout and on-the-fly pattern adjustment system is proposed in Chapter Six. This encompasses leveraging all of the local automation tools on the drill to accomplish the concept of intelligent drilling which is also introduced and discussed. The concluding chapter provides results and discussion for the research conducted and modelling work completed and suggests avenues for future work.

Where appropriate, developed models and algorithms are provided in the Appendices.

Chapter One – Introduction. This chapter provides an explanation of the problem to be explored in the research and discusses the author’s methodology and corresponding purpose and goals.

Chapter Two – Literature Review. All background concepts and theories necessary for the development of the autonomous solution are reviewed in this

chapter. Specific topics covered include drill bit design and its influence on drilling, rotary blasthole drill equipment design and operation, control techniques and strategies, machine movement and positioning research, and bit wear research and studies.

Chapter Three – Advanced Drill Control. This chapter provides a detailed review of the drilling application and requirements that a drill control system must accommodate. An advanced and novel drill control solution is developed based upon these requirements.

Chapter Four – Drill Control Field Testing. This chapter details the field testing of the advanced and novel drill control solution. The results are discussed. The influence of bit design and condition are also explored.

Chapter Five – Considerations for Automation – Additional Drill Cycle Components. This chapter examines the movement of the drill to the target design hole location and the required positioning. A propel and positioning algorithm is presented, and field test results of the algorithm are reviewed and discussed. In addition, the drill cycle step of levelling / un-levelling is discussed. An auto-level algorithm is presented.

Chapter Six – Smart Pattern Layout. This chapter reviews the best practices in drill and blast pattern design and provides an understanding of the variables and

how a pattern is ultimately defined by the drill and blast engineer. The concept of intelligent drilling is presented, and a theoretical solution proposed that would allow for automatic pattern design and layout. How this concept of intelligent drilling would influence other aspects of surface mine production and operations is also discussed. The feature of On-The-Fly Pattern Adjustments is introduced and further builds on the concept of intelligent drilling; the ability to tune and adjust blast designs based upon what the drill “sees” as it drills a pattern is explored. A self-tuning and adjusting intelligent drill solution is theorized and presented.

Chapter Seven – Conclusion. This chapter presents the conclusions of the current research and highlights the original contributions of this doctoral dissertation. In addition, recommendations for future work are provided.

## Chapter 2

### Literature Review

For surface mining applications there are two categories of blasthole drills: hydraulic drills and electric drills. The difference between the two types of drills are their power plants. The hydraulic drill category encompasses all drills that are powered by an onboard diesel engine. Whereas the electric drills derive their power from an onboard compressor which is supplied electricity by the mine site grid. Typically, the hydraulic drills are a smaller machine which leads to the electric drills commonly being known as large electric blasthole drills.

When comparing the two drills, cost per operating hour is often lower for the electric drills however the hydraulic drills offer more flexibility for the mine operation since they do not require an established electrical grid within the operating pit. In addition, the scale of the mining operation must be large enough to realize the potential operating cost savings of the larger electric machines. For smaller scale operations such as a quarry hydraulic drills are the dominant drill type.

Beyond the required mine site infrastructure and power plants, from an operational point of view there is little difference between hydraulic and electric drills. While this research was conducted predominantly on electric drills the results and discussion should be equally applicable to both categories of machine. In addition, the electric drill's requirement of a trailing cable for power adds complexity to an autonomous drill solution that is not present for a hydraulic drill. Therefore, an autonomous drill solution for a

hydraulic drilling application would be a simplified version of the solution presented in this research.

## **2.1 Large Electric Rotary Blasthole Drills**

As mentioned in the Introduction the purpose of the rotary blasthole drill is to drill blastholes according to the mine design. In turn, the purpose of a blasthole is to be filled with a liquid-slurry explosive mixture that will then form an explosive column through the material that is to be mined. Once blasted this explosion fractures the material allowing for efficient removal by shovel and truck operation. This section shall provide a description of one such large electric rotary blasthole drill – the P&H 120A – and a description of its key components. The P&H 120A was one of the machine types used for experimentation during this research. Along with a description of the drill itself and its core components, example machine specifications will be given that apply to the P&H 120A (the drill). Globally the P&H 120A's market segment is shared with two other manufacturer's drills: the CAT MD6640 and the Atlas Copco Pit Viper 351. While the mechanical fundamentals and corresponding machine descriptions are common between the three machines some of the specifications do vary. The P&H 120A is the largest and most powerful drill in its class however it is a valid assumption to consider the supplied specifications as a good approximation for both the CAT MD6640 and AC PV351.

Large electric drills are capable of being equipped with one or multiple pieces of drill pipe to allow for single-pass or multi-pass drilling. Together, these one or many drill pipe segments are called the drill string. Single pass drilling is common in surface mining. Most large drills only drill vertical holes, but options are available for angled drilling if

---

requested. Rotary and vertical drilling motion use electric motors and drill propel motion uses hydraulic motors. The hydraulic power is provided by a double-shafted electric motor, coupled on one end to the air compressor and on the other end to the hydraulic pump drive transmission (Harnischfeger Corporation, 2006).

The P&H 120A drill can produce a pulldown bit load of up to 68,039 kg and has been optimized to drill single-pass or multi-pass holes of up to 0.5588 m in diameter. The total machine weight is approximately 165,564 kg. The standard pipe rack provides storage for one 19.8 m pipe with 0.05 m pipe wall thickness and up to 0.273 m diameter. A second pipe rack is available as an option for additional pipe (Harnischfeger Corporation, 2006).

For reference overviews of the external components and internal components of the P&H 120A have been provided with applicable nomenclature in Figure 2-1 and Figure 2-2, respectively.

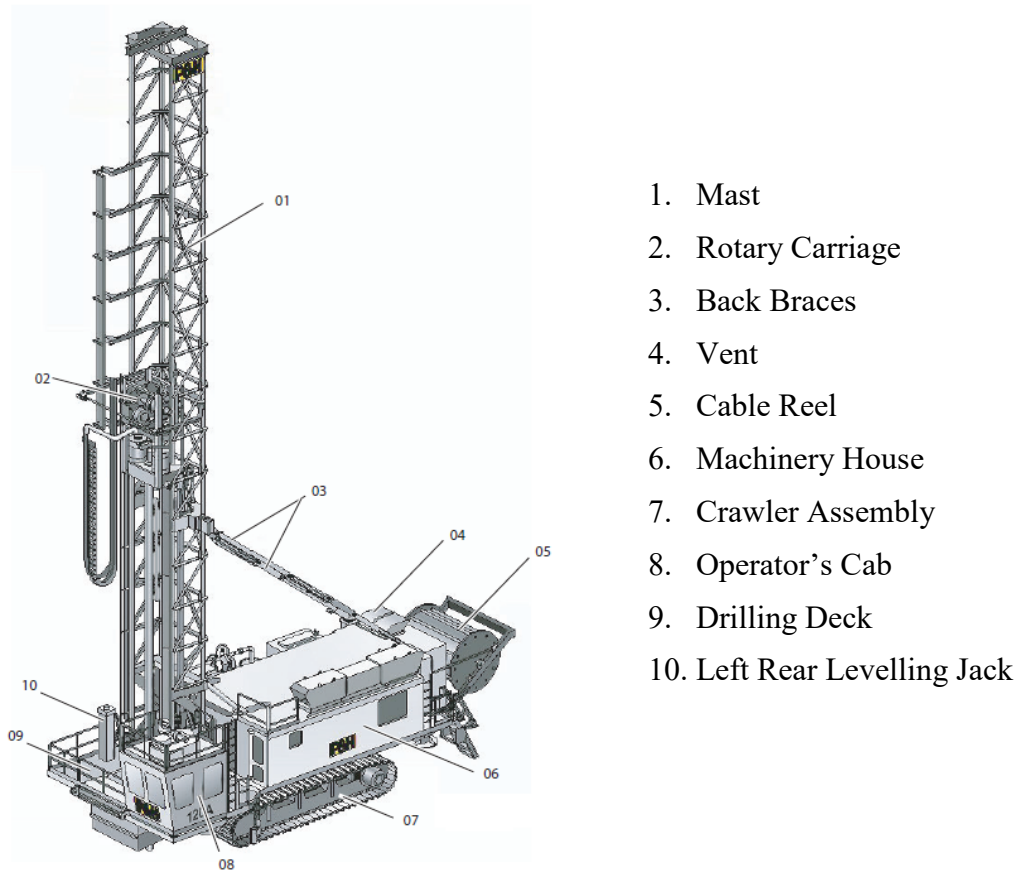


**Figure 2-1: P&H 120A Large Electric Rotary Blasthole Drill (Harnischfeger Corporation, 2006)**

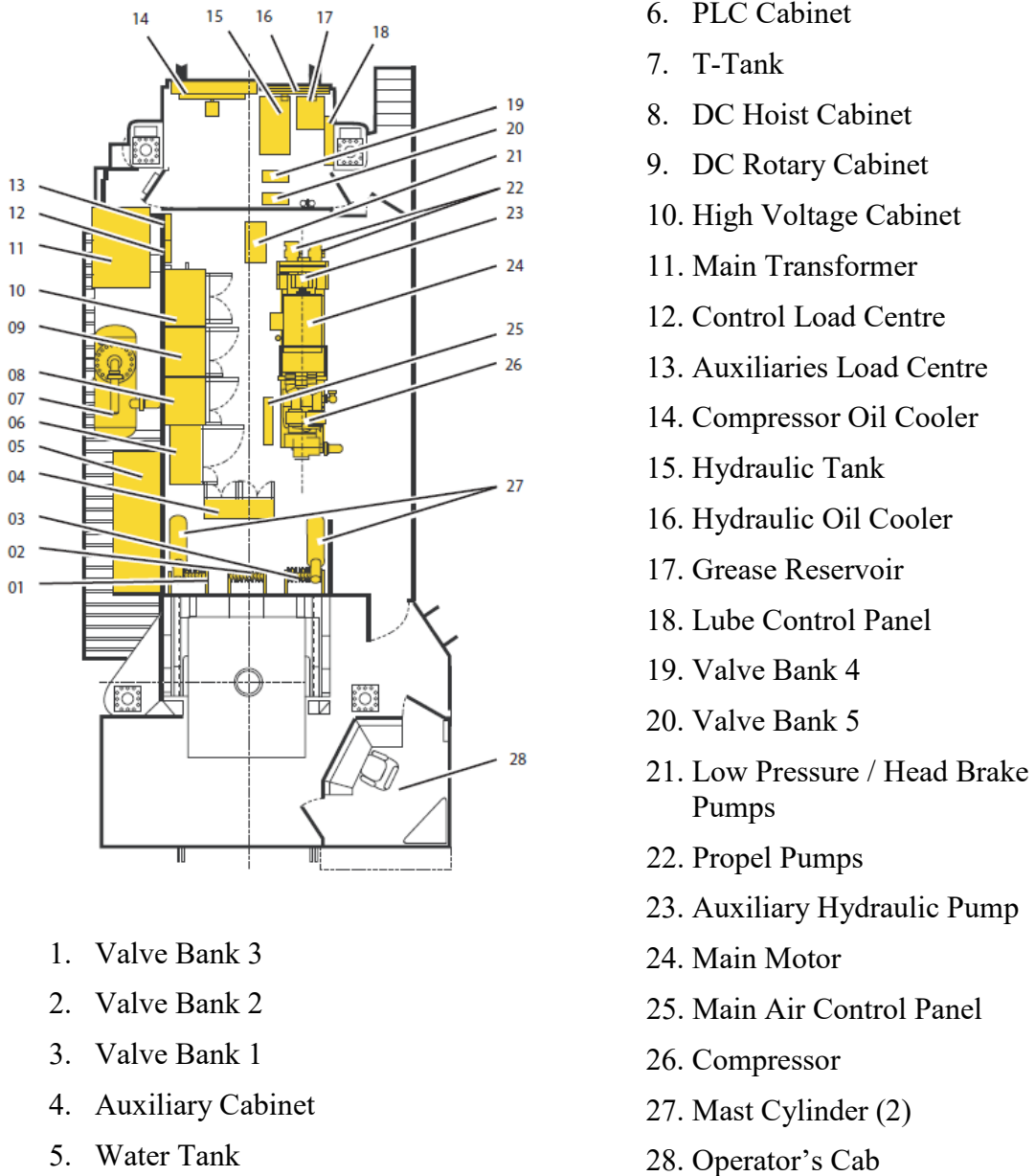


**Figure 2-2: P&H 120A Drill Deck Plan (Harnischfeger Corporation, 2006)**

### 2.1.1 Power Unit Assembly

The drill is powered by a 700HP main AC electric motor that can be configured for the voltage and frequency available at the mine site which allows for deployments of the drill throughout the globe. The main AC electric motor is provided electricity via a trailing cable connected to the mine site power grid. Mine site power can be more variable than a

---

typical power grid and the drill's electrical system can accept mine voltage up to plus 10% or minus 15% from nominal (Harnischfeger Corporation, 2006).

Both the hydraulic pump drive transmission (PDT) and the main air compressor are driven by the main AC motor. The AC motor rotates at 1,800 rpm for mine voltage at 60 Hz and at 1,500 rpm for mine voltage at 50 Hz. The AC motor has been designed to function for the potential mine site voltage fluctuation mentioned. The main air compressor is a rotary screw type that provides a rated output of 3,600 SCFM. To ensure smooth operation it is coupled to the main electric motor via a flexible coupling. All three of the assembly's components (the main motor, air compressor and PDT) are mounted on a skid to provide isolation from the drill's mainframe which protects from potential distortions due to drill levelling or propel (Harnischfeger Corporation, 2006).

### **2.1.2 Track Assembly**

Two crawler tracks are attached to the underside of the drill's main frame by a fixed rear axle and an oscillating front axle. This crawler assembly was chosen to increase stability and to provide isolation to the main frame from excessive loading when the drill is propelling over potentially rough terrain. The crawler units are heavy duty with a rating of over 200 tons of drill weight. The crawler shoes are of lug-and-tumbler design with 58 crawler shoes per track one third of which are cleated, and two thirds un-cleated. Each crawler track is independently driven by drive tumblers with planetary transmissions directly bolted to the crawler frame. Individual hydrostatic motors power each planetary transmission. The motors are designed for a plug-in style connection and are nested within the drive tumbler for protection from travel damage in rough areas with loose

---

debris. Each planetary transmission has an integral spring-set, hydraulically released wet-type multiple disc parking brake. Each crawler track is capable of counter-rotation to allow for maximum manoeuvrability for tight turning and rapid travel from hole to hole. Two identical axial piston pumps with crossover-centre variable displacement provide speed and direction control for the hydraulic motors that drive the drill propel motion. These two hydraulic circuits are closed loop (Harnischfeger Corporation, 2006).

### **2.1.3 Rotary Carriage and Pulldown Mechanism**

Two electric drive motors power the rotary driveshaft through the rotary gear case. The rotary drive shaft protrudes from the bottom of the rotary gear case for connection to the drill string. Pulldown functionality is accomplished by means of a rack and pinion drive. The rack is mounted vertically on the mast and the drive pinion on the rotary carriage shipper shaft. The rotary carriage guide rollers are provided with an eccentric arrangement for adjustment of rack/pinion gear backlash and alignment with the mast. An electric DC motor drives the hoist/pulldown pinions through the pulldown transmission (Harnischfeger Corporation, 2006). All the above can be seen in Figure 2-3.

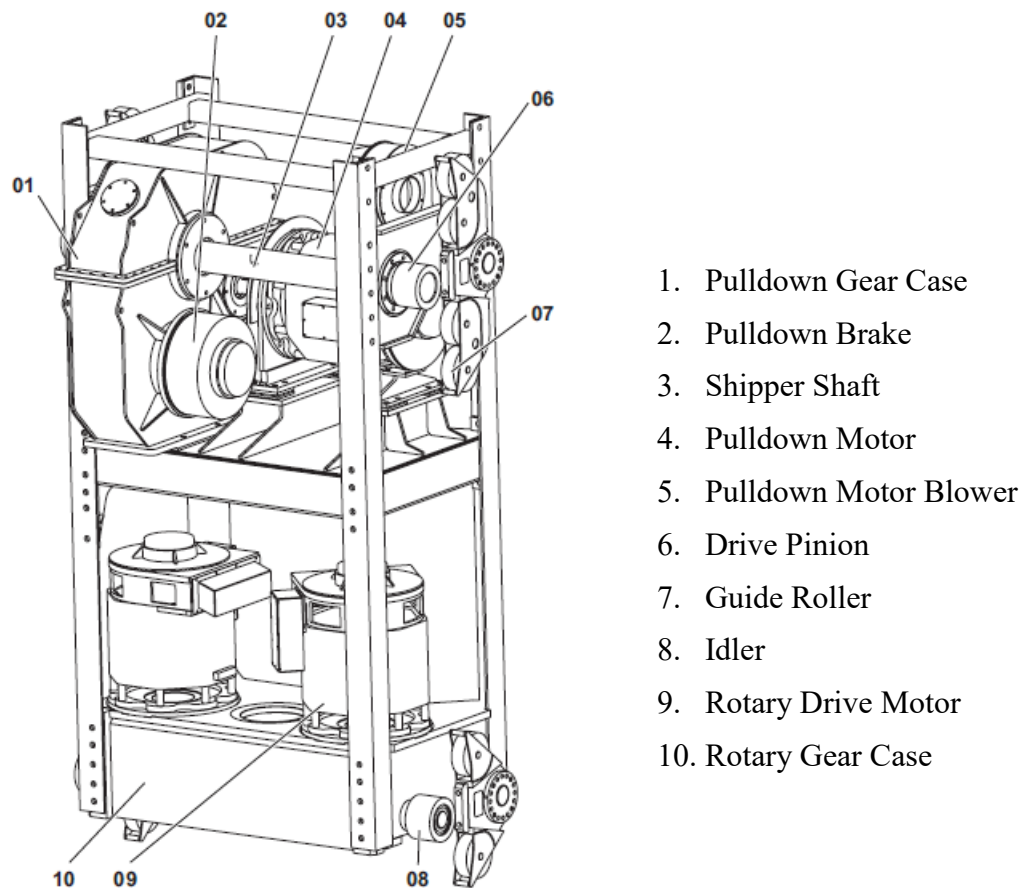


**Figure 2-3: Rotary Carriage and Pulldown Mechanism (Harnischfeger Corporation, 2006)**

#### **2.1.4 Mast and Back Brace Assembly**

The mast chords utilize structural steel members. The mast safety sling ensures retention of a falling drill pipe without structural damage to the mast. The mast is raised and lowered by two hydraulic cylinders and is locked in the vertical position by two hydraulically actuated mast lock pins located below the drilling deck. The position of these pins is monitored by the drill's PLC-based (Programmable Logic Controller) control system. The back braces fold and unfold automatically when the mast is raised or lowered. Two back brace locking collars slide over the folding knee joints between the

upper and lower back braces to keep the back braces rigid, locking the mast in the vertical drilling direction (Harnischfeger Corporation, 2006).

## **2.2 Drilling and Drill Control**

There are two styles of drilling that can be employed: percussive and non-percussive. In surface mining non-percussive drilling is the most commonly used and was the style investigated for this research. Percussive drilling will be briefly discussed but not examined in detail.

For non-percussive drilling, rotary blasthole drills utilize two styles of drill bits: tri-cone or fixed-type. Fixed-type bits have no moving parts and cut through rock only by shearing. Two examples of fixed-type bits are claw or drag bits. Due to a fixed type-bit's reliance on shearing rock their application is limited to only the softest material (Atlas Copco Drilling Solutions LLC, 2012). Since the open pit mining environment consists largely of harder, coarser, in-tact material tri-cone rotary bits are preferred and are the industry standard.

These bits rely on crushing and spalling of the rock by transferring downforce, known as pulldown, to the bit while rotating to drive the carbides into the rock as the three cones rotate about their respective axes (Atlas Copco Drilling Solutions LLC, 2012). The bit-rock interaction will be described in detail in subsection 2.2.2. Rotary and pulldown force is supplied by hydraulic or electric motors mounted onboard the blasthole drill. A summary of this process can be seen in Figure 2-4.

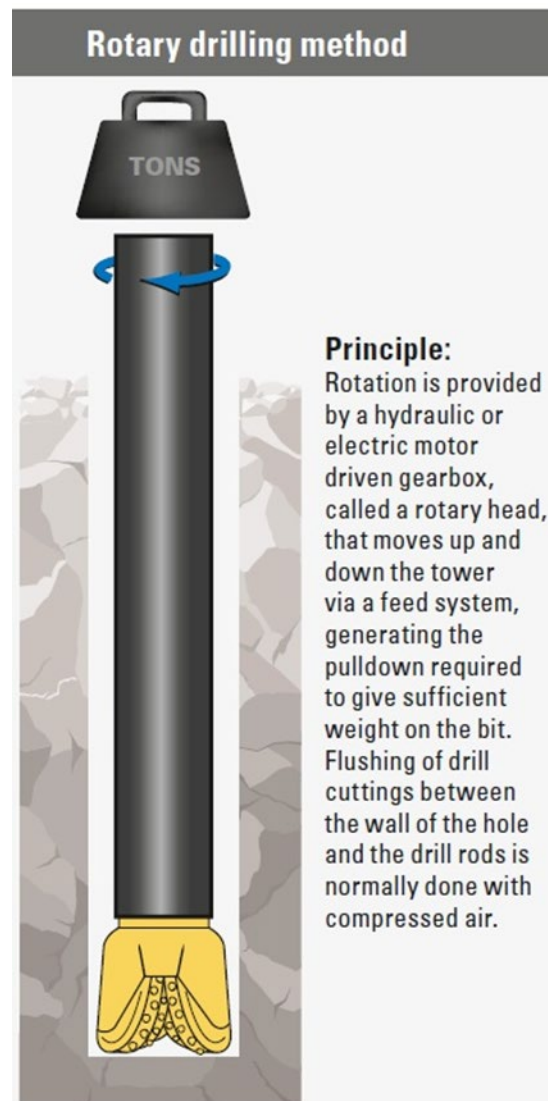


**Figure 2-4: Tri-cone rotary drilling method (Atlas Copco Drilling Solutions LLC, 2012)**

Since tri-cone rotary drill bits are the industry standard for use in open pit mining the research will focus exclusively on this style of bit and ignore the lesser used, unsuitable, fixed-type bits.

A simple overview of a traditional drilling process is given in Figure 2-5. The drill operator will input the desired rotary speed, weight-on-bit (pull-down force) and bailing

air pressure set-points to the drilling unit. These set-points are then transmitted through the drilling system via the machine dynamics and on to the bit.

The bit-rock interface can be examined as a multivariable system, where  $P()$  is a function of ground conditions, rock type, bit type, bit wear, etc. The inputs to  $P()$  are: weight-on-bit, rotary speed and bailing air pressure. The outputs will primarily consist of: bit penetration rate, rotary torque, vibration excitation, bailing air pressure rise (if broken rock is blocking the bit orifices), and other secondary variables (Aboujaoude, 1991).

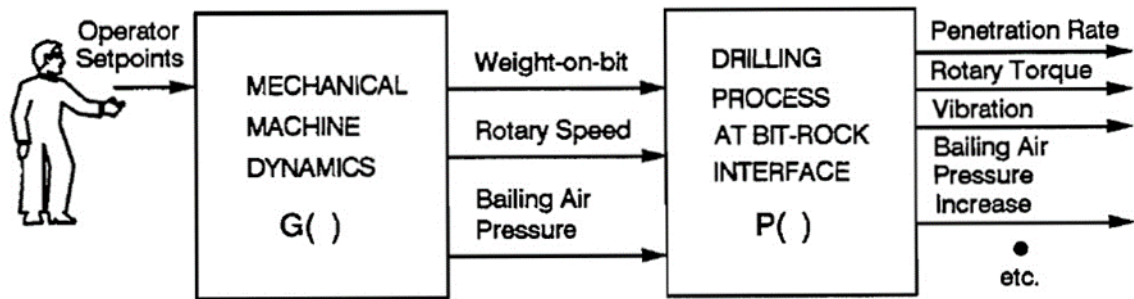


**Figure 2-5: Simple overview of the drilling process (Aboujaoude, 1991)**

A more advanced drilling system can be implemented using feedback control strategies either independent of, or in tandem with, the operator. The most common practice in industry is to employ an in tandem approach where the operator provides the initial set-points and then allows a drilling control system to continuously monitor and fine-tune the drilling process about the set-points. The operator's role is then limited to providing a higher level supervisory control function to the drilling system; the operator only intercedes for exceptional drilling conditions.

In general, control is based around the premise of trying to illicit a desired response or output from any system by manipulating (or controlling) input variables (Franklin G. ,

---

1980). The system that is to be controlled can be simple, such as speed control of an electric motor, or more complex, such as a fully autonomous aircraft.

To further expand on the simple model of speed control of an electric motor; the input variable with which we could control the system would be the speed set-point conveyed to the motor in a voltage signal. The system's output variable would, of course, be the actual speed attained by the motor. The motor speed desired could then be reached by altering the speed request voltage signal until the actual motor speed attained matches our desired speed. The premise is the same in the more complex example, however, the input and output variables have become both more numerous and complex in nature.

The goal of control systems engineering is to induce a desired response from a system regardless of plant and environmental effects. Other associated goals usually involve minimizing steady state error, rise time, settling time, and overshoot (or undershoot), etc. (Franklin G. , 1980).

The type of control that will be applied in this thesis is a modified form of PID control which is a commonly used type of closed loop feedback control. PID control is comprised of three types of control actions: Proportional, Integral and Derivative.

**Proportional control** uses a control signal  $[u(t)]$  proportional to the error signal  $[e(t)]$ .

This control signal is then multiplied by the proportional gain  $[k_p]$ . If a system has zero error, then proportional control will give no signal. A stable system can reach equilibrium in which the proportional control signal is constant, and a constant steady state error will exist. The proportional gain can be increased to reduce the steady-state error.

The control law for proportional feedback control is

$$u(t) = k_p e(t), \tag{2.1}$$

with the error signal from the plant defined as

$$e(t) = u_c(t) - y(t), \quad (2.2)$$

where the feedback loop has a set-point  $[u_c(t)]$  and a process output  $[y(t)]$ .

The corresponding controller transfer function  $[D_c(s)]$  is

$$\frac{U(s)}{E(s)} = D_c(s) = k_P. \quad (2.3)$$

**Integral control** has a control signal that is proportional to the time integral of the error.

The presence of integral control improves the steady state error by one order and ensures that if constant steady state error exists it will be reduced to zero. However, it must be noted that since a system with integral control is one which is higher by one order its introduction makes the system inherently less stable. The control law for integral control is

$$u(t) = k_I \int_{t_0}^t e(\tau) d\tau, \quad (2.4)$$

and the transfer function for integral control is

$$\frac{U(s)}{E(s)} = D_c(s) = \frac{k_I}{s}. \quad (2.5)$$

**Derivative control** gives a control signal proportional to the derivative of the error signal.

The derivative of the error represents the slope which is the rate of change of the error.

For this reason, derivative control is known as predictive control as it can be successfully used to minimize large overshoots. However, if constant steady state error exists derivative control is ineffective at reducing it. Due to this, derivative control is ineffective without either of the other two control actions and cannot be used alone. The control law for derivative control is

$$u(t) = k_D \frac{de}{dt}(t), \quad (2.6)$$

and the transfer function for derivative control is

$$\frac{U(s)}{E(s)} = D_c(s) = k_D s. \quad (2.7)$$

The three control actions defined above when placed in combination is known as **PID control** and can be expressed as the following transfer function

$$\frac{U(s)}{E(s)} = D_c(s) = k_P + \frac{k_I}{s} + k_D s. \quad (2.8)$$

Reviewing the above control actions, proportional control used alone will reduce error to a constant, steady state. Proportional control paired with derivative control will give even more damping to the system, but steady state error will persist. Pairing proportional and integral control would aid with the steady state error but will slow rise and settling time. For the above reasons PID control has wide acceptance throughout industry.

The author's previous work on rotary blasthole drilling has shown an optimal feedback control strategy to be that of a Proportional-Integral-Velocity controller (Lucifora, 2012).

The transfer function for PIV control is shown in 2.9 and a block diagram of the controller is shown in Figure 2-6.

$$u(s) = \left[ k_P + \frac{k_I}{s} \right] e(s) - \left[ \frac{k_V}{1+T_n s} \right] y(s) \quad (2.9)$$

For this control scheme, derivative control is applied to the plant output  $[y(s)]$  instead of to the error  $[e(s)]$ . In addition, the output  $y$  is first low pass filtered, using a first order filter, to avoid the use of a noisy feedback signal as input.

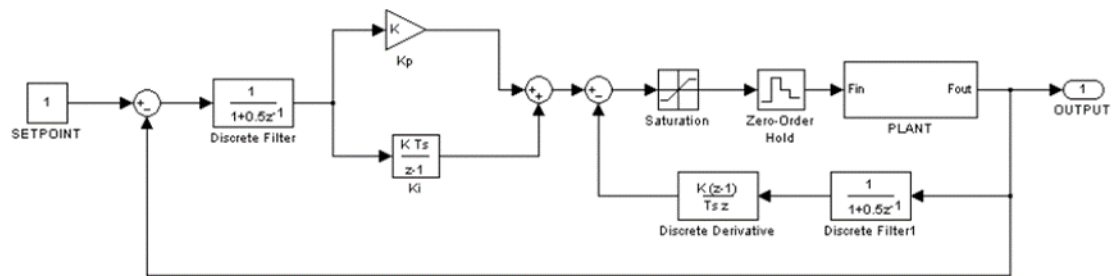


**Figure 2-6: Block diagram representation of a PIV controller (Lucifora, 2012)**

Upon further consideration of Figure 2-6, of the four main outputs from the bit-rock interface all but one lends themselves very well to feedback control. The exception is vibration. The uniqueness of the vibration plant output and its potential as a controllable variable are further discussed in subsections 2.3.3 and 2.3.4.

### 2.2.1 Drill Bit Design

Drill bit design has been evolving for over 100 years. The modern drill bit design has its origins in the Two-Cone Bit designed by Howard Robard Hughes, Sr. in 1909. This bit enabled drilling to advance to much greater depths which allowed for the recovery of oil reserves that were previously thought to be unattainable. Figure 2-7 shows a Hughes Two-Cone drill bit.



**Figure 2-7: Hughes Two-Cone drill bit (Baker Hughes Inc., 2009)**

In 1933 the Hughes Tool Company further advanced the world of drill bit design with the introduction of the tri-cone rotary drill bit. This drill bit represented an improvement over the two-cone bit in many ways and to this day remains the industry standard. Further improvements in drill bit design included: the introduction of tungsten carbide inserts in 1951 which allowed for faster drilling of hard, abrasive formations with 3 – 10 times the footage attained per drill bit, the introduction of an O-ring sealed journal bearing in 1970 which dramatically increased the life of a tri-cone rotary bit, and the first metal-sealed roller cone bearing in 1987 which allowed for high-speed, high-temperature drilling with enhanced bit life in even the toughest of conditions (Baker Hughes Inc., 2009).

The assembled components of a typical tri-cone rotary drill bit can be seen in Figure 2-8 with a cut-away of one lug for illustrative purposes. The tri-cone rotary drill bit consists of several components: three roller cones which have the cutting structure mounted on their external surface, and the bearings in their interior, the cutting structure which consists of either Tungsten Carbide Insert teeth or milled steel teeth, three lugs – each of which has the bearing journals which match up with the cone bearing bore, inner and outer roller bearings, and ball bearings (Atlas Copco Drilling Solutions LLC, 2012).

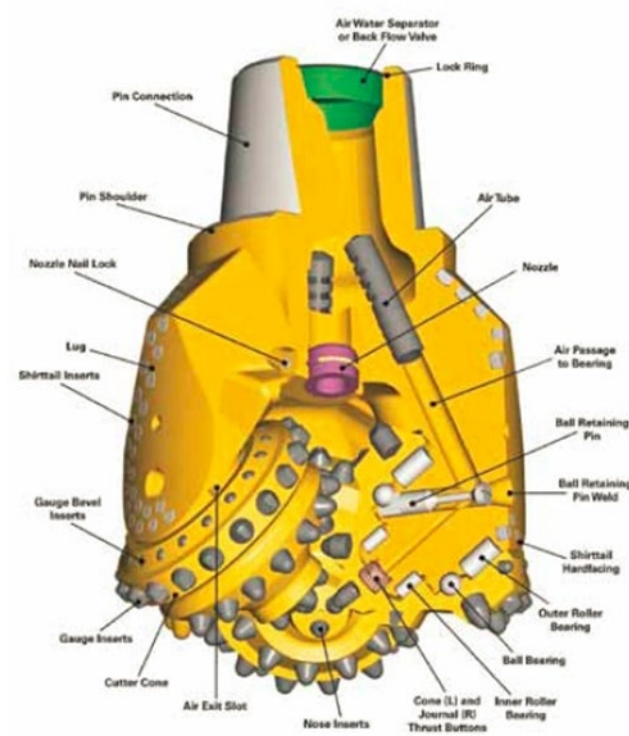


**Figure 2-8: Assembled components of a tri-cone rotary drill bit (Atlas Copco Drilling Solutions LLC, 2012)**

The assembly process consists of the components being assembled into individual cones before being assembled into the final tri-cone arrangement. Once the bit has been

---

assembled into the final tri-cone arrangement the bit pin connection is threaded with the appropriate connection size and type for the given bit diameter.

The bit shown in Figure 2-8 has air passages from the bit interior into the bit bearing area. That is because it is an air bearing bit. There are two other types of bit bearing configurations available: open (or fluid) bearing bits and sealed bearing bits. Open bearings do not have any internal air passages and the back of the cones are open to the external environment to allow for bit bearing cooling. Sealed bearings are completely enclosed and have no internal air passages. These bearings are sealed off from the external environment and are filled with pressurized grease to prevent overheating (Atlas Copco Drilling Solutions LLC, 2012).

The cutting structure is mounted on each of the roller cones for a tri-cone rotary drill bit. The cutting structure consists of arrays of tungsten carbide inserts (or teeth) aligned in several rows with four rows being standard. The cones have different geometry and are designed to rotate freely about a fixed axis. The inserts are extremely resistant to abrasive wear and breakage and are designed with the goal of giving consistent performance over the life of the drill bit. The insert length is usually row and cone dependant (Aboujaoude, 1991).

Tri-cone rotary bits may have a slight shearing action in soft rock but are primarily designed to drill by breaking the rock into chips by indentation of the inserts under an applied force (weight-on-bit) paired with a rotating torque which will cause the desired spalling action in the broken rock. The broken rock chips will then be removed from the cutting face by pressurized air sent down the centre of the drill string. The return air and chips then leave the cutting face and go to surface along the outside of the drill string.

The distance between adjacent rows on the cutting structure is designed to maximize free surface area to allow the spalling rock chips to propagate and be removed by the circulating air without being completely ground into dust. If this action occurs properly efficient drilling has been realized.

A wide assortment of drill bits are manufactured which offer a range of: geometry, diameter, shape of inserts and insert length. Typically, bits designed for hard rock drilling have short ovoid-shaped inserts, whereas bits designed with soft rock drilling in mind have longer tooth-shaped inserts.

### **2.2.2 Bit-Rock Interaction**

To understand exactly what is occurring at the bit-rock interface it is useful to simplify the process down to an examination of the interaction between a single insert impacting upon the rock mass. The interaction of this single insert is representative of the interactions between the rock mass and the many inserts that cover a typical tri-cone rotary bit.

A study by Maurer produced a model which has formed the basis for understanding the bit-rock interaction which occurs in the drilling process (Maurer, *The Perfect Cleaning Theory of Rotary Drilling*, 1962). The bit-rock interaction occurring between a single insert on a drill bit and the rock mass being drill can be seen in Figure 2-9.

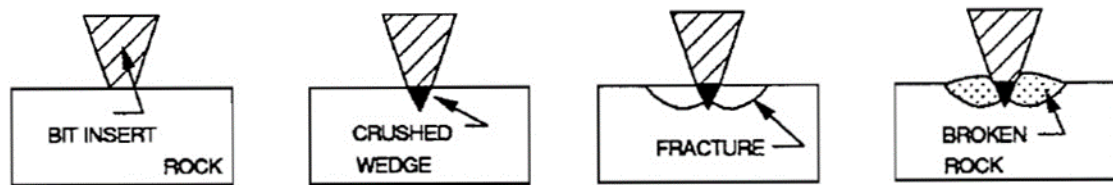


**Figure 2-9: Bit-rock interaction between a single insert and the drilled rock mass (Maurer, *The Perfect Cleaning Theory of Rotary Drilling*, 1962)**

Examining Figure 2-9 from left to right: a bit's insert impacts the rock and causes the rock to elastically deform until the crushing strength of the rock is exceeded, at this point a wedge of crushed rock is created below the insert (Hartman, 1959), (Simon, 1953).

Additional force is then applied to the insert which causes the crushed material to compress and exert high lateral forces on the solid, undisturbed material surrounding the wedge of crushed rock (Fairhurst, 1956). Once the lateral forces exceed the compressive strength of the rock mass being drilled, fracture propagation at the free surface of the rock occurs. The trajectories of these fractures intersect the principal stresses at a constant angle as predicted by Mohr's and Griffith's theories of failure (Clausing, 1959), (Maurer, 1959), (Simon, 1953).

### **2.2.3 Optimal Rotary Drill Bit Performance and Depth of Cut**

As with any physical system, there are clear limitations to the penetration rate that can be attained by different types of drill bits. The limitations are dictated mechanically by the insert's height on the drill bit. If the teeth become buried during drilling, the bit will not function efficiently, and this can lead to excessive torque overloading, bit and bearing failure and, in turn, reduced bit life (Lucifora, 2012).

---

A measure of the optimal penetration rate for a given drill bit is given by the Depth of Cut performance metric which relates penetration rate ( $R$ ) to rotary speed ( $N$ ), where some ratio represents efficient drilling for that bit (United States of America Patent No. 5,449,047, 1995).

$$\text{Depth of Cut} = \frac{R}{N} \quad (2.10)$$

Over penetration can cause the bit to ‘choke’ which occurs when cuttings are trapped between the cone shell and the rock and cannot be blown free by the down hole air pressure (Zink, Optimizing Drilling Productivity and Bit Life with "Depth of Cut" Studies, 2005). This leads to the drill bit not functioning properly which results in inefficient drilling, premature component wear and possible machine damage. Typically, a good starting set-point for Depth of Cut is 0.5. However, the optimal set-point is very much bit design dependant. It is best to follow an iterative field testing procedure to determine what Depth of Cut is optimal for each bit. Once optimal Depth of Cut has been determined, if the drill can drill above that set-point there becomes a risk of over penetration. Figure 2-10 illustrates over penetration and Figure 2-11 shows over penetration’s impact on drill bit performance.

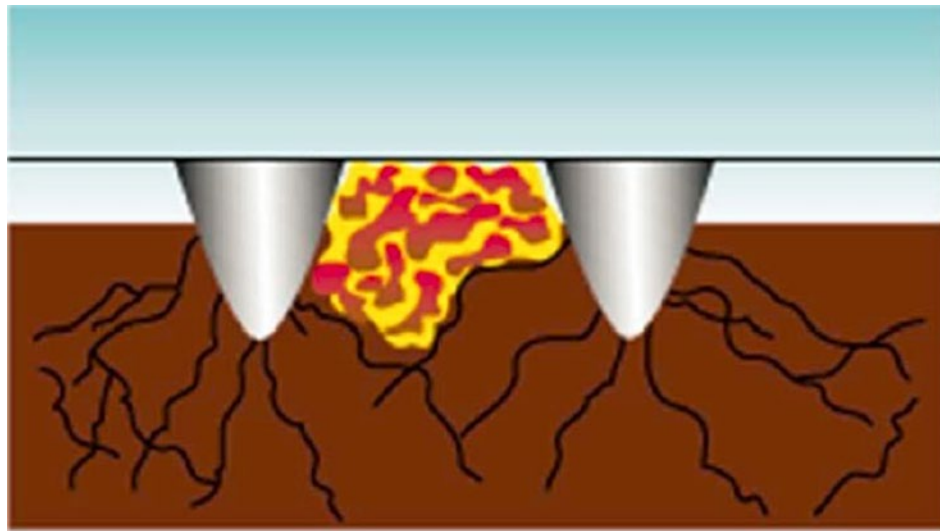


**Figure 2-10: Illustration of over penetration (Zink, Optimizing Drilling Productivity and Bit Life with "Depth of Cut" Studies, 2005)**

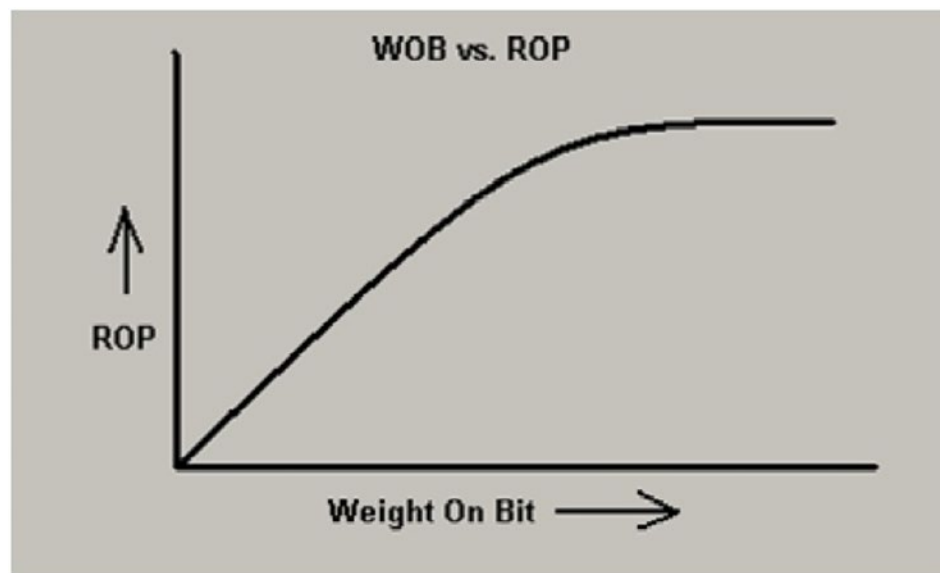


**Figure 2-11: Drill bit performance given by penetration rate with respect to weight on bit (Zink, Optimizing Drilling Productivity and Bit Life with "Depth of Cut" Studies, 2005)**

The results of a Depth of Cut that is too high, which leads to over penetration, can be seen in Figure 2-11. Penetration rate can be seen to increase continually with increases in

---

weight-on-bit until a plateau is reached. At this point increased weight-on-bit does not increase penetration rate and the added down force only serves to damage the drill and decrease component life. The plot shown in Figure 2-11 is somewhat optimistic in that some studies have shown penetration rate to not just plateau but to decrease with excessive weight-on-bit [Zink, 2005]. For these reasons Depth of Cut is a crucial measure that must be monitored closely to ensure optimal drill performance.

## **2.3 Bit Wear**

### **2.3.1 Total Drilling Cost Curve and Bit Wear**

The driver behind determining a reliable measure of bit wear is to ensure efficient drilling which will protect the drill from damaging vibrations and shortened component life while keeping drill productivity high and, in the end, save the mine operator from unnecessary expenses and lost potential production. One indicator of bit wear and the optimal drill bit change point is the total drilling cost curve. Preliminary studies have shown this to be a promising approach.

This process consists of monitoring several variables over the course of a given drill bit's life: initial drill bit purchase price, mine site's drilling costs/hour, total depth drilled, and total drilling time. From these variables one can calculate the Rate of Penetration and the Total Drilling Cost per hole. An example plot of this process is shown in Figure 2-12 and the Total Drilling Cost calculation is

$$TDC = \frac{\text{Bit Price } [\$]}{\text{Total Drilled Depth} [\Sigma m]} + \frac{\text{Drill Operating Cost} \left[ \frac{\$}{hr} \right]}{\text{Penetration Rate} \left[ \frac{m}{hr} \right]} \quad (2.11)^2$$

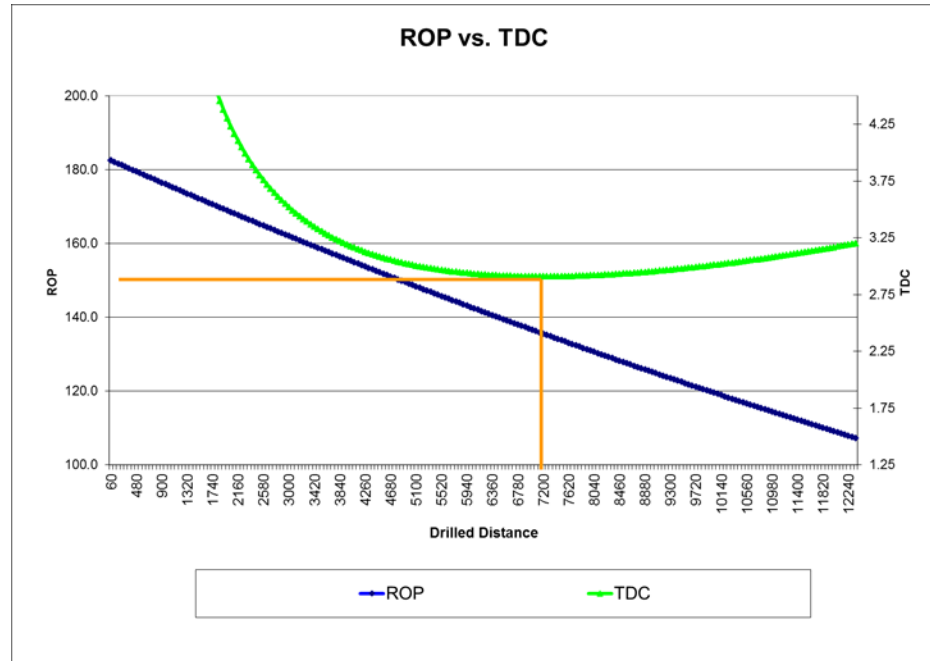


**Figure 2-12: Total Drilling Cost curve<sup>3</sup>**

Some preliminary studies were performed at a working mine site in which the working drill bit was pulled from the drill at the point when the total drilling cost curve started its upward climb from its lowest point (in Figure 2-12 this would be at approximately the 7,200 feet drilled distance point). These studies demonstrated that by removing the worn bit at that point and installing a new bit the mine site would end up saving more money in operating costs than if the worn bit was used to failure (Zink, 2007).

The premise of monitoring the total drilling cost curve as a means to dictate drill bit change frequency is a type of performance-based drill bit wear monitoring.

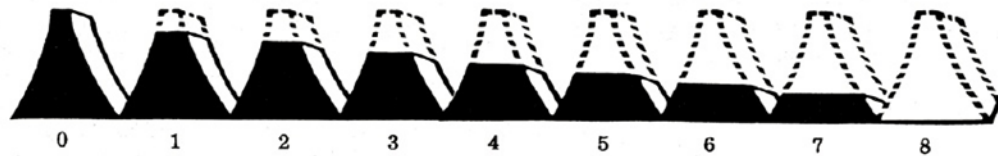
<sup>2</sup> While this is a standard equation used in industry, it is overly simplistic and fails to account for the impact of the opportunity cost of the lost production time incurred due to a drill bit change.

<sup>3</sup> It should be noted that the example TDC curve is very specific to scenarios where bit life is very long. It is not applicable to the more common scenario of catastrophic bit failure due to operational inputs or drastic changes in in-situ geology.

### 2.3.2 Drill Bit Wear Monitoring

Drill bits are a consumable component and, as such, are designed to wear over time with as limited performance degradation as possible until a replacement is required. Insert or tooth wear is currently measured and recorded using industry standards defined by the International Association of Drilling Contractors (IADC) Tooth Wear Grading System. Under this system tooth wear is graded in increments of 1/8 of the initial insert height, where: a new, unused bit would have inserts of a condition equal to zero, a worn bit with half worn teeth would have a condition equal to four, and a heavily worn bit with teeth totally gone would have a condition equal to eight. Bearing wear is graded in a similar way (new = 0, failed = 8) and shirrtail and cone wear is also examined and noted. Figure 2-13 shows a simplified illustration of the IADC Tooth Wear Grading System.

Tooth wear is graded in “eighth’s” (1/8’s) of the insert missing:



New, unused = 0.                      Half gone = 4.                      Totally gone = 8  
Steel Tooth and Tungsten Carbide cutting structures are graded the same.

**Figure 2-13: IADC Tooth Wear Grading System**

It should be noted that the IADC Tooth Wear Grading System is only meant to be applied as a form of condition monitoring and recording. It is not meant to be used as a failure analysis. It is only a tool with which to record drill bit condition at a certain point in the drill bit’s life for the purpose of future reference.

---

Currently, the method most widely used to evaluate bit wear is a performance based one similar to what was proposed in prior research by Peck. The current state of bit wear is determined by monitoring penetration rate and torque (Peck, 1989). Assuming a constant rock type, and therefore a uniform rock strength, and constant operating conditions penetration rate will decrease over time as bit wear increases. Once the penetration rate has fallen below a predetermined value or the torque has risen above a predetermined value the bit should be replaced (Peck, 1989).

The aforementioned procedure is applicable for slow tooth and cone wear. For cone bearing failures the torque must be monitored. Any observation of a rapid rise in torque while under constant operating conditions is a sign of bearing failure. A bearing failure requires immediate bit replacement (Cooper G. e., 1987).

Unfortunately, the requirement of constant operating conditions and rock type is often not an option in the open pit mining environment. Typically, several rock layers are encountered during the drilling of a single hole. Some layers may even be composed of entirely broken and non-homogenous rock material. At some particularly dynamic mine sites rock layers can be encountered in differing orders from one hole to the next within the same drill pattern. This dynamic, and often unmodeled, in-situ geology makes it incredibly difficult to determine if penetration rate is decreasing or torque is spiking because of bit wear/failure or because a new rock layer is being encountered. This puts clear limitations on performance-based drill bit wear monitoring and is a driver behind exploring a vibration-based model. Some future work has been proposed which would attempt to correlate the bit performance data with drilling rock recognition data however this has not yet progressed past the proposal stage (Cooper G. , 2002).

Another possible approach to bit wear monitoring is optical profiling of the drill bit over time. As the bit progresses through the various stages of bit life from new to replacement required there will be a definitive volume change as the bit wears. This volume change could be captured by using some type of three-dimensional mapping tool to take images of the surface of the tri-cone rotary drill bit. These images would then be processed using a software tool and a data analysis would be carried out. Based upon volume changes bit wear state could be determined upon which bit wear replacement decisions could be based.

A study was carried out on impregnated diamond drill bits using an optical 3D mapping profilometer (Pelletier, 1993). This study concluded that drill bit profiles could be used to determine current wear states. The data was also thought to be of use as a feedback tool to drill bit designers for design and performance improvements. An overall accuracy of 5 mm<sup>3</sup> for volumetric measurements and 2.5 µm for surface height variations could be realized.

This method of drill bit wear monitoring is very similar to the method of visual condition inspection outlined earlier. However, it is an improvement over visual condition inspection and recording in that it is incredibly exact, precise and repeatable. But much like visual condition inspections it is an invasive technique which requires the drill bit to be removed from the hole and cleaned for inspections. This is not ideal as it requires the drill to be in a non-operating mode during the inspection periods. For this reason, the Optical Profiling method is not an ideal form of bit wear monitoring and is not suitable for industrial applications.

Due to the limitations and shortcomings of the above mentioned bit wear monitoring strategies, vibration monitoring for bit wear is seen as a field of study with great potential.

### **2.3.3 Vibration in Drilling**

Previous work examining vibration in drilling can be used as a guideline for the frequency ranges that can be expected for each component of the blasthole drill rig. Full modelling of the mast itself would be a complex task but is also likely unnecessary. The natural frequency of a blasthole drill's mast was observed to be in the 300-400 Hz range (Branscombe, 2010). This was seen to be well above the vibration frequencies associated with tri-cone bit activity or even with drill string steel activity (the components of interest).

The drilling-induced vibrations can be of use for modelling bit depth, rotary speed, and bit wear but also because they are responsible for the high-displacement vibrations that can cause damage to the drill rig and health risks to human operators. These are of a much lower frequency, so the high frequency vibrations are of little interest (Branscombe, 2010).

Additional work succeeded in showing that the blasthole drill could be modelled as a mass-spring-damper system with the drill string itself modelled as a spring due to its spring-like nature and that the drill string's oscillations were shown to have a period directly related to the length of the drill string (Jardine, 1994).

Previous work has found that low frequency drilling vibrations (0-20 Hz) are the main range of interest for tri-cone rotary drill bit modelling. Drill string steel was found to have

resonant frequencies of 75-80 Hz. While many of the higher frequency vibrations are caused by onboard rotating components such as motors and compressors (Aboujaoude, 1997). In addition, it was shown that mass imbalances due to bent drill string steel can cause lateral oscillations at 1 times the rotation speed with sympathetic oscillations in the axial (2 times rotation speed) and torsional (1-2 times rotation speed) directions (Besaisow, 1986). Additionally, misalignments and buckling in the drill string can cause lateral oscillations at 1 times the rotation speed (primary) and possible secondary axial and torsional oscillations at 2 times the rotation speed.

As well asymmetric hole bottoms can cause lateral oscillations at 2 times the rotation speed due to moment of inertia variations. Tri-cone rotary drill bit effects have been shown to cause axial and torsional oscillations at 3 times rotation speed (Deily, 1968), (Besaisow, 1986). For our application we can assume a rotation speed of between 40-120 rpm. This would give the primary vibration frequency range of interest for tri-cone rotary drill bit effects to be between 0.6-6 Hz.

An initial study by Cooper showed that the vibration spectrum produced by a tri-cone rotary drill bit caused by the successive impacts of the bit teeth with the rock, could be associated with impacts coming from particular rows of teeth on a particular cone. Over time the vibration peaks were seen to accelerate as the drill bit teeth wore down (Cooper G. e., 1987).

The vibration frequency of a cone, in particular, accelerates with wear because the individual cone must move faster to cover the same distance as its size diminishes due to

the wear. Wear is not necessarily uniform across all three cones, so they must be examined and modelled individually.

A loss of vibration peak sharpness was seen to occur as a result of a cone bearing failure. This would mimic the vibration phenomenon seen with poor hole cleaning. Torsional acceleration was seen to be a particularly good indicator of bearing failure. Large spikes appeared in the torsional acceleration when a bearing had failed. These peaks were not present for a bit with three good bearings.

In addition to providing an indication of drill bit wear and bearing failure, vibration was also shown to have the potential to identify different rock types. Cooper's work also observed that for tri-cone rotary drill bit effects there was little use for vibration signals of greater than 100 Hz and that cone rotation speeds were 1.00 – 1.25 times bit rotation speed which was lower than previously hypothesized.

Although Cooper's work seemed promising the conclusions included a caveat that vibration data collection is easy in the lab but seemed impractical and possibly unfeasible in the field. However, this caveat was directed at petroleum drilling which has extremely deep drill holes compared to the shallow holes seen in surface production mining. In general capturing vibration signals from the drill bit in a surface mining environment should not be as challenging as in deep well drilling.

Additional work explored the axial bit vibration spectra data to attempt to show a bit wear correlation. It was shown that tooth vibration peaks accelerated toward higher frequencies as wear progressed. Through continuous monitoring of axial bit vibration spectra detection of bit tooth wear was accomplished by detecting spectral peak shifts. As

well, it was shown that the cone from which the spectral peaks arose could be identified (Naganawa, 2012). These results were consistent with the previous vibration related work, albeit more elaborate and included an overall improved contribution with respect to the prior research.

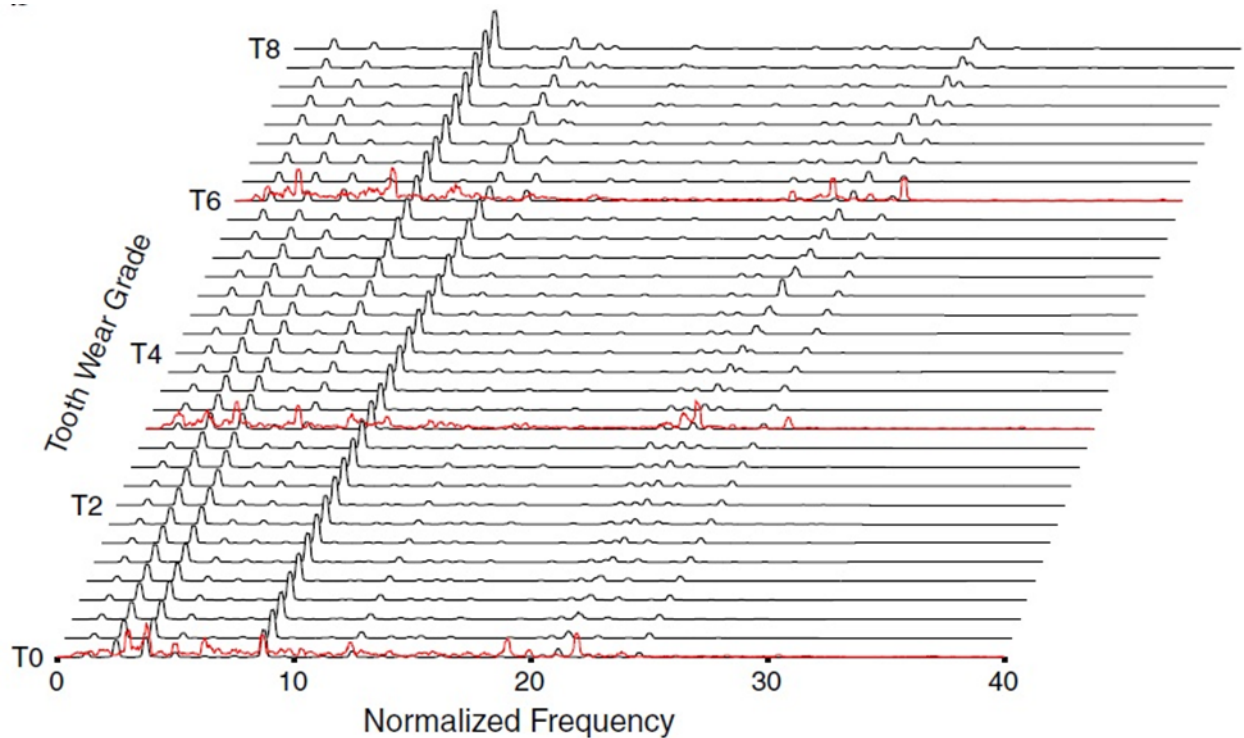


**Figure 2-14: Behaviour of weight on bit vibration spectra for tri-cone rotary drill bit with different tooth wear grades in a constant rock type (Naganawa, 2012)**

Figure 2-14 clearly shows that the tooth vibration peaks accelerate to higher frequencies as tooth wear progresses. In the plot T0 is the lowest tooth wear and T8 is the highest. The vibration peaks at approximately 20 Hz accelerate from 20-30 Hz as the tooth wear progresses from low to high.

Additional simulation work showed that bearing failure could be detected in a similar fashion. However, it was found that missing tooth detection would be a more difficult

---

task to accomplish. Only the first row of teeth made enough of an impact to detect when a tooth was missing, on the subsequent rows this did not appear possible (Naganawa, 2012).

It must be noted that this testing was only accomplished in a laboratory setting and it is expected that downhole while drilling data will be much noisier and more difficult to interpret because of non-homogenous in situ material and the corresponding effect of vibrations from orientations other than axial.

Prior research done at McGill University has shown that as the length of drill string steel in the hole increases, the natural frequency of the drill string steel decreases (Aboujaoude, 1991), (Aboujaoude, 1997). This was subsequently reinforced by work done at Queen's University which highlighted the importance of accelerometer placement on the drill's mast when recording the drill string steel's natural frequency with respect to depth (Branscombe, 2010). In addition, Branscombe demonstrated a relationship between the 6-times rotary speed frequency and rotary speed. When the dominant or secondary vibration frequency was considered this relationship was demonstrated to have a very favorable fit ( $R^2$ ) of 0.9959. Thus, the 6-times rotary speed frequency value should be favoured during a vibrational analysis for bit wear.

#### **2.3.4 Vibration and Wear as Controllable Variables**

Vibration had been suggested as an input to a drill control system in prior McGill based research (Aboujaoude, 1997). Aboujaoude demonstrated that by utilizing vibration as a signal in a feedback control loop drilling related vibration could be lessened and kept at acceptable levels. This was accomplished by regulating the rotary speed request signal

---

based upon the optimal drilling set-point and the plant vibration signal as feedback.

During periods of low vibration, the rotary speed would be set to the pre-defined optimal point and when vibrations increased the rotary speed would be reduced until vibration levels subsided. The lower limit for rotary speed under this control scheme was also pre-defined.

In addition, drilling vibration holds the potential to assist an autonomous drilling system that cannot rely on the presence of a human operator. All drilling induced vibration is caused by events at the bit-rock interface and the corresponding actions or inactions of the operator or drilling control system. Rock is a heterogeneous material which can contain significant and unknown variation. Cracks, inclusions, transition zones, voids and other factors can cause the optimal drilling set-points to be in constant flux (Bailey, 1960). One can consider the bit-rock interface to be a time-varying environment with unknown variations and it is these variations which result in the drilling vibrations that subsequently propagate through the blasthole drill rig. The information-rich vibration data could be utilized to better define the bit-rock interface at any given time. This data could then be used, in conjunction with rock recognition data, to optimize the drilling process via the drill control system. In this way, it is proposed that the output of an analysis of the vibration data could be used as a low frequency, supervisory control loop – much in the same way as the operator currently is utilized.

Bit wear has not been previously utilized as an input to a drill control system nor has it been proposed as one. However, research by Peck did show that as a drill bit wears its performance characteristics change and higher levels of rotary torque, vibration and air pressure can be seen as well as potentially reduced penetration rates. The same research

showed that drilling performance could be used to determine the type of in-situ material presently being drilled. This research led to the now industry standard rock recognition software that is commonly used by many mine sites. The same research showed that not only would wear influence drilling performance but that it would also influence the rock recognition system and Peck suggested that future research should work to address that (Peck, 1989). However, to date no research has been done on this phenomenon.

Additionally, the patent by G.P. Shively, Jr. proposed that optimal tri-cone drilling occurred at a depth of cut based upon the insert heights on the drill bit (United States of America Patent No. 5,449,047, 1995). Since it was shown that those insert heights lessen as the drill bit wears over its life cycle the present wear state could also be of use when a drill control system is using depth of cut based control.

Based upon the above research drill bit wear would be a valuable feedback signal to a drill control system for both drilling set-point optimization and rock recognition normalization.

## **2.4 Industry State of the Art Drill Control**

While having a variety of names [Autodrill, Auto Drill, PDC (Programmable Drilling Control)], the present drill control offerings from the three leading blasthole drill OEMs are extremely similar. All offer the same basic functionality based upon penetration rate control and some offer limited enhancements that attempt to address high rotation torque or vibration levels. This section will examine the most advanced drill control systems presently offered (Harnischfeger Corporation, 2006), (Bucyrus International, Inc., 2005), (Atlas Copco Drilling Solutions LLC, 2012).

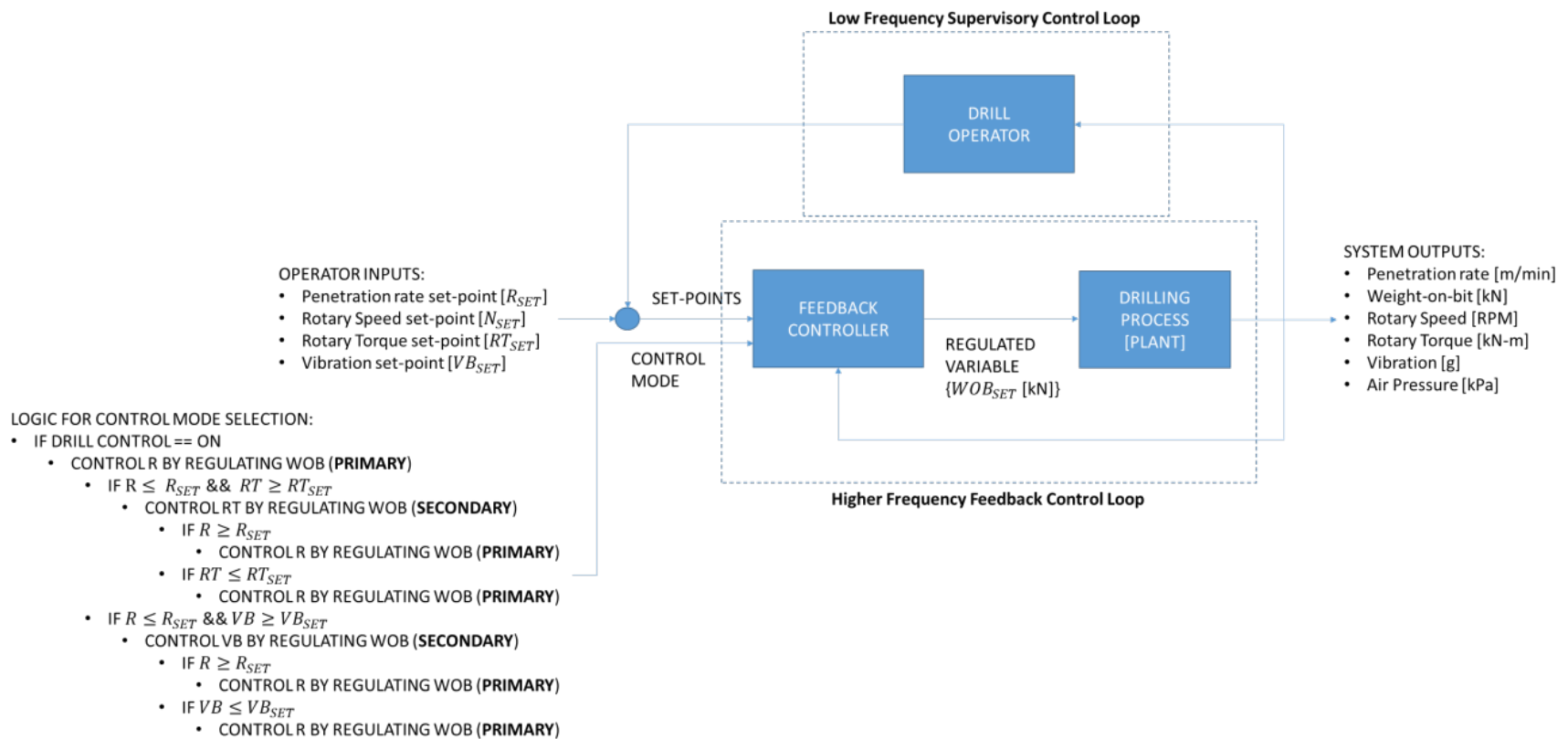


Figure 2-15: State of the art OEM drill control system

---

As illustrated in Figure 2-15, the primary control mode is penetration rate control and the corresponding logic for control mode selection is also provided. Some pre-set penetration rate [m/min] is selected and the drill control system regulates weight-on-bit [kN] in an attempt to reach and maintain the desired penetration rate. If the chosen penetration rate set-point is too high to be attained for the given drilling conditions the weight-on-bit will saturate at the maximum attainable by the drill. If the penetration rate chosen is too low for the given drilling conditions the weight-on-bit from the machine will become negative in an attempt to hold back the bit from advancing too quickly.

Two secondary control modes are offered: rotation torque and vibration. The secondary control modes only activate if the primary control mode of penetration rate is satisfied. If, while in a secondary control mode, penetrate rate exceeds the set-point the system will switch back to regulating penetration rate.

If rotation torque [kN-m] exceeds a pre-set rotation torque value the drill control system will regulate weight-on-bit in an attempt to reach and maintain the desired rotation torque.

Alternately, if vibration [g] exceeds a pre-set value weight-on-bit will be reduced following some pre-defined methodology. If at any time the vibration level exceeds a higher OEM defined value drilling will suspend for several seconds and a restart sequence will be followed. The restart sequence is allowed a maximum of three restarts before the drill control system will switch off and the operator must take control.

---

Additional hard stop limits are defined by the OEM for rotation torque and air pressure. If these thresholds are exceeded machine operation will be suspended and must be restarted by the operator.

None of the OEM drill control systems consider the specifications or design of the drill bit employed or the in-situ environment. In addition, none have the capability to address a variety of exceptional drilling conditions and offload this requirement to the operator who acts as a required supervisory control loop.

## **2.5 Propel Control**

Blasthole drills position using two tracks on either side of the drill deck; a left track and a right track. Each track is independently driven by a dedicated track motor, mounted on a common axis which is capable of moving the track in the forward or reverse direction (Harnischfeger Corporation, 2006).

This configuration makes the blasthole drill propel function similar to a differential drive mechanism. While a differential drive has been speculated to be the simplest possible drive mechanism for a ground contact robot, a tracked vehicle is more complex because it relies on ground slip or skid in order to change direction. A differential drive vehicle with wheels allows the assumption of perfect rolling contact which cannot be made for a tracked vehicle. However, tracked vehicles have the advantage of being more robust to terrain variations and can cross small voids in the surface and can climb steeper gradients than comparable wheeled vehicles (Dudek, 2010). This makes them the logical choice for surface mining applications.

Another complication introduced by tracked vehicles' reliance on slip between the treads and the ground surface in order to change orientation arises when attempting to use the vehicle kinematics to compute its pose. Although tracked vehicles can be approximated as differential drive vehicles with "extended" wheels, the large amount of slip between the treads and the ground makes it impossible to predict accurately a tracked vehicle's motion from the motion of its treads. Thus, tracked vehicles must rely on some other external mechanism for determining their motion rather than just examining the motion of the treads (Dudek, 2010).

Also, from Dudek and Jenkin, differential drive kinematics with linear and rotational speed equations are given below (Dudek, 2010).

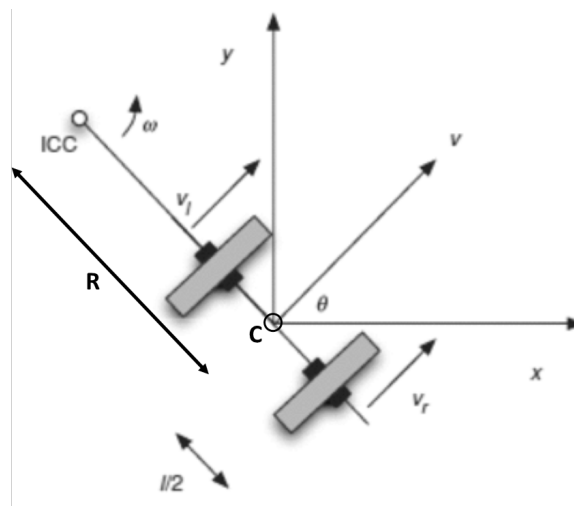


**Figure 2-16: Differential drive kinematics**

Examining Figure 2-16, the left track and right track velocity are denoted by  $v_l$  and  $v_r$ , respectively, the angular velocity is defined as  $\omega$ , and the velocity of the rotational centre of the vehicle ( $C$ ) is  $v$ . The distance between the tracks is defined as  $l$  and the vehicle heading in the  $x - y$  plane is denoted by  $\theta$ . The point in space about which the vehicle

rotates is known as the ICC (Instantaneous Centre of Curvature).  $R$  is the distance from the ICC to the rotational centre of the vehicle ( $C$ ). The blasthole drill right track velocity is

$$v_r = \omega(R + l/2), \quad (2.12)$$

and the left track velocity is

$$v_l = \omega(R - l/2), \quad (2.13)$$

where the distance from ICC to the rotation centre of the blasthole drill is

$$R = \frac{l(v_l + v_r)}{2(v_r - v_l)}, \quad (2.14)$$

and the drill's angular velocity is

$$\omega = \frac{v_r - v_l}{l}. \quad (2.15)$$

Given a fixed speed and radius, linear and angular velocity are related by  $v = \omega r$  (Giancoli, 2000).

Therefore, the velocity of the rotational centre of the vehicle is given by

$$v = \omega R = \frac{1}{2}(v_l + v_r). \quad (2.16)$$

Previous work saw the problem of exponential stabilization of the kinematic and dynamic model of a simple wheeled mobile robot addressed and solved using a discontinuous, bounded, time invariant, state feedback control law. The properties of the closed-loop system were studied in detail and its performance in the presence of model errors and noisy measurements were evaluated and discussed (Astolfi, 1999).

Astolfi explored the problem of attempting to move a differential drive, wheeled vehicle from some starting point to a pre-defined end-point location. In this way Astolfi's problem is not dissimilar to the surface mining application of propelling a blasthole drill

from a starting position to the desired blasthole location. Astolfi's robot kinematics model are given below with target location ( $G$ ) included.

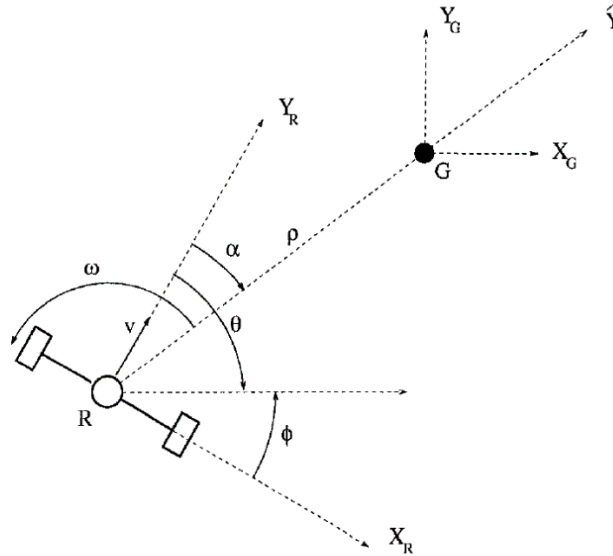


**Figure 2-17: Robot kinematics for Astolfi's problem (Astolfi, 1999)**

Astolfi considered the following coordinates transformation

$$\begin{aligned}\rho &= \sqrt{x^2 + y^2} \\ \alpha &= -\theta + \arctan\left(\frac{-y}{-x}\right) \bmod\left(\frac{\pi}{2}\right) \\ \phi &= \frac{\pi}{2} - \theta.\end{aligned}\tag{2.17}$$

Astolfi proposed the following control law with some gains  $k_\rho$ ,  $k_\alpha$ , and  $k_\phi$

$$\begin{aligned}v &= k_\rho \rho \\ \omega &= k_\alpha \alpha + k_\phi \phi.\end{aligned}\tag{2.18}$$

Through experimentation and discussion, it was shown that the proposed dynamic system was locally stable with the following constraints

$$k_\rho > 0$$

$$k_\phi < 0$$

$$k_\alpha + k_\phi - k_\rho > 0. \quad (2.19)$$

Therefore it was found that any choice of gains for  $k_\rho$ ,  $k_\alpha$ , and  $k_\phi$  that satisfies the constraints defined in 2.19 will result in a stable controller that will exponentially drive the vehicle to the coordinate frame's origin  $(x, y, \theta) = (0,0,0)$  (Astolfi, 1999).

The figure below illustrates the vehicle's path using Astolfi's controller with no disturbances or model errors.

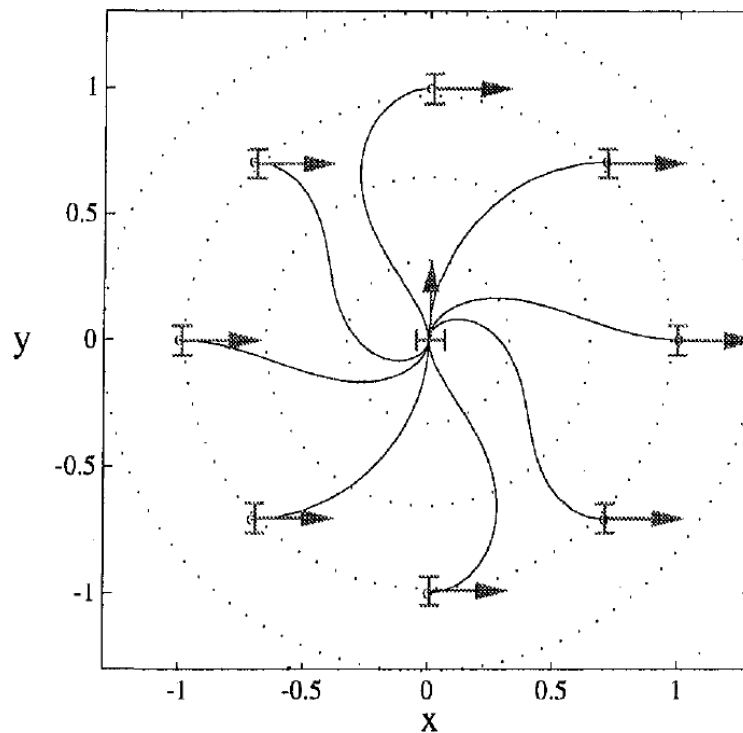


**Figure 2-18: Idealized vehicle path using Astolfi's controller (Astolfi, 1999)**

## 2.6 Extraterrestrial Drilling

In situ investigations in space began with the Luna and Apollo missions and have continued to present day which, paired with the rover exploration programs, have led to

an increased interest in drilling for extraterrestrial application. To achieve the goal of detecting habitable zones or signs of past or present life, the objectives for planetary exploration missions often include in situ sampling and analysis which requires subsurface exploration usually via drilling. An added complexity is introduced due to the harsh planetary and lunar environments which include extremely low temperatures and vacuum (Briggs, 2002), (Zacny, 2008).

The first extraterrestrial drilling occurred in the 1970s when the Soviet Luna 16 lander collected a 101 gram sample of lunar soil and returned it to Earth. The Apollo 15 mission saw astronauts operating a manual drill called the Apollo Lunar Surface Drill (ALSD) which was a 500 W rotary-percussive drill with a coring bit capable of acquiring a continuous 2 cm diameter core to a depth of approximately 2.4 metres. It was equipped with an auger for moving cuttings to the surface (Bar-Cohen, 2009).

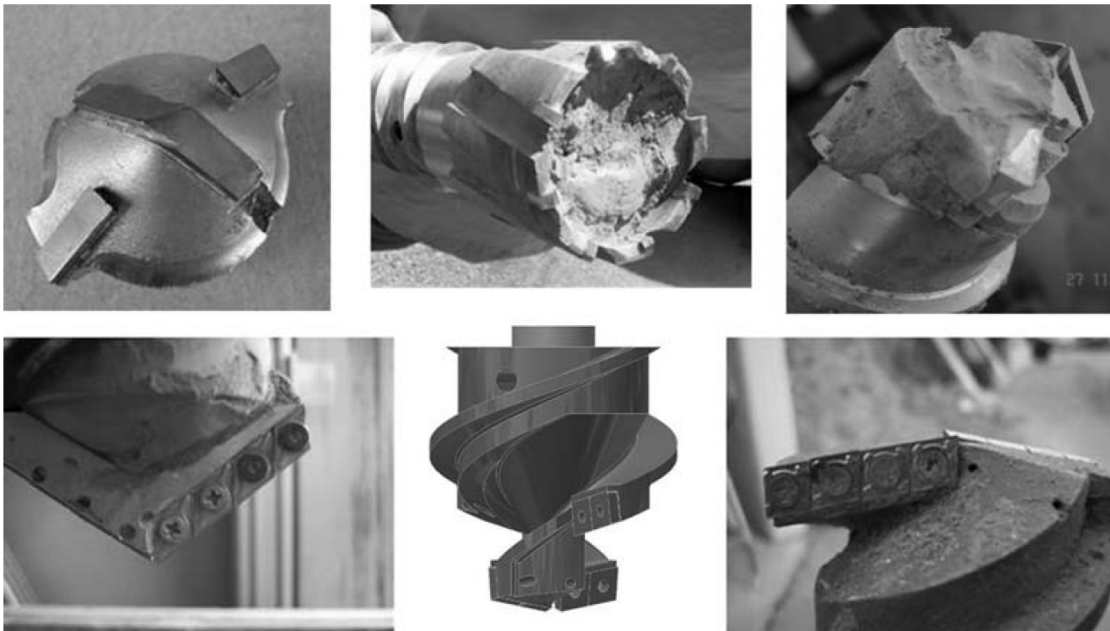


**Figure 2-19: Various drill bits used on the DAME drill (Bar-Cohen, 2009)**

The extraterrestrial environment is one of low temperatures and pressures which makes the use of drill fluid not feasible. Therefore, the style of bit is a fixed type or tool style auger or similar device (see Figure 2-19). To date most of the drills used in extraterrestrial missions have been rotary however research has shown that incorporating a percussive action may increase drilling ability while also respecting the low payload weight and power requirements associated with the application. One such drill was developed to be used on the 2011 Mars Science Laboratory mission which had two independent actuators to produce impact and rotation together with a specialized control system for synchronized operation. For scientific analysis, a core sample offers much more information than sample cuttings thus most drills designed for extraterrestrial exploration are core drills (Bar-Cohen, 2009).

For an extraterrestrial application deep drilling is considered depths greater than 2 metres. For future in situ exploration achieving depths of up to 10 metres is desired. The Subsurface Planetary Exploration Core Extracting System (SPECES) was developed to experiment with the deeper drill holes. During field trials at the Arizona Desert Rose Sandstone mine near Buckeye, Arizona the drill successfully drilled a 10 metre layer of sandstone using a single bit. This took 7 days of operation and after drilling the custom dry drilling coring bit was seen to have negligible wear. The drill's power levels were maintained between 80 and 100 Watts throughout the testing which comparable to a standard light bulb (Bar-Cohen, 2009).

Additional work has continued between the NASA Johnson Space Center and Baker Hughes Inc. with the development of a low-mass and low-power planetary drilling approach based on a dry rotary-coring wireline Bottom Hole Assembly (BHA). The BHA

---

is 8.5 kilograms and was designed to recover a continuous record of 2.6 centimetre diameter by 15 centimeter length cores. Typical operation occurs at 100 Watts of electric power at a 20 centimetre per hour ROP in consolidated sandstone. The drill has been field tested in both the United States and the Canadian Arctic in sandstone and ice with eventual plans for a Mars mission (Bar-Cohen, 2009).

Some obvious and great differences exist between the terrestrial production drilling application explored in this thesis and the extraterrestrial application explored in the referenced research. For this research these differences include: non-percussive drilling, non-core drilling, drilling with a tri-cone style bit and not a fixed type or tool bit, greater than a standard light bulb's power supply, and relatively unlimited weight requirements. Due to the less restrictive application of terrestrial drilling more advanced drilling technology and techniques can be utilized.

### **2.6.1 Drilling Automation and Intelligence for Extraterrestrial Applications**

The Drilling Automation for Mars Exploration (DAME) project explored drilling automation for extraterrestrial applications in detail with the primary purpose of the DAME drill build being to advance intelligent drill control software. The testing was limited to hole depths of 3.2 metres (Bar-Cohen, 2009).

The DAME drill system utilized an array of above and below ground sensors as well as an intelligent control method which enabled the system to autonomously detect and recover from drilling problem situations – in total six such situations were developed (Bar-Cohen, 2009):

- 
- For normal drilling situations, rate of penetration was controlled to keep the drill operating below the maximum weight on bit and the maximum operating power thresholds.
  - *Auger binding* – one of two situations where controlling ROP does not reduce operating power to less than the threshold. Related to bit torque compared to auger torque, vibration frequency of the drill and other factors.
  - *Auger choking* – the second of two situations where controlling ROP does not reduce operating power to less than the threshold. Related to bit torque compared to auger torque, vibration frequency of the drill and other factors.
  - *Bit jamming* – high bit torque or stalled auger.
  - *Bit inclusion* – oscillating WOB and bit torque.
  - *Drilling hard material* – high WOB, low ROP, and low bit torque.
  - *Auger corkscrewing* – high negative WOB.

The developed drilling controller in the current research addresses all of the above problem situations as well as numerous others as outlined in Table 3-2 which lists all of the exceptional scenarios considered by the author.

In addition to autonomous drilling the DAME project explored profiling the material being drilled. Using drill telemetry data to correlate to material and composition using a pre-built library of various material types (Bar-Cohen, 2009).

The material profiling appeared to heavily focus on rate of penetration to define what type of in situ material was present. For terrestrial drilling applications, this is considered

a simplistic approach to rock recognition and is not as advanced as the methods proposed by Teale and Peck (Teale, 1965), (Peck, 1989).

While Earth based teleoperation is feasible for the Moon, due to light speed associated time delays (tens of minutes) drills used for environments beyond the Moon (Mars, Europa, Titan, etc.) must be self-contained and autonomous (Bar-Cohen, 2009).

When discussing automation there are various levels of complexity and functionality all of which are often referred to simply as autonomous. As such, it is valuable to have an autonomy rating system to clearly understand what level or category of autonomy is achieved. One such autonomy rating system is given below (Mukherjee, 2006).

Category	Description
A0: automated	Open-loop control for drilling, sample acquisition and delivery
A1: semi-autonomous	Some closed-loop control: closed-loop drilling control with respect to drill rate and platform reaction forces
A2: semi-autonomous	Primarily closed-loop control: closed-loop drilling, sample acquisition and delivery
A3: autonomous	Primarily closed-loop control: failure diagnosis and recovery for drilling and sampling
A4: fully autonomous	Closed-loop control: failure diagnosis, failure recovery/avoidance, and performance optimization for drilling and sampling

**Table 2-1: Autonomy rating system (Mukherjee, 2006)**

The presented research proposes an autonomous surface rotary blasthole drilling system. Based on the referenced autonomy rating system the author's proposed system would be classified as fully autonomous<sup>4</sup>. While the sampling component is not considered due to the production drilling application, in addition to fully autonomous drilling rig movement and pre-drilling setup are included in fully autonomous rig operation. Sporadic human

<sup>4</sup> While one could argue the results of this research could fall into the autonomous or the fully autonomous category, it is the author's opinion that the results are fully autonomous as they include performance optimization for drilling.

---

operator intervention may be required for the author's proposed fully autonomous solution but this would be analogous to having intermittent Earth based mission control commands for the extraterrestrial application.

## Chapter 3

### Advanced Drill Control

As a first step toward understanding the requirements for an advanced drill control solution, the author undertook a detailed research study and review of the state of the art technology offerings available in industry. The results of this study are documented in Section 2.4 – Industry State of the Art Drill Control.

After developing an understanding of the industry state of the art offerings for drill control a drill audit was conducted at five Canadian surface mines. The mine sites visited operated drills built by two of the three leading OEMs (Caterpillar and P&H) and between them operated a total of 16 large electric rotary blasthole drills. A detailed breakdown of the machine type by mine site is provided in Table 3-1 (where OEM #1 and OEM #2 represent Caterpillar and P&H, respectively).

The purpose of the audit was to acquire an understanding of the drill control systems capabilities and limitations as well as observe how the technology is received and utilized in an operational context. Manual practices were also observed and noted.

Mine Site	Total Drills	OEM #1	OEM #2
Mine Site #1	4	4	0
Mine Site #2	3	3	0
Mine Site #3	3	2	1
Mine Site #4	4	1	3
Mine Site #5	2	2	0
<b>Total</b>	<b>16</b>	<b>12</b>	<b>4</b>

**Table 3-1: Drill audit, equipment distribution by site**

For the following discussion on the drill control systems observed it may be useful to refer to the drill control architecture outline illustrated in Figure 2-15.

During the audit it was observed that the rotary torque control mode was only available on the newest drills (those purchased within the last calendar year) and was not offered on the other drills. This resulted in only three of the 16 drills having a rotary torque control feature.

An additional limitation for rotary torque control was that to be activated the operator would manually have to elect to have the drill control system operate in rotary torque control mode instead of the primary penetration rate control mode. Automatically switching between the control modes was beyond the scope of the drill control systems. This was thought to be a significant design limitation.

To complicate the issue of having the operator decide when rotary torque control should be used instead of penetration rate control, all of the operators met during the audit did not understand the purpose of rotary torque control. The operators reported that they rely on the regional OEM representatives to educate them on how to best use the features of the drill and the OEM staff had never mentioned the alternate control mode. This highlighted a further flaw in the design decision to have the control modes switch manually instead of automatically – necessary reliance on regional resources understanding and educating customers on the merits of new technology.

A design issue with the OEM vibration control module was observed during the design review stage and further reinforced by field observations during the audit. Vibration control is designed so that when high levels of vibration are detected (but not high enough to warrant a process stop) the drill control system will attempt to control (lower)

---

vibration by regulating (decreasing) weight-on-bit. However, this action often increases vibration levels because it, in effect, decreases the mass of the vibrating body (in this case the drill string). This concept can be seen in the simple frequency of motion equation (Giancoli, 2000)

$$f = \frac{1}{2\pi} \sqrt{\frac{k}{m}}, \quad (3.1)$$

where  $f$  is the frequency of motion (Hz),  $k$  is the spring constant of the system (N/m) and  $m$  is the mass of the system. In the application of a blasthole drill the mass of the system is made up of two parts: the physical weight of the components (which is a constant) and the weight-on-bit. When the vibration control feature decreases the weight-on-bit in response to the presence of vibration, the mass of the overall blasthole drill system is decreased. Thus, decreasing the denominator of 3.1 and increasing the corresponding frequency of motion (vibration). As was demonstrated in the previous research to properly control vibration rotary speed should be the regulated variable not weight-on-bit (Aboujaoude, 1997).

Based upon the above two observations when considering the OEM drill control solutions operating in the field, the logic for control mode selection and control mode input fields shown in Figure 2-15 can be discounted. The OEM drill control solutions can and should be thought of as a simple penetration rate cruise control type solution with thresholds added for rotary torque and vibration that, if met, trigger a process stop.

Unfortunately, it was also observed that often the penetration rate selected by operators was ill-suited for the given ground conditions, the drill or the application in general.

When this occurs, it prevents the OEM drill control solutions from delivering efficient drilling even in normal ground conditions.

It appeared that the mine site culture was such that the operators all saw production (or meters drilled) as the primary measure of what made a good operator. Indeed, at several sites the drill operators had to read their production statistics out over the mine site radio which acted as a way to glorify high performers and shame those that had not drilled as many metres. In general, this led to them choosing penetration rate set-points that were either unattainable or too aggressive. There seemed to be no consideration paid to drilling efficiently with all attention on attempting to have the machine reach some high penetration rate that the operators believed would allow them to reach their chosen production goal.

The lowest penetration rate set-point observed was 1.524 metres per minute (which is likely a suitable choice) however most were 2 m/min or above with some as high as 5 m/min.

Often the chosen penetration rates were simply unattainable because of physical limitations and constraints on the system. The machine is limited by its hoist and rotary motor specifications and the in-situ material is often too hard or sticky to allow for high penetration rates. Even if the high penetration rate set-point can be physically attained it is likely beyond the optimal operating conditions of the tri-cone rotary drill bit used. As has been discussed, if the penetration rate is too high it will result in the bit becoming buried and instead of allowing broken rock chips to spall and be flushed out of the hole the chips are trapped beneath the bit and re-grounded into a powder which results in premature bit wear, slower penetration rates and higher vibration and torques on the drill

---

rig. So a penetration rate set-point that is too high for the machine and drill bit will actually result in a lower penetration rate realized than if a lower set-point is chosen.

It was also observed that no consideration was paid to the type of bit used by the drill operator. At all of the mine sites visited for the audit the drill and blast engineer chose the drill bits to be used but the bits chosen had no impact on the drill control operating set-points which were either chosen by the individual drill operator or the OEM regional representative for that site. All of the sites visited would use drill bits from at least two different OEMs as they like to encourage competition and feel that it yields a better purchase price for them. It was observed that some sites would alternate the use of bits for soft formations and bits for hard formations. Even if they were using the bits in the appropriate type of in-situ material they would not change the drill control set-points even though each bit was designed for very different operating characteristics.

Based upon the literature review and the mine site drill operational audit, this research proposes an advanced drill control solution that differs considerable from the state of the art drill control solution offered by the OEMs. A three-tiered drill controller is proposed with a high frequency feedback control loop as the primary control mode, a lower frequency supervisory control loop that will automatically switch between control modes as required, and a low frequency (rare) operator loop that will be required for extremely exceptional conditions or drill control resets due to process stops or timeouts.

Instead of being a simple penetration rate cruise control type control system, the advanced drill control solution proposed would only accept bit specifications for the installed drill bit as inputs. Based on the optimal drilling conditions for the drill bit and in combination with the known machine specifications the advanced drill control solution

---

would choose the operational set-points. This would remove the operator prejudice for high penetration rate set-points by not giving them the input option.

The primary control philosophy proposed for the advanced drill controller is the depth of cut method. Based upon the bit-rock interactions depth of cut would be utilized or switch out for one of the alternate control philosophies available. In order to understand the different drilling methods required an understanding of the various potential exceptional drilling conditions is necessary. This is reviewed in the next section.

### **3.1 Exceptional Drilling Conditions**

To understand the various drill control modes required for an advanced drill control solution the various potential exceptional drilling conditions were compiled. The list can be seen in Table 3-2. Also included in the list is the typical adjustment required by the drill operator (these were compiled through field observations during the drill audit and from the available OEM literature) and the applicable drill control mode that would address the listed exception. The drill control modes listed are for the developed advanced drill control solution. The various drill control modes are explored in detail in Section 3.2 and the overall controller with associated hierarchy is presented in Section 3.2.

It should be noted that there are several exceptional conditions that are not addressed by any mode in the advanced drill controller. These include Risk of Flooded Hole, High Dust Output, and Worn Bit.

For both risk of flooded hole and high dust output additional sensing hardware is required to detect the presence of excess water in the ground and to detect dust particulate in the

air above the hole while drilling. Both of these technologies do exist and could be handled with additional inputs to the drill control system in the future if integration was desired.

Both scenarios of a completely stuck bit and a bit that must be changed would be addressed through the controller's rare and infrequent operator intervention loop.

Exception ID#:	Result	Typical Adjustment(s)	Applicable drill control mode
<b>1.0 Soft Ground</b>			
1.1	Increased penetration rate	Regulate based on R/N	Depth of cut control
1.2	Risk of blasthole caving	Regulate based on R/N	Depth of cut control
1.3	Increased importance of mud wall	Ensure proper WF & R & N	Depth of cut control
<b>2.0 Wet Ground</b>			
2.1	Risk of flooded hole	↓ WF	None
2.2	Risk of jammed bit	↓ WF	Critical, bit plugging control
<b>3.0 Synclines</b>			
3.1	Dynamic ground conditions	Regulate based on R/N	Depth of cut control
<b>4.0 Off Horizontal / Dipping Hard Rock Bands in Softer Strata</b>			
4.1	Potential bit deflection	↓ R	Depth of cut control
4.2	Potential high torque	Regulate based on RT	RT control
4.3	Potential high vibration	↓ N	Vibration control
<b>5.0 Strata with Voids or Cracks that can Provide an Escape Path for the Bailing Air</b>			
5.1	Decreased air pressure	Regulate based on R/N	Depth of cut control
5.2	Issues with bailing chips not escaping	Regulate based on RT	Rotation torque control
5.2.1		Regulate based on VB	Vibration control
<b>6.0 Soft Materials Seams with Hard Cap and Seat Strata</b>			
6.1	Risk of high penetration rate & bit dama	Limit R	Depth of cut control
<b>7.0 Soft / Granular or Fractured Material Causes Hole Caving</b>			
7.1	Risk of hole caving	Regulate based on R/N	Depth of cut control
7.2	Increased importance of mud wall	Ensure proper WF & R & N	Depth of cut control
<b>8.0 Fractured Shales and Other Non-Consolidated Materials</b>			
8.1	Risk of high penetration rate & bit dama	Limit R	Depth of cut control
8.2	Potential high vibration	↓ N	Vibration control
8.3	Risk of bit walking	↓ WOB & ↓ N	Depth of cut control

9.0 Excessive Dust		
9.1	High dust output	↑ WF None
10.0 High Feed Force & Torque		
10.1	Mechanical stress on drill string, bit & m	↓ WOB Depth of cut control & Rotation torque control
11.0 Low Penetration Rate		
11.1	Slow, inefficient drilling	↑ WOB Depth of cut control
12.0 High Rotation Speed		
12.1	Grinding, bad penetration	↓ N Depth of cut control
12.2	High vibration	↓ N Vibration control
13.0 Low Rotation Speed		
13.1	Bad penetration rate, inefficient drilling	↑ N Depth of cut control
14.0 Air Flow Too Low for Penetration Rate		
14.1	Cutting accumulation at bottom of hole	↓ R Depth of cut control
15.0 Too Much Air Flow for Ground Conditions		
15.1	Risk of hole caving	Regulate based on RT Rotation torque control
15.1.2		Regulate based on VB Vibration control
16.0 Bit Plugging		
16.1	High air pressure	↓ WOB Critical, bit plugging control
17.0 Upward Resistance		
17.1	Cutting accumulation above the bit	Turn AP off & pause bit retract Retraction
17.2	Bit stuck	Reverse direction of R Retraction
18.0 Bit Stuck in Normal Drilling		
18.1	Drilling cannot progress	Manually retract bit using jacks None
19.0 Void		
19.1	Increased penetration rate	Regulate based on R/N Depth of cut control
19.2	Risk of high penetration rate & bit damage	Limit R Depth of cut control

20.0 High Vibration		
20.1	Inefficient drilling, bit & machine damage	↓ N Vibration control
21.0 Worn Bit		
21.1	Inefficient drilling	Change bit None
22.0 Crest Hole (Thick Layer of Broken Material Before Intact Rock)		
22.1	Risk of bit walking	↓ WOB & ↓ N (deeper collar) Collar
22.2	Risk of high torque	Regulate based on RT Rotation torque control
22.3	Risk of high vibration	↓ N Vibration control
<b>Legend:</b>		
N - Rotation Speed	AP - Air Pressure	
WOB - Weight-on-Bit	VB - Vibration	
RT - Rotation Torque	WF - Water Flow	
R - Penetration Rate	R/N - Depth of Cut (Penetration Rate / Rotation Speed)	

**Table 3-2: List of exceptional drilling conditions with typical outcome, adjustment and applicable advanced drill controller mode**

### **3.2 Controller Hierarchy**

The advanced drill control solution was created to address exceptional drilling conditions that may be encountered while drilling production holes in surface mining. It was designed to do this by considering various drill control modes, each designed to address a specific limitation to the drilling process introduced by one or more exceptional drilling condition. The advanced drill controller was designed to incorporate best operator practices, respect the OEM specifications for drill and drill bit use, and react more quickly than a typical operator. Overall, the advanced drill controller should outperform a mine's fleet performance, however, it may not outperform the very best human operator.

The various drill control modes implemented are each triggered by some set of drilling conditions; it is common for more than one drill control mode to be relevant at any given point of drill operation. To properly orchestrate the various drill control modes the advanced drill controller has a control mode hierarchy. This hierarchy is illustrated in the graphic presented in Figure 3-1; control modes are shown with priority decreasing from the centre to the exterior of the circular graphic.

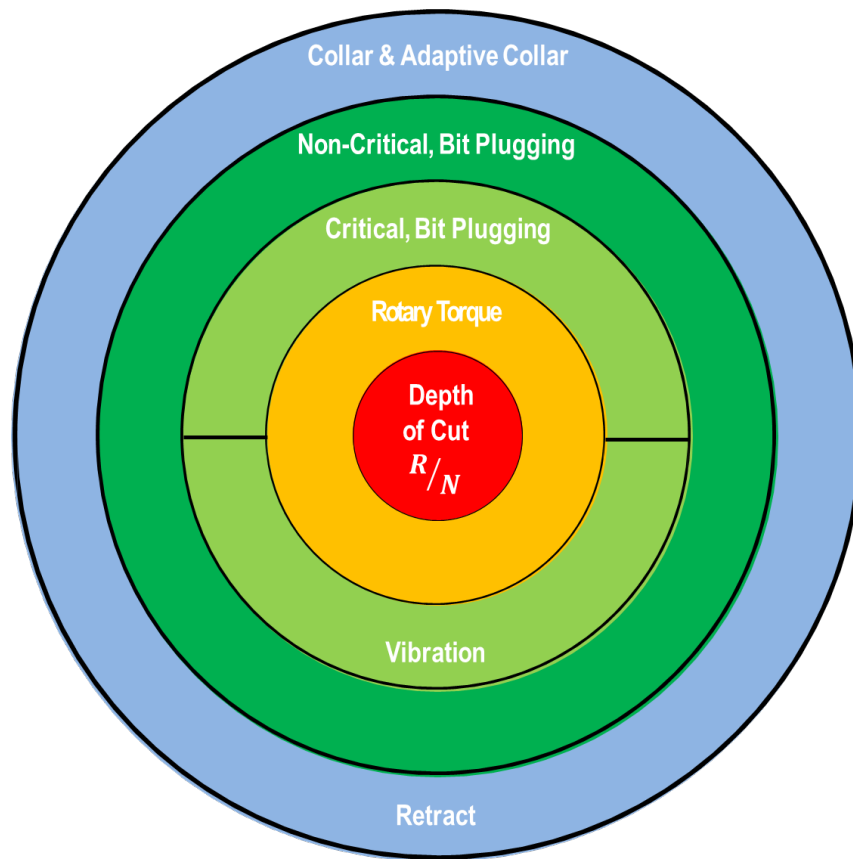


**Figure 3-1: Hierarchy of various control modes**

With reference to Figure 3-1, the advanced drill controller was implemented with the following hierarchy:

1. **Depth of Cut** is the primary control method and is the default control philosophy if no exceptional drilling scenarios are encountered. If another control mode is active, at its conclusion the controller reverts to this mode.
2. **Rotary Torque** is the secondary control method. If a high torque is encountered this control method will be active until the torque has been appropriately addressed. At that time the controller will activate any of the other control modes or revert to depth of cut control.

3. **Critical, Bit Plugging and Vibration** (equally weighted in the control hierarchy).  
Provided there is no high torque, high air pressure or high vibration will activate the respective control mode. Both modes are equally weighted, and activation is based upon which exceptional scenario is encountered first.
4. **Non-Critical, Bit Plugging** is low in the control hierarchy as it is a somewhat passive control mode. Its operation happens more or less in the background, during a drilling scenario where no critical issue is occurring but when one may be anticipated and prevented.
5. **Collar & Adaptive Collar and Retract** are shown on the perimeter of the control hierarchy graphic. This represents that they are only functional during defined and delineated segments of the drilling process; at the start and end of each drilled production hole.

While not shown in Figure 3-1, an important feature of the controller is rotary speed feedback control. This control mode is active during all operation and for all control modes.

### 3.2.1 Closed Loop Control of the Drill-Plant Model/System

The overall closed loop control implementation is described in this section; this description is valid for the controller implementation used for the simulated drill-plant model and for the implementation used for the physical drill-plant model at the partner mine sites. More details around the implementation of the individual control modules can be found elsewhere in Chapter 3. The high-level implementation of the controller is shown in Figure 3-2.

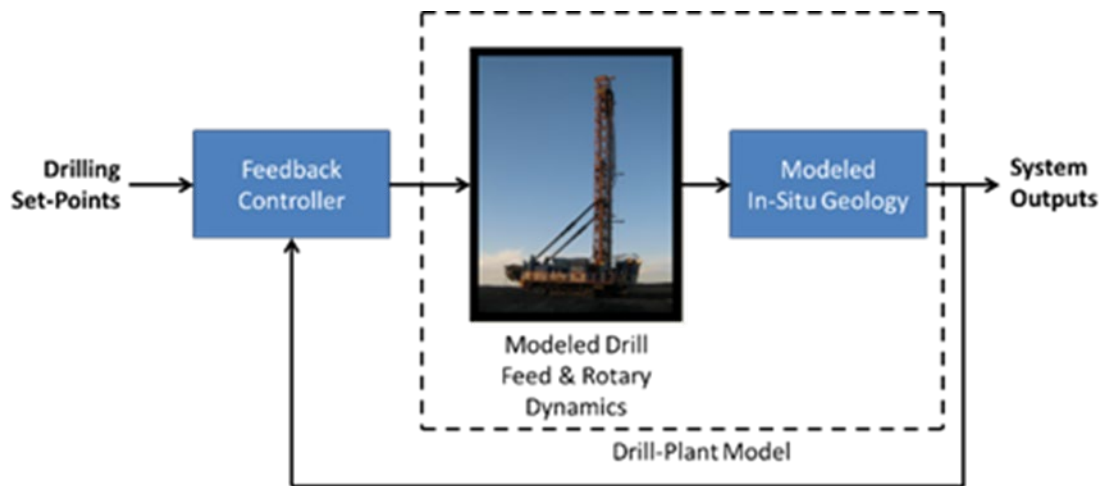


**Figure 3-2: Advanced drill control interface to drill-plant model**

The modelled drill feed and rotary dynamics are described in detail in Appendix A: Feed Motor and Rotary Motor Response Testing, Modelling. The modelled in-situ geology used for testing and simulation was based on that developed during previous work (Aboujaoude, Modeling, Simulation and Control of Rotary Blasthole Drills, 1991). The geological models developed in this work were adapted (using Aboujaoude’s methodology) to better represent the partner mine sites used for eventual field testing of the developed advanced drill control solution.

A more detailed version of the controller during normal drilling is shown in Figure 3-3. This plot shows how the various drill control modules described in Section 3.3 interface to the drill-plant model and operate within the feedback control loop when appropriate. A supervisory control loop determines which control module should be active based upon observed plant signals and applies switching logic to the feedback control loop.

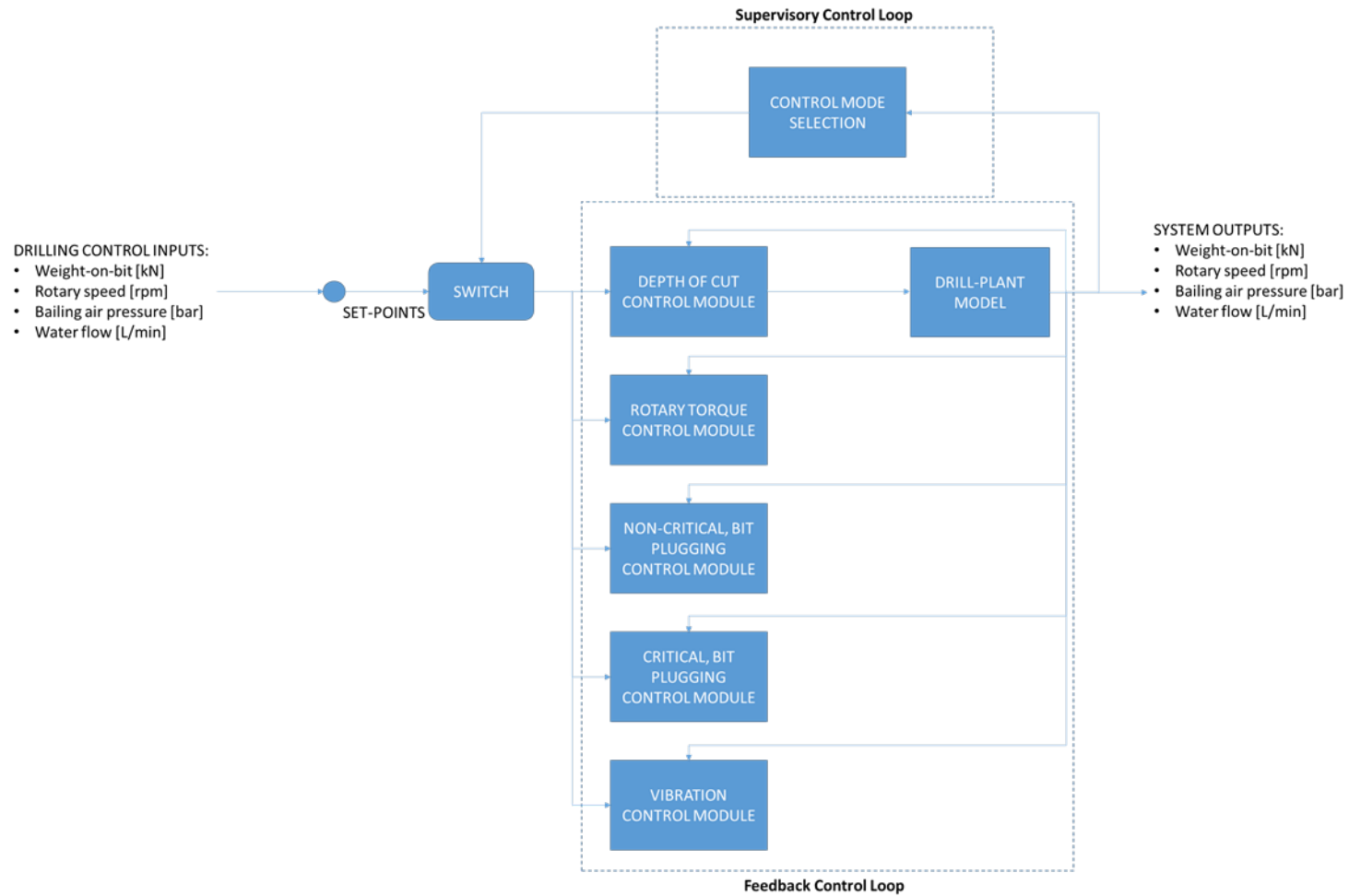


Figure 3-3: Various control modules within the advanced drill control solution

### **3.3 Various Drill Control Modes**

This section discusses the various control modes supported by the developed advanced drill control system. Each feature is defined, and its implementation is then detailed.

#### **3.3.1 Collaring & Adaptive Collar Feature**

Collaring is a necessary and important step in the drilling of a blasthole. The start of the blasthole must be drilled properly as this ensures that the hole will remain “true” and that angle deviations over the length of the blasthole with respect to the designed blast patterns are kept to a minimum.

While it is important to follow the blast design to ensure good blasting efficiency, more important concerns are component damage due to high stresses on the drill string from slanted holes and a worker safety hazard due to the bottom of hole location being outside of the planned area. High stresses on the drill string can result in string breakage which is an added cost for the mine site and results in lost productivity as the partially drilled hole will need to be abandoned and a new blasthole drilled. If the bottom of hole location is outside of the planned area there is a risk of potentially un-blasted explosive materials being drilled during the next mining bench step which can present a dangerous situation for the drill operator and anyone working in the bench location.

The start of the blasthole is particularly susceptible to hole deviation as the first several metres of ground are often made up of pre-fragmented and broken material due to the mine activity that previously occurred during the mining of the preceding bench. This area of broken ground can be soft and easy to drill through which can lead to hole

deviation if collaring occurs too quickly. Even slight deviations in the collar zone can lead to significant bottom of hole deviations so care must be taken during collaring.

Collaring can be accomplished using depth of cut control, however using a lower depth of cut ratio than is optimal for normal drilling is advised to ensure any loose and broken material is able to be properly ejected from the hole. For a given drill bit, assuming an optimal depth of cut of 1.0 for normal drilling, an approximate depth of cut of 0.4 would be a suitable, approximate choice for collaring. This approximation is based upon OEM operational literature, observed industry practice and the conducted field testing.

Collaring is typically necessary for the first 0.5 to 2.0 metres of the blasthole but in especially broken ground up to 4.0 metres of collaring may be required.

Most mine operations use a conservative pre-set collar depth that is chosen based upon average site conditions. This depth would then be used for every ground condition no matter how broken or intact the in situ material may be. It is suggested that instead of using a pre-set collar depth an adaptive collar solution be implemented so that all ground conditions are handled appropriately.

An adaptive collar solution can be built using the observed weight-on-bit as the collar zone is drilled. The drill string assembly has a constant weight of approximately 7,000 kg. If the drill string is in air and it is desired that the drill string be held still (penetration rate = 0 m/min) then the weight-on-bit will actually be a negative value equal to the string weight (-7,000 kg). If the drill string is in contact with a very strong, intact rock mass then to hold the drill string still the weight-on-bit will be closer to 0 kg. If in between,

---

broken ground scenario is considered then the following can be considered true

$(0 \text{ kg} \geq WOB \geq -7,000 \text{ kg})$ .

For collaring mode, the collar depth of cut set-point of  $0.4 \cdot \frac{R}{N}$ , will be kept constant during the entire collaring zone, where the depth of cut will be dictated by the drill bit specifications. In addition, a constant rotary speed  $N$  will be supplied by the adaptive collar module. Therefore, the penetration rate  $R$  will be determined by the two pre-set values of collar depth of cut and rotary speed but will be constant for the collar zone.

Since  $R_{collar}$  will be constant, the  $WOB_{collar}$  will vary with the ground conditions as described for the zero penetration rate example above. Based upon the knowledge that the in-situ material is an intact rock mass of some sort underneath a shallow layer of broken, pre-fragmented material a maximum weight-on-bit collar threshold can be selected. For the adaptive collar module, this threshold is selected so that:

*IF  $WOB_{actual} > WOB_{collar-max}$ , THEN drill mode: collar  $\rightarrow$  normal drilling*

The adaptive collar module can be seen in Figure 3-4. Note that the air flow and the water flow set-points are some value between 0 and 100 which regulates the air flow from the air compressor and the water flow from the water pump. Feedback control may or may not be used for these drilling variables.

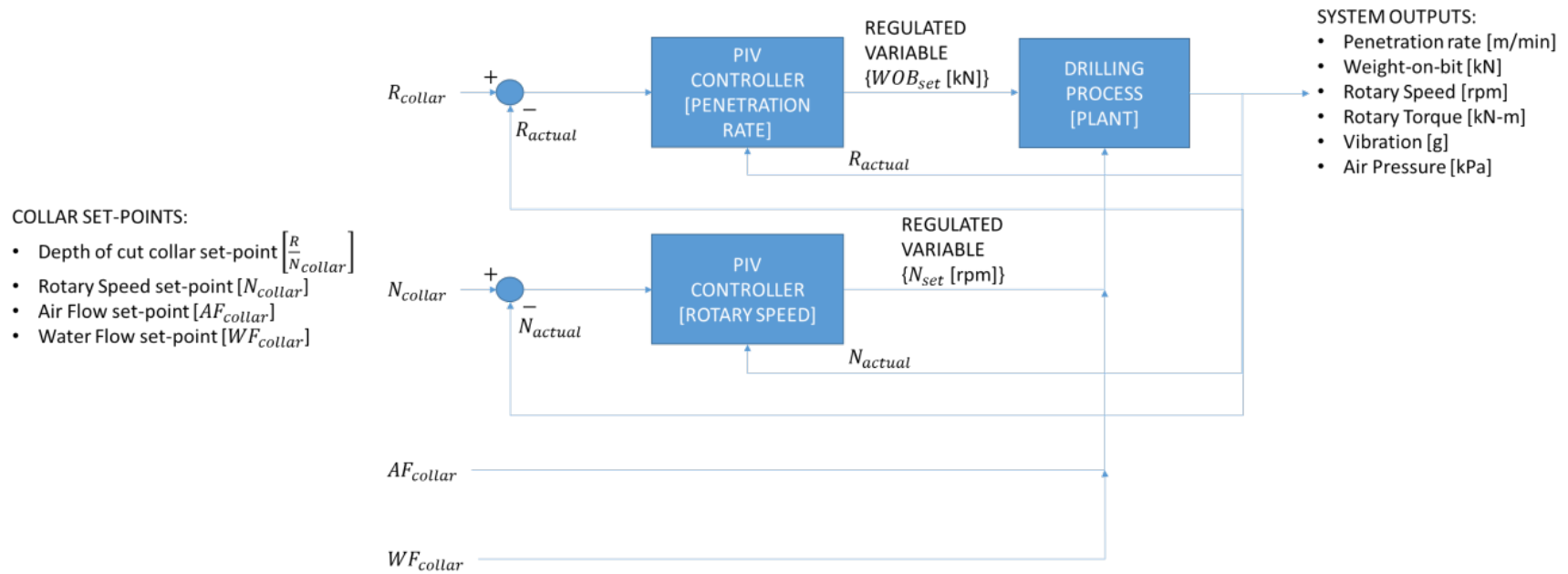


Figure 3-4: Adaptive Collar Module

### 3.3.2 Primary Control: Depth of Cut

The proposed primary control mode is based upon the depth of cut method which has been previously reviewed. The required inputs and how the controller will use them are given below.

- Bit IADC code [#-#-#]: International Association of Drilling Contractors drill bit code that provides three numbers which correspond to the Series (insert material and formation strength), the Type (formation strength) and the Bearing (bearing design and type). In addition, the IADC code denotes the insert (bit tooth) height. In combination with bit diameter, insert height determines the optimal depth of cut for the operating drill bit as well as any rotary speed and weight-on-bit limitations or any air and water flow requirements.
- Bit Diameter [m]: The same style (IADC code) of drill bit is available in various diameters. However, the diameter of the drill bit can affect its operating specifications. To be used in combination with bit IADC code to look up the optimal depth of cut for the operating drill bit as well as any rotary speed and weight-on-bit limitations or any air and water flow requirements.
- WOB operating range [kg]: The mine site may wish to limit or expand the weight-on-bit operating range allowed.
- N operating range [rpm]: The mine site may wish to limit or expand the rotary speed operating range allowed.

- 
- Bit Wear (optional) [%]: Not required for controller to work but if available could be used to refine the depth of cut set-point to better match the present drill bit wear state. Could be supplied as some combination of operator observations (IADC bit dull grading), total metres drilled, or output from a bit wear monitoring system.

The primary control mode will use the above inputs in combination with plant outputs via feedback to control the weight-on-bit and rotary speed request supplied to the plant.

PIV controllers will be used in parallel to control both weight-on-bit and rotary speed.

This design will allow for a robust drill controller that can accommodate a variety of in-situ conditions from very hard to very soft and from brittle to sticky. If hard material is encountered the weight-on-bit will saturate at the maximum value, potentially without attaining a high penetration rate. This would see rotary speed be limited due to the lower penetration rate value and the depth of cut set-point, thus accommodating very hard material. Alternately, if soft material is encountered the penetration rate will be very high with relatively low weight-on-bit required. This would see rotary speed saturate at the maximum value, which would force the weight-on-bit to be decreased to limit the penetration rate to ensure the system maintains the depth of cut set-point. In this fashion, very soft material would also be accommodated.

The depth of cut module (primary control mode) can be seen in Figure 3-5. Once again, the air flow and the water flow set-points are some value between 0 and 100 which regulates the air flow from the air compressor and the water flow from the water pump. Feedback control may or may not be used for these drilling variables.

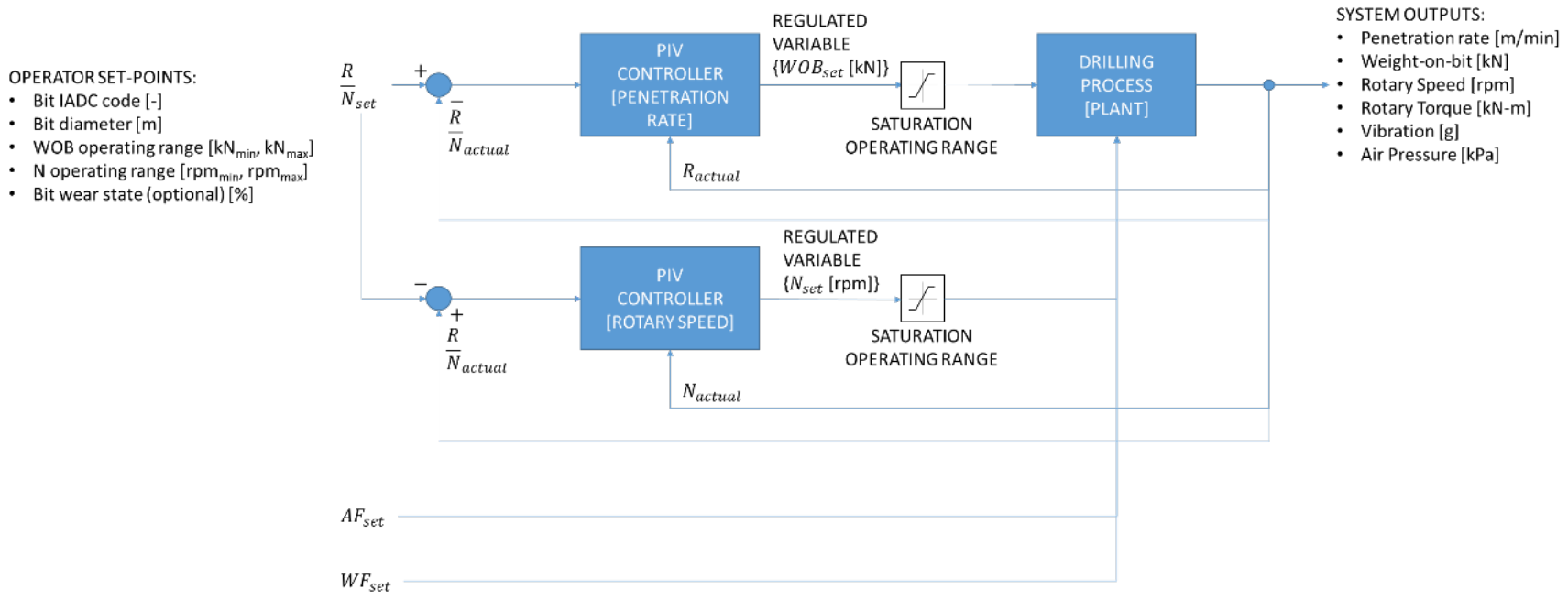


Figure 3-5: Depth of cut control module

### 3.3.3 Rotary Speed Feedback

Presently OEMs do not implement a feedback control loop for rotary speed. Instead they rely on a scaling table which is based upon voltages for the rotary drive motor taken at the factory. This introduces issues which were observed in the field where the rotary speed request does not quite equal the actual rotary speed attained by the motor. These issues can occur as the motor ages, gets damaged, or may be introduced due to small differences from one motor to the next. In manual operation these issues would not be observed as the rotary speed is set via a rheostat which has the operator turning a dial clockwise for a speed increase and counter clockwise for a speed decrease. When the operator sees the desired speed displayed on the instrument panel he or she will stop turning the dial. However, during drill control the OEM control system requests a rotary speed and based upon the scaling table expects the motor to attain it which is not always the case.

To improve rotary speed motor performance and accuracy a feedback control loop is added for both the primary control mode as well as the secondary and all alternate control modes. The rotary speed control loop is included in the primary control mode illustrated in Figure 3-5. Below a rotary speed feedback loop is illustrated independently from other control modes. Also included is a fully detailed proportional-integral-velocity controller<sup>5</sup> which is displayed as a closed system in the other control loop diagrams.

---

<sup>5</sup> A discrete-time PIV controller is shown with an Integrator element based on the Forward Euler method and a Derivative element based on the Backward Euler method. All PIV controllers used in this work match the controller illustrated in Figure 3-6.

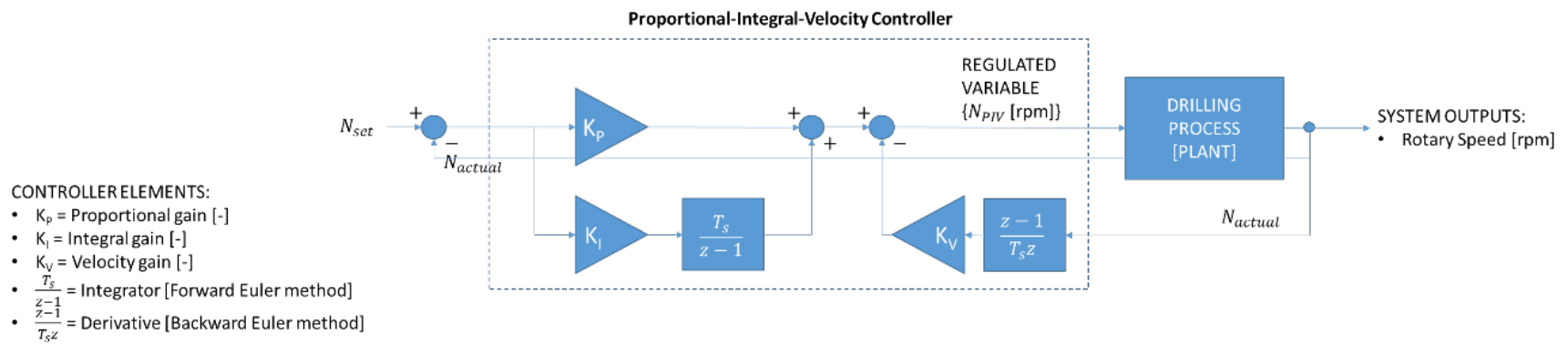


Figure 3-6: Rotary speed control loop

### 3.3.4 Secondary Control: Rotary Torque

The choice of control variable for rotary torque control requires an understanding of what rotary torque is and how it is caused in the drilling application. During the drilling process there is a downward force provided by the hoist motor and also a rotation torque caused by the downward force from the hoist motor interacting with the resulting forces from the bit-rock interface and the rotation movement driven by the rotary motor. As such the rotation torque has two components: hoist (weight-on-bit) and rotary (rotary speed). Either could be chosen as the control variable but the one which most impacts rotary torque is the best choice.

As was explored in previous work, a simple rotation speed step test was done using a blasthole drill operating in the field. The test was done in air, with the bit not in contact with the rock. As such the test is representative of the rotation speed component of the actual rotary torque incurred by the motor. Table 3-3 shows the rotation speed step inputs to the drill with the resulting rotation torque incurred. Figure 3-7 is a plot of these values with trend line and resulting rotary torque equation and  $R^2$  value by linear regression.

Rotation Speed (rpm)	Rotation Torque (kN-m)
10.44	1.2
15.39	1.3
19.22	1.4
25.74	1.6
31.95	1.7
36.81	1.8
40.95	1.9
45.27	2.1
49.55	2.2
56.66	2.5
64.75	2.7
69.66	2.9
78.03	3.2
84.11	3.4
90.36	3.6
92.7	3.7

**Table 3-3: Rotation speed in air step test inputs**

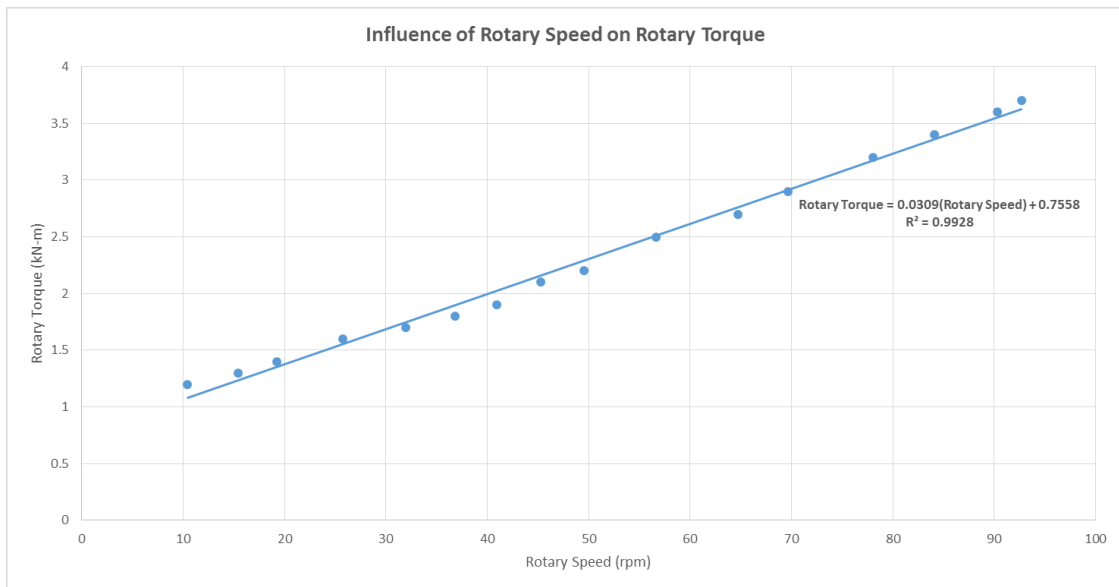


**Figure 3-7: Influence of rotary speed on rotary torque**

Examining Figure 3-7 it is apparent that there is a linear relationship between rotation speed and rotation torque over the test range of 10 – 93 rpm. The maximum speed tested (93 rpm) can be considered the maximum rotation speed that the drill will attain during normal operation. However, based upon the drill specifications and observed drill

---

operation the maximum rotary torque that may occur during drill operation is 25.7 kN-m.

Since the maximum rotation speed contribution to rotary torque is less than 4 kN-m, it can be concluded that the best option for the controllable variable for rotary torque control is weight-on-bit and not rotary speed.

The rotary torque control module can be seen in Figure 3-8.

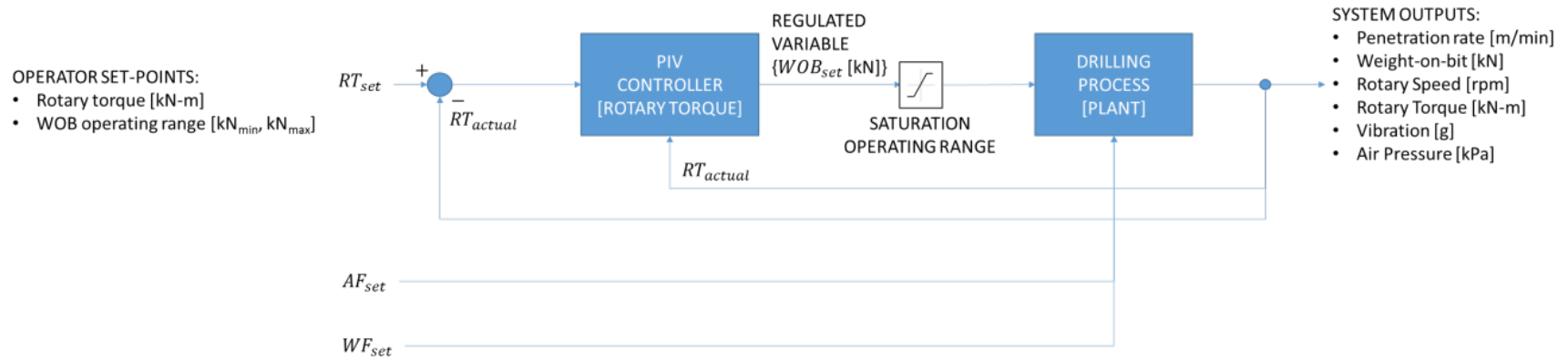


**Figure 3-8: Rotary torque control mode**

### **3.3.5 Alternate Control: Non-Critical, Predictive Bit Plugging**

Bit plugging is a common cause for manual drill operator intervention. A bit is considered plugged when its orifices are blocked and prevent the bailing air from escaping and clearing away the broken material from the bit rock interface. A bit can become plugged due to the build-up of mud on the drill bit's surface or due to the accumulation of broken materials at the bit rock interface. In addition, a bit could be considered blocked even in the event of an up-hole blockage that prevents the bailing air from leaving the bit-rock interface and escaping the hole.

Since bit blockages plug the orifices on the drill bit and prevent the bailing air from escaping from either the bit itself or from the bottom of the hole a good indication of a blocked bit is high air pressure. Based upon field observations and data analysis it was noted that air pressure would build up over time before reaching a critical level and if monitored a bit blockage could be prevented. For this reason, air pressure rate of change is the monitored variable for predictive bit plugging control. This type of control is implemented in non-critical bit plugging scenarios.

Under this control scenario, the monitored air pressure rate of change is used as an input to the controller and weight-on-bit is adjusted based upon feedback from the plant. Once triggered this control mode will run until the air pressure rate of change has decreased below the rate of change set-point and continue to run for some pre-set time delay off period. In addition, water flow is decreased during this control mode to discourage bit plugging. This is shown in Figure 3-9.

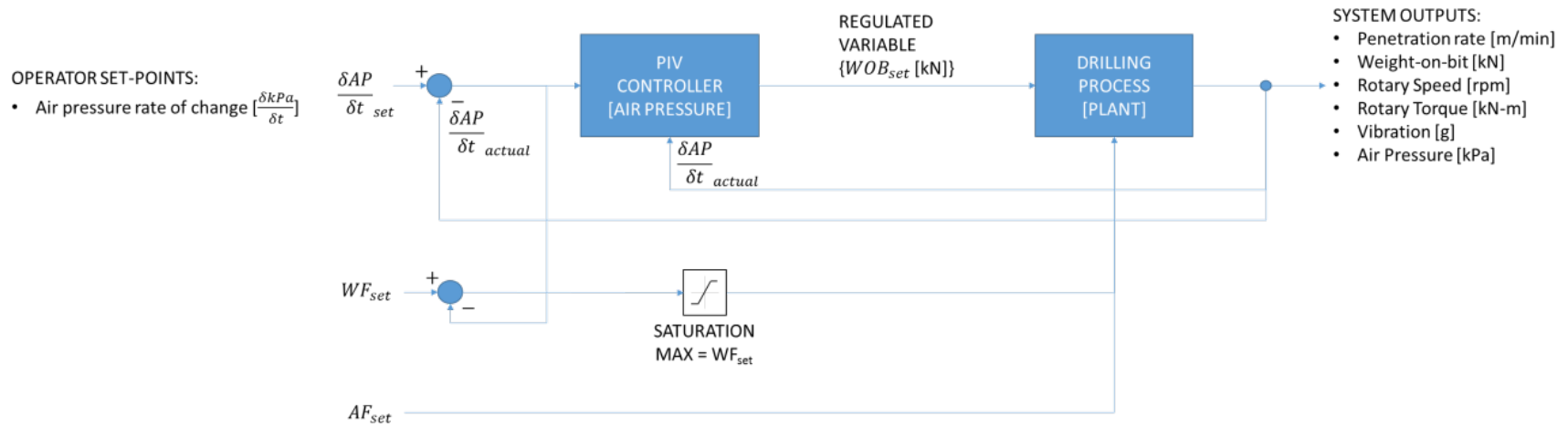


**Figure 3-9: Non-critical, predictive bit plugging control mode**

### 3.3.6 Alternate Control: Critical, Bit Plugging

Even with the implementation of the predictive bit plugging control mode described in the previous subsection, there may still be scenarios that lead to critical bit plugging.

These must be addressed via a dedicated control mode.

An air pressure set-point is chosen that is representative of the onset of a critical, bit plugging scenario. When this threshold is reached the alternate control mode is selected which attempts to decrease the system air pressure via weight-on-bit manipulation (decreases). The control mode will continue to lower weight-on-bit until, either, the air pressure is successfully decreased for some pre-set duration of time or the weight-on-bit reaches 0 kN. If the weight-on-bit reaches 0 kN, then both the water flow and air flow set-points will be set to 0 %. Setting the water flow to 0 % stops additional water from being added to the bit-rock interface which alone could lower the air pressure sufficiently. Setting the air flow to 0 % allows any up-hole blockage the opportunity to fall back to the bottom of the hole. It should be noted that with no air flow supplied to the bit-rock interface broken chips can no longer be flushed out of the hole, however in this control scenario the weight-on-bit would already be at 0 kN so no bit advancement will be occurring at this time regardless of air flow.

Both the air flow and water flow set-points will be held at 0 % for some pre-set period of time, at the conclusion of which normal drilling will resume or manual intervention will be required.

The described control mode is shown in Figure 3-10.

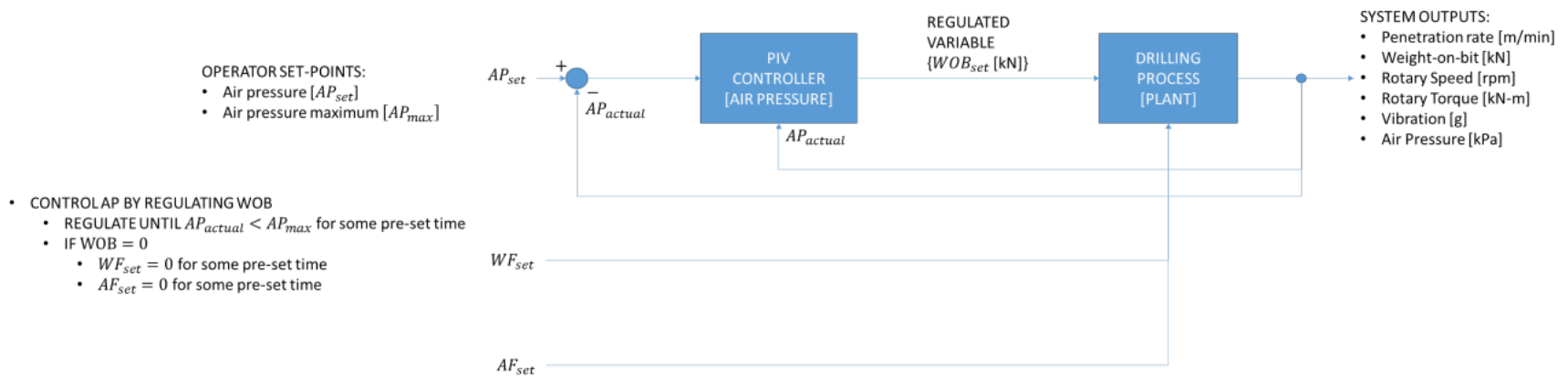


**Figure 3-10: Critical, bit plugging control mode**

### **3.3.7 Alternate Control: Vibration**

Drilling vibration is another common cause for manual drill operator intervention. During drill operation normal vibration activity is expected however excessive vibration can lead to drill machine damage and has the potential to cause operator injury. A vibration threshold should be chosen which is high enough that the vibration control module should intervene in the drilling process but not high enough that a machine shutdown must occur.

When the vibration threshold is reached the alternate control strategy of feedback vibration control is utilized. This control mode attempts to control vibration by regulating rotary speed so that some acceptable vibration level is reached. Once the plant vibration signal has been below the vibration threshold for a pre-set depth increase or time increment normal drill operation will resume.

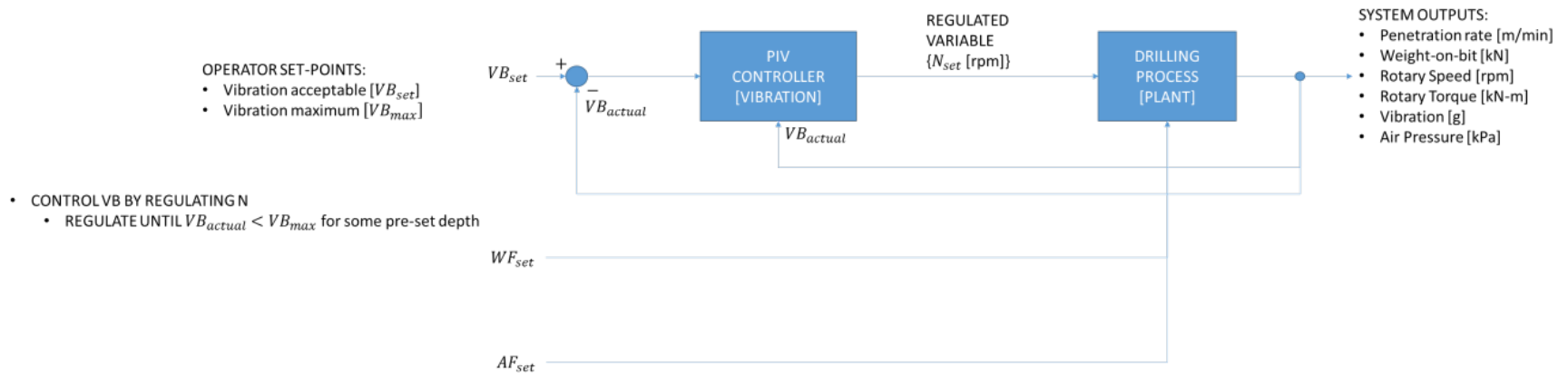


**Figure 3-11: Vibration control mode**

### 3.3.7.1 Dynamic, dual-axis vibration control

During field testing on a Caterpillar MD6640 at a mine site that was particularly prone to vibrational events it was observed that the regular vibration control module was not reactive enough to vibrational events and a more aggressive vibration control approach was desired. A dynamic, dual-axis vibration control module was developed for this purpose. The underlying logic is provided in Figure 3-12<sup>6</sup>.

The revised vibration control module considers both the dominant axis of drilling vibration (vertical) as well as the secondary axis of drilling vibration (horizontal). This vibration control module acts as a gain on the rotary speed set-point.

Where,

$V_{VB}$  is plant vertical vibration in physical units;

$H_{VB}$  is plant horizontal vibration in physical units;

$V_{VBSET}$  is the vertical vibration setpoint in physical units;

$H_{VBSET}$  is the horizontal vibration setpoint in physical units;

$K_{VB}$  is the output gain applied to the rotary speed set-point (unitless);

$r$  is some configurable parameter for calculating the output gain (unitless);

$k$  is some configurable parameter for calculating the output gain (unitless);

$t$  is time in seconds; and,

---

<sup>6</sup> While the experimented control philosophy is a sequential/logical application of heuristic rules, the output is applied as a gain to feedback control for simpler integration with the underlying architecture of the development advanced drill control solution.

$t_{OFFDELAY}$  is an off delay time in seconds.

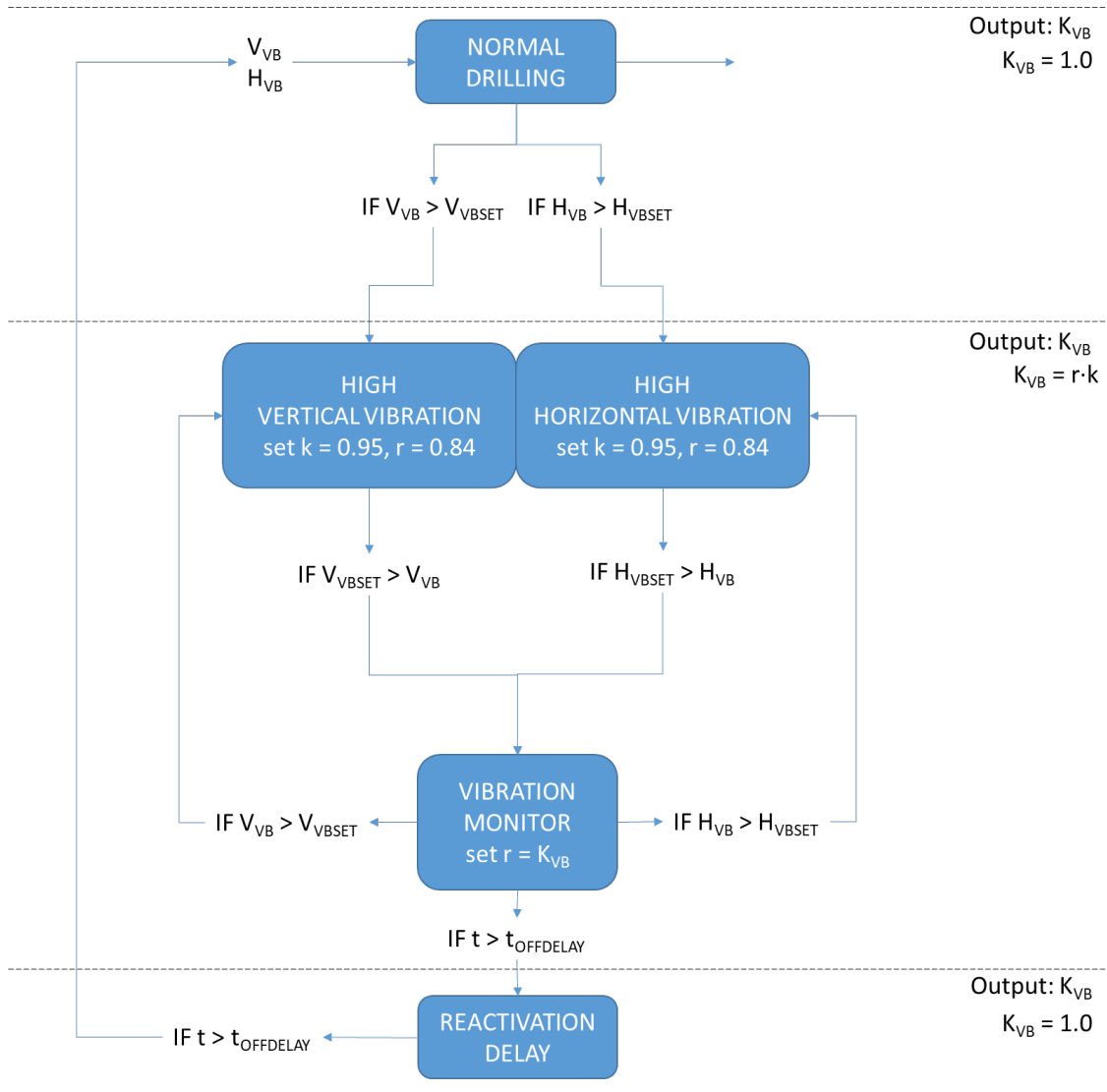


**Figure 3-12: Logic diagram of dynamic, dual-axis vibration control scheme**

Field testing on the Caterpillar MD6640 drill rig showed promising results for this vibration control philosophy in high vibration prone drilling conditions.

---

### 3.3.8 Alternate Control: Retract

When the end of hole depth is reached the drill bit must be retracted back to its start point, above the drill deck at the base of the mast. This is the desired bit stop location between holes as it is a suitable place for the bit during drill propel movement from the completed hole to the next design hole.

A common critique of industry standard drill control solutions by drill operators is that they are often limited to a maximum speed during retraction that is much slower than the retraction speed drill operators use in manual operation. Field observations showed that retractions speeds were indeed limited to approximately 1/5 of the speed typically used when in manual retraction. The OEMs choose to limit drill retraction speed because they do not have recovery logic in place in the event of a bit jam during retraction. So, to decrease the likelihood of a jam they greatly limit the retract speed. While this is an effective measure it does add unnecessary time to the drill cycle. Drill operators have the option of using the higher retraction speed because they can manually recover the bit if a jam occurs.

To address this scenario an additional control mode specifically designed for end of hole drill bit retraction was designed. Figure 3-13 shows the five steps from end of hole to drill bit returned to above drill deck as well as the corresponding blasthole zones with accompanying operational set-points.

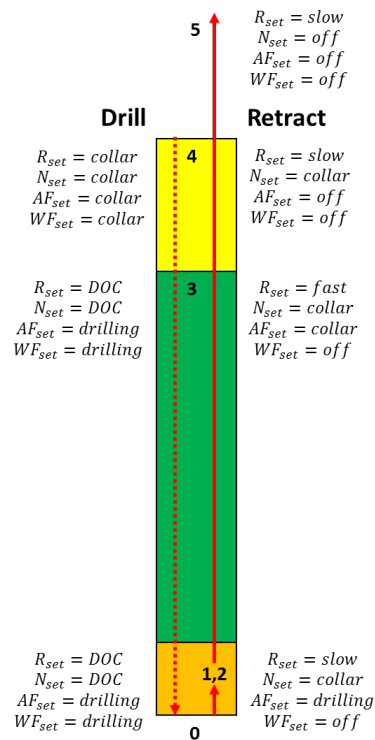


**Figure 3-13: End of hole retraction zones and corresponding logic**

With respect to Figure 3-13 the displayed numbers correspond to the following:

0. End of hole (final) depth [dictated by drill plan, approximately 15 metres];
1. Hole near bottom zone [dependant on ground conditions, typically 2 metres from final hole depth; 13-15 metres];
2. Exit from hole near bottom zone / entry to fast feed zone [dependant on ground conditions, typically greater than 2 metres from final hole depth; <13 metres];
3. Exit from fast feed zone / entry to collar zone [dependant on ground conditions and dictated by adaptive collar point, typically 2 metres from ground level; 0-2 metres];
4. Exit from collar zone / hole top [ground level; 0 metres];

5. Final return position above drill deck [dependant on drill rig model, typically 1 metre above drill deck].

With respect to Figure 3-13 the displayed setpoints are defined as follows:

$R_{\text{set}}=\text{collar}$ , is penetration rate as defined by the adaptive collar mode;

$N_{\text{set}}=\text{collar}$ , is the rotary speed as defined by the adaptive collar module;

$AF_{\text{set}}=\text{collar}$ , is the air flow during collar (on or reduced);

$WF_{\text{set}}=\text{collar}$ , is the water flow during collar (on or reduced);

$R_{\text{set}}=\text{DOC}$ , is the penetration rate as defined by the depth of cut control module;

$N_{\text{set}}=\text{DOC}$ , is the rotary speed as defined by the depth of cut control module;

$AF_{\text{set}}=\text{drilling}$ , is the air flow during drilling (on);

$WF_{\text{set}}=\text{drilling}$ , is the water flow during drilling (on);

$R_{\text{set}}=\text{slow}$ , denotes a limited retraction speed ( $R < 5$  metres per minute);

$WF_{\text{set}}=\text{off}$ , denotes water flow is turned off;

$R_{\text{set}}=\text{fast}$ , denotes a high retraction speed ( $5 < R < 25$  metres per minute);

$AF_{\text{set}}=\text{off}$ , denotes air flow is turned off;

$N_{\text{set}}=\text{off}$ , denotes rotary speed is off.

During retraction bit jamming is the primary concern and can be avoided by monitoring rotary torque. If high torque is sensed the penetration rate will be controlled directly until torque decreases back to acceptable levels. The detection of a high torque event during the retraction process and above the hole near bottom zone will result in the hole being reamed before the drill bit is returned to position 5. The rotary torque control during retraction module is shown below.

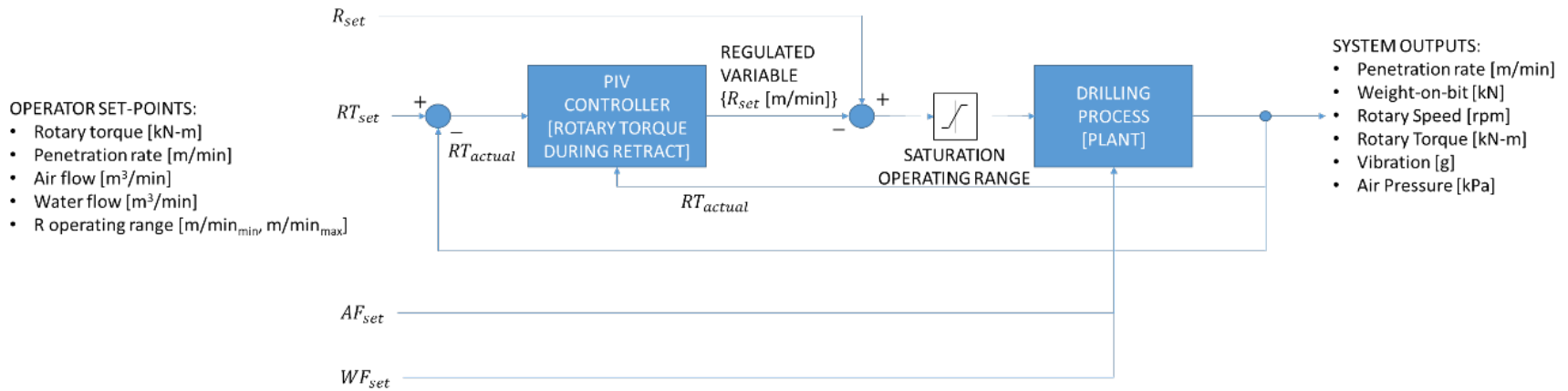


Figure 3-14: Retraction jamming control mode

### 3.3.9 Alternate Control: Operational Limits

Despite the implementation of all of the aforementioned control modes and corresponding logic there may still be operational scenarios where the advanced drill controller will fail to adequately control the drilling process. An overriding safety layer will be supplied to address these rare but possible conditions. This safety layer will be supplied in the form of operational limits that dictate an immediate suspension of drilling activity and necessitate manual (human) operator intervention. This should ensure machine protection and also limit the risk of injury to an operator if onboard the drill.

The operational limits apply for the following parameters:

- Penetration Rate (m/min)
- Rotary Torque (kN-m)
- Vibration (g)
- Air Pressure (kPa)

In addition, minimum operational thresholds are applied for the following:

- Weight-On-Bit (kN)
- Rotary Speed (rpm)

If any of the operational limits are met or exceeded the drill controller will change all operational set-points (weight-on-bit, rotary speed, air flow water flow) to zero. In addition, if any of the minimum operational thresholds are not met (except in the case of weight-on-bit during retract) the drill controller will change all operational set-points to zero.

The operational limits act to protect the machine and operator from potential damage and injury. The minimum operational thresholds act to catch any unusual drill operation that likely requires operator intervention.

An optional recovery scenario can be implemented that begins with the bit being retracted a short distance from the bit-rock interface and normal drill operation resuming.

The recovery scenario is limited to several restart attempts before manual operator intervention is required.

## **Chapter 4**

### **Drill Control Field Testing**

#### **4.1 Drill Rig Instrumentation and Interfacing**

Field testing occurred on two different drill rig models: a Caterpillar MD6640 and an Atlas Copco Pit Viper 351. While mechanically similar, each rig had a unique control system. The Caterpillar MD6640 utilized an Allen-Bradley PLC based control system (Figure 4-1). The Atlas Copco PV351 utilized a CANbus based control system as part of their proprietary Rig Control System (RCS) feature (Figure 4-2).

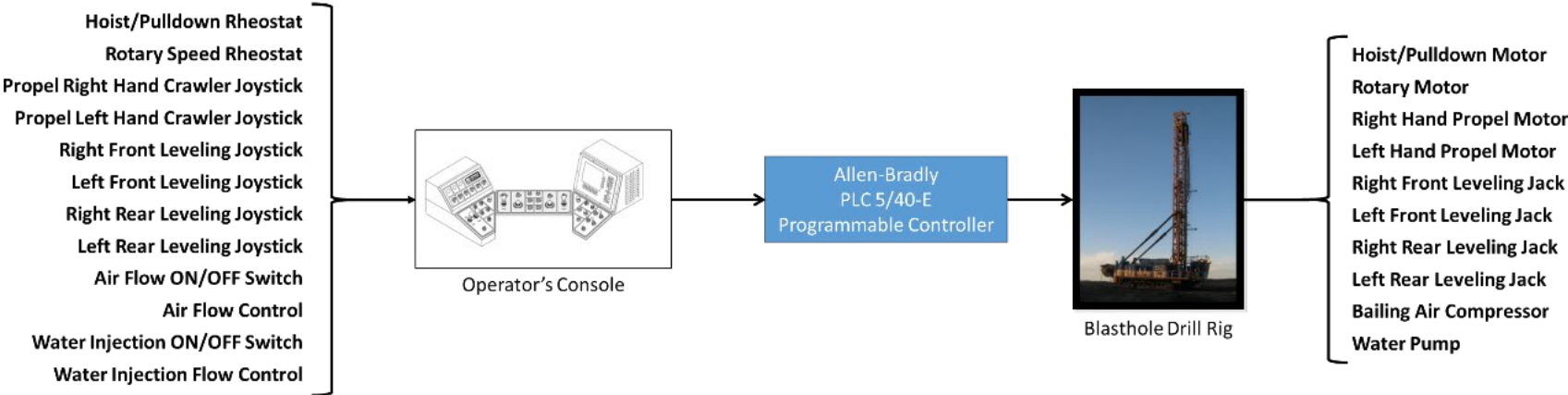
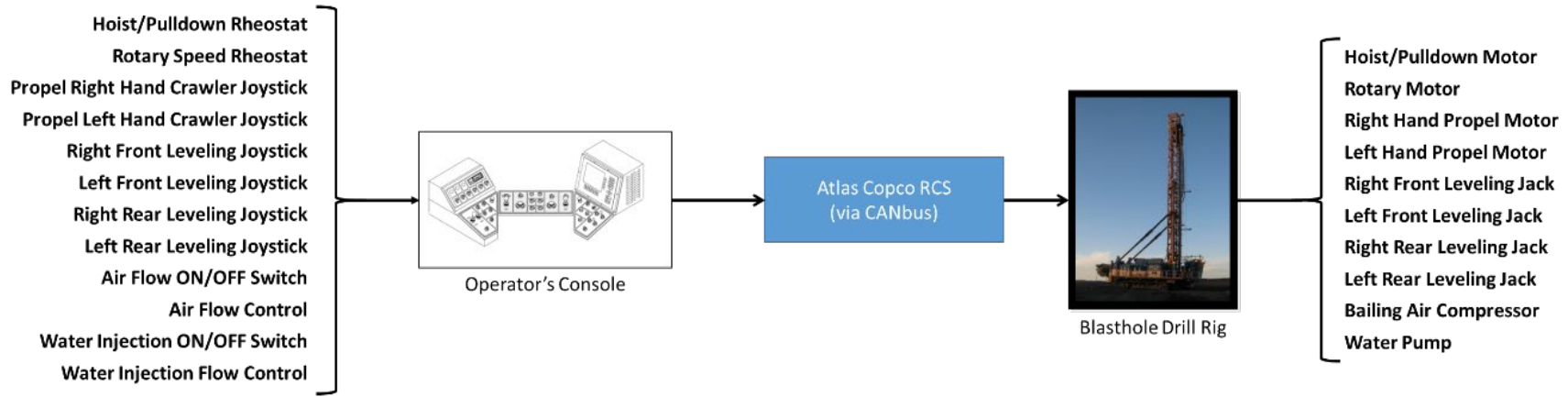


Figure 4-1: Caterpillar MD6640 control system



**Figure 4-2: Atlas Copco PV351 control system**

---

Data collection on the Caterpillar MD6640 was conducted using an industrial data logger called the DATAQ 718-Bx. The DATAQ was interfaced to the drill rig's Allen-Bradley PLC rack. The configuration used for the DATAQ is shown below.

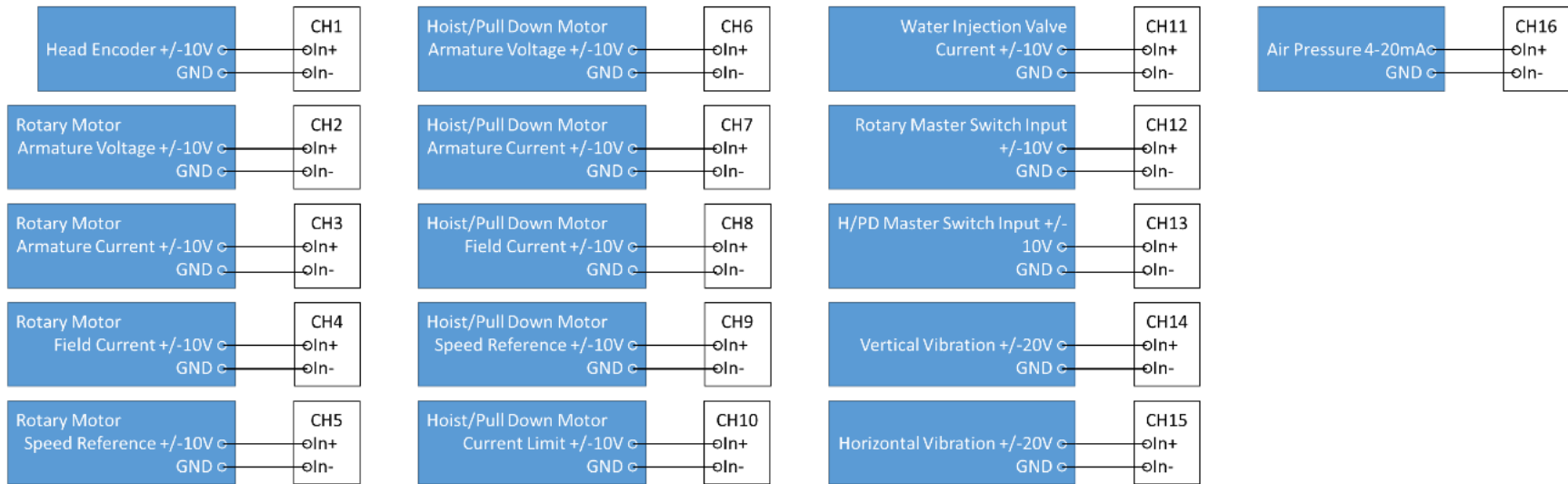
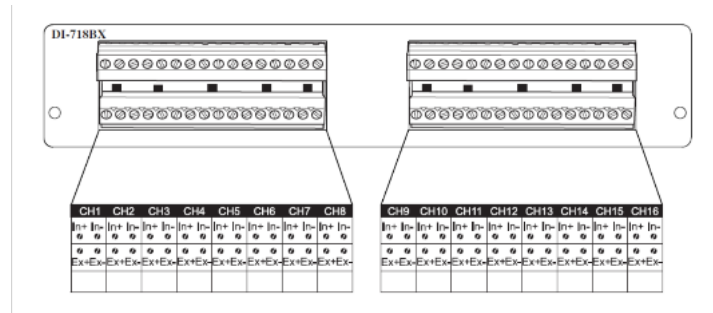


Figure 4-3: DATAQ 718-Bx input channels with signal detail

Control of the CAT MD6640 drill rig for field testing was accomplished through the interfacing shown in Figure 4-4. A mechanical switch was implemented to facilitate autonomous operation. The switch toggled operation between the operator's console (for manual operation) and the drill controller (for autonomous operation). The physical switch consisted of a bank of industrial relays which was designed and implemented by an Original Technology Manufacturer that partnered in the research. The signals of interest as well as the controllable range are provided.

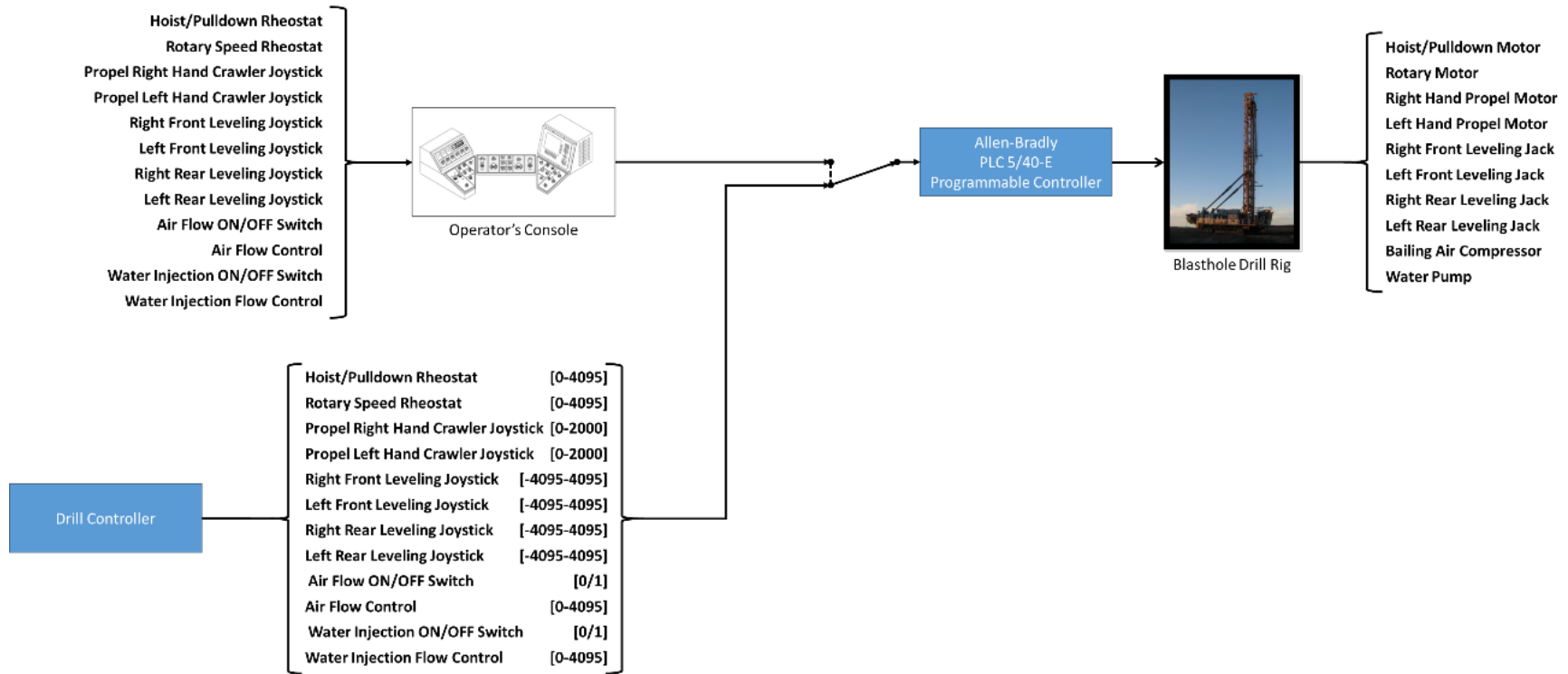


Figure 4-4: CAT MD6640 drill rig interfacing for autonomous drill control testing

Data collection and control of the Atlas Copco PV351 drill rig was accomplished via RCS with the assistance of the drill OEM. For data collection the standard RCS high frequency logging to USB feature was utilized. For rig control during field testing, the advanced drill control algorithm was created in Simulink and then coded to C++ by the author. The advanced drill control algorithm (in C++) was then incorporated as a module in RCS by the OEM. Field testing on the Atlas Copco PV351 drill rig only consisted of in-hole drilling control. Field testing on the CAT MD6640 drill rig also included propel and level control testing.

#### **4.2 Experimental Testing**

The experimental testing of the developed advanced drill control system reviewed in this section was conducted using two working rotary blasthole drills at two operating surface mine sites. The testing was performed over two individual field periods in 2014 and 2015. Each field period occurred at a different surface mine; a copper mine in North America as well as an iron ore mine. In total two weeks of in-field, on-machine, operational testing was completed. At the conclusion of the in-field test period at the iron ore mine the advanced drill controller was left operational for long term operational use.

The rotary blasthole drills used for the testing were both produced by Atlas Copco, which is one of the three leading OEMs for global surface mining production drills. Although the test drill rigs were both produced by the same OEM they were not the same drill model. The test drill rig at the copper mine was the largest model produced by that OEM (Pit Viper 351) while the iron ore machine was a mid-sized model (Pit Viper 271).

The size of the drill can be represented by the diameter of drill bit that can be utilized during production drilling. Available drill bit diameters range from 1 inch to 16 inches and are split between the two types of blasthole drills; percussive and rotary. Rotary drills do not operate with bit diameters of less than 4 inches and percussive drills do not operate with bit diameters greater than 8 inches. The copper machine (Pit Viper 351) could accommodate a drill bit range of 11 – 16 inches. The iron ore machine (Pit Viper 271) could accommodate a drill bit range of 7 – 10.5 inches. A list of the technical specifications related to the drill control application is given below for each machine.

<b>Copper Machine</b>	
Drilling Method	Rotary - Single pass
Hole Diameter	270 mm - 406 mm
Maximum Pulldown Force	534 kN
Maximum Weight On Bit	56,700 kg
Maximum Rotary Speed	100 rpm
Maximum Pullback Force	267 kN
Single pass depth	19.8 m
Maximum hole depth	41.1 m
Maximum Feed Speed	0.6 - 0.8 m/s
Maximum Rotary Torque	25.7 kN-m
Estimated machine weight	175 - 188 tonnes

**Table 4-1: Technical specifications of interest for the Copper Machine**

Iron Ore Machine	
Drilling Method	Rotary or DTH - Single pass
Hole Diameter	171 mm - 270 mm
Maximum Pulldown Force	311 kN
Maximum Weight On Bit	34,000 kg
Maximum Rotary Speed	150 rpm
Maximum Pullback Force	156 kN
Single pass depth	16.8 m or 19.8 m
Maximum hole depth	32 m
Maximum Feed Speed	0.6 m/s
Maximum Rotary Torque	11.8 kN-m
Estimated machine weight	84 tonnes

**Table 4-2: Technical specifications of interest for the Iron Ore Machine**

Although both drills were capable of multi-pass drilling the two surface mines only operated using single pass. Upon examination of Table 4-1 and Table 4-2, it can be seen that the copper machine is capable of operating at much higher Pulldown Forces, Rotary Torques and slightly higher Feed Speeds. While it can also be seen that the iron ore machine is cable of operating at higher Rotary Speeds. However, the operating set-points for the drill rigs are dictated by the type (diameter and configuration) of drill bit used. Both sites used similar drill bits (copper, IADC 6 and IADC 7) (iron ore, IADC 6) and therefore had similar operating set-points for their rigs.

#### 4.2.1 Collaring & Adaptive Collar Feature

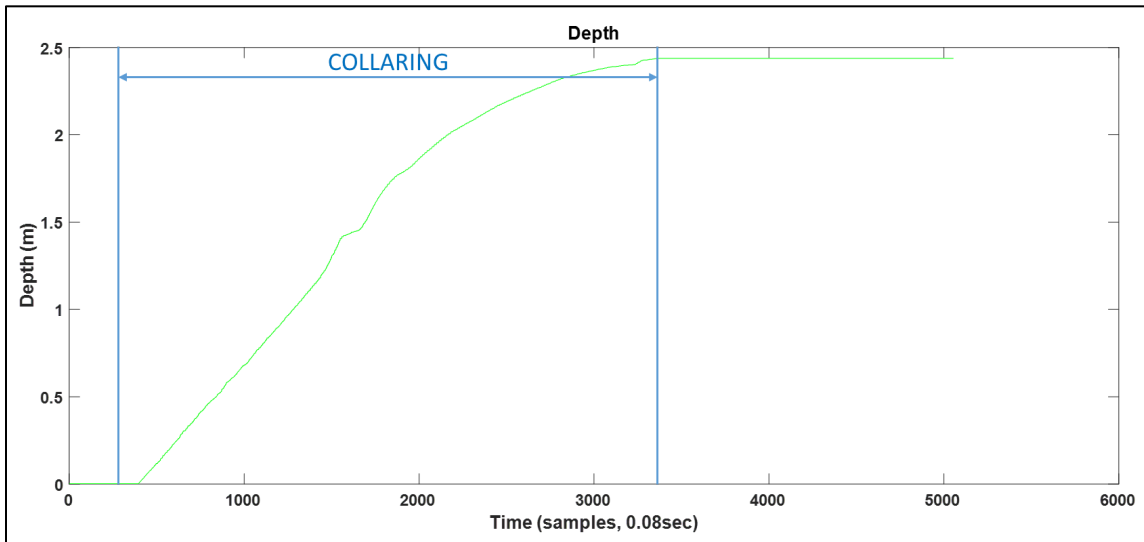
The present industry standard practice for collaring is to drill with reduced weight on bit and rotary speed set-points for some pre-defined depth – typically 1 to 4 metres depending on ground conditions. If collaring is ended prematurely poor hole quality can follow and an aborted or lost production hole may occur which would require a new blasthole be drilled. If collaring is ended too late some production is potentially lost.

---

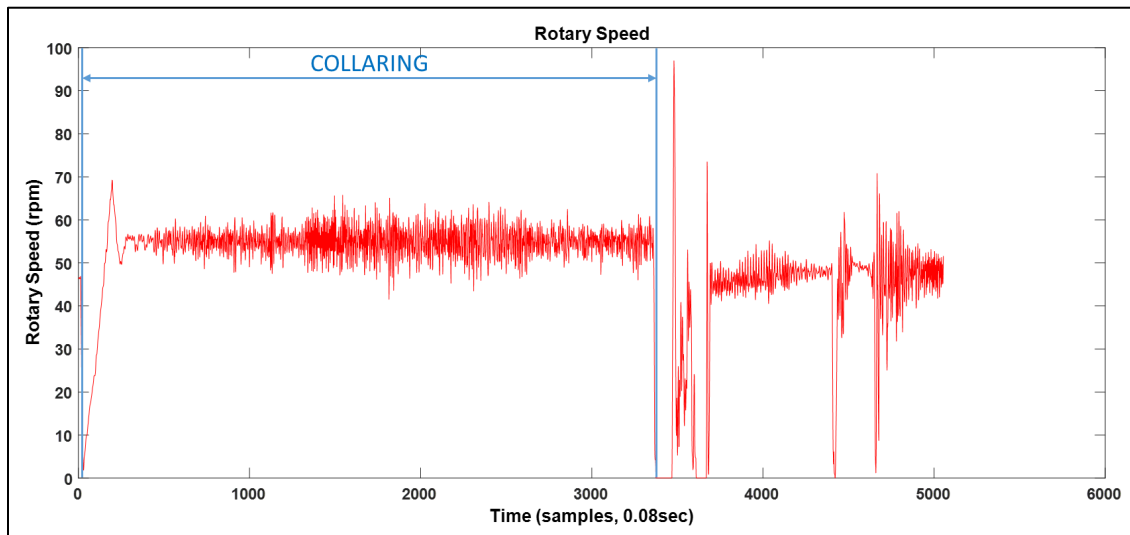
Since some lost production is more palatable than completely re-drilling production holes the standard industry practice is to collar to a depth beyond what is necessary based upon ground conditions. Some operators will always collar to the same depth regardless of the instruction from mine planning or the ground conditions encountered.

For the reasons stated, an adaptive collar feature would be a useful tool for mine operators. An adaptive collar feature could contribute to reducing lost production holes due to poor hole quality and improve production through the reduction of overly restrictive drilling inputs in non-collar ground conditions.

A typical collar scenario will be examined based upon data recorded during testing on the copper machine. The following three plots show hole depth, rotary speed and feed force through the first several metres of a drilled production hole. The drill starts from rest at zero depth and progresses through the collar zone into normal drilling (normal drilling set-points begin at approximately 2.4 metres). Figure 4-5 shows the hole depth for the collar scenario examined, Figure 4-6 shows the rotary speed, and Figure 4-7 shows the weight on bit. The change from collar set-points to normal drilling set-points is readily identifiable based upon the rotary speed which is regulated at 55 rpm during collar regardless of penetration rate. From Figure 4-6, collaring ends at time sample 3359; or 2.438m in Figure 4-5.



**Figure 4-5: Hole Depth – collar scenario**



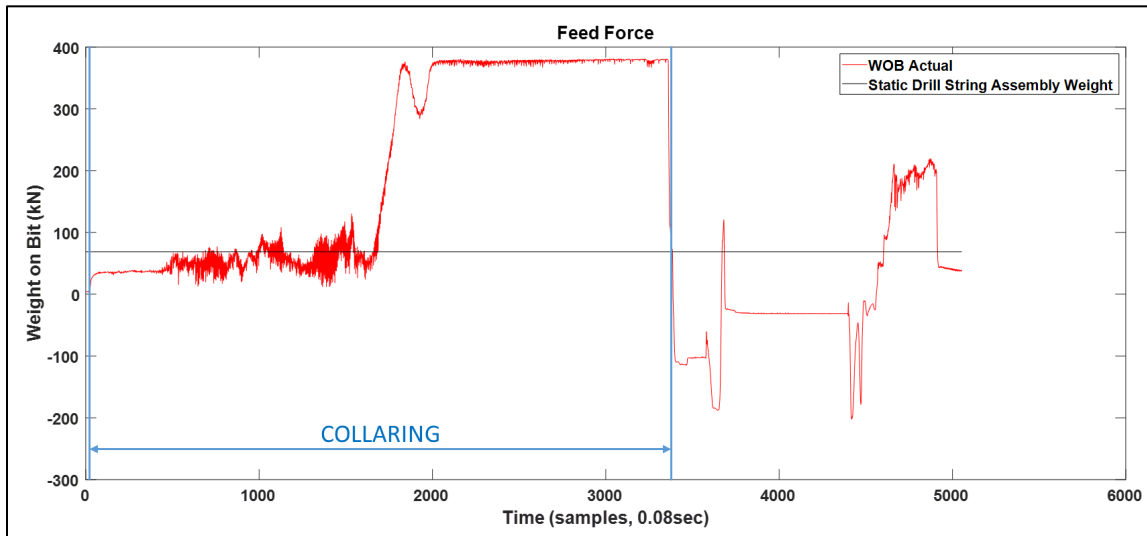
**Figure 4-6: Rotary Speed – collar scenario**

Figure 4-7 shows the weight on bit (in red) and also the static drill string assembly weight (in black). For the copper machine the static drill assembly weight was 7,112kg or 68.7kN. When examining the weight on bit plot, any weight on bit above the static drill assembly weight is provided by the drill’s feed motor while anything below is facilitated by a negative weight on bit (or pullback) from the feed motor. Pullback situations are

representative of extremely broken ground where the controller is attempting to prevent a penetration rate that is too high.

Collaring is required in broken ground and, when examining Figure 4-7, is required from hole start to approximately time sample 1682 (or 1.484m). Beyond this point the weight on bit quickly increases to 370kN which is representative of intact, strong in-situ material where collaring is no longer required or appropriate. However, since an adaptive collar feature was not utilized the collaring continued for another one metre until the pre-set collar end depth was reached. This resulted in reduced productivity from the drill rig during this continued but unnecessary collar period. This translates into lost production for the mine operator.

Although for a single hole this only accounted for one metre, the entire hole depth is typically approximately 15m. This equates to 1/15 (or 6.7%) of the blasthole being drilled at an artificially low rate. When considered over many production holes and across a fleet of several drills at a surface mine this single metre of reduced production quickly inflates to a not insignificant amount. This illustrates the utility of the proposed adaptive collar control module.



**Figure 4-7: Weight on Bit – collar scenario**

#### **4.2.2 Primary Control: Depth of Cut**

The developed advanced drill control system was built with depth of cut as the primary control philosophy. This was first tested using the copper machine. As was previously mentioned depth of cut involves controlling both feed speed and rotary speed in an attempt to maintain a predetermined optimal ratio based upon the drill bit's design with which the most efficient drilling will occur. In this subsection, a production hole drilled by the copper machine under the control of the advanced drill control system and using the depth of cut control philosophy will be examined.

The drilled production hole is shown by depth in Figure 4-8. The collaring, drilling, and end of hole zones are displayed for reference.

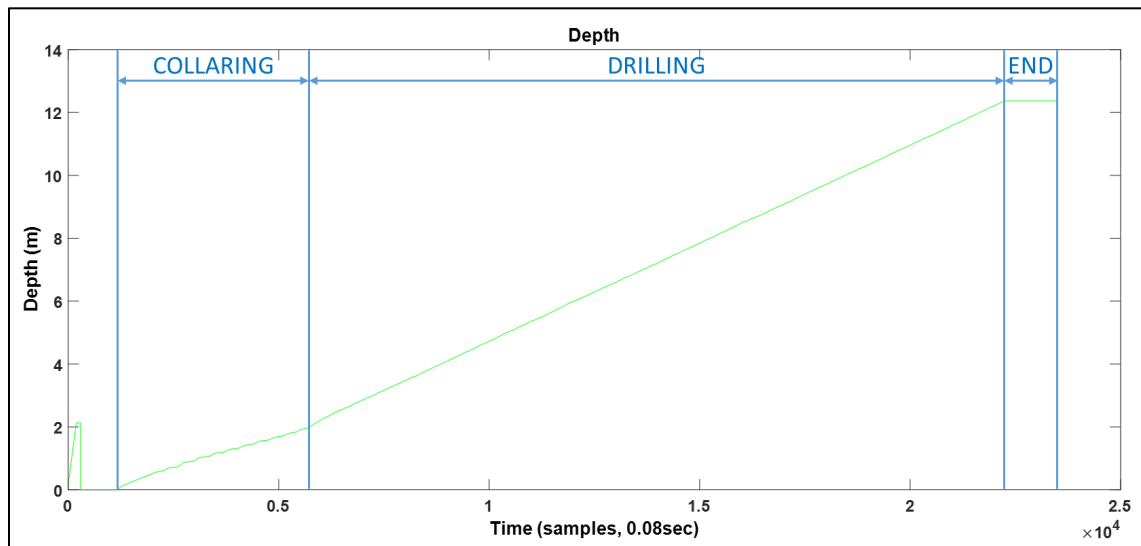


**Figure 4-8: DOC example hole – depth**

Due to a pre-set fixed collar depth, collaring occurs from zero metres to a depth of two metres. Normal drilling occurs from two metres to the final hole depth of 12.37 metres. Examining the normal drilling zone, and more precisely the slope of the depth line, it can be seen that penetration rate for the example production hole was quite consistent indicating uniform ground conditions and/or the execution of effective depth of cut based control. In the collar section the penetration rate is more variable which is consistent with broken ground conditions.

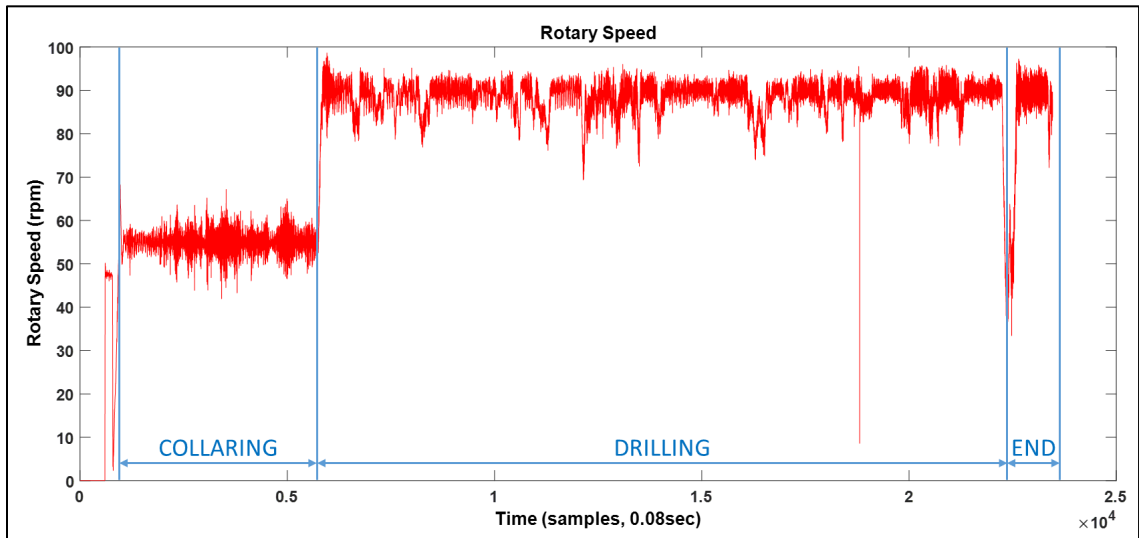


**Figure 4-9: DOC example hole – rotary speed**

Figure 4-9 shows the rotary speed over the drilled production hole; once again the hole zones are denoted. In the collaring zone the rotary speed is kept at the collar rotary speed set-point of 55 rpm which was chosen for the field testing based upon the OEM drill rig specifications and common site practices. Although, the rotary speed signal is quite noisy which is indicative of fractured ground that is typical of ground in the hole collar zone. In the drilling zone the rotary speed stays near 90 rpm (the maximum speed the controller was set to allow) which is indicative of a high penetration rate. Although there are times in the drilling that the rotation speed drops from 90 rpm (at one point it falls to near 70 rpm) which is indicative of a lower penetration rate at those sections of the production hole.

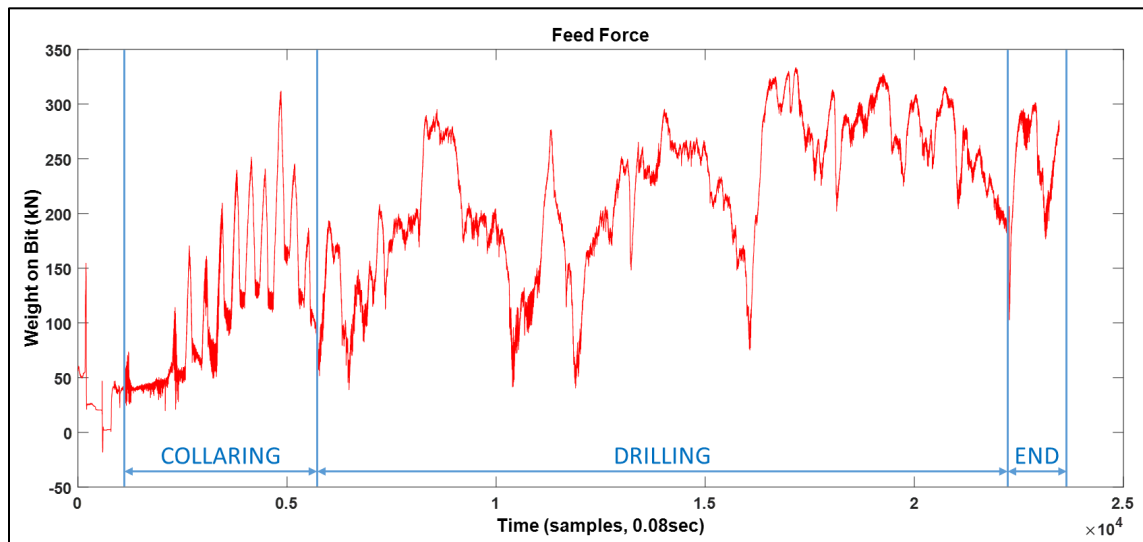


**Figure 4-10: DOC example hole – weight on bit**

While both weight on bit and rotary speed are manipulated to regulate depth of cut, the primary controlled variable is weight on bit. Figure 4-10 shows this. The weight on bit fluctuates greatly in the collaring zone. This is due somewhat to the presence of broken ground in the collar zone but more so is because rotary speed is kept constant which causes weight on bit to be the only way for the controller to attempt to reach the pre-set depth of cut.

In the normal drilling zone, the weight on bit also fluctuates but it is of a more gradual nature. The depth of cut control philosophy tends toward high rotary speeds if the depth of cut set-point is attainable given the ground conditions. So, the changes in weight on bit values over the production hole are representative of ground quality [or how difficult (slow) it is for the drill bit to pass through various sections of the hole]. The higher the weight on bit, the more difficult the drilling; the lower the weight on bit, the easier the drilling.

Comparing the weight on bit fluctuations displayed in Figure 4-10 to the consistent rate of change of the depth (penetration rate) displayed in Figure 4-8 illustrates how variable the in-situ ground conditions were. This confirms the effectiveness of the advanced drill control system at delivering the depth of cut control method.

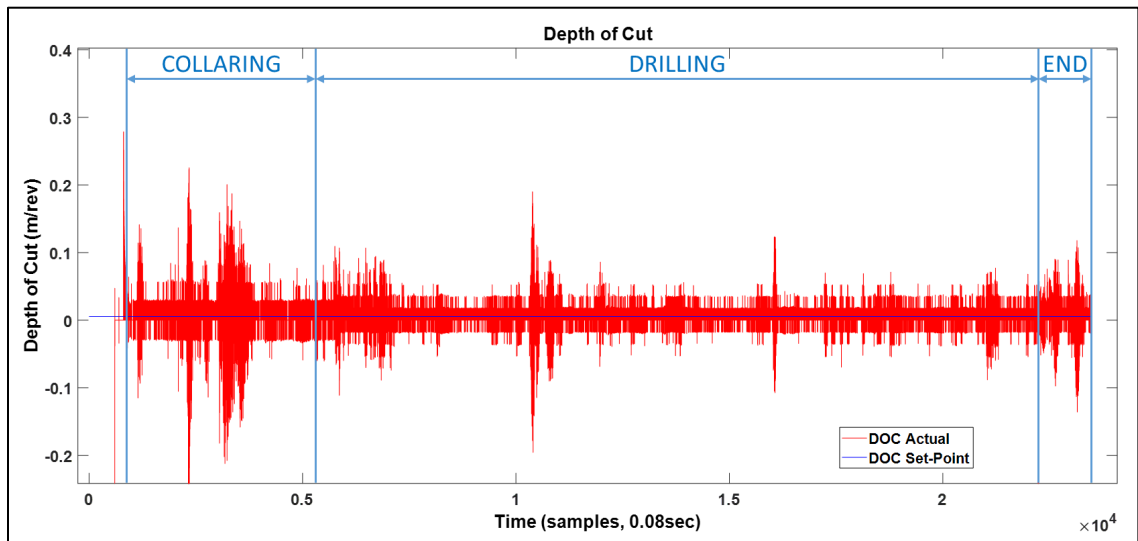


**Figure 4-11: DOC example hole – depth of cut**

While under the control of the advanced drill control system, the depth of cut that the copper machine achieves is compared to the depth of cut set-point in Figure 4-11. For the example production hole, the depth of cut set-point was 5.21 millimetres per revolution. For this production hole the collar depth of cut was the same as that of the normal drilling zone.

While the achieved depth of cut signal is quite noisy, it can be seen to follow the depth of cut set-point quite well. As expected the collar zone's depth of cut is the noisiest due to the fractured ground. The beginning of the normal drilling also sees some additional noise in the depth of cut signal which is likely due to the rotary speed increasing from 55

to 90 rpm. There are several other spikes in the depth of cut signal which are caused by varying in-situ geology requiring the controller to compensate accordingly.

### 4.2.3 Rotary Speed Feedback

Rotary speed feedback control was implemented using a PIV controller. The controller directly regulated rotary speed based upon the rotary speed set-point and the associated error between the set-point and the plant rotary speed feedback. The feedback signal was supplied from a sensor on the rotary motor.

A good example of the utilized PIV control for rotary speed can be seen in Figure 4-12. The plot of drilling while collaring with a fixed collar rotary speed set-point of 55 rpm. The drill starts from rest at time sample zero and reaches a steady state at time sample 249, where one sample is equal to 0.08 seconds. Some overshoot can be seen as the rotary speed increases from a state of rest to the desired set-point. However, the responsiveness is quite good and, more importantly, the steady state error is negligible.

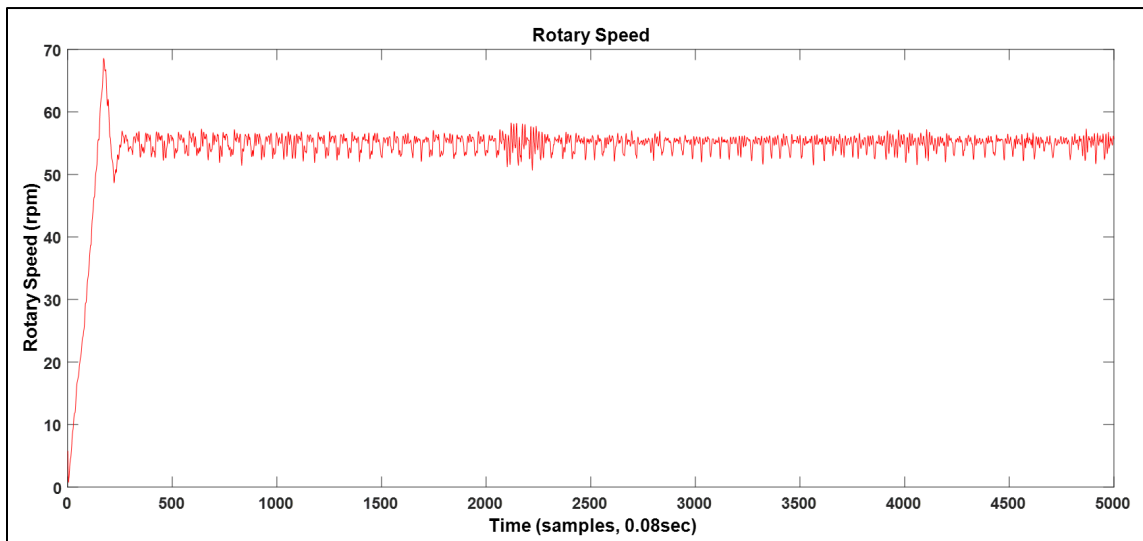


**Figure 4-12: PIV control of rotary speed**

The improvement realized via feedback control becomes quickly apparent when examining the rotary speed response data from the same drill prior to the implementation of PIV control for rotary speed. A series of input-output test were conducted to better understand the base machine application and for the purposes of modelling the rotary dynamics of the target drill rig. A more detailed review of input-output testing for the modelling of a production drill's rotary and feed dynamics can be found in Appendix 1: Feed Motor and Rotary Motor Response Testing, Modelling. Figure 4-13 shows the response testing with the blue representing the rotary speed request (input) signal and the red representing the actual rotary speed (output) attained by the drill.

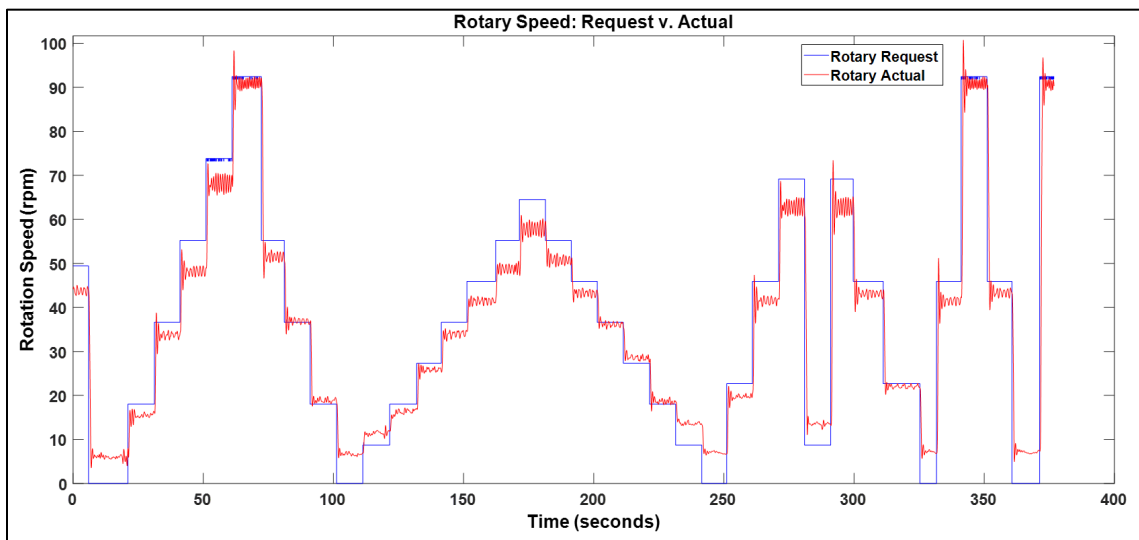


**Figure 4-13: Rotary speed response testing – no feedback control**

Examining the data recorded during the response tests it can be seen that apart from near the maximum and minimum of the rotary speed range the drill only coarsely delivers the requested rotary speed. For a better comparison between the performance of the PIV controller a fixed set-point of 55 rpm is examined (similar to Figure 4-12). Figure 4-14 includes a labelled portion of rotary speed response testing when 55 rpm was requested.

With only open loop control<sup>7</sup> when 55.2 rpm is requested the drill rig reaches a steady state about 48.8 rpm. This represents a steady state error of approximately 6 rpm (or over 10% of the requested value). Examining Figure 4-12 one can observe that feedback (PIV) control provides the requested rotary speed with negligible steady state error.

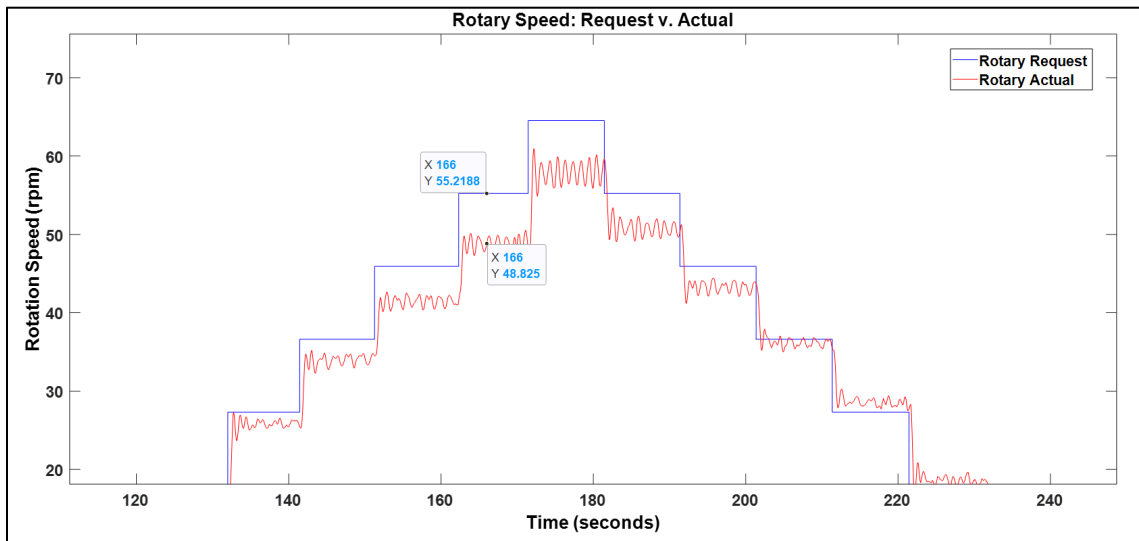


**Figure 4-14: Rotary Speed Request of 55 rpm – no feedback control**

#### 4.2.4 Secondary Control: Rotary Torque

The developed advanced drill control system was built with rotary torque as the secondary control philosophy. This was first tested using the Pit Viper 351 drill. Rotary torque is an important consideration during drilling as high rotary torques can damage the drilling components such as the rotary motor, drill string steel and drill bit. In addition, high torques can be indicative of inefficient drilling and can lead to additional problems such as unnecessary wear and tear on the drill rig.

<sup>7</sup> Open loop control refers to a control system implementation where there is no closed path or loop around which the signals go in a control block diagram (Franklin, Powell, & Emami-Naeini, 2002). With respect to this application, open loop control denotes that the OEM controller does not use a rotary motor speed reading as feedback to alter the initial set-point; rather it simply sends the requested set-point to the motor and makes no correction based upon the system's subsequent response.

For the example production hole, the maximum rotary torque was set to 6.8 kN-m and the rotary torque set-point was set to 5.4 kN-m. Rotary torque control would activate if the maximum rotary torque was exceeded and no other exceptional conditions are active.

Rotary torque control would deactivate once the rotary torque was less than the set-point.

Figure 4-15 shows the rotary torque control module operating on the Pit Viper 351. The rotary torque feedback signal from a sensor on the rotary motor is shown in green. The feed command signal from the controller to the plant is shown in black. The chosen maximum rotary torque is displayed in red and the rotary torque set-point is displayed in blue.

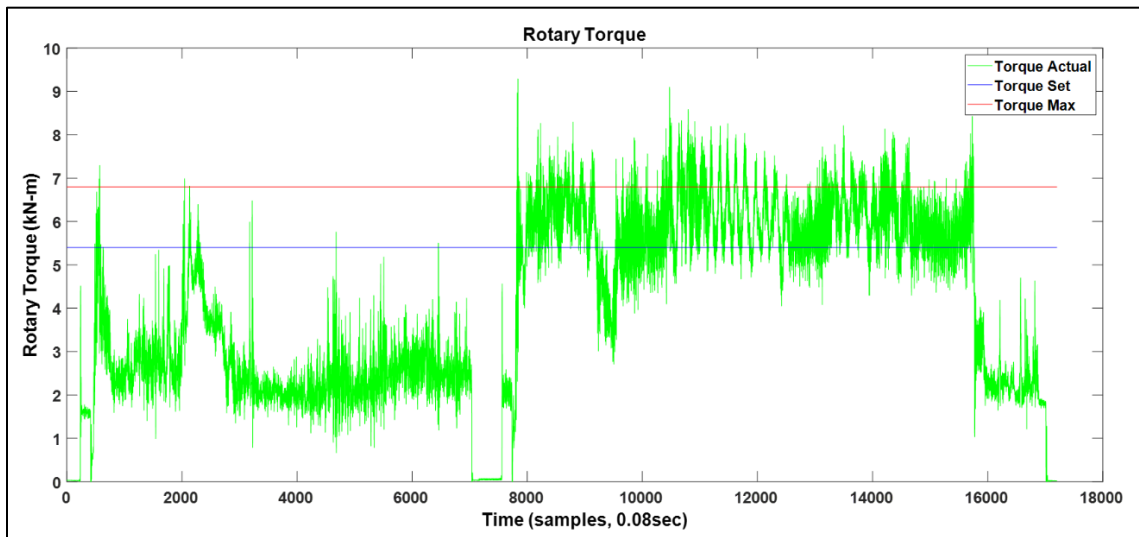


**Figure 4-15: RT example hole – rotary torque**

The advanced drill control system can be seen to react quickly when the plant exceeds the maximum torque limit. Whenever the torque exceeds the threshold the system quickly decreases the torque resulting in torque exceptions of no more than 3 seconds at a time.

Once the plant torque subsides to 5.4 kN-m or less the weight on bit is quickly increased

as the controller returns to the primary control mode. It should be noted that there are several periods displayed in Figure 4-15 where the rotary torque control module doesn't seem to be decreasing the feed command even though there is a high torque event – this is due to the vibration control module already being active. The system has been designed so that high vibration events supersede high torque events (see 3.2 Controller Hierarchy).

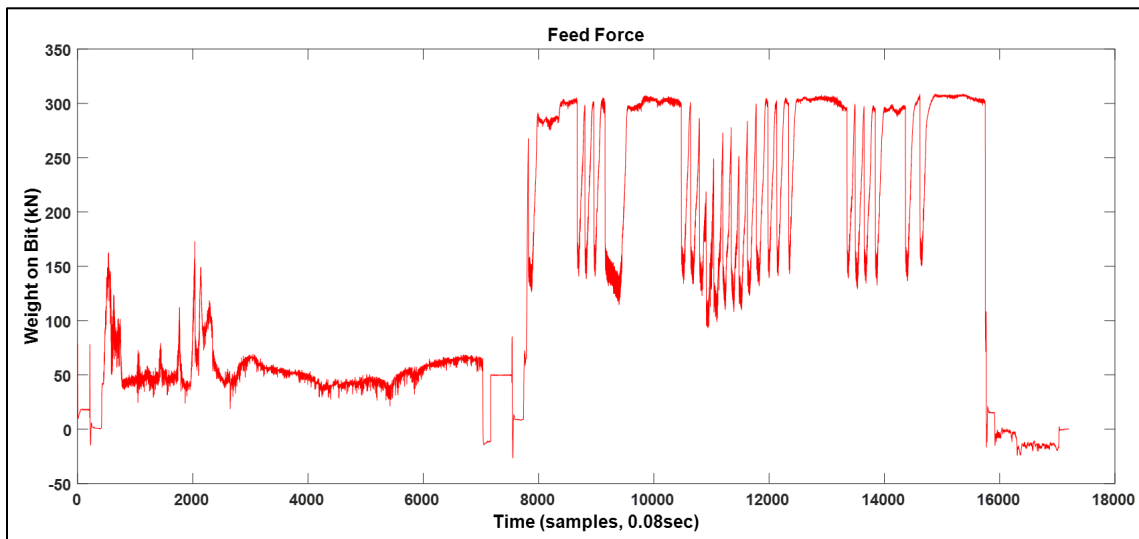


**Figure 4-16: RT example hole – weight on bit**

Rotary torque is controlled by modulating the weight on bit. This is evident in Figure 4-16. Despite the seemingly drastic modulations in weight on bit the overall penetration rate of the Pit Viper 351 through the production hole is relatively smooth albeit with an inconsistent penetration rate (Figure 4-17). This was thought to be an acceptable trade-off for avoiding potentially machine damaging high rotary torque levels.

Examining Figure 4-17 it should be noted that there is an inconsistency in the depth (and the data) between 4.2 m and 11.2 m. During this depth range other, unrelated tests were conducted that are not relevant to the rotary torque control discussion. Therefore, that data was omitted from this subsection.

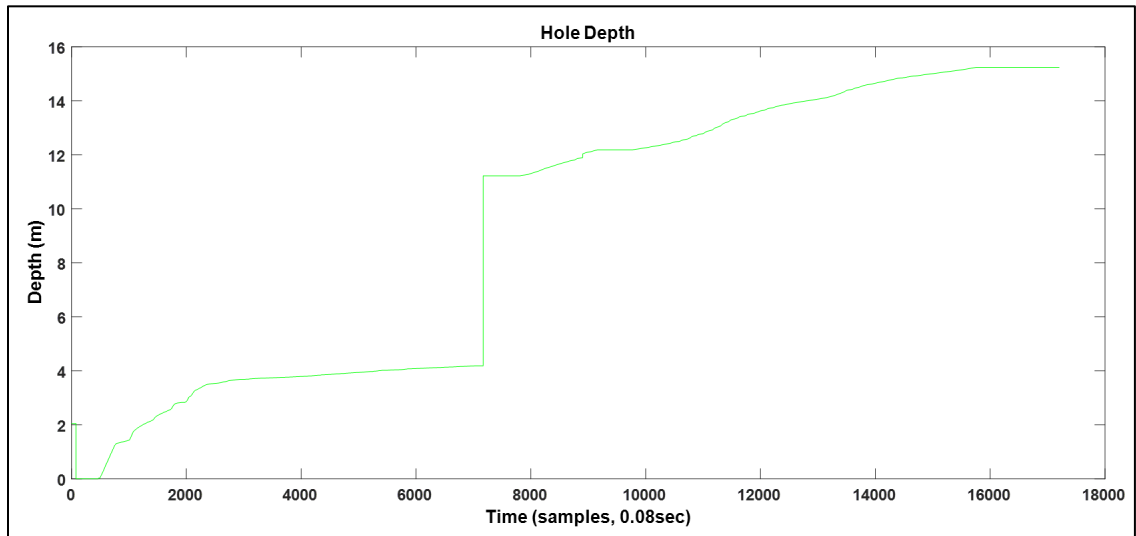


**Figure 4-17: RT example hole – depth**

#### **4.2.5 Alternate Control: Non-Critical, Predictive Bit Plugging**

To fully appreciate the predictive bit plugging control method employed by the advanced drill controller during non-critical increasing air pressure scenarios, an understanding of the industry standard controller's approach to bit plugging is required. In this subsection the reaction of an industry standard controller to a high air pressure (bit plugged) scenario is explored.

A depth plot of a production hole drilled using an industry standard controller is shown in Figure 4-18. The y-axis displays the hole depth in metres and the x-axis is time in samples at a frequency of 12.5 Hz. Examining the plot, three points of drill bit retraction are apparent. The drill bit retractions occurred at approximate times of  $0.837 \times 10^4$ ,  $1.401 \times 10^4$ , and  $5.441 \times 10^4$ . From the plot the last drill bit retraction occurred at a depth of 20.56 m which corresponds to the end of the hole. Of particular interest is the first such

bit retraction at a time of  $0.837 \times 10^4$  samples and a depth of 5.52 m – this retraction was due to a bit plugging event.

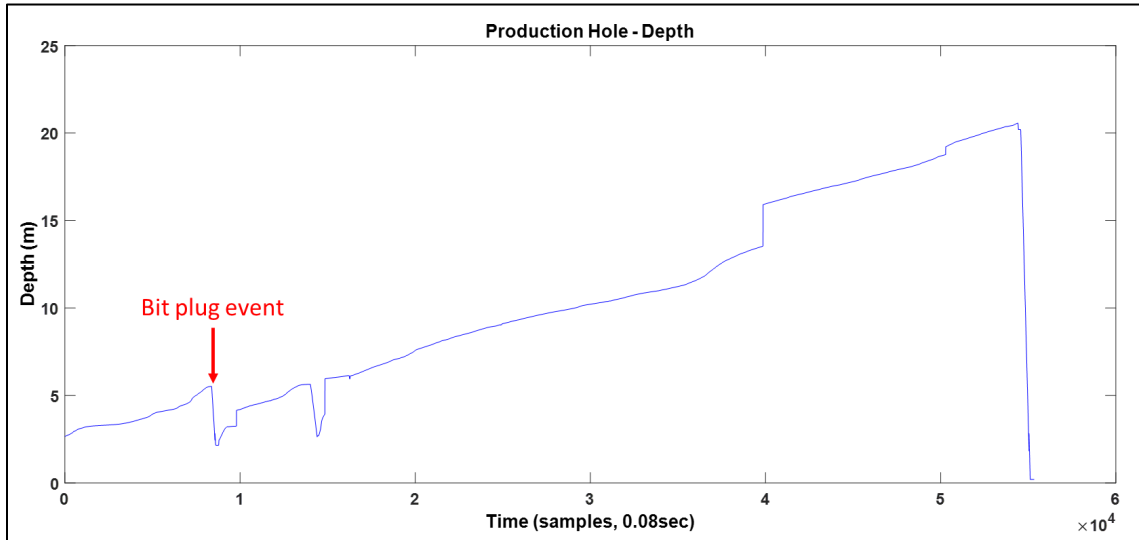


**Figure 4-18: Industry Standard Controller – Bit Plugging example hole, depth**

From the example production hole, the bit air pressure jam threshold was set at 6.2 bar. At or above that air pressure the controller would consider the bit plugged and react accordingly. Figure 4-19 shows that at  $0.738 \times 10^4$  samples the bit air pressure began to rapidly rise to a zenith of 6.8 bar which is well above the 6.2 bar set-point. At this point the controller's adjustments are able to take effect and a decrease of air pressure back to the baseline of 5.0 bar was achieved.

Figure 4-20 and Figure 4-21 illustrate that the controller achieved the air pressure decrease through a reduction of weight-on-bit to the minimum possible for the corresponding feed motor's hydraulic circuit and rotary speed to zero. This response from the controller caused an interruption in drill production and was not effective at avoiding a plugged drill bit. Furthermore, once the bit has plugged it is very difficult to resume

drilling and will likely require manual operator intervention. For both productivity and automation, avoiding a plugged bit is extremely beneficial.

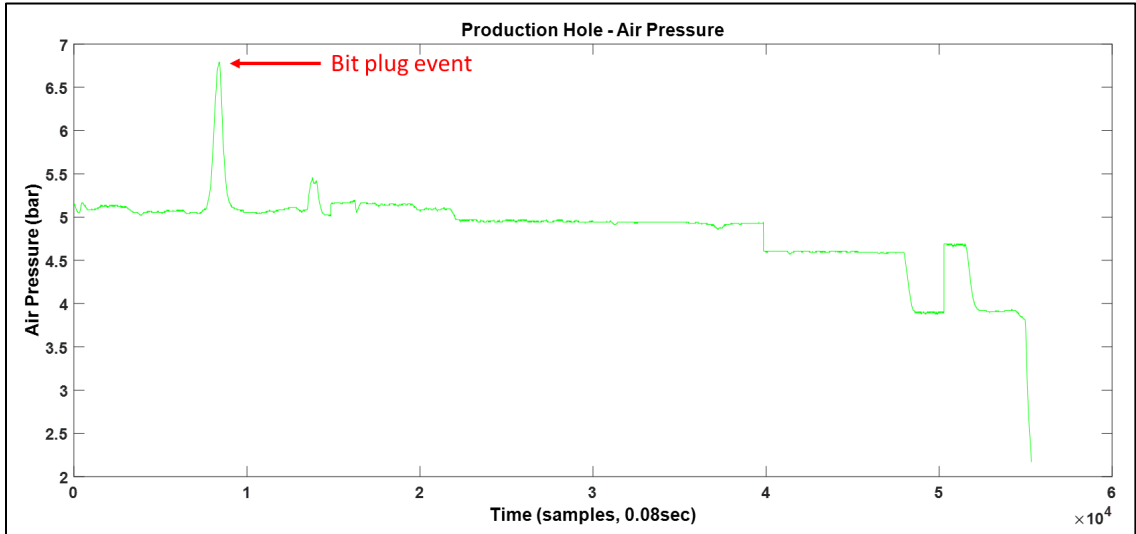


**Figure 4-19: Industry Standard Controller – Bit Plugging example hole, air pressure**

The predictive control method that was created attempted to intervene and prevent bit plugging prior to the air pressure surpassing or even approaching the jam threshold – it was designed to control air pressure during non-critical air pressure scenarios.

Referencing Figure 4-19, this was the operational period of the initial air pressure rise from 5.0 bar to the jam threshold of 6.2 bar. For this example, the total time to reach a critical air pressure was 59.68 seconds.

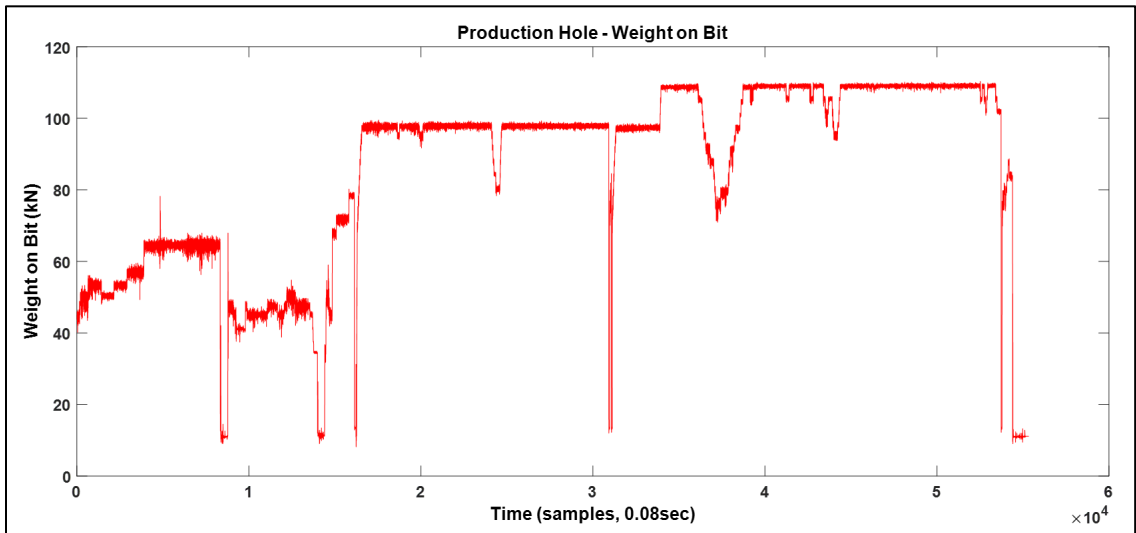


**Figure 4-20: Industry Standard Controller – Bit Plugging example hole, weight on bit**

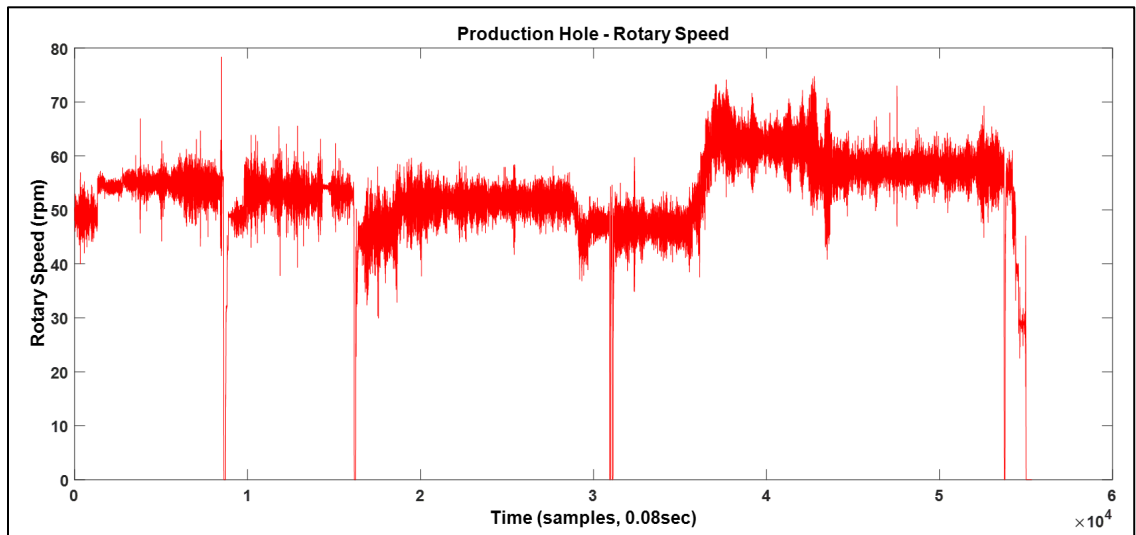


**Figure 4-21: Industry Standard Controller – Bit Plugging example hole, rotary speed**

For comparison, an example production hole which was drilled while utilizing the predictive bit plugging control method will now be explored. The controller was configured with an air pressure rate of change set-point of 0.05 bar per second calculated

---

by measuring the root mean square value of the plant air pressure signal. The RMS value of the plant air pressure signal was calculated over a running average window of one cycle of the fundamental frequency. The specified fundamental frequency chosen was 29 Hz (or 3.35 seconds of plant operation). This fundamental frequency was chosen based on various simulations of air pressure control using the modeled in situ geology and plant dynamics in the Simulink modelling environment.

Figure 4-22 is a plot of the air pressure rate of change used by the controller as described above. The set-point is represented by the horizontal red line. Anytime the calculated plant air pressure rate of change rose above the set-point the predictive control method was utilized. The controller regulated weight-on-bit based upon the predictive bit plugging method until the rate of change remained below the set-point for a total of 300 samples (24 seconds). This time delay off for the air pressure control method was chosen based on simulation-based and field testing.

Examining Figure 4-22 the plant air pressure rate of change first exceeded the set-point at 3079 samples and only returned to being consistently below the set-point at 4214 samples.

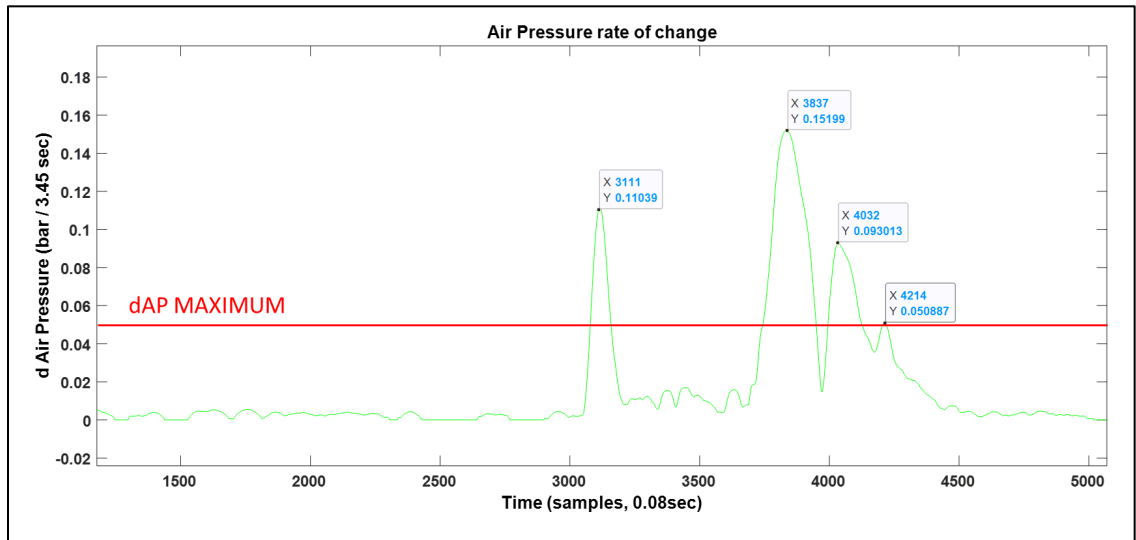


**Figure 4-22: Predictive Bit Plugging example hole – air pressure rate of change**

When the predictive, alternate control method was active the controller attempted to regulate the plant air pressure about some set-point through variation of the weight-on-bit. The set-point for this example was 4.8 bar. The air pressure regulation via weight-on-bit manipulation can be seen in Figure 4-23 (plant weight-on-bit) and Figure 4-24 (plant air pressure). These two plots demonstrate the controller manipulating weight-on-bit to successfully regulate plant air pressure at or below the defined set-point (4.8 bar for this example).

Figure 4-25 is a plot of the example production hole's depth. Examining the depth and the depth derivative (penetration rate) provides a good approximation of the control method's impact on drill productivity during the non-critical air pressure exceptional scenario. The depth plot appears smooth throughout the exceptional scenario and is consistent with the normal drilling situations that bookend the drilling exception in Figure 4-25.

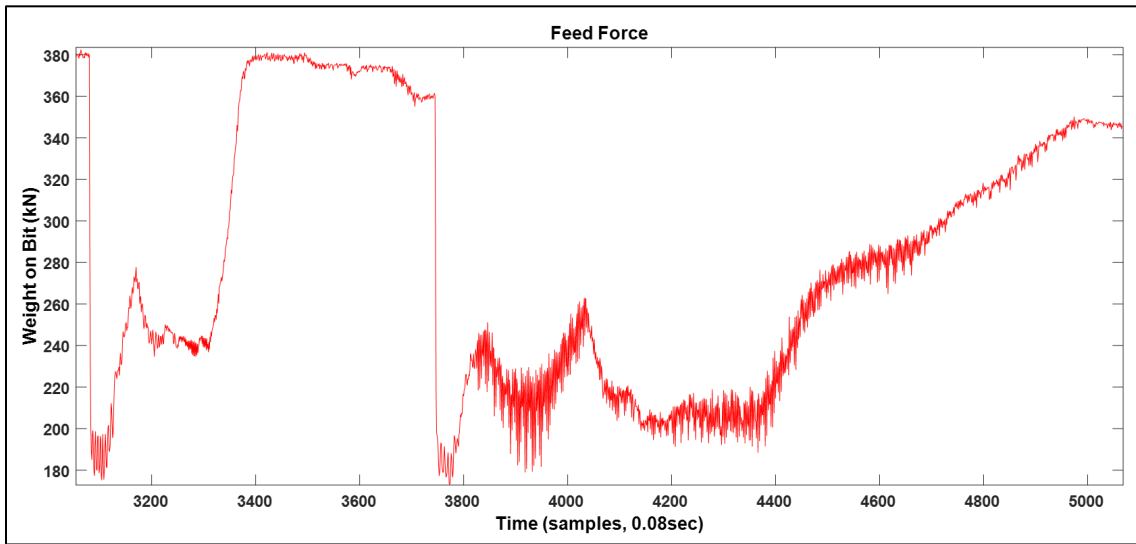


Figure 4-23: Predictive Bit Plugging example hole – weight-on-bit

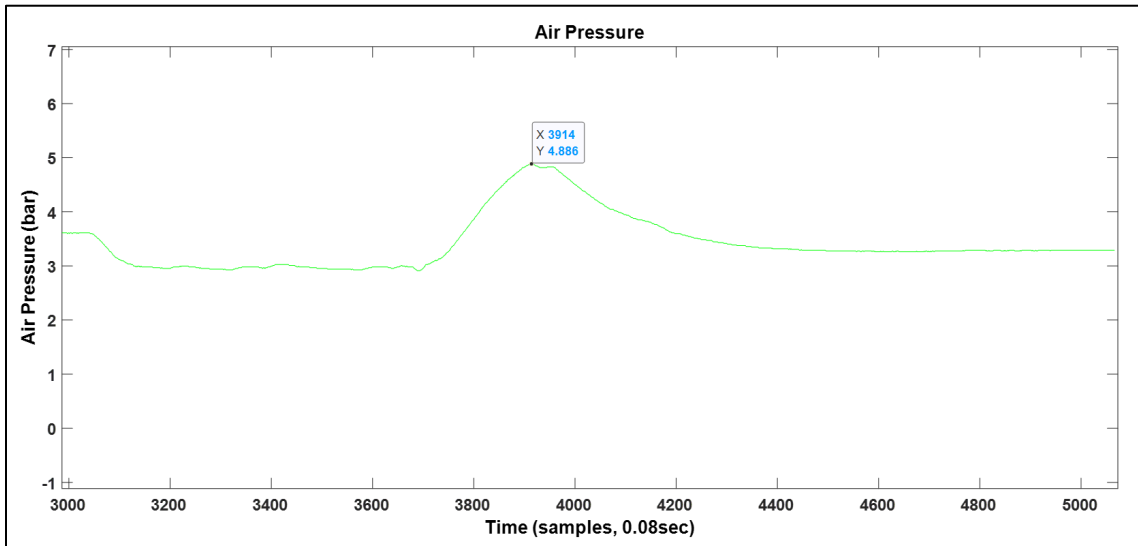
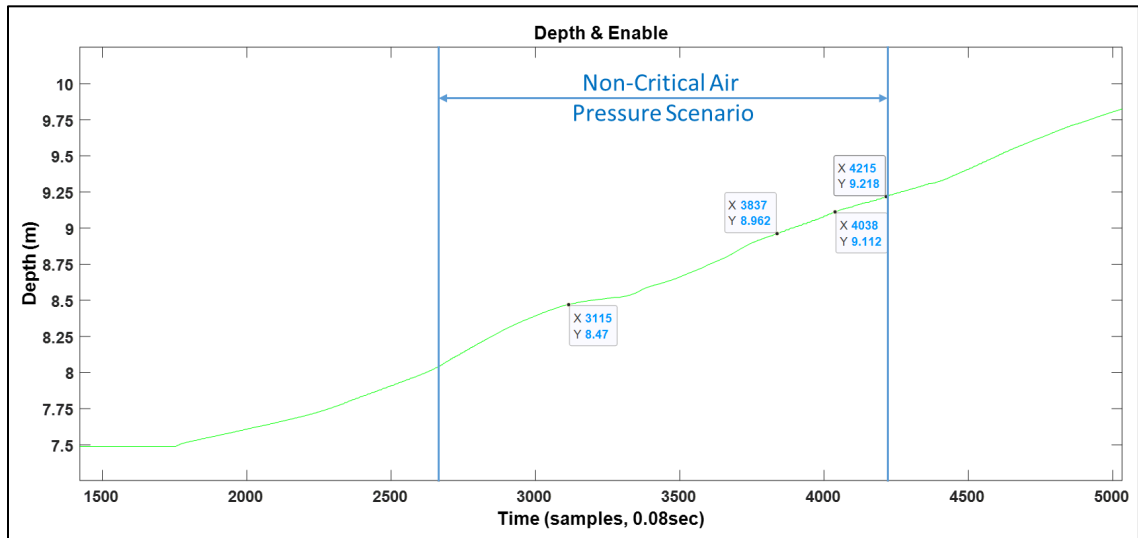


Figure 4-24: Predictive Bit Plugging example hole – air pressure



**Figure 4-25: Predictive Bit Plugging example hole – depth**

In addition, the predictive control method successfully prevented a critical air pressure scenario by preventing the plant air pressure from exceeding 4.8 bar which was well below the 6.2 jam threshold. At no time was the 6.8 bar peak approached unlike in the previous example of the industry standard air pressure control strategy.

#### 4.2.6 Alternate Control: Critical, Bit Plugging

During the field testing, it was difficult to induce a critical bit plugging exceptional drilling scenario; even with aggressive drilling set-points. It was theorized that this was due to the control hierarchy implemented which saw an inability to disable the predictive non-critical bit plugging control strategy while also keeping the critical bit plugging control strategy active. While the controller design could be changed in a laboratory setting it proved not possible in the field environment.

Eventually a bit plugging scenario was artificially induced by increasing the water flow set-point to its maximum and the air flow set-point to 75% of its maximum. For field

testing, the critical bit plugging threshold was set to 4.8 bar. Figure 4-26 and Figure 4-27 show the plant water flow and air flow command in litres per minute and percent request, respectively. The periods of raised water and air flow are highlighted in the two figures; they do not cover the same periods but there is overlap.

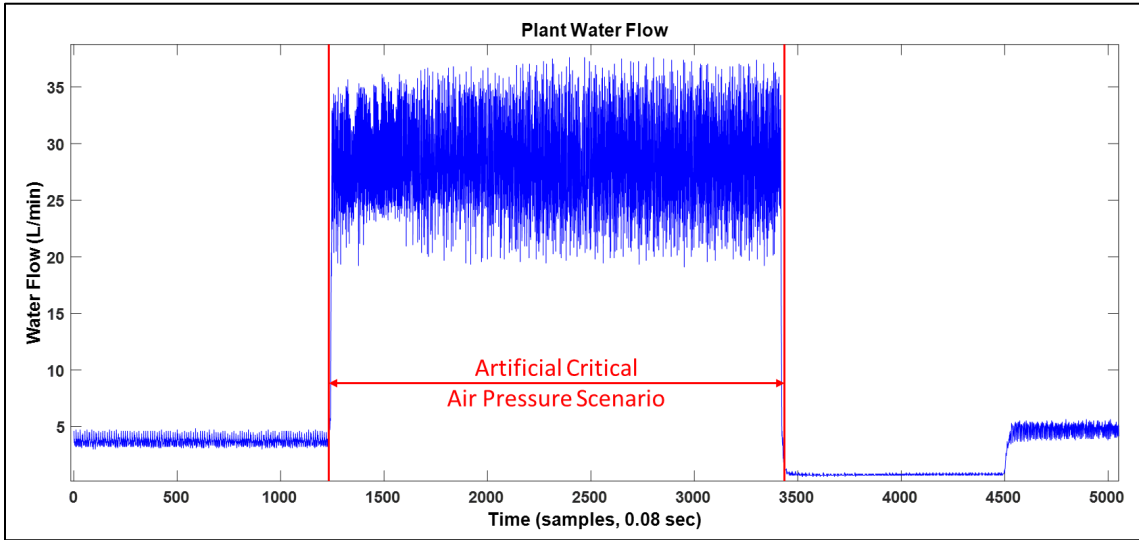


**Figure 4-26: Critical Bit Plugging example hole – water flow**

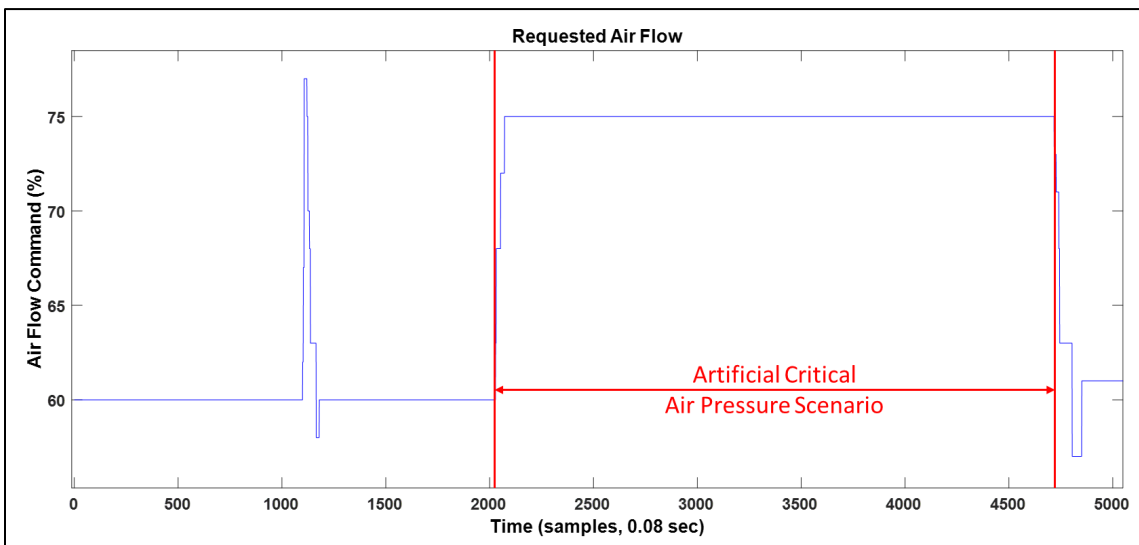


**Figure 4-27: Critical Bit Plugging example hole – air flow command**

The resulting plant air pressure can be found in Figure 4-28. Air pressures that trigger critical bit plugging control (4.8 bar and above) are noted in the plot as are the periods of 100% water flow and 75% air flow.

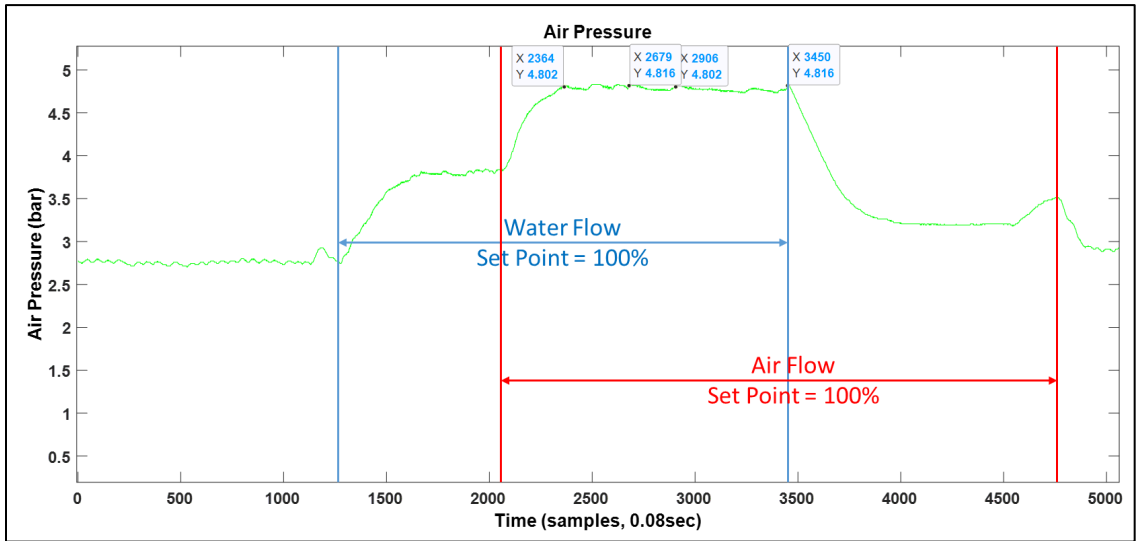


Figure 4-28: Critical Bit Plugging example hole – plant air pressure

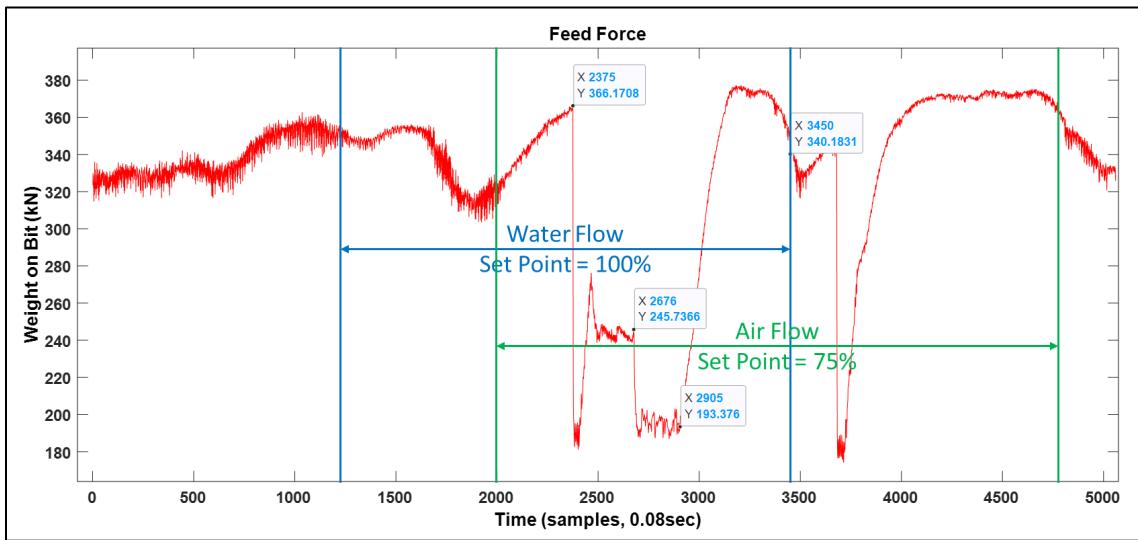


Figure 4-29: Critical Bit Plugging example hole – plant weight-on-bit

---

The weight-on-bit regulation that corresponded to the critical air pressure levels is shown in Figure 4-29. Several key points are noted within the plot. At sample 2,375 the weight-on-bit was reduced to avoid the critical bit plugging scenario. The WOB dropped from approximately 360 kN to 246 kN. Some undershoot can be observed which saw the WOB decrease to 180 kN before subsequent overshoot returned the WOB to 280 kN, followed by a WOB steady state at 246 kN. At sample 2,676 WOB was again reduced from 246 kN to 193 kN in response to a critical air pressure value; however in this instance no overshoot occurred. In response to a sustained period of air pressure below the set-point of 4.8 bar WOB was increased at sample 2,905 from 193 kN to 370 kN. At sample 3,450 WOB was reduced again due to high air pressure albeit at a more gradual rate.

The observed overshoot and undershoot indicate that the weight-on-bit modulation of the critical bit plugging controller may be slightly too aggressive. This can be further refined via gain tuning. Although, it must be noted, aggressively avoiding a critical bit plugging situation is greatly preferred to drilling into a jammed bit.

Overall, the weight-on-bit modulation shown in Figure 4-29 effectively controlled (and avoided) critical air pressure levels. Examining Figure 4-28 this is reinforced as high air pressures were present during the period of both high water flow and high air flow however they rarely exceeded the chosen threshold of 4.8 bar. When the threshold was exceeded the overage was quite low and brief. Further examining Figure 4-28, it should also be noted that while drilling high air pressures only occurred during periods of both high water flow and high air flow. Individual periods of only high water flow or only high air flow did not result in air pressures that approached the critical plugging

threshold. This demonstrated the effectiveness of the multi-layered air pressure control approach utilized.

#### 4.2.7 Alternate Control: Vibration

The vibration control feature was created to minimize incidences of high drill string vibration and to avoid periods of sustained high drill string vibrations. To accomplish this the controller regulates rotary speed as the primary control variable and keeps weight-on-bit static. The vibration control feature is activated once high vibrations have been detected (beyond a configurable time delay on) and remains active until a period of low vibrations has been observed. The period of low vibration can be indexed to either distance drilled or time elapsed.

For the example hole explored, the vibration set-point was set to 9.0 centimetres per seconds squared. Figure 4-30 shows the observed plant vibration for the example hole as well as the chosen set-point (denoted by the red line).

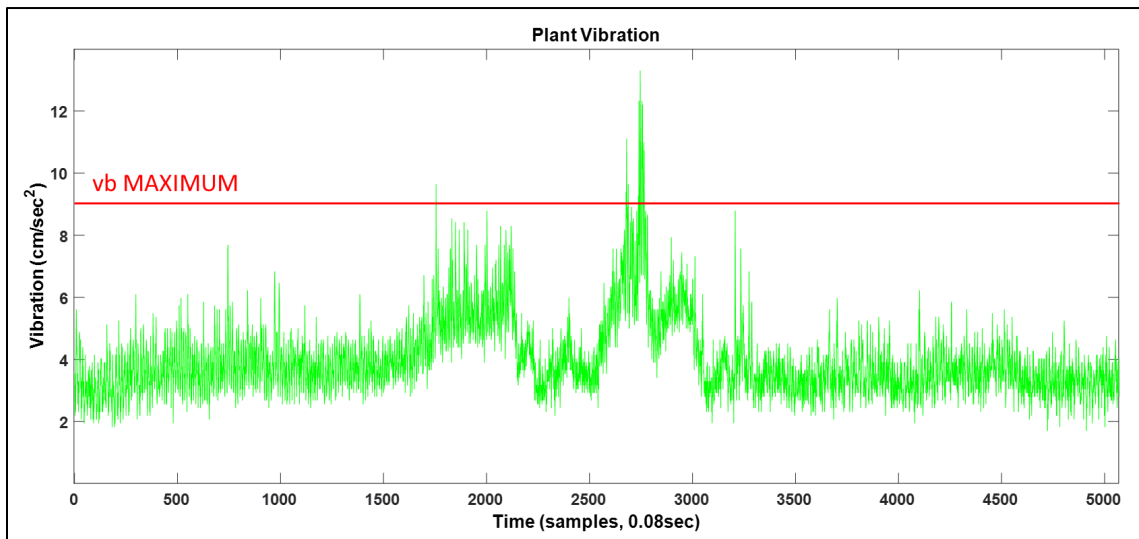


**Figure 4-30: Vibration example hole – plant vibration**

The vibration event that occurred at approximately sample 2,700 in Figure 4-30 caused the vibration control feature to activate. The vibration control was active between sample 3,000 and sample 4,000 (approximately) in Figure 4-31. The vibration control feature reduced the rotary speed from 90 rotations per minute (the maximum for normal operation) to the pre-set 55 rpm for vibration control. This remained the rotary speed until no further high vibration events were observed for the chosen time delay off period (approximately sample 4,000). At that point the rotary speed was once again defined by the depth of cut ratio and began to fluctuate with plant penetration rate.

For reference the corresponding weight-on-bit during the vibration control activity is provided in Figure 4-32.

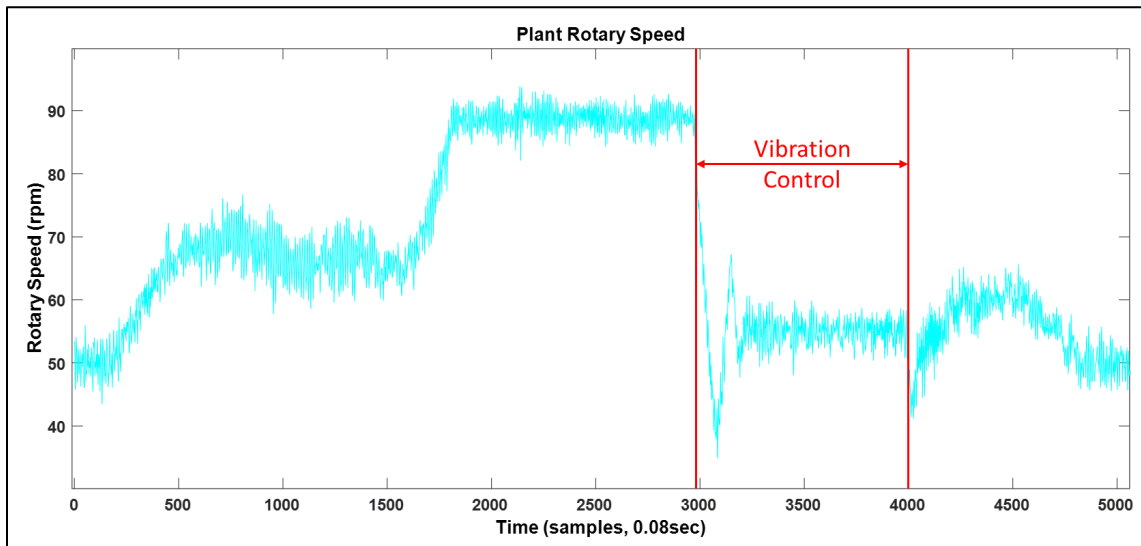


**Figure 4-31: Vibration example hole – plant rotary speed**

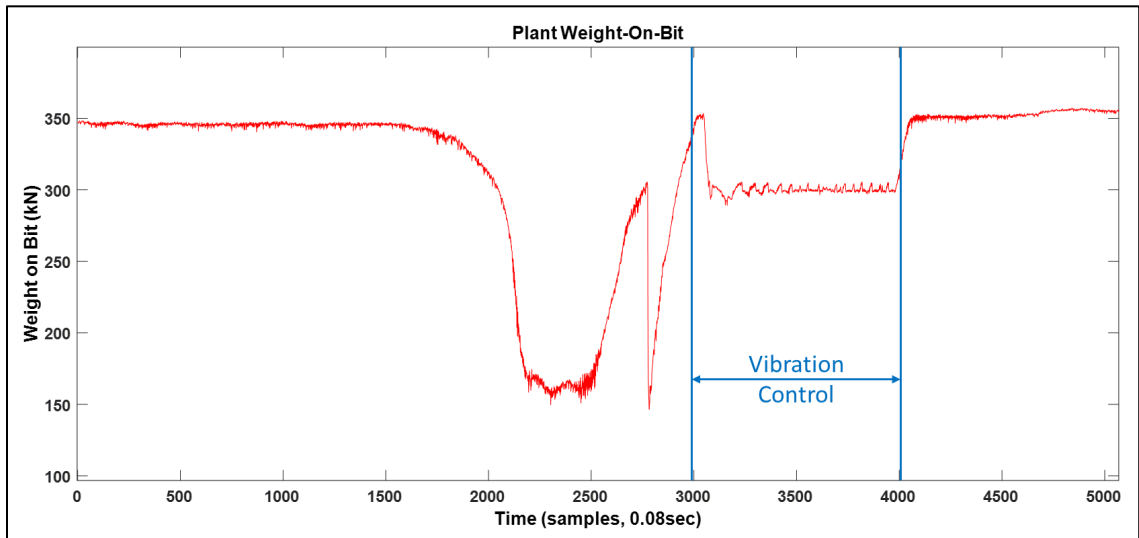


**Figure 4-32: Vibration example hole – plant weight-on-bit**

#### 4.2.8 Alternate Control: Retract

The retraction control feature of the advance drill controller is critical in ensuring that high retract speeds can be delivered but bit jamming issues avoided, thus striking the necessary balance between productivity and reliable autonomous operation. Figure 4-33 shows the end of hole sequence for the example hole. The various retraction zones are noted. These zones correspond to those previously defined in Figure 3-13.

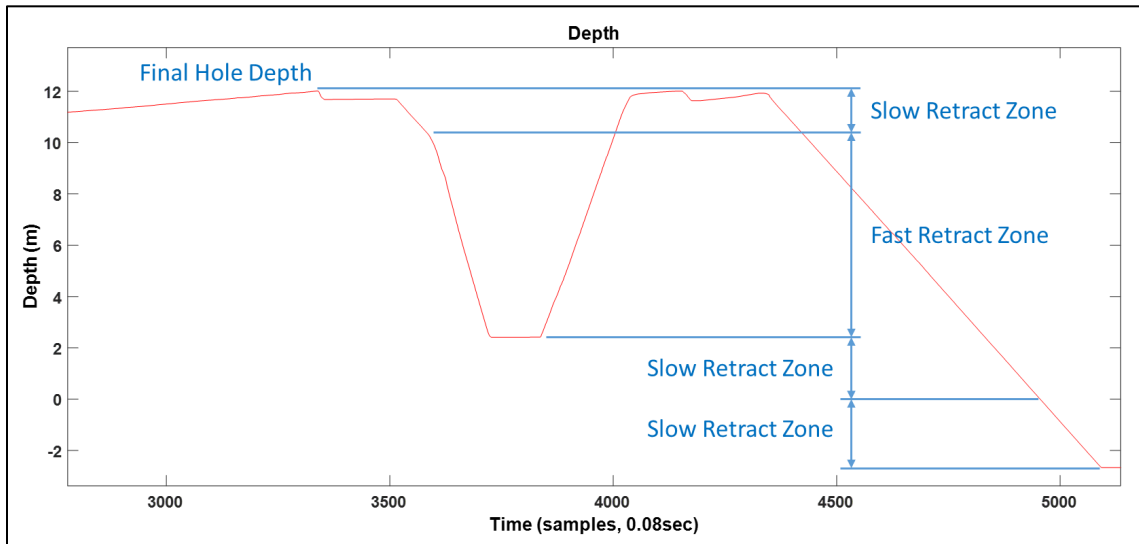


**Figure 4-33: Retract example hole – bit position**

During bit retraction bit jam conditions are predominantly indicated by high torque levels. One such high torque event occurred during the first retraction displayed in Figure 4-34. Upon detection of the high torque the retraction control mode decreased the speed of the drill bit's retraction from the hole (penetration rate). This was done until the high torque value subsided, at which time the retraction speed was once again increased. The retraction speed manipulation is shown in Figure 4-35 where a potential jam condition was successfully avoided.

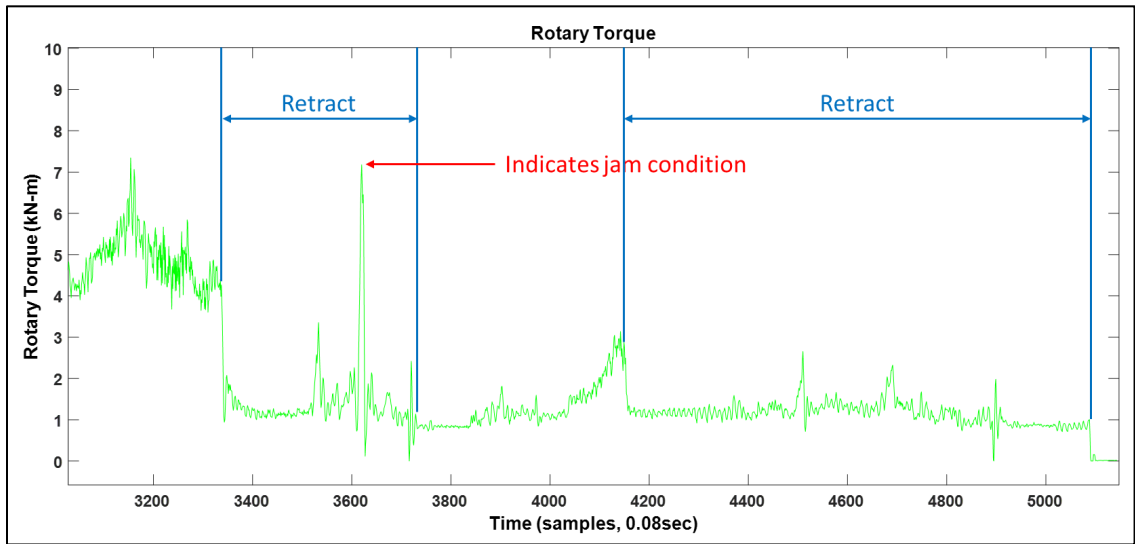


**Figure 4-34: Retract example hole – rotary torque**

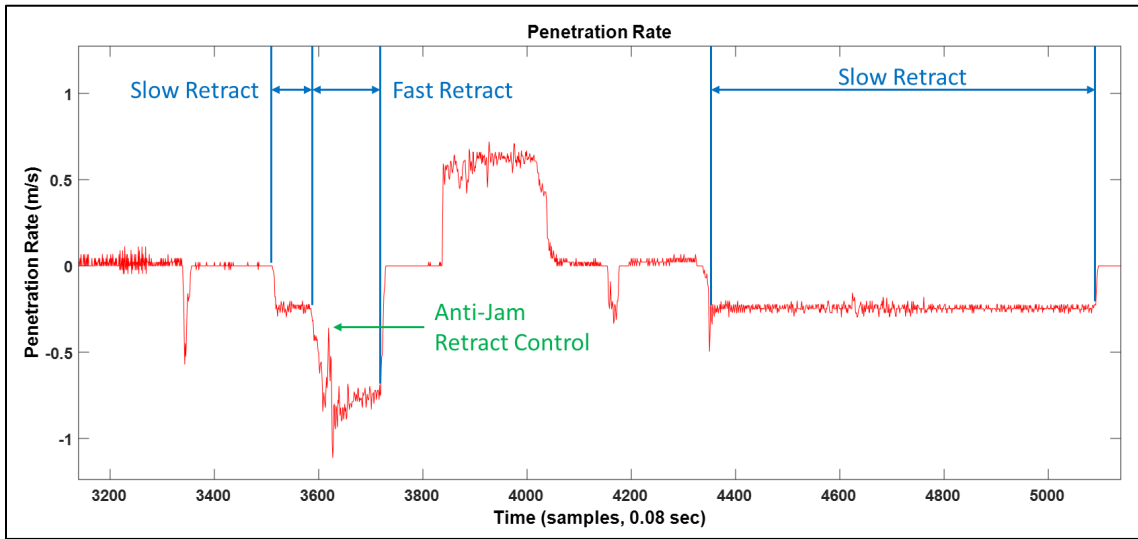


**Figure 4-35: Retract example hole – penetration rate**

In addition to the anti-jam retraction logic discussed, an auto hole cleaning feature was developed. This feature would monitor any jams that occurred during the drilling of a production hole. If the number of jams was above some configurable amount the hole would be cleaned (or reamed) upon completion. If the number of jams was below the

---

configurable amount, the hole would not be cleaned. Figure 4-33 shows a hole cleaning sequence<sup>8</sup>.

#### **4.2.9 Alternate Control: Operational Limits**

The operational limits (maximum and minimum) were implemented as described in Section 3.3.9. A recovery scenario was not implemented as the advanced drill control testing was executed with a human operator onboard the drill and was therefore not required. For potential autonomous operation a recovery scenario is thought to be beneficial. This could be implemented as a high-level “wrapper” style module.

#### **4.2.10 Exception Handling: Drilling Through a Void**

In situ voids encountered while drilling are a common occurrence that must be properly accommodated by the developed drill control solution. To test the ability of the controller to facilitate drilling in a void condition a production hole was drilled to completion and cleaned, the drill rig was then kept in place and the previously drilled hole was then used for the void test. The controller was reset with the drill bit retracted from the hole. The controller was then restarted at the zero meter depth point (or the ground contact point) and proceeded to drill the pre-drilled hole with a pre-set sequence that began with hole collaring for the first three meters. Hole depth progress can be seen in Figure 4-36.

---

<sup>8</sup> A hole cleaning sequence occurs at the end of a drilled production hole and is done to ensure all the broken material has been ejected from the hole. It involves retracting the drill bit from the bottom of the completed hole to a point near the surface, then lowering the drill bit back to the bottom of the hole, if necessary “cleaning” of material at the bottom of the hole by drilling and loose material ejection via air flow, then retracting the drill bit back to the surface and stowing the drill string assembly for movement to the next production hole.

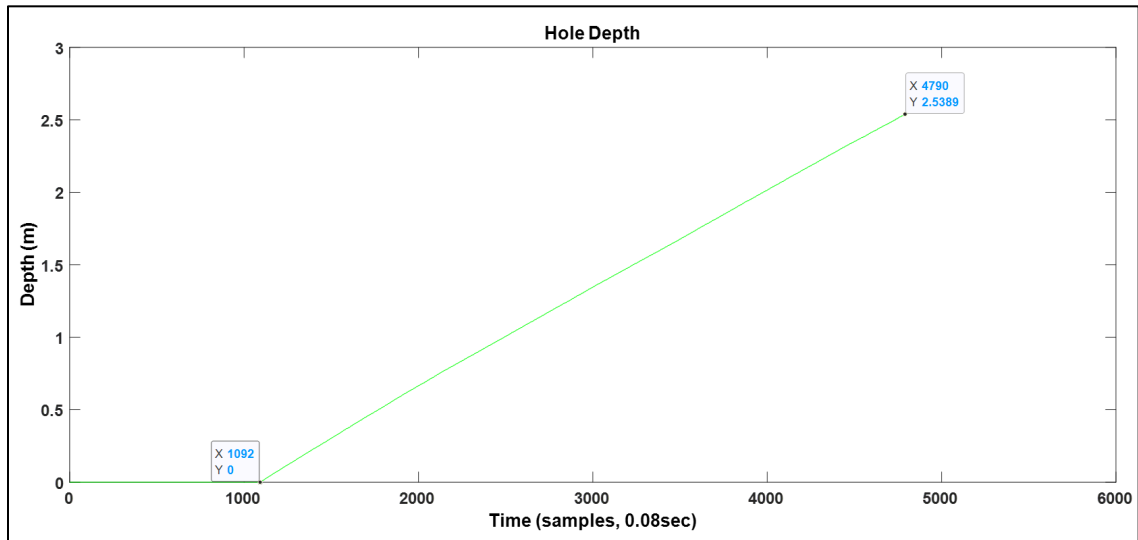


**Figure 4-36: Hole depth through void zone**

Examining Figure 4-36, the penetration rate was relatively constant through the void from 0 to 2.5 meters. During this period of drilling the penetration rate was approximately 0.5 meters per minute. Beyond this zone the penetration rate slows as some loose and caved material from the hole wall was encountered. While the penetration rate set-point for collar drilling was 2.084 millimeters per revolution (0.4 times 5.21 mm/rev), field testing showed that 0.5 meters per minute during drilling in a void was the lowest positive penetration rate that could be achieved by the test drill rig. This was due to the mechanical properties of the drill rig, the drill head weight and the feed motor specifications. For drilling in broken or solid material a slower penetration rate was achievable.

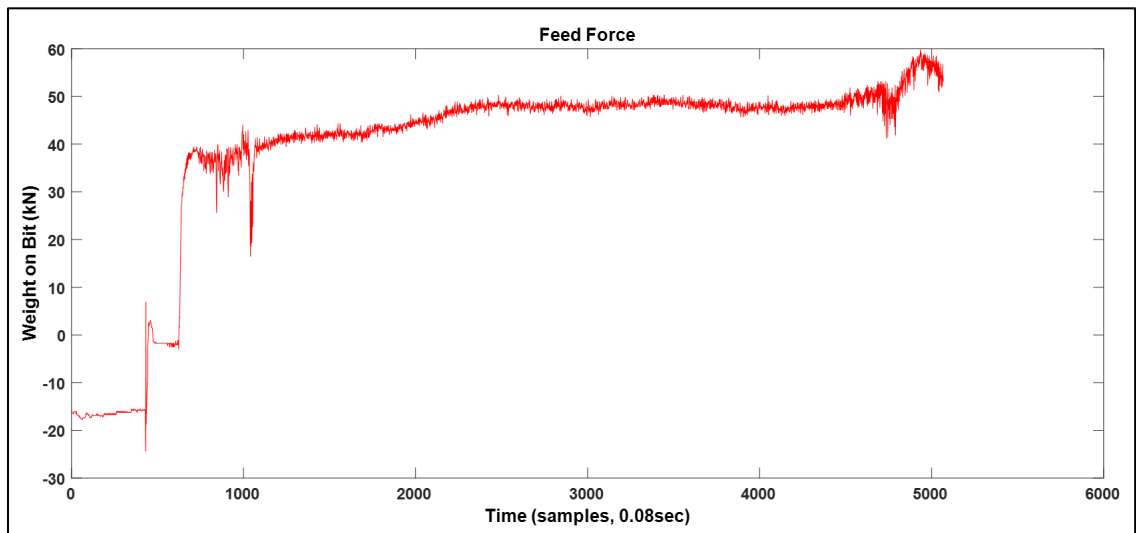


**Figure 4-37: Feed force through void zone**

The feed force applied by the drill rig in the void zone is shown in Figure 4-37. For reference the drill string head weight is approximately 69 kilo Newtons (7,000 kg). Therefore, the drill rig was holding back the full weight of the drill string and only allowing 40 to 50 kN of down force to be applied through the 0 – 2.5 meter void zone. In general, an indication of the presence of a void zone is when there is feed force less than the force component associated with the drill string weight.

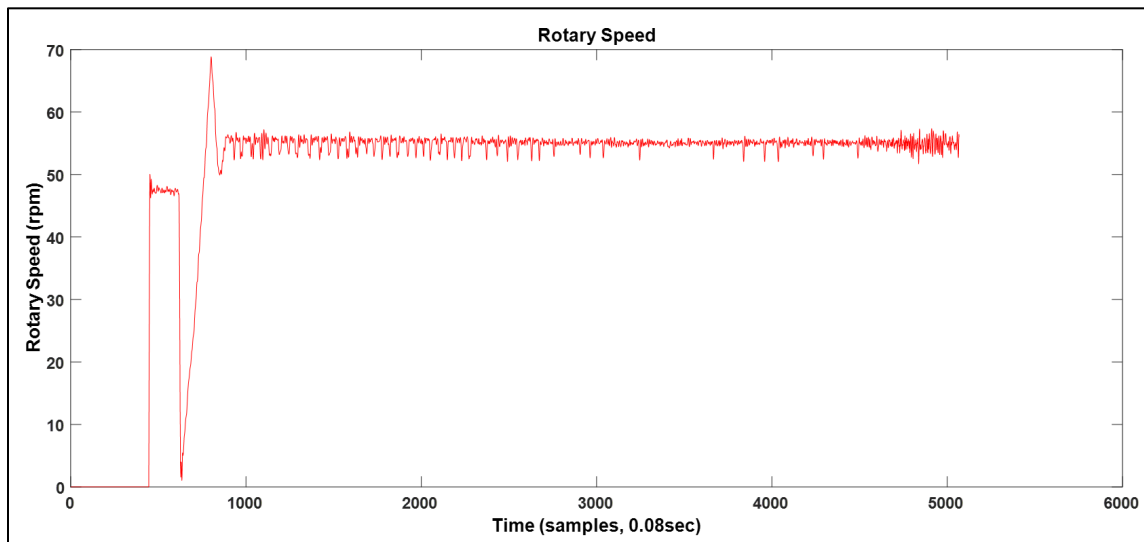


**Figure 4-38: Rotary speed through void zone**

Figure 4-38 shows the rotary speed through the void zone which was the collaring rotary speed set-point of 55 rpm. Based upon the penetration rate from Figure 4-38 an approximate depth of cut for the void zone can be calculated to be 0.1 meters per revolution. Based on the results of the field testing, this was shown to be a stable penetration rate and depth of cut for void zones. In addition, the controller repeatedly achieved this result in various void zones encountered throughout the testing which resulted in the conclusion that the controller appropriately handled void scenarios.

### **4.3 Advanced Drill Control Results & Discussion**

As mentioned, the advanced drill control solution was field tested at two surface mine sites: A North American copper mine and an Australian iron ore mine. The field test at the copper mine consisted of one week of supervised field testing; the field test at the iron ore mine consisted of one week of supervised field testing followed by several months of normal operational use. The results of supervised field testing at the copper mine and the

several months of normal operational use at the iron ore mine will be summarized and discussed in this section.

#### 4.3.1 North American Copper Test Results

During the one week of supervised field testing all control modes were tested and validated and the advanced drill control solution was used to drill 162 metres of production holes. The results were logged as were the drilling performance of the same drill rig (Drill #1) without the use of the advanced drill controller (manual operation or industry standard drill controller) and another drill rig (Drill #2) that was the same OEM and drill model (Pit Viper 351) but did not have the advanced drill controller installed. These results provided a good performance comparison and are given in Table 4-3.

Drill	Depth (m)	Time (min)	Pen. Rate (m/min)
Drill #2	679	2378	0.29
Drill #1	604	1915	0.32
Drill #1 with Advanced Drill Control	162	351	0.46

**Table 4-3: Field test results, North American copper mine**

Comparing the penetration rate between the test drill rig (Drill #1) with the advanced drill control system enabled or disabled yields a penetration rate improvement of 46 percent. When comparing the test drill rig with the advanced drill control system enabled to the comparable drill rig (Drill #2) there is a 61 percent penetration rate improvement.

Due to the relatively short duration of the field test the advance drill control solution's influence on bit wear could not be determined based upon the North American copper mine results.

#### 4.3.2 Australian Iron Ore Test Results

During the one week of supervised field testing the various control modes were further tested and refined. During this time production data was not tracked as a long-term trial consisting of normal operational use was planned. The data presented here is representative of the first four months of that long-term trial.

Description	Penetration Rate (% improvement)	Bit Life (% improvement)
Advanced Drill Control vs. Manual Operation / Industry Standard Drill Control	9.8	22

**Table 4-4: Field test results, Australian iron ore mine**

Table 4-4 shows how the operation of the advanced drill control solution performed in comparison to the mine's average manned drill performance during the long-term field trial. The results show a productivity improvement of 9.8 percent with a bit life improvement of 22 percent over the four month period.

#### 4.3.3 Discussion

Based upon the results of the two field test periods the following observations were made:

- 
- All control modes functioned as designed and performed well in both the copper and iron ore surface mines. This demonstrated a versatility of the controller with respect to in-situ geology and mine conditions.
  - The controller functioned well on two different models of drill rigs with different performance specifications (Pit Viper 351 and Pit Viper 271). This demonstrated a versatility of the controller with respect to the base drill rig.
  - Productivity improvements were seen at both test sites. However, a much larger productivity improvement was observed at the copper mine whereas a more modest (albeit still significant) improvement was seen at the iron ore mine. It is the opinion of the author that the added productivity improvement attained at the copper mine is due to the more conservative drilling set-points used by the fleet of operators. At the iron ore mine the approach to drilling was more aggressive overall and therefore less added productivity could be realized through the enhanced controller.
  - While overall the drilling set-points utilized by the advanced drill controller are typically more aggressive than those utilized by most human operators they are always configured to be within the OEM performance specifications and are always driven toward optimizing drilling efficiency with respect to drill bit design. This is not typically the case with human operators. This leads to a somewhat counterintuitive situation, where more conservative drilling set-points may actually lead to damage and a decrease of the lives of drill rigs and their components.

- Over longer-term use a noticeable improvement in drill bit life was observed. This reinforced that the advance drill controller succeeded in accomplishing not just more productive but also more efficient drilling. An improved drill bit life of almost one quarter is quite significant and could represent a good cost savings via reduced consumable purchasing for the mine operators.

#### **4.4 Influence of Drill Bit Design (and Wear) on Drill Control**

As discussed in Chapter 2, sub-section 2.2.3, Shively Jr. proposed a method for optimal penetration rate, and therefore efficient drilling, for any given tri-cone drill bit. This was termed depth of cut. The depth of cut is a ratio between penetration rate and rotation speed. Shively Jr. advised that to ensure efficient drilling the optimal penetration rate cannot exceed the drill bit's insert (tooth) height for any given rotation of the bit. If the insert height is exceeded, this leads to the drill bit interacting with the rock face at the surface of its three cones. This is an inefficient drilling method and can lead to regrinding as material becomes trapped and cannot be bailed from the bottom of the production hole. In addition, this can lead to accelerated bit wear and premature failure.

In general, there are five classes of tri-cone rotary bits with Tungsten Carbide Inserts. Figure 4-39 shows the five IADC classes of bits and their corresponding in-situ rock type. The rock type is given by its Unconfined Compressive Strength (UCS) in psi; the higher the UCS the harder the material. Table 4-5 provides the OEM operational guidelines for each class of bit.

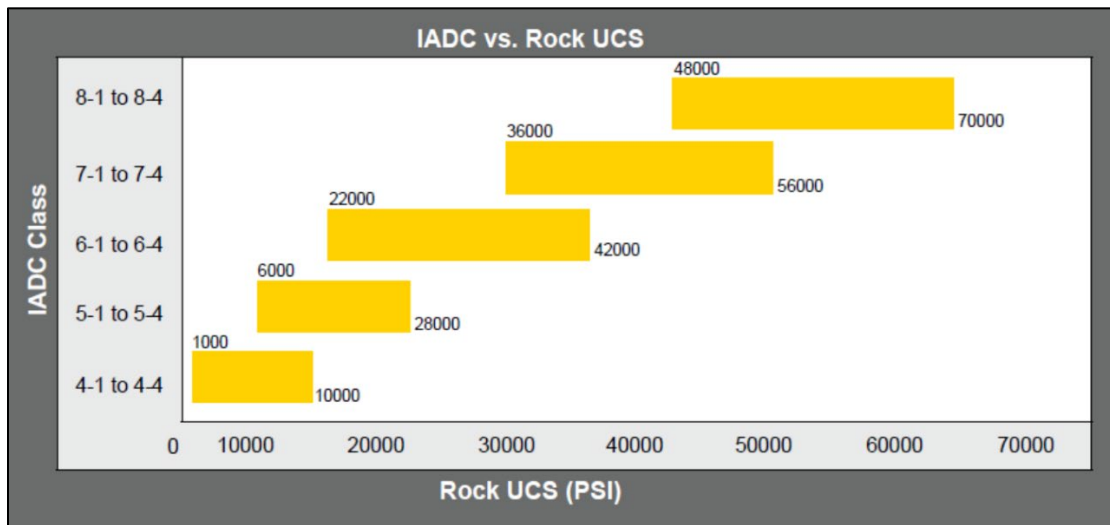


**Figure 4-39: IADC bit class and corresponding rock type (Atlas Copco Drilling Solutions LLC, 2012)**

Bit Class	Rotation Speed	Weight-on-Bit
4-1 to 4-4 IADC	50 - 150 rpm	454 - 2,268 kg
5-1 to 5-4 IADC	50 - 150 rpm	1,361 - 2,948 kg
6-1 to 6-4 IADC	50 - 120 rpm	1,814 - 3,175 kg
7-1 to 7-4 IADC	50 - 90 rpm	1,814 - 3,629 kg
8-1 to 8-3 IADC	40 - 80 rpm	2,722 - 4,082 kg

**Table 4-5: OEM operational guidelines for various tri-cone bit classes (Atlas Copco Drilling Solutions LLC, 2012)**

The two mine sites at which the drill control research (described in Chapter 4) was conducted used three classes of tri-cone drill bits: IADC 5, IADC 6, and IADC 7. The insert heights of these bits were measured, and the results are given in Table 4-6.

Bit Class	Insert Height
IADC 5	6.40 mm
IADC 6	5.18 mm
IADC 7	4.57 mm

**Table 4-6: Measured insert height by observed bit class**

The observed insert heights dictate the depth of cut ratio for each class of bit. Based upon the chosen performance range for the test drill rigs the minimum and maximum rate of penetration can be determined. This information is displayed below in Table 4-7. The performance range was dictated by the partner mine sites in consultation with the drill OEM's specifications. The rotary speed range was 50 to 90 rotations per minute at both test sites.

Bit Class	Depth of Cut	ROP <sub>MIN</sub>	ROP <sub>MAX</sub>
IADC 5	6.40 mm / rev	0.320 m / min	0.576 m / min
IADC 6	5.18 mm / rev	0.259 m / min	0.466 m / min
IADC 7	4.57 mm / rev	0.229 m / min	0.411 m / min

**Table 4-7: Depth of cut and range of penetration rates for observed bit classes**

The operational rate of penetration range by observed bit class is displayed in Figure 4-40. For reference the observed insert height for each bit is also provided. This plot illustrates the range over which each bit class can operate while providing efficient bit-rock interaction. In this range bit chip size is kept within the optimal size range and drill bit life is maximized. In addition, drill energy usage is optimized. As shown in the plot, the operational rate of penetration range is dictated by the chosen operational rotary speed. Rotary speeds above 90 rotations per minute are possible for drill bit types of IADC 6 or less. For the drill rig itself, this is especially relevant on the smaller drill rigs that typically operate at higher rotary speeds but with lower weight-on-bit.

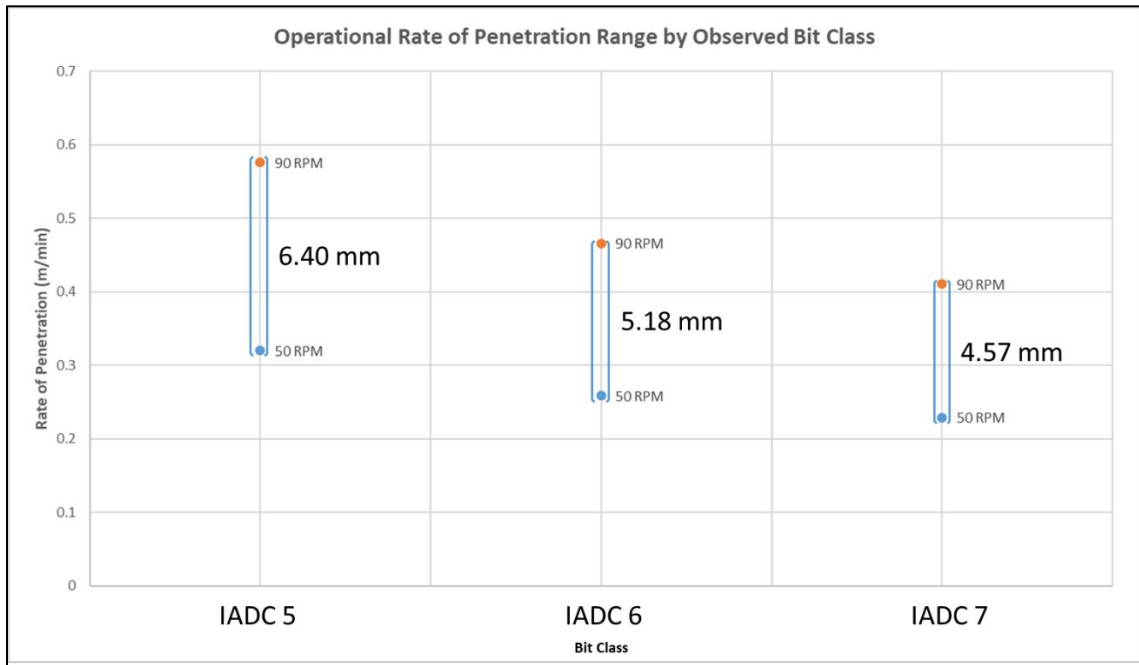


**Figure 4-40: Operational rate of penetration range by observed bit class**

Based upon the observed insert heights during the field testing a linear regression analysis was performed for the relationship between rate of penetration and insert height. The analysis included operational rate of penetration at rotary speeds of 50 and 90 rotations per minute. Figure 4-41 shows the results of the linear regression analysis as well as operational rates of penetration for various insert heights (both observed and projected). The bit type associated with the observed insert heights are noted on the plot. The results of the linear regression for both rotary speed set-points had a fit of  $R^2 = 1$  which denotes a very high fit for the linear trendline. The equations generated by the linear regression for rate of penetration by insert height are

$$y = 0.09x \text{ and} \tag{4.1}$$

$$y = 0.05x, \tag{4.2}$$

for 90 rpm and 50 rpm, respectively.

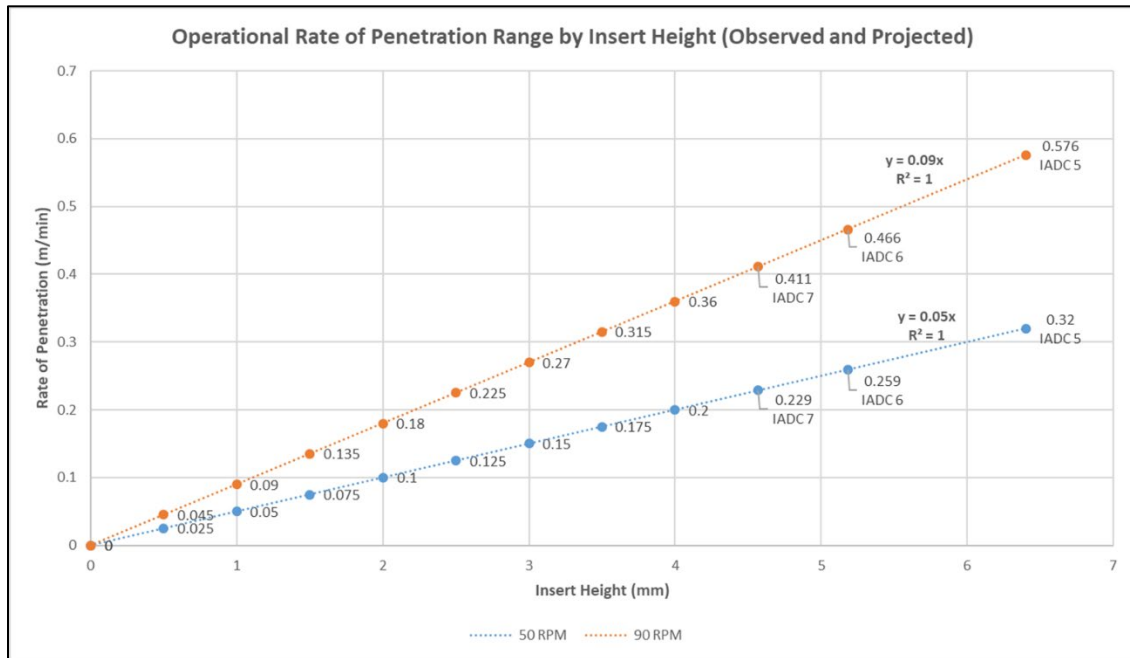


**Figure 4-41: Operational rate of penetration range by bit height (observed and projected)**

Examining Figure 4-41, as the insert height approaches zero so too does the corresponding rate of penetration independent of chosen rotary speed. Thus, it can be stated that for efficient drilling, rate of penetration is proportional to insert height,

$$R \propto \text{insert height} \tag{4.3}$$

Over its operational life the height of a drill bit’s inserts will reduce from full height on a new bit to zero on a completely worn (bald) bit<sup>9</sup>. This phenomenon is illustrated in Figure 4-42 and based upon this it can also be stated that insert height is inversely proportional to total bit operating hours,

$$\text{insert height} \propto \frac{1}{\Sigma t} \tag{4.4}$$

<sup>9</sup> It should be noted that during normal operation a drill bit should be changed at some point before its inserts reach a height of zero, so a drill bit with an insert height of zero would be an over-worn bit.

---

Therefore, using the previous equations for efficient drilling, rate of penetration is inversely proportional to total bit operating hours,

$$R \propto \frac{1}{\Sigma t}. \quad (4.5)$$

However, while typical drill bit operating hours are provided by the OEM, exceptional drilling conditions or poor operator practice can adversely impact the condition of a bit independent of its operating hours. Therefore, present bit condition must also be considered,

$$R \propto C \cdot \frac{1}{\Sigma t}. \quad (4.6)$$

Based upon the above analysis, the input to a drill control system from a bit wear monitoring solution should attempt to quantify the present bit condition and track the total operating hours with respect to OEM specifications for the bit. The drill control system should then select the appropriate rate of penetration based upon this bit wear input.



**Figure 4-42: Comparison of new and completely worn drill bit**

---

## Chapter 5

### Considerations for Automation – Additional Drill Cycle Components

#### 5.1 Hole to Hole Movement (Propel)

The propel function moves the blasthole drill from hole to hole as well as to various locations on a mining bench. The drill may also be propelled over longer distances from one location within the mine to another. However, due to the relatively slow speeds with which the drill rig propels the drill will often be towed on a flatbed for any long distance repositioning. If a drill rig is powered electrically then the trailing cable and corresponding power supply also make longer distance movement problematic thus reinforcing towing.

The blasthole drill rig studied for this chapter utilizes two axial piston variable hydraulic motors with a nominal pressure of 350 bar and a peak pressure of 400 bar. Each hydraulic motor drives the propel circuit for one crawler track (left and right). Of the three industry leading OEMs, two are confirmed to use the model of propel motor analyzed in this Chapter. The third OEM uses an equivalent style of hydraulic motor for propel.

##### 5.1.1 Propel Motor Response Testing and Modelling

For propel motor response testing, a test drill rig at a partner mine site was instrumented with track motor speed sensors. The partner mine site was a working Canadian surface mine. The speed sensors utilized were a Hall-effect style dual sensor for contactless speed measurement. The speed sensor is offered as an option by the hydraulic motor manufacturer. The hydraulic motors are internally designed to be instrumented for

potential scalability to autonomous application. However, prior to testing the mine operator was not using any drill autonomy and the drill OEM did not offer an autonomous option.

During field testing motor response data was collected. The data is shown in Figure 5-1 below.

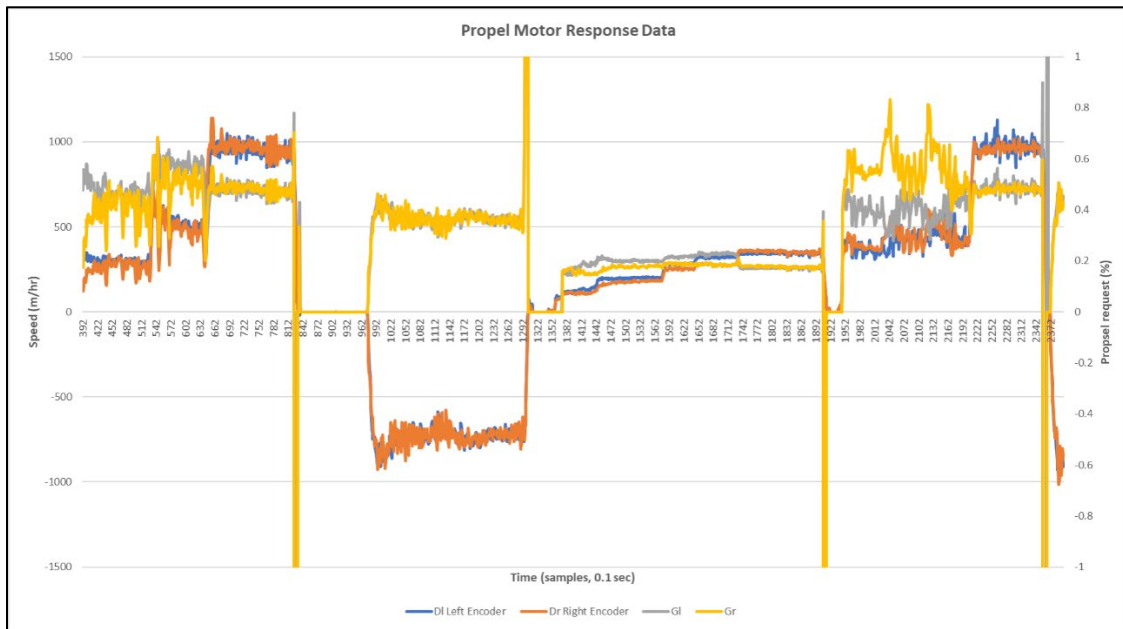


**Figure 5-1: Propel motor response data**

Examining Figure 5-1, it should be noted that four signals are displayed: Left Encoder Displacement (DI), Right Encoder Displacement (Dr), Left Track Gain (GI), and Right Track Gain (Gr). For this plot Gain is defined as the ratio of track encoder displacement to track voltage input request. Included within the logged response data the signals track voltage input request (left and right) are also available. It should also be noted that the plot contains track responses for both available propel speeds (normal and slow). In

Figure 5-1 the period of slow propel speed response testing is denoted. The rest of the response testing was conducted at normal speed.

For reference the two available propel speeds for the test rig are given below.

- Slow speed range: 0 – 0.44 km/h
- Normal speed range: 0 – 1.45 km/h

The OEM recommends the slow propel speed for inexperienced operators or when manoeuvring in tight locations or for hole to hole movement within blast patterns. The OEM recommends the normal propel speed for experienced operators or when moving from one site to another (outside of hole to hole movement). For an automated drill cycle application slow propel speed applies.

For a better understanding of how each propel motor performs the left and the right crawler tracks are explored independently.

Figure 5-2 and Figure 5-3 show the unscaled input-output responses for the left and right propel motors, respectively.

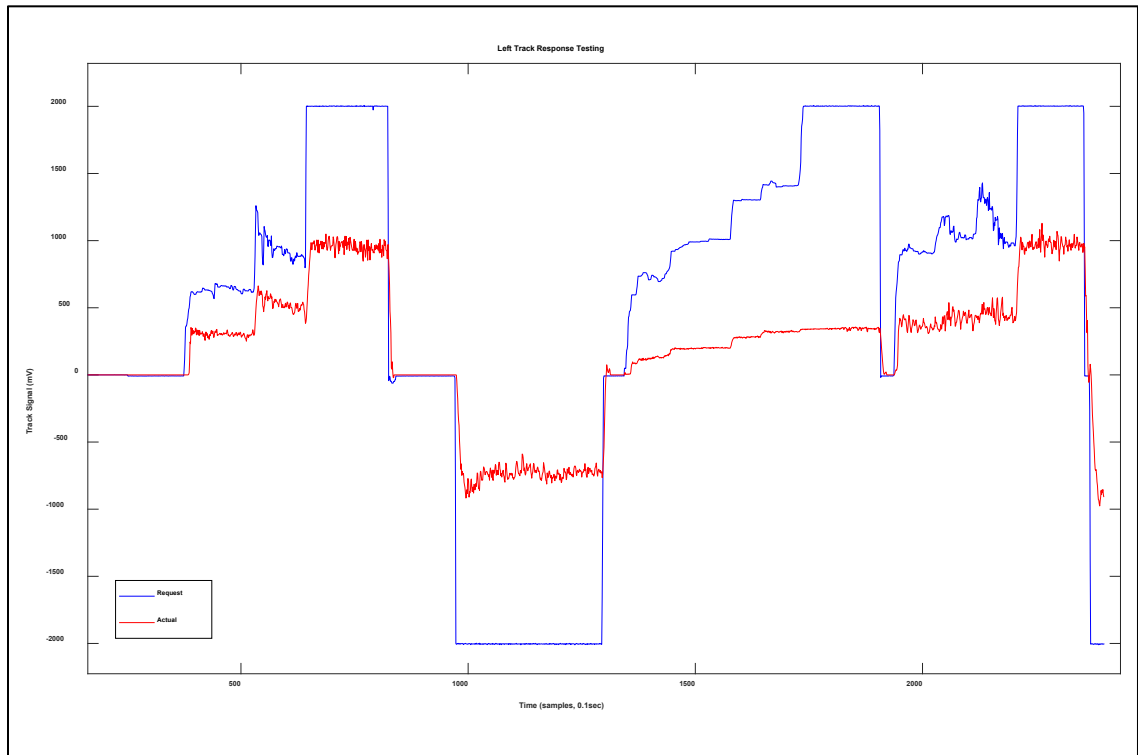


**Figure 5-2: Left propel motor input-output (unscaled)**

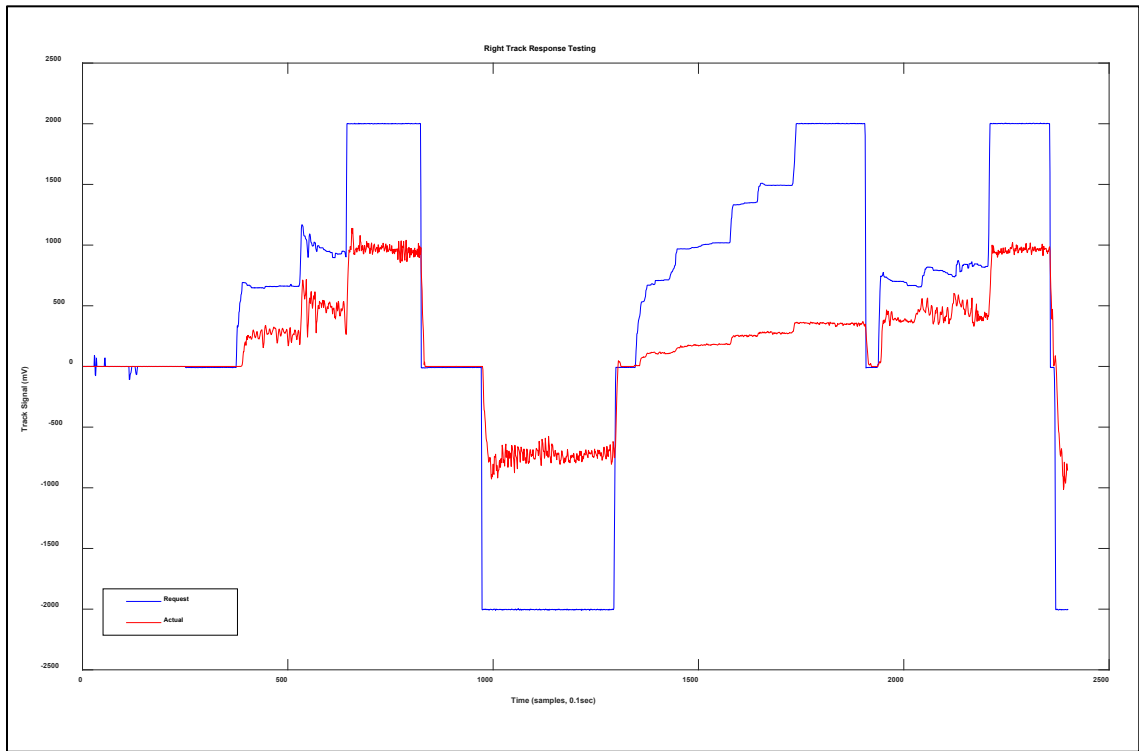


**Figure 5-3: Right propel motor input-output (unscaled)**

Examining Figure 5-2 and Figure 5-3 with emphasis on the slow propel speed section, it becomes apparent that the input signal and output response are not consistent with the normal propel speed sections and, therefore, the track motor speed ranges must be modelled independently.

The following two figures are the scaled left and right track input-output responses, respectively. For the normal propel speed sections the fit between the signal request and track motor output is more easily understood with scaling applied. The scaling assumes that an input of 2 volts is equal to 100% track motor request – this assumption is based on field testing and observation. Also, it assumes that the track motor encoder value of 1,000 is equal to 100% track motor output. At this time both conversions are assumed linear

from 0 to 100%. The scaling coefficients were taken from the respective OEM literature for the drill rig and the hydraulic motor.

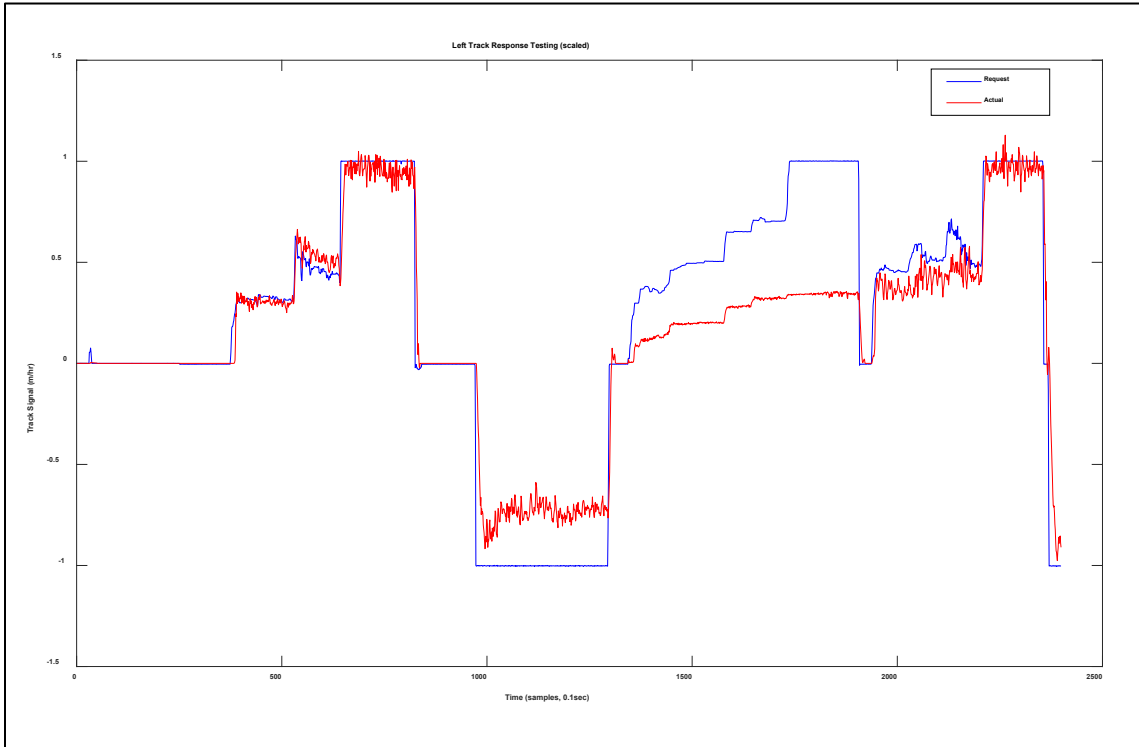


**Figure 5-4: Left propel motor input-output (scaled)**

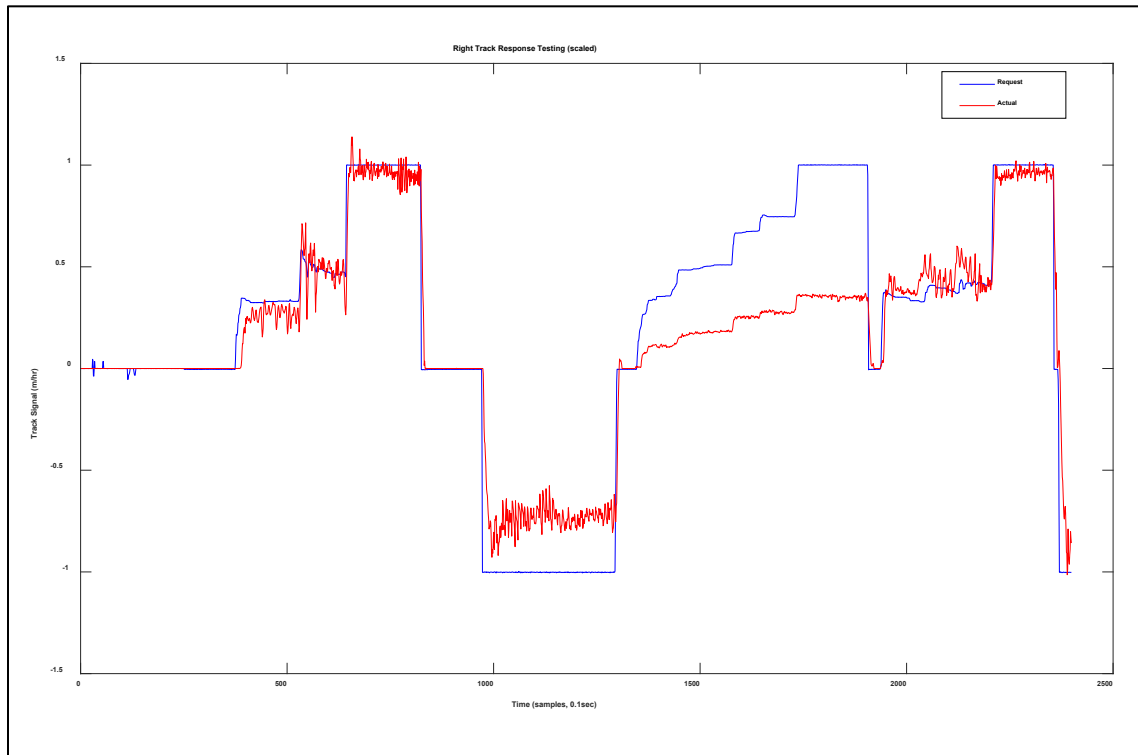


**Figure 5-5: Right propel motor input-output (scaled)**

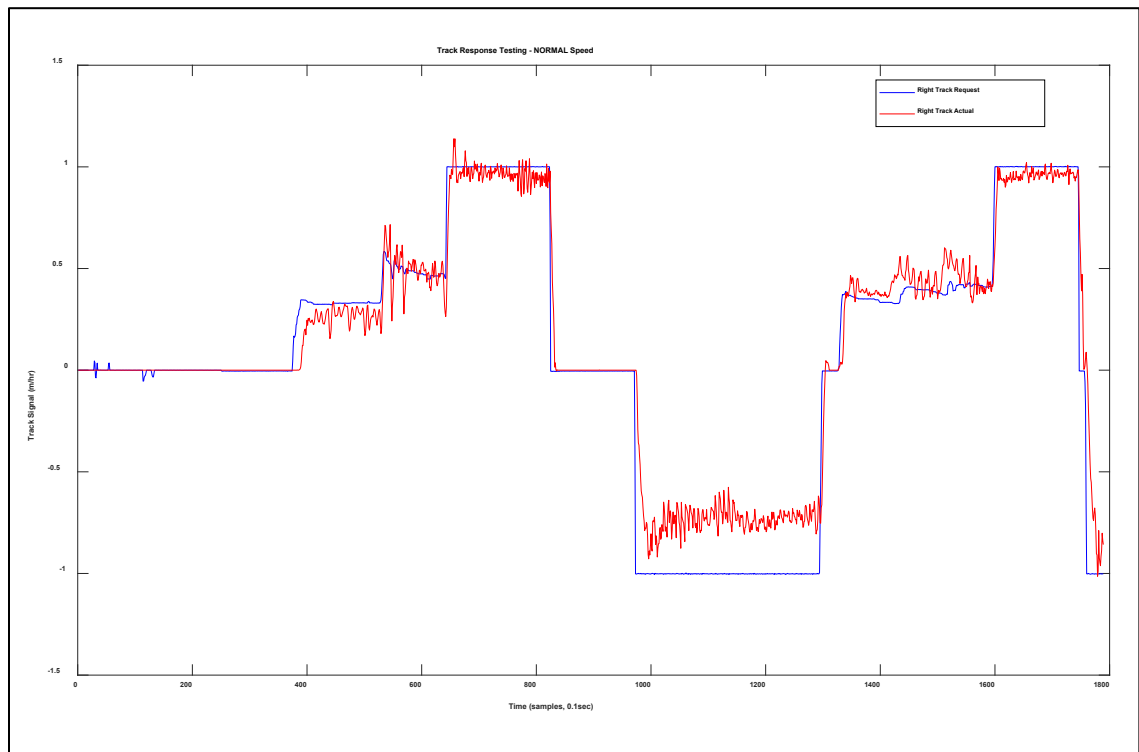
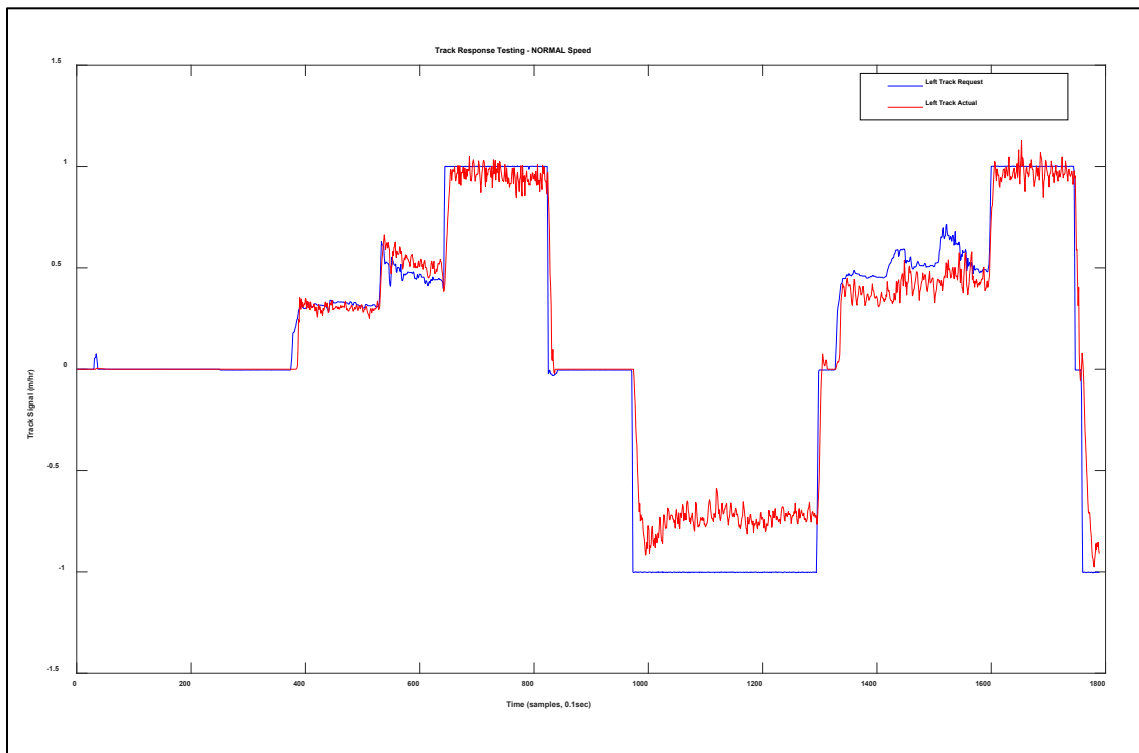


**Figure 5-6: Normal propel speed track response testing (scaled)**

---

Figure 5-6 shows that the inputs for the left and right propel motors do not match. This is due to the manner in which the response testing was conducted – manually via the propel master joysticks which was a non-exact input mechanism for non-zero and non-maximum inputs. Figure 5-6 also shows that the responses of the left and right propel motors, while similar, do have minor variations.

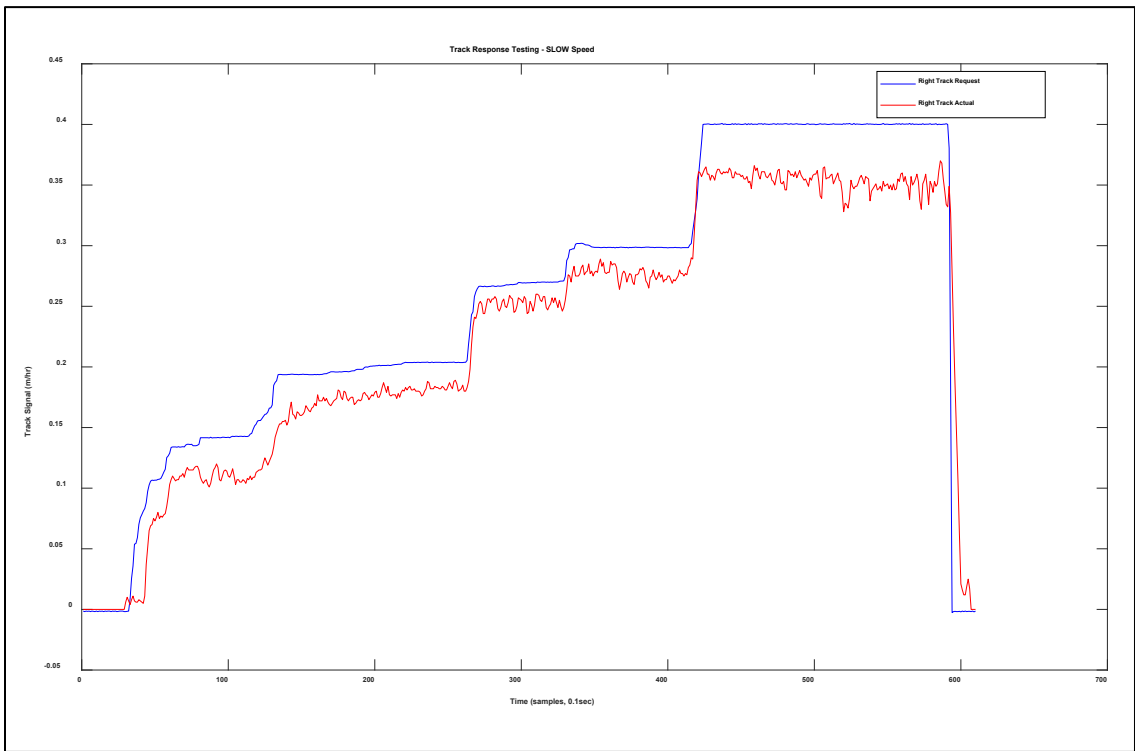
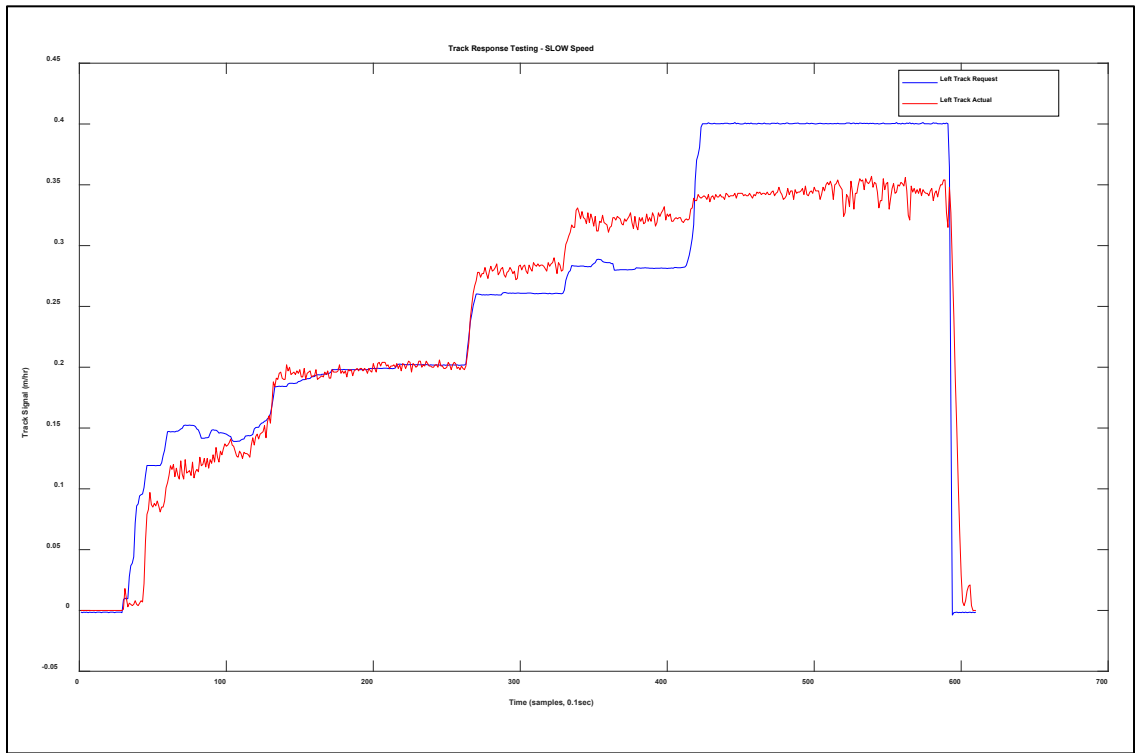


**Figure 5-7: Slow propel speed track response testing (scaled)**

---

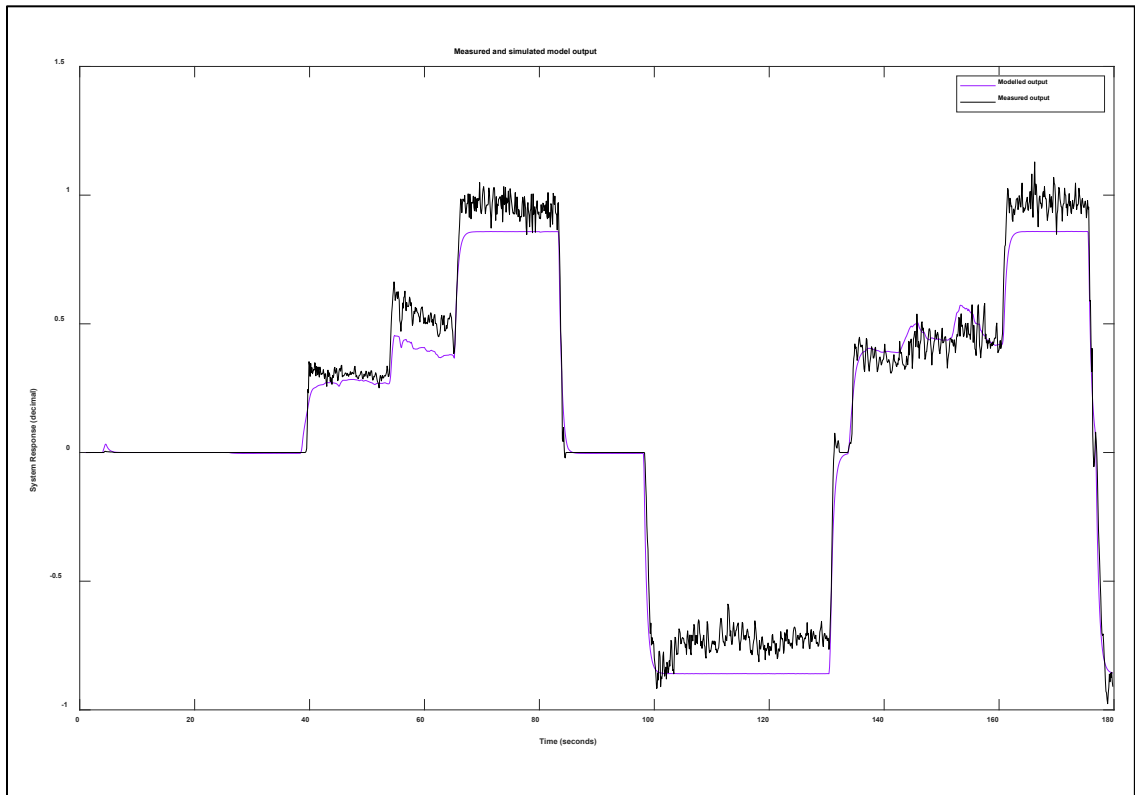
To scale the slow propel speed track motor input-output data it was assumed that 100% input request corresponded to 40% track motor output response. This assumption was based on a visual inspection of the data. A more precise conversion was not available as the OEM documentation lacked this information.

Examining Figure 5-7 it is once again evident that the inputs for the left and right propel motors do not match and that the responses of the left and right propel motors, while similar, do again have minor variations.

Using the track response test input-output data, dynamic system models were created for the left and right propel motors at both slow propel and normal propel operating speeds. This was done using the MATLAB System Identification Toolbox.

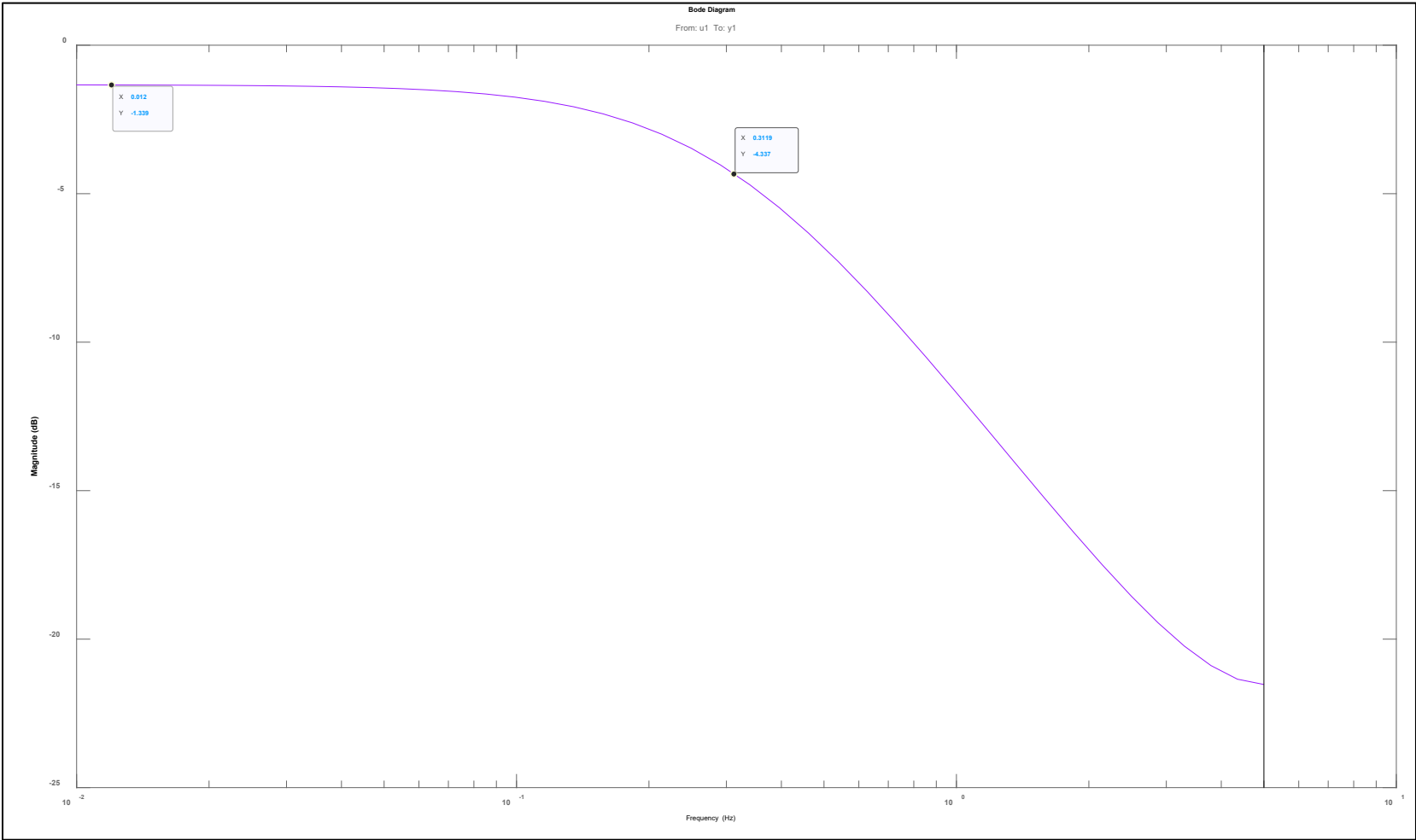
The left track, normal propel speed model had a fit of 83.45. This fit was considered acceptable for simulation based testing. Although unnecessary, with more response test data it was expected that the fit could be improved. Figure 5-8 and 5.1 show a comparison of measured to simulated model output and the corresponding transfer function for the derived model, respectively.

Figure 5-9 shows a magnitude only Bode plot of the left track, normal propel speed model defined by 5.1. Highlighted on the plot is the -3 dB point relative to the d.c. gain, at a frequency of approximately 0.312 Hz. This is indicative of the natural frequency of the system. Note that the Bode plot is only defined up to 5 Hz since that is the Nyquist frequency for a 10 Hz sampling rate.



**Figure 5-8: Left propel motor, measured and simulated model output – normal propel speed**

$$H(z) = \frac{0.1538z}{z^2 - 0.8218z} \tag{5.1}$$

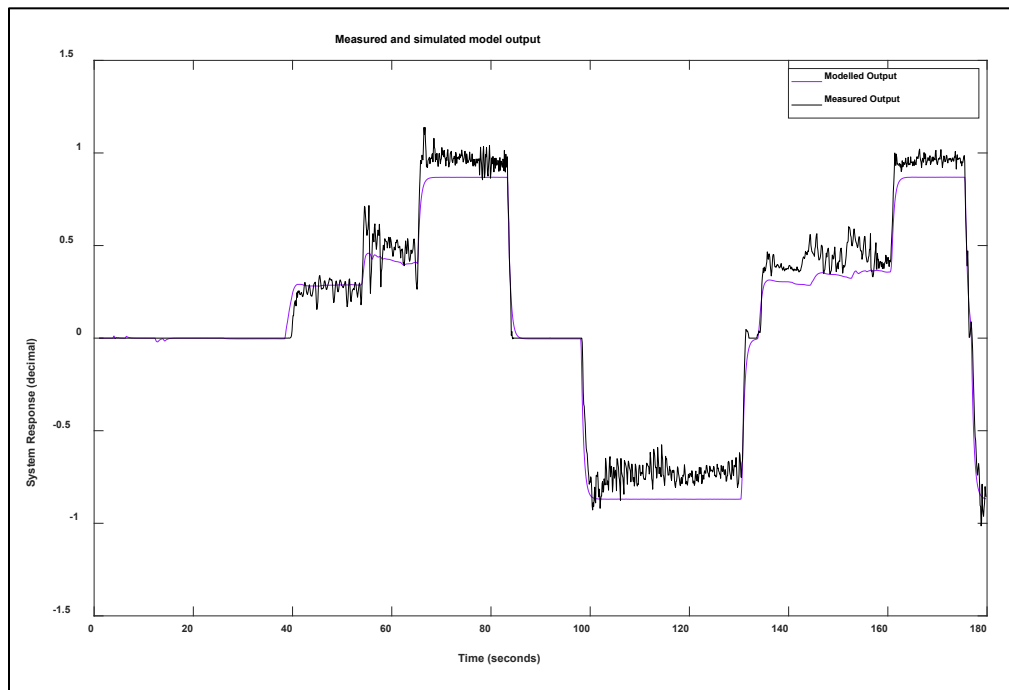


**Figure 5-9: Bode magnitude plot – left propel motor, normal speed**

The right track, normal propel speed model had a fit of 81.91. This fit was considered acceptable for simulated testing. Although unnecessary, with more response data it was expected that the fit could be improved. The comparison of measured to simulated model output and the corresponding transfer function for the derived model is provided.

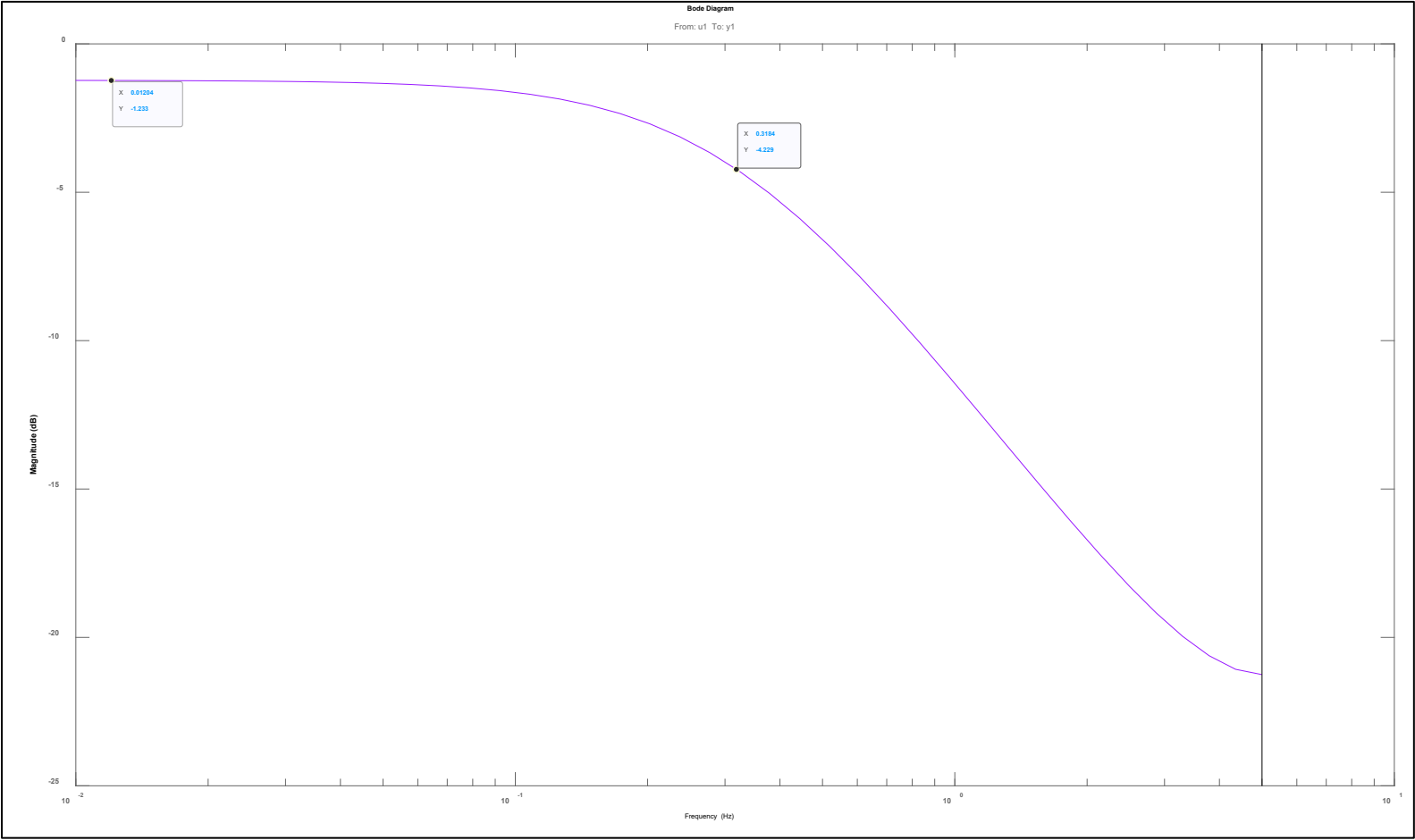
Examining 5.1 and 5.2 it can be seen that models for the left and right track motors at normal propel speed are almost identical. Based upon the data available these motors can be thought of as interchangeable at normal propel speed operation.

Figure 5-11 shows a magnitude only Bode plot of the right track, normal propel speed model defined by 5.2. Highlighted on the plot is the -3 dB point relative to the d.c. gain, at a frequency of approximately 0.318 Hz. This is indicative of the natural frequency of the system. Note that the Bode plot is only defined up to 5 Hz since that is the Nyquist frequency for a 10 Hz sampling rate. The Bode plot reinforces the observed equivalency of the left and right propel motors during normal speed operation.



**Figure 5-10: Right propel motor, measured and simulated model output – normal propel speed**

$$H(z) = \frac{0.1574z}{z^2 - 0.8187z} \tag{5.2}$$



**Figure 5-11: Bode magnitude plot – right propel motor, normal speed**

The left track slow propel speed model had a fit of 70.16. This was the worst fit of the four derived models however was still considered acceptable for simulated testing. More response data is recommended for all input-output testing but particularly for the left track at slow propel speed operation. However, the validity of this model was strengthened due to its similarity to the right track, slow propel speed model that will be subsequently presented and discussed. The comparison of measured to simulated model output and the corresponding transfer function for the derived model are provided in Figure 5-12 and 5.3. The Bode magnitude plot is given in Figure 5-13.

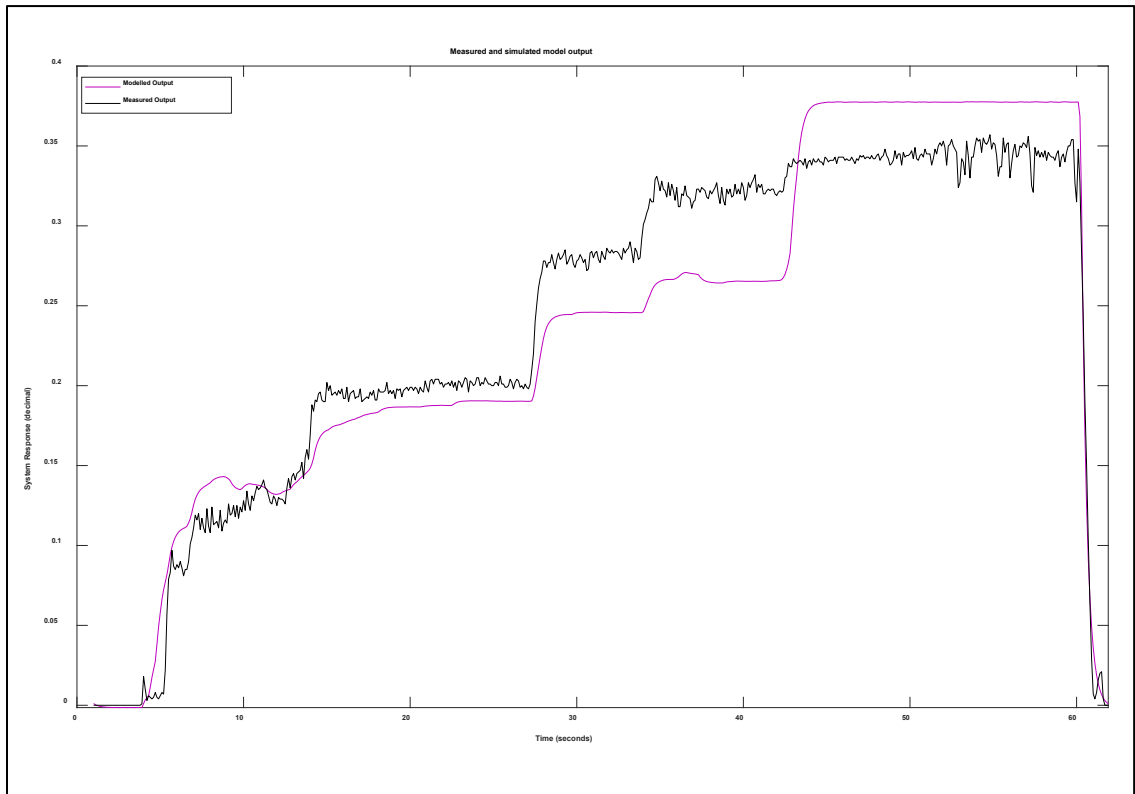


**Figure 5-12: Left propel motor, measured and simulated model output – slow propel speed**

$$H(z) = \frac{0.2467z}{z^2 - 0.7383z} \tag{5.3}$$

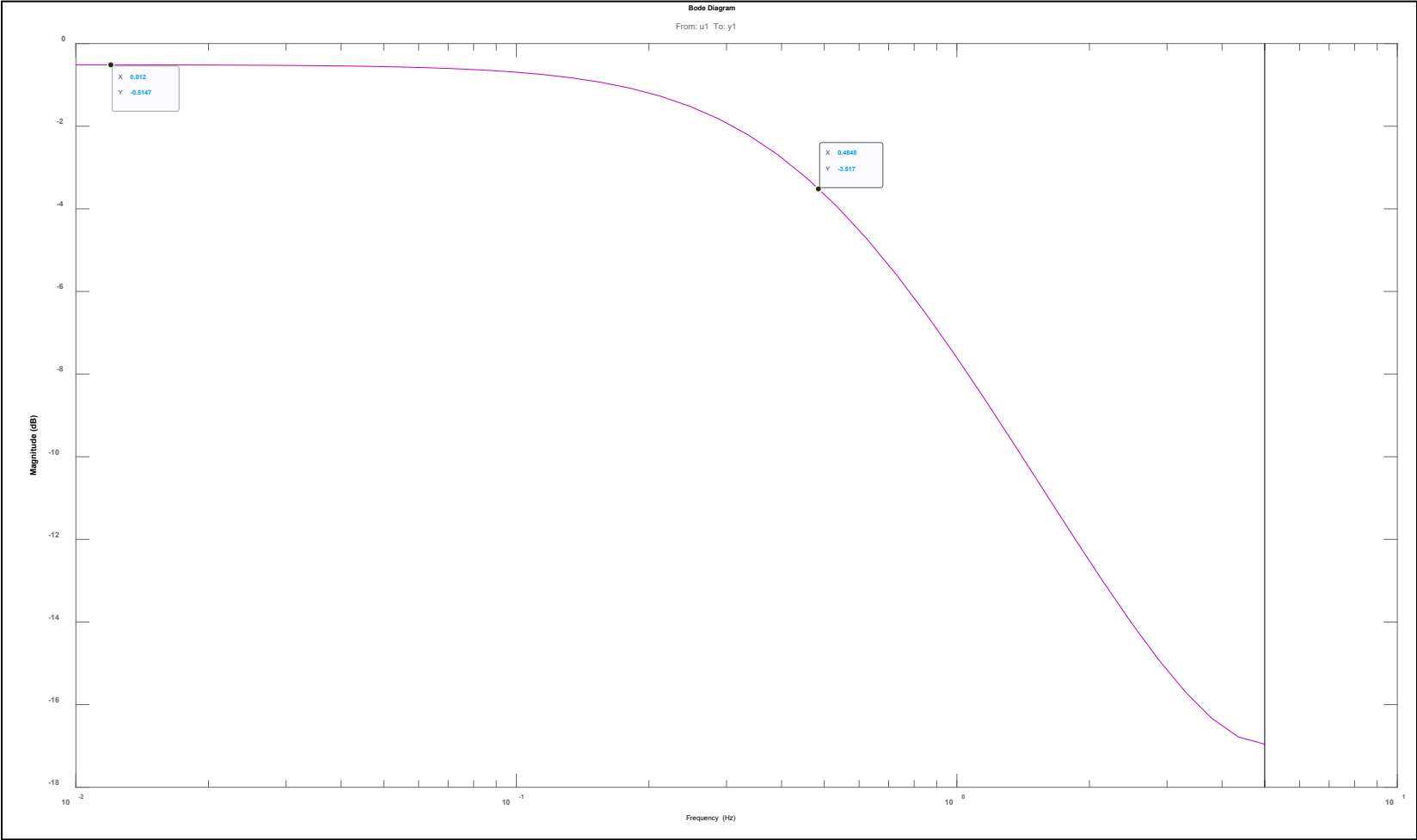
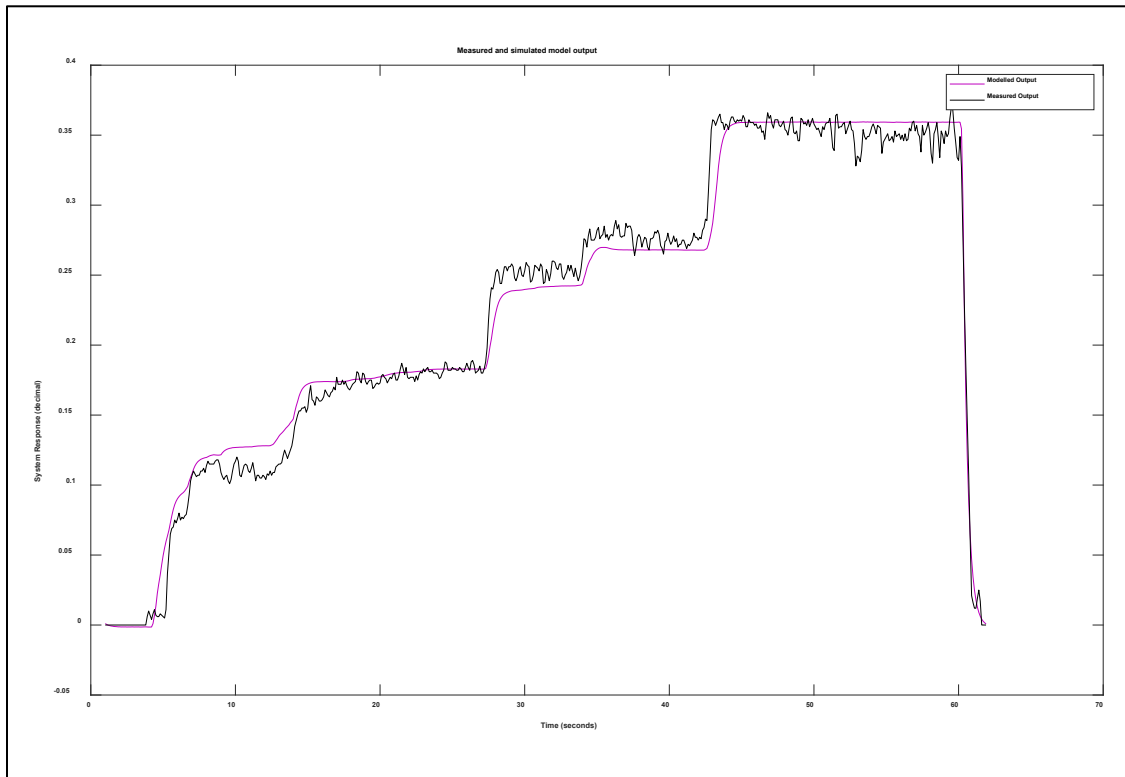


Figure 5-13: Bode magnitude plot – left propel motor, slow speed

The right track slow propel speed model had a fit of 87.78. This was the best fit of all the models and was considered acceptable for simulated testing. Although unnecessary, with more response data the fit may be further improved. The comparison of measured to simulated model output, the corresponding transfer function for the derived model, and the Bode magnitude plot are provided.



**Figure 5-14: Right propel motor, measured and simulated model output – slow propel speed**

$$H(z) = \frac{0.2369z}{z^2 - 0.7361} \tag{5.4}$$

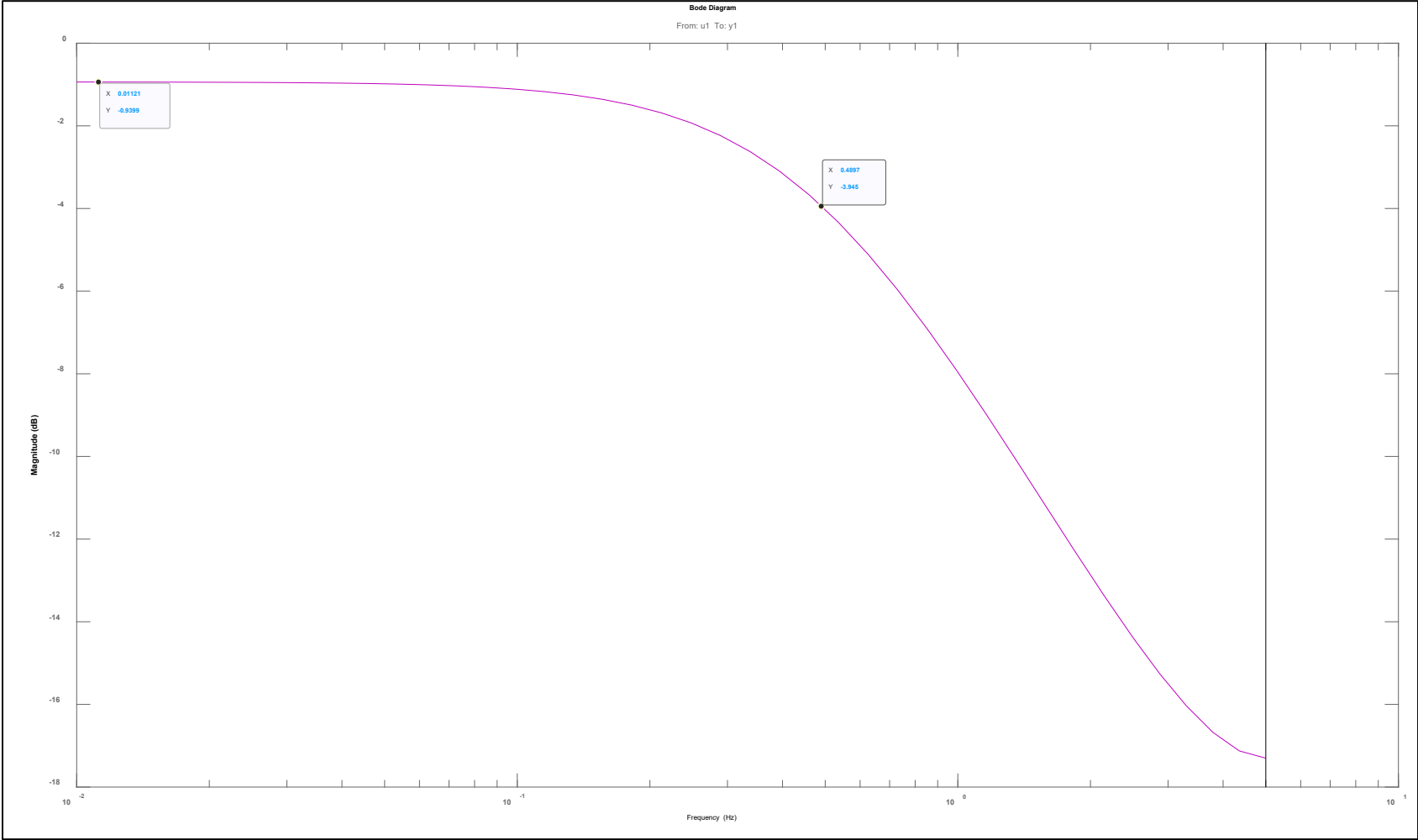


Figure 5-15: Bode magnitude plot – right propel motor, slow speed

As previously stated, examining 5.3 and 5.4 it can be seen that the models for the left and right track motors at slow propel speed are almost identical. From this observation and the previously observed similarity of the left and right normal propel speed models, the validity of the left slow propel model is strengthened despite the worse fit. Based upon the data available the derived models show that the left and right track motors on drill 226 (the test rig) have some differences but they are relatively minor and can be modelled as interchangeable.

In addition, the results show that the motor responses vary based upon operating speed. However, the same feedback controller could be used for both operating speeds so long as the inputs are properly scaled to the corresponding operating speed and the integral gain block (if used) is reset when operating speed is altered to avoid integral wind-up.

Section 5.1.2 explores feedback control for the propel motors as well as an overall control solution for drill rig propel and positioning.

### **5.1.2 Propel and Positioning Control**

Based upon the propel motor response testing, analysis and modelling in Section 5.1.1 it was demonstrated that a feedback control loop would be well suited for the propel motor speed control application. A classic two-tiered feedback control solution is proposed to accommodate both the propel motor speed application and the overall drill rig hole to hole positioning application. The proposed two-tiered controller is shown in Figure 5-16.

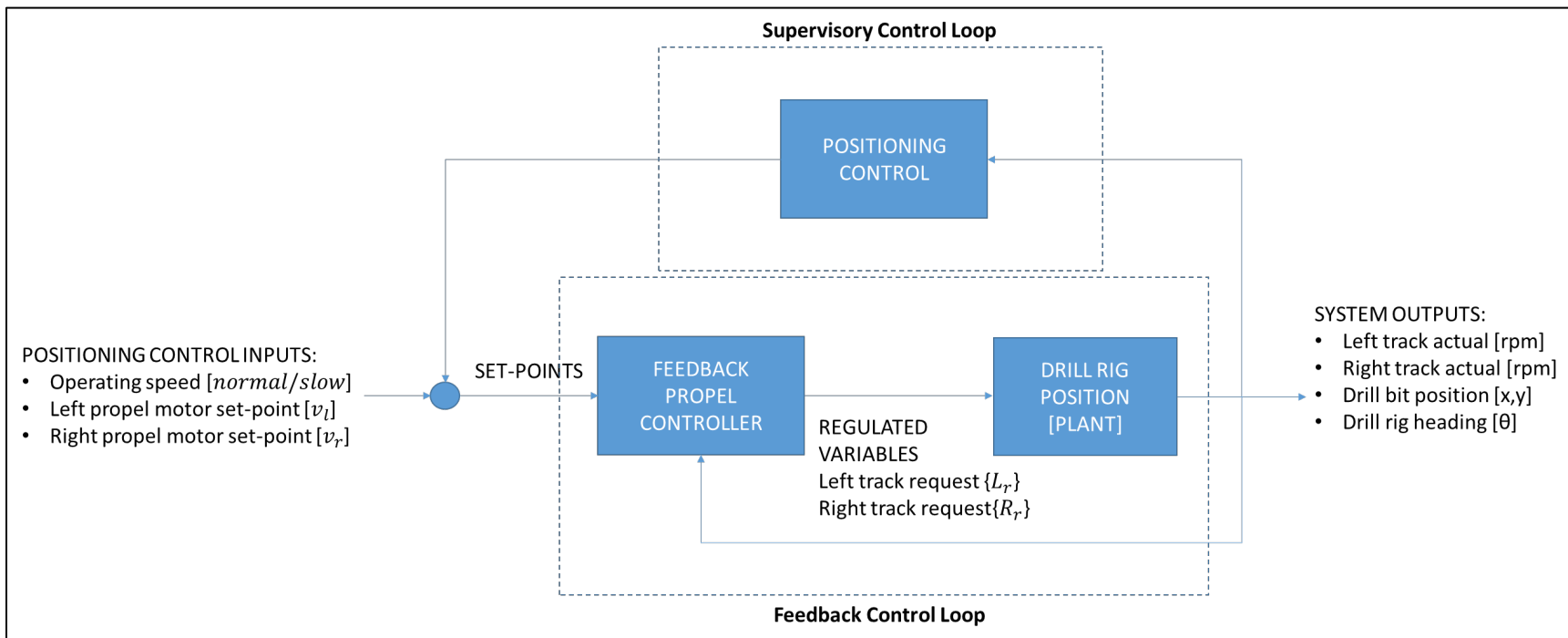


**Figure 5-16: Two-tiered propel and positioning controller**

With reference to Figure 5-16, the lower level, higher frequency feedback control loop is for propel motor speed control. The set-points to the propel controller are left and right track speed request (in rpm). The feedback signals to the propel controller are left and right track speed actual (in rpm). The purpose of this control loop is to provide a correction based on observed error in the actual track speeds with respect to the requested track speeds.

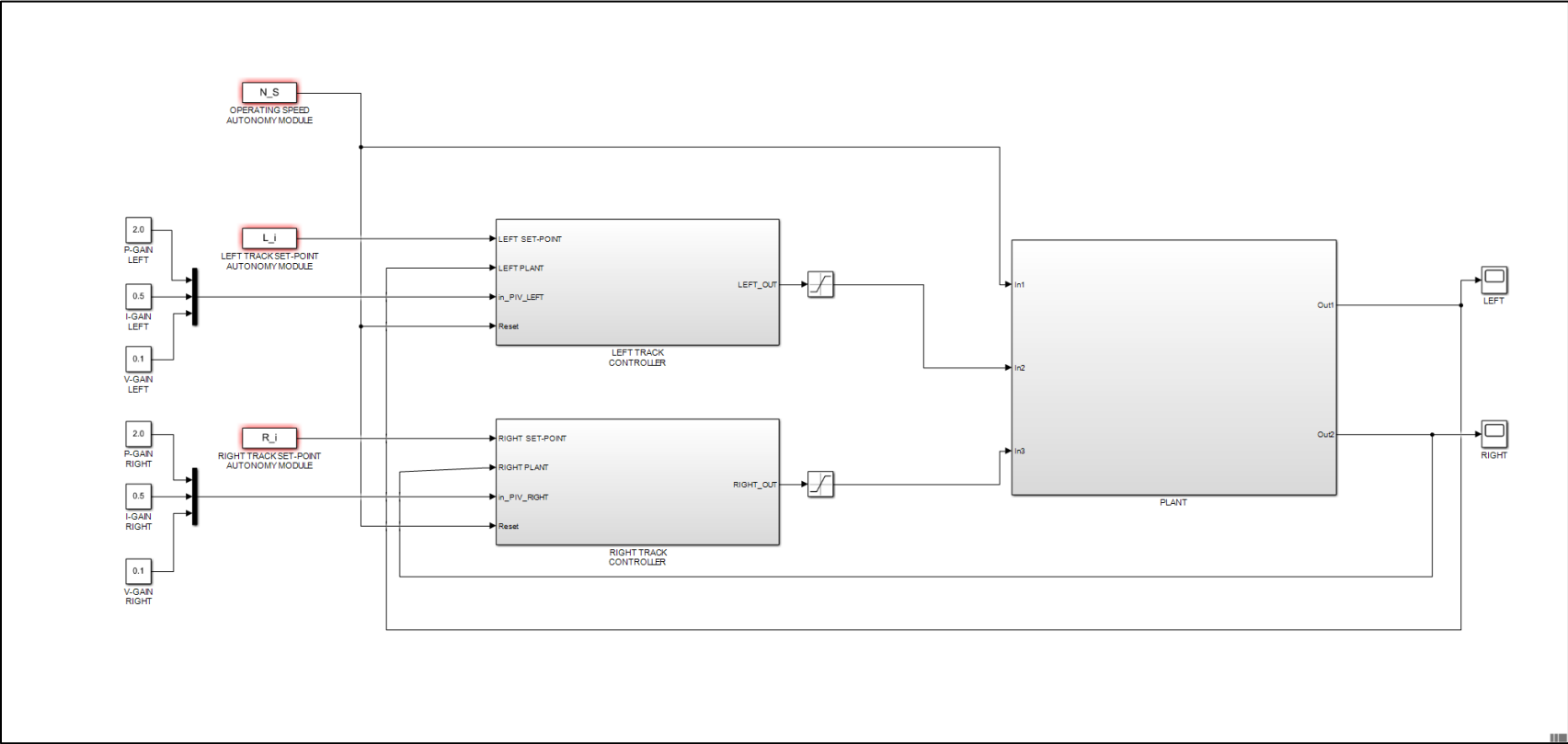
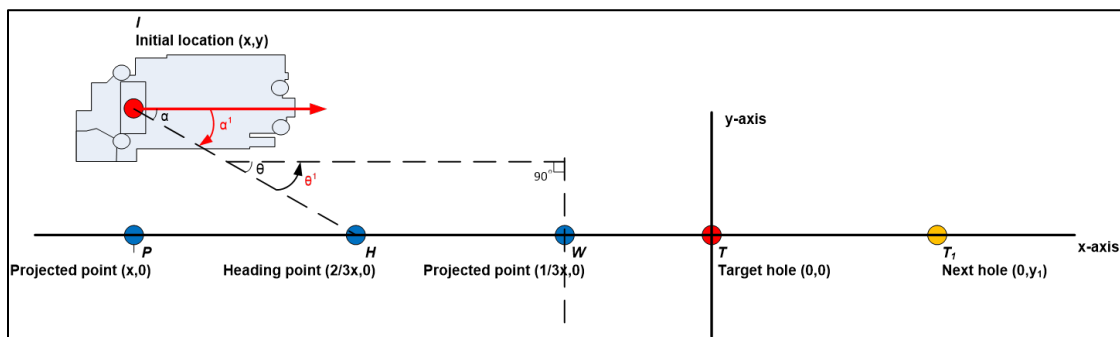


Figure 5-17: Propel motor speed control solution

Figure 5-17 shows the propel motor speed controller in more detail. The left and right track set-points are provided by the higher level supervisory controller. The gains for the track set-points are provided by the higher level supervisory controller. The gains for the PID controllers are separately configurable for the left and right propel motor to allow for variations in motor performance over the life of the equipment. The controller has also been designed to operate effectively in normal or slow propel speed however for the hole to hole movement application only slow propel speed will be used.

The higher level, lower frequency supervisory control loop is for drill rig position control. The set-points to the position controller are drill bit position request (in x and y GPS coordinates) and drill rig heading request (in degrees). The feedback signals to the position controller are drill bit position actual (in x and y GPS coordinates from the mine site HPGPS solution) and drill rig heading actual (in degrees). The purpose of this control loop is to provide a correction based on observed error in the actual drill bit position and drill rig heading with respect to the requested drill bit position and drill rig heading. The overall drill rig position control philosophy employed is illustrated in Figure 5-18 and is described in detail below.



**Figure 5-18: Drill rig position control philosophy**

---

When the drill rig position control is activated the drill rig is located at the initial location ( $I$ ).  $I$  will have some initial coordinates  $(x,y)$ . The target production hole ( $T$ ) is supplied to the controller in mine site GPS coordinates. A local x-y coordinate system is established by the propel controller based upon assigning  $T$  the x-y position  $(0,0)$ . The drill rig's initial position ( $I$ ) is subsequently also defined. The x-axis of the local coordinate system is established so that both  $T$  and the next hole ( $T_1$ ) in the autonomous mission are along the x-axis. Therefore,  $T_1$  can be given the x-y position  $(0, y_1)$ .

Gateway points are defined in a manner consistent with what is described above. The projected point ( $P$ ) is simply the point on the x-axis that corresponds to the x-component of  $I$ . Therefore,  $P$  is located at  $(x,0)$ . The heading point ( $H$ ) is one third of the distance between  $T$  and  $P$  and the projected point ( $W$ ) is two thirds of the distance between  $T$  and  $P$ .

The first controller induced drill rig movement is to align the drill rig's heading with the heading point  $H$ . This movement is purely rotational and is denoted by  $\alpha^1$ . The movement is accomplished by propelling with one crawler track only thereby pivoting the drill about its centre of rotation. For the example drill rig and target hole orientation in Figure 5-18, this step would be accomplished by the left track propelling and the right track being held stationary.

The second controller induced drill rig movement is to attempt to reach the project point  $W$  through the implementation of Astolfi's control law. This law is reviewed in detail in Section 2.5. The rig movement is controlled in such a way as to attempt to minimize the error in all three positioning components (x-position, y-position, and heading) to zero.

This is accomplished through the movement of the drill rig from  $I$  to  $W$ . The rotational component for heading control is denoted by  $\theta^1$ .

The final component of drill rig movement via the propel controller is a contingency step that ends with the arrival of the drill bit to the target hole  $T$  with the drill rig's heading aligned with the next hole  $T_1$ . This step also implements Astolfi's control law albeit most of the error reduction is accomplished during the previous step. This final component can be thought of as fine tuning on final approach to the target hole.

Once the target hole has been drilled and movement is required from  $T$  to  $T_1$  the same procedure described above is executed by the two-tiered propel and positioning controller. However, since the drill rig's heading should now be aligned with the next hole the required rig movement should be less complex than for the initial target hole. In addition, the frame of reference for the next propel and position sequence resets around the next hole  $T_1$  and the subsequent hole  $T_2$  thereby allowing the propel and positioning controller to be continuously adjusting as a multi-hole mission is executed.

### 5.1.3 Auto-Propel Field Test Results and Discussion

An auto-propel algorithm that implemented the positioning control philosophy outlined in Section 5.1.2 was field tested at a partner Canadian surface mine site on an operating large electric blasthole drill. The following performance metrics were a requirement for the application and both had to be met to consider the auto-propel testing successful:

- Required mine design positioning accuracy 30 cm or better
- Safety mandated positioning accuracy threshold of 65 cm

The first metric for positioning accuracy of 30 cm or better was the pre-existing mine site requirement for manually positioning drill rigs. This was defined by mining engineering and was meant to be a reachable target (considering the mechanical properties of the drill rig and drill bit) that also conformed to the drill and blast design as created by the responsible engineer.

The second metric of upper accuracy threshold for positioning safety is mandated by the mining engineering team and is meant to protect the equipment and human workers from potentially unexploded material from the previously mined bench that sits near the surface of the present to-be-drilled bench. The point of the 65 cm target zone is to ensure that the drill is never drilling into a location that is directly below the bottom of the previously mined bench's production holes and that an appropriate safety offset is respected.

To determine the 2-D positioning accuracy in an x-y coordinate frame of the tested auto-propel algorithm the following root mean square equation was appropriately adapted to 5.6.

$$x_{rms} = \sqrt{\frac{1}{n}(x_1^2 + x_2^2 + \dots + x_n^2)} \quad (5.5)$$

$$d_n = \sqrt{\frac{1}{2}(x_n^2 + y_n^2)} \quad (5.6)$$

The auto-propel algorithm was tested in the movement of the drill rig to 12 production holes. The results of the field testing are provided below.

Time of Test	Positioning Error (distance) [m]
10:17 AM	0.09
10:44 AM	0.20
11:02 AM	0.20
11:22 AM	0.07
11:42 AM	0.07
12:05 AM	0.14
12:37 AM	0.07
1:04 PM	0.07
1:28 PM	0.09
1:53 PM	0.08
2:16 PM	0.07
2:39 PM	0.04

**Table 5-1: Results of auto-propel field test**

Examining the field test results presented in Table 5-1, for the sample set the mean error was less than 10 cm and the recorded positioning error did not exceed 20 cm for any positioning sequence. These results are well within both the safety and design requirement for the application. Based upon these field test results the proposed positioning control philosophy can be considered valid for the application.

**5.2 Auto-Level**

Before a production hole can be drilled the drill rig must be raised and leveled. Raising the rig is required to remove weight from the undercarriage; if the crawler tracks are engaged with the ground during drilling the vibration and resulting drill movement leads to premature component wear and failure of those expensive mechanical components. Levelling the rig is required to ensure that the hole is drilled precisely to plan and that any angle introduced is consistent with the drill and blast design and accomplished through angled drilled via the drill mast as designed by the OEM. Both raising and

levelling of the rig are done simultaneously and are therefore commonly referred to simply as levelling. This terminology will be used in this thesis as well.

For surface rotary blasthole drills levelling is accomplished via four hydraulic cylinders (known as jacks) located near each corner of the machine. The jacks are referred to by their location on the drill as shown in Figure 5-19. The sides of the drill are referred to as cab side or non-cab side in reference to the location of the operator's cabin. The ends of the drill are known as front and rear where, somewhat counterintuitively, the operator's cabin is located at the rear of the drill. While most drills have four hydraulic cylinders some drill models have only three, with the two front jacks having been combined into one larger diameter rear jack. However, the levelling process proposed in this chapter applies to rigs with four jacks or three jacks.

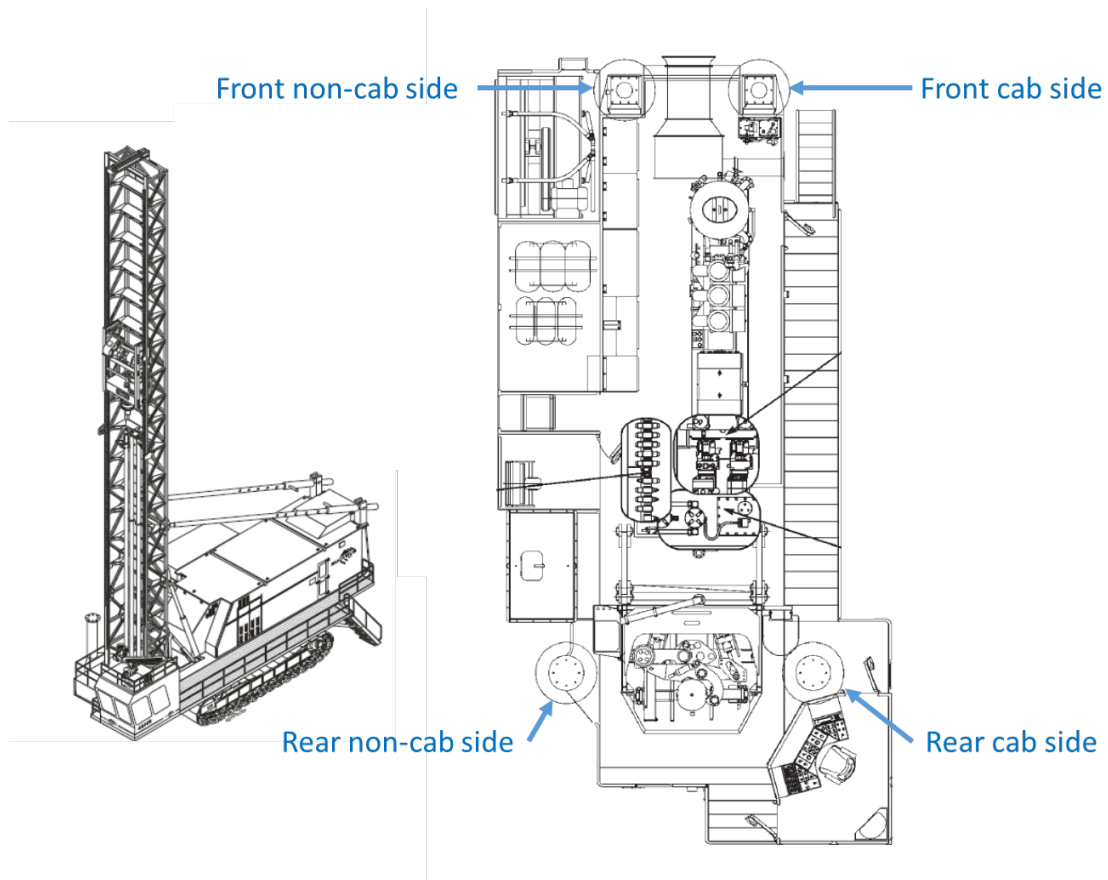


**Figure 5-19: Levelling jacks – location and naming convention**

This section will describe a proposed autonomous level (auto-level) procedure. It will be described on a step by step basis. The procedure will start with the drill rig in an un-leveled state and with all the cylinders fully retracted. The procedure will end with the drill rig raised off the undercarriage and in a leveled state ready to drill.

It should be noted that each hydraulic cylinder is equipped with a ground contact sensor and cylinder full-retract sensor. These will be leveraged by the proposed auto-level solution.

**5.2.1 Ground Contact**

The purpose of this step of auto-level is to capture the initial pitch and roll (and store it as a reference) and to ensure all jacks have attained ground contact. Pitch is measured from end to end; roll is measured from side to side. To prevent tipping drill OEMs provide operational limits for both pitch and roll. The auto-level solution must respect these limits. Once both tasks are accomplished this step has succeeded and auto-level will proceed to the next step. If the tasks cannot be completed the auto-level sequence will abort.

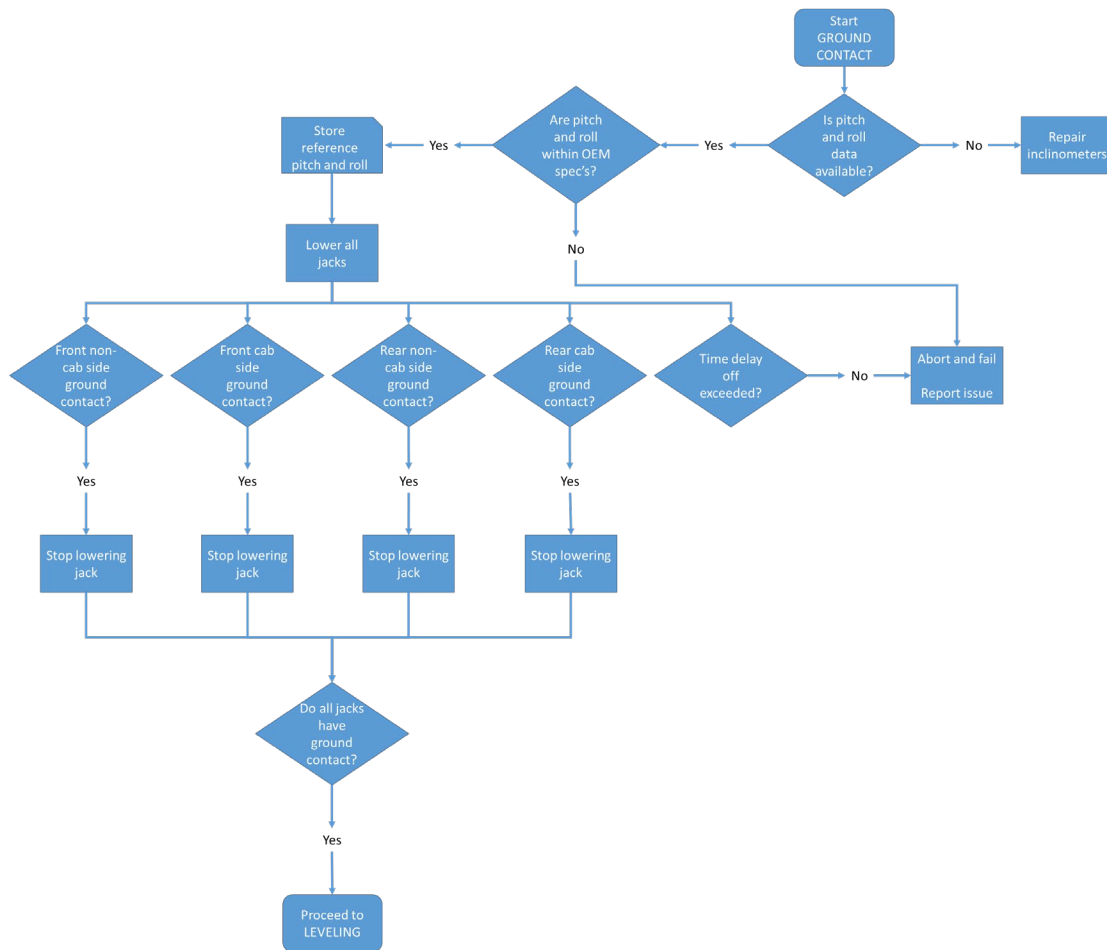


**Figure 5-20: Auto-Level – ground contact**

### 5.2.2 Levelling

This step of the auto-level solution encompasses the main purpose of auto-level – levelling of the drill rig. During this step OEM pitch and roll limits are constantly monitored and auto-level is aborted if any limits are exceeded. At the end of this step the drill is raised, and level and drilling may commence.

To explore levelling, data was collected from a drill rig operating at a working surface mine site and the results provided in the figures below. A typical levelling sequence is shown in Figure 5-21 and Figure 5-22 which display the drill rig roll and pitch, respectively. The target level state for each is also provided on the plots. The OEM suggested levelling sequence is to first accomplish a rig level state side to side (roll) and then proceed with attaining a rig level state front to back (pitch) while at the same time maintaining the side to side level state.

Examining the figures, the drill rig first attains a level state with respect to roll before attaining the level state with respect to pitch. While the pitch angle is adjusted the roll angle is maintained constantly at the level angle position. At the end of the levelling sequence both axes are in an acceptable level state.

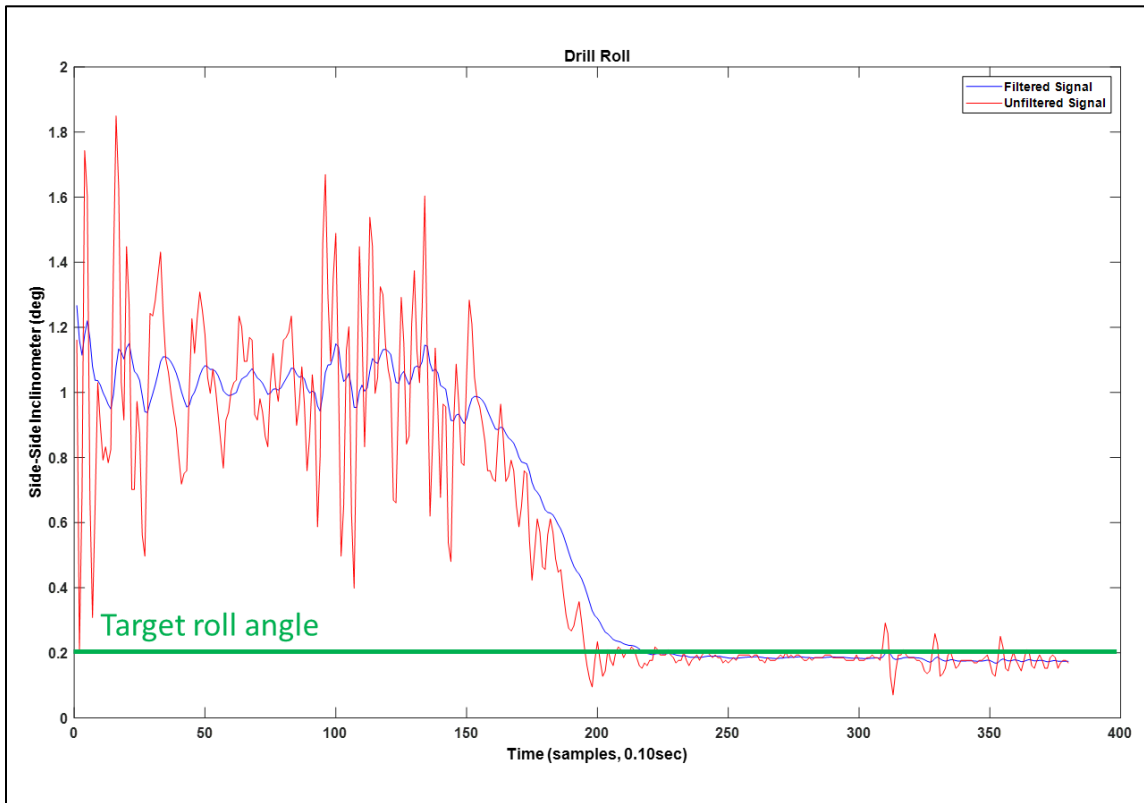


**Figure 5-21: Level sequence – drill rig roll axis**

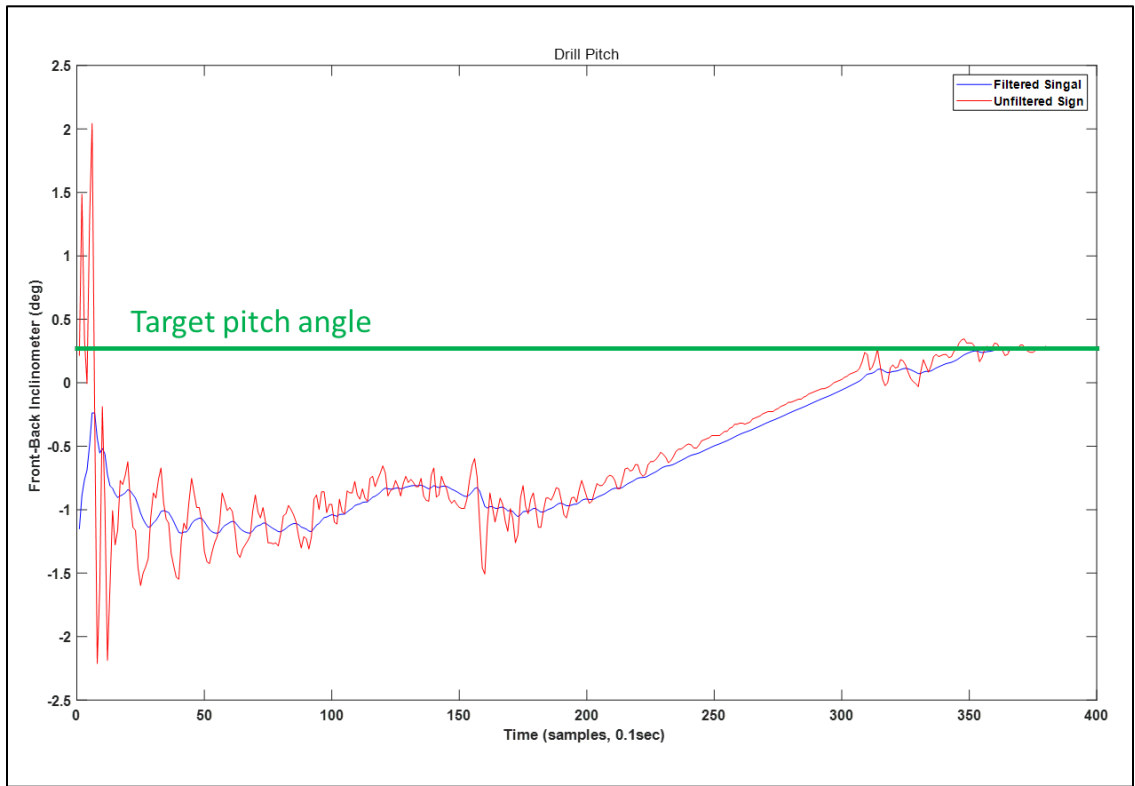


**Figure 5-22: Level sequence – drill rig pitch axis**

The proposed auto-level sequence is provided in Figure 5-23 below.

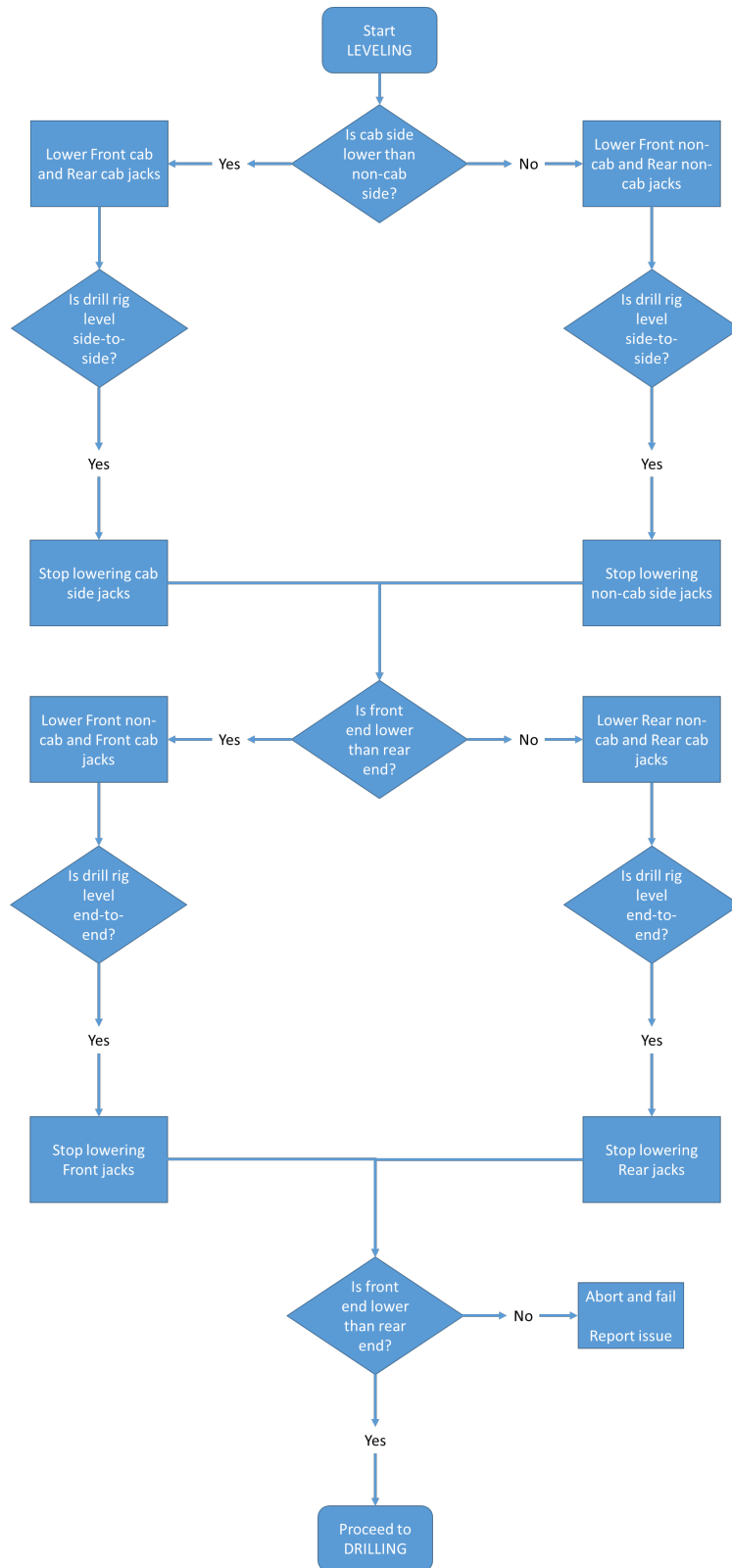


Figure 5-23: Auto-Level – levelling

### **5.2.3 Lowering**

Once drilling has completed, the drill rig must be lowered back to ground level so that all weight is resting on the undercarriage (crawler tracks). This is required even if the drill is going to be left idle in the near term. Throughout the lowering process it is very important that the drill remain level. When operating on a level surface this is easier as it just entails retracting all jacks simultaneously; when operating on a sloped surface this is challenging as the jacks must be retracted in such a way that the drill remains level and excessive twisting of the main frame is avoided. For the auto-level solution sloped ground must always be assumed. The lowering sequence reviewed below is designed to accommodate sloped ground and will also facilitate lowering on a level surface.

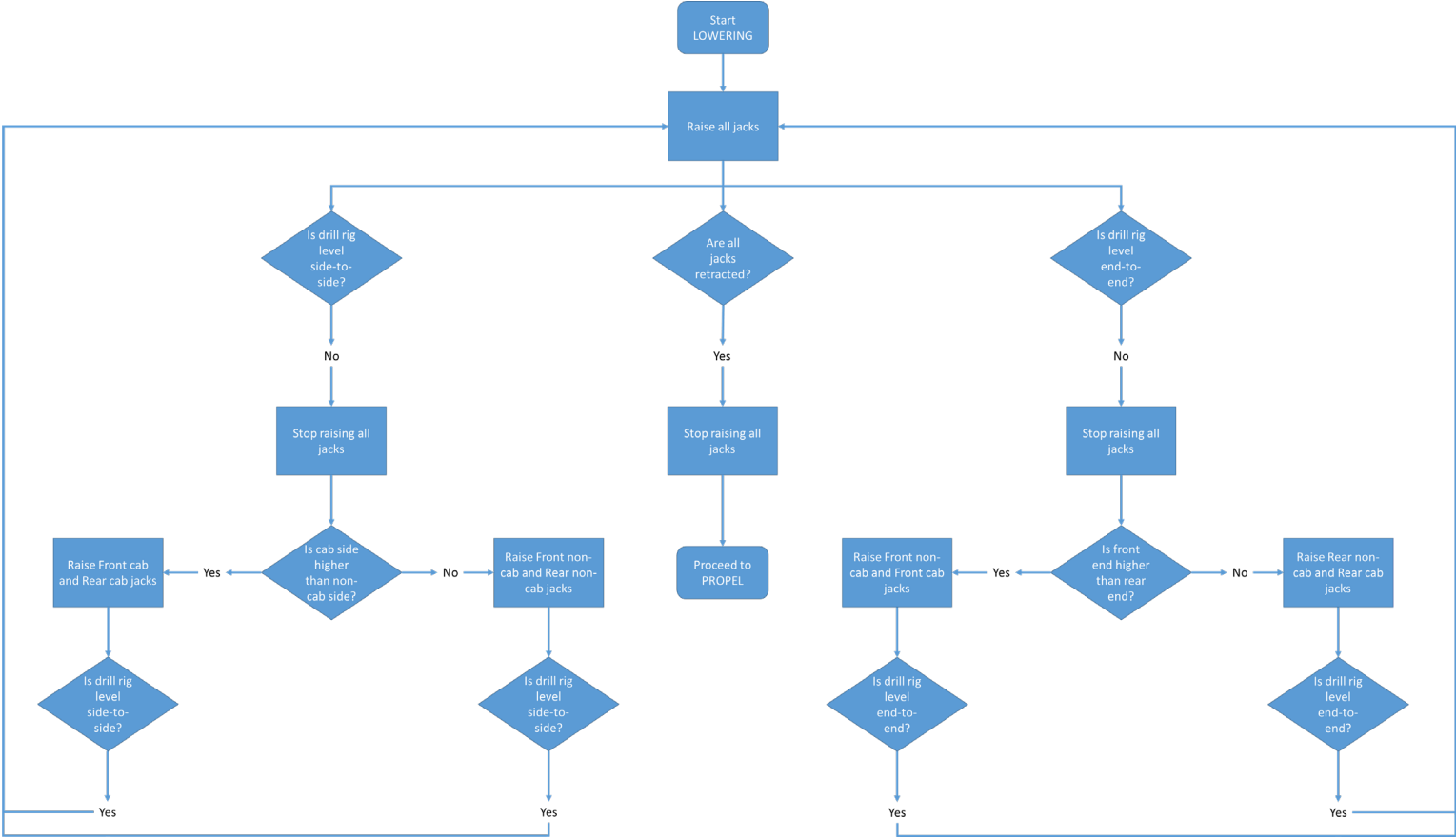


Figure 5-24: Auto-Level – lowering

## Chapter 6

### Smart Pattern Layout

This chapter will describe a proposed autonomous blast pattern layout function (referred to as *smart pattern layout*). The purpose of the smart pattern layout tool is for utilization by the proposed autonomous drilling solution. As such, the smart pattern layout tool's functionality will be limited to conventional blasting and vertical, single pass holes.

These restrictions are consistent with the proposed autonomous drilling solution's operation.

A blast pattern used for production drilling in surface mining has several variables that can be configured to suit the mine site's production targets and the in-situ environment of the zone that is to be blasted. These variables and the associated blasting nomenclature are given in Figure 6-1.

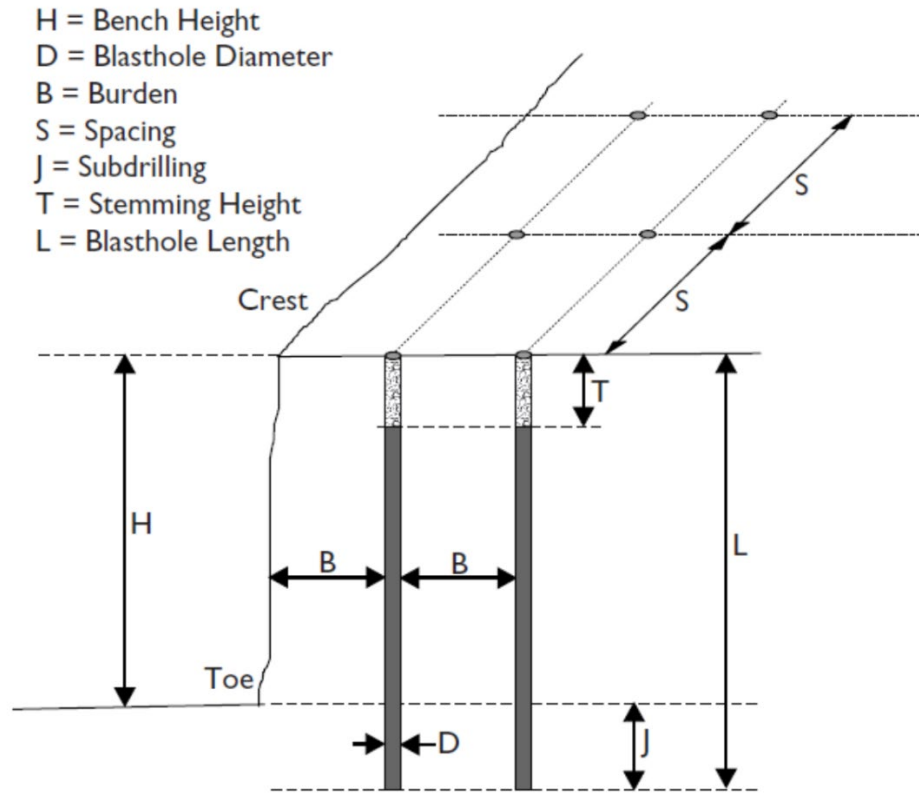


**Figure 6-1: Nomenclature of a blast pattern (Gokhale, 2011)**

### 6.1 Blast Pattern Geometry

The general layout of the blast pattern may be termed square, rectangular, or triangular; each for the layout of the blastholes when viewed from above. Research has shown that the post-blast fragmentation around a blasthole is influenced by the overall pattern layout.

Figure 6-2 shows the fragmentation zones with respect to the blastholes where the illustrated square pattern can be thought of as analogous to the rectangular pattern.

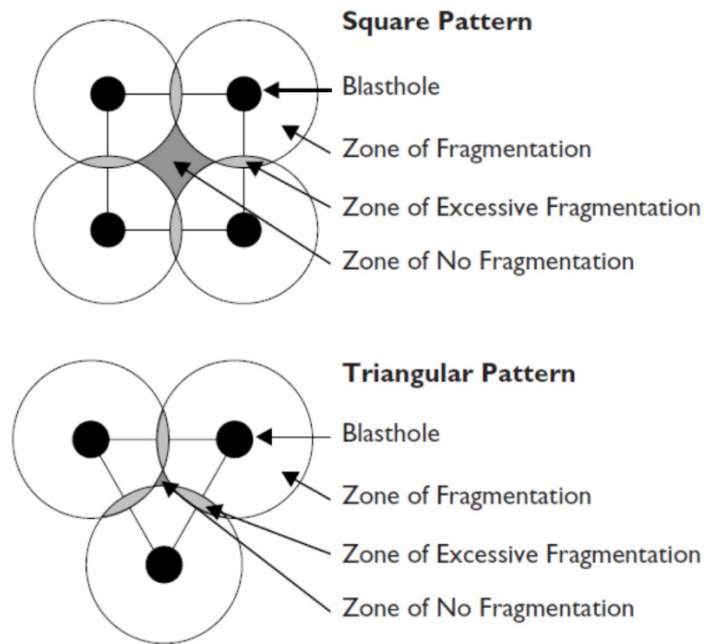


**Figure 6-2: Zones of fragmentation with respect to pattern geometry (Gokhale, 2011)**

Due to the pattern geometries and the fragmentation spreading circularly from the blasthole zones of excessive fragmentation and of no fragmentation appear as a function of pattern geometry and spacing. When attempting to decrease the zone of no fragmentation, one increases the corresponding zone of excessive fragmentation. Based on the above, the zone of no fragmentation is most readily minimized (while also minimizing corresponding zones of excessive fragmentation) using the triangular blast pattern layout. A comparison between the two blast pattern geometries when the zone of fragmentation is zero is given below (Gokhale, 2011):

- Square blast pattern with zone of no fragmentation = 0
  - Zone of excessive fragmentation =  $0.570796 \cdot r^2$

- Triangular blast pattern with zone of no fragmentation = 0
  - Zone of excessive fragmentation =  $0.181172 \cdot r^2$

The zones of excessive fragmentation are provided as functions of blasthole radius. It is shown that when the no fragmentation zone is set to zero, the zone of excessive fragmentation is much less using the triangular blast pattern than the square or rectangular patterns.

In industry it is not unusual for square or rectangular blast patterns to still be used. However, based on the above the smart pattern layout tool will employ the triangular blast pattern exclusively.

The overall size of the blast pattern should be dictated by mining engineering based upon the operation's production goals, the mining equipment utilized at the operation, short and long range mine planning objectives, and various other considerations. The smart pattern layout tool is proposed to accept x-y GPS coordinates as inputs from mine engineering. These GPS coordinates would define the required surface area and location of the planned blast. The smart pattern layout tool would then design the blast within that zone and properly tailor the blast pattern variables described below.

## 6.2 Blasthole Diameter

The selection of blasthole diameter is dictated by the type of excavation equipment used (and indirectly by the mine's target production rate). Generally, blast patterns with smaller diameter, closely spaced holes provide the finest fragmentation which is more suited for smaller excavation equipment. Larger diameter blastholes do not guarantee more coarse fragmentation but it is possible.

$$\text{Production rate } \left[ \frac{m^3}{hr} \right] \propto \text{Dig tool capacity} [m^3] \propto \text{Blasthole diameter} [m] \quad (6.1)$$

The relationship between production rate and blasthole diameter (6.1) (Gokhale, 2011) makes practical sense as a larger diameter hole drilled results in a larger zone of fragmentation. This larger amount of fragmented material then requires a larger dig tool capacity to efficiently excavate it. This larger dig tool capacity then results in a higher production rate for the mine site.

Literature suggests that an approximation can be made between the dig tool capacity and the blasthole diameter used. This is shown in Table 6-1 and should be thought of as an approximate operational guideline.

Dig tool capacity (m <sup>3</sup> )	Blasthole diameter (inch)
4.5	3 - 5
7.5	5 - 8.5
9.17	6 3/4 - 9 3/4
11.5	7 3/4 - 10 1/2
15.3	9 - 12 1/4
20	9 3/4 - 13 3/4
35	10 3/4 - 15
50	12 1/4 - 17 1/2

**Table 6-1: Blasthole diameter by dig tool capacity (Gokhale, 2011)**

While hole diameter is also interrelated to bench height and desired fragmentation it is primarily dictated by the mine site's production requirements. The smart pattern layout tool should consider bench height and desired fragmentation but the most weight should be given to desired rate of production.

### 6.3 Blasthole Length

Blasthole length is dictated by the height of cut of the excavation equipment used. In general, larger excavation equipment has a larger height of cut which requires a larger blasthole length. The blasthole length should never be less than the height of cut of the excavation equipment used by the mine site (Gokhale, 2011),

$$\text{Blasthole length} \geq \text{Height of cut.} \quad (6.2)$$

For reference the height of cut for popular excavation equipment is given in the table below.

OEM	Model	Height of cut (m)
Komatsu	P&H 4800XPC	18.0
Komatsu	P&H 4100XPC	16.8
Komatsu	P&H 2800XPC	16.6
Komatsu	P&H 2300XPC	13.5
Caterpillar	CAT 7495 HF	16.8
Caterpillar	CAT 7495 HD	14.9
Caterpillar	CAT 7395	14.9
Caterpillar	CAT 7295	13.7

**Table 6-2: Height of cut for commonly used electric rope shovels**

### 6.4 Burden

From Gokhale, burden by material hardness is defined by the following equation,

$$B = 25 \cdot D, \text{ for hard material}$$

$$B = 40 \cdot D, \text{ for soft material} \quad (6.3)$$

where,  $B$  is burden,  $D$  is diameter, and both are in metres. 6.3 can be used for varying material hardness by altering the constant value used over the range of values between 25

to 40. The smart pattern layout tool assumes that burden to diameter relationship over this range is linear with respect to the transition of soft to hard in-situ material.

### 6.5 Spacing

From Gokhale, spacing by blasthole diameter is defined by the following relationship (Gokhale, 2011)

$$S = 1.1 \cdot B, \text{ for large diameter blastholes}$$

$$S = 1.5 \cdot B, \text{ for small diameter blastholes} \quad (6.4)$$

where,  $S$  is spacing,  $B$  is burden, and both are in metres. 6.4 can be used for varying blasthole diameter by altering the constant value used over the range of values between 1.1 to 1.5. The smart pattern layout tool assumes that spacing to burden relationship over this range is linear with respect to the transition of large to small blasthole diameter.

### 6.6 Subdrilling

From Gokhale, subdrilling is defined by the following table.

In-situ material	Subdrilling in intact rock ( $J$ )	Subdrilling in highly fractured rock ( $J$ )
Soft rock with easy toe	$0.1 \cdot B - 0.2 \cdot B$	$0.07 \cdot B - 0.15 \cdot B$
Medium rock with normal toe	$0.3 \cdot B$	$0.25 \cdot B$
Hard rock with difficult toe	$0.4 \cdot B - 0.5 \cdot B$	$0.3 \cdot B - 0.4 \cdot B$

**Table 6-3: Definition of subdrilling by material type and fracture level**

Where,  $J$  is subdrilling,  $B$  is burden, and both are in metres. Table 6-3 provides several equations for subdrilling based upon the in-situ material being drilled as well as the level of fracturing present. The smart pattern layout tool will assign material properties and fracture levels based upon input from the mine site geologist.

---

## 6.7 Desired Fragmentation

The purpose of the drill and blast cycle is to break the rock to allow for ease of movement by loading and haulage equipment and eventual processing and refinement by the mine's plant. The post-blast particle size distribution is known as fragmentation. The desired fragmentation is determined by several factors, the primary drivers being: size to facilitate practical loading and hauling and desired input size to the crusher (first processing stage within the mine's plant).

If post-blast material is over-sized it can cause premature wear and damage to the loading and haulage equipment as well as pose a potential injury risk to equipment operators and other mine site staff.

The blasting process is the cheapest and most efficient way of comminution available to a mine operation. The more mined material that is properly sized post-blast, the cheaper (and more profitable) the mine operation will be. If material is drastically oversized (and not safely moveable via loading and haulage) secondary drilling is required. If material is oversized but moveable fragmentation via the crusher occurs. Both add costs to the mining process resulting in a reduction in profitability of the operation.

Based upon the loading and haulage equipment available, the mineral processing equipment and the type of operation a desired fragmentation can be determined.

A combination of the in-situ environment and the various blast pattern variables described in Sections 6.1 to 6.6 determine the actual fragmentation realized.

Several prediction models exist for forecasting of post-blast particle size distributions; the most widely used is the Kuz-Ram model. This model is a combination of the adapted

Kuznetsov equation and the adapted Rosin-Rammler equation. The model is provided and described in the following sub-section (Cunningham, 2005).

### 6.7.1 Kuz-Ram Model for Prediction of Fragmentation

The adapted Kuznetsov equation,

$$x_m = AK^{-0.8}Q^{1/6} \cdot \left(\frac{115}{RWS}\right)^{19/20}, \quad (6.5)$$

where,

$x_m$  = mean particle size in centimetres;

$A$  = rock factor (varies between 0.8 and 22; determined by the rock factor equation);

$K$  = powder factor in kilogram of explosive per cubic metre of rock;

$Q$  = mass of explosive in the hole in kilograms;

$RWS$  = weight strength relative to ANFO (where, 115 is the RWS of TNT).

The adapted Rosin-Rammler equation,

$$R_x = \exp\left[-0.693\left(\frac{x}{x_m}\right)^n\right], \quad (6.6)$$

where,

$R_x$  = mass fraction retained on screen opening;

$x$  = screen opening in centimetres;

$n$  = uniformity index (usually between 0.7 and 2; determined by the uniformity equation).

The uniformity equation,

$$n = \left(2.2 - \frac{14B}{d}\right) \sqrt{\left(\frac{1+S/B}{2}\right)} \left(1 - \frac{W}{B}\right) \left(\text{abs}\left(\frac{BCL-CCL}{L}\right) + 0.1\right)^{0.1} \frac{L}{H}, \quad (6.7)$$

where,

$B$  = burden in metres;

$S$  = spacing in metres;

$d$  = hole diameter in millimetres;

$W$  = standard deviation of drilling precision in metres;

$L$  = charge length in metres;

$BCL$  = bottom charge length in metres;

$CCL$  = column charge length in metres;

$H$  = bench height in metres.

The rock factor equation,

$$A = 0.06(RMD + RDI + HF) \cdot C(A), \quad (6.8)$$

where,

$RMD$  = rock mass description which is an assigned number based upon the rock condition and its jointing (based on various jointing factor constants and a joint factor equation);

$RDI$  = density influence of the rock (based on various density factor constants);

$HF$  = hardness factor which is based upon the physical characteristics of the rock (specifically the elastic modulus and the unconfined compressive strength).

In summary, the Kuz-Ram model is used through the following procedure:

- Using 6.5 (Adapted Kuznetsov equation), determine the mean particle size yielded by the blast based upon the various geological properties of the in-situ material and the various blast pattern variables.

- An input to 6.5 is 6.8 (Rock factor equation) which is based upon the in-situ conditions of the rock mass, the density of the rock mass, and the physical properties of the rock mass.
- Using 6.6 (Adapted Rosin-Rammler equation) determine the mass fraction remaining on the screen opening (which is the input to the plant). This is based upon the mean particle size yielded by the blast (as determined by 6.5) as well as the blast pattern variables.
  - An input to 6.6 is 6.7 (Uniformity equation) which is based upon the blast pattern variables.

It should be noted that while the Kuz-Ram model is for prediction of post-blast fragmentation its purpose is for guidance not for precise fragmentation prediction. The Kuz-Ram model is really a collection of best practices and should be used as a check to ensure the blast pattern variables selected are suitable for the in-situ environment that is to be blasted. While the Kuz-Ram model has been shown to be suitable for verifying that fragmentation size from a blast will be suitable for the downstream loading and haulage equipment, it has been found to not be useful for determining blast pattern variables.

### **6.8 Methodology of Proposed Smart Pattern Layout Tool**

This section explains the proposed methodology used by the smart pattern layout. An iterative process is proposed where the smart pattern layout tool would generate a blast design, check the design against the Kuz-Ram model, and then either proceed with the execution of the designed blast pattern or refine the design if predicted fragmentation

---

from Kuz-Ram does not satisfy the operational requirements. Multiple iterations would be used as required.

1. **Determine the surface area of the To-be designed blast pattern.** Based upon input GPS coordinates layout a triangular blast pattern within the desired blast zone.
  - Required inputs from mining engineering: x-y GPS coordinates of desired blast zone.
2. **Determine the blasthole diameter.** Based upon the desired rate of production and the available drilling and excavation equipment determine the blasthole diameter to be used in the blast design. Also, consider desired fragmentation.
  - Required inputs from mining engineering: Desired rate of production, available production drills (and available bit diameters for each), available excavation equipment tool capacity, desired fragmentation, and available excavation equipment height of cut.
3. **Determine the blasthole length.** Based upon the available excavation equipment's height of cut design the blast pattern's blasthole length.
  - Required inputs from mining engineering: Available excavation equipment.
4. **Determine the burden.** Based upon the supplied in-situ material properties and the previously selected blasthole diameter design the blast pattern's burden.
  - Required inputs from mine geology: In-situ material properties.

- 
5. **Determine the spacing.** Based upon the previously selected blasthole diameter design the blast pattern's spacing.
    - Required inputs: None.
  6. **Determine the subdrilling length.** Based upon the supplied in-situ material properties design the blast pattern's subdrilling length.
    - Required inputs from mine geology: In-situ material properties.
  7. **Validate the designed blast pattern using the Kuz-Ram model.** Using the Kuz-Ram model, validate the designed blast pattern and its underlying variables by comparing predicted fragmentation to desired fragmentation.
    - Required inputs from mine geology: In-situ material properties.
    - Required inputs from mine engineering: Desired fragmentation.
  8. **Revise designed blast pattern (if required).** Iteratively revise the designed blast pattern until an acceptable Kuz-Ram fragmentation prediction is reached.
    - Required inputs: None.

## 6.9 On-The-Fly Pattern Adjustments

As described earlier in Chapter 6, the in-situ geology influences various components of the blast pattern design process. Both designed burden and designed subdrilling are influenced by the in-situ geological properties. However, the primary influence of the in-situ material is on post-blast fragmentation. This is illustrated in the various equations that comprise the Kuz-Ram model as presented in sub-section 6.7.1.

Since the ultimate purpose of all the blast pattern variables is to facilitate rock comminution to desired fragmentation, the in-situ geology directly and indirectly influences all elements of the blast design. The smart pattern layout tool proposed earlier in Chapter 6, relies upon the mine site geology department to fully characterize the in-situ environment. The geologists accomplish this using a dataset which compiles various geological logs including exploration hole information, results of in-field testing using geophysical logging tools, and in-mine observation of present conditions. The granularity of the datasets available to the mine site geologist is generally limited by cost. Since all the input information requires labour and materials outside of the normal mining production process mines attempt to minimize these efforts as much as possible resulting in geological datasets that are incomplete or of minimal use. This leads to approximation and assumptions that may be invalid and lead to poorer blast results than if the in-situ environment were more fully detailed and defined.

However, work by Peck (Peck, 1989) showed that a production drill could be used as a logging tool to better define the in-situ environment. Since a production drill is a required part of the normal mining production process, gathering in-situ geological information in parallel to production yielded a valuable, non-invasive, geological logging tool. This work built upon the previously defined concept of specific energy (Teale, 1965).

$$e = \left(\frac{F}{A}\right) + \left(\frac{2\pi}{A}\right)\left(\frac{NT}{\mu}\right), \quad (6.9)$$

where,

$e$  = specific energy in pounds per cubic inch;

$F$  = thrust force in pounds;

$T$  = torque in pounds inch;

$N$  = rotation speed in revolutions per minute;

$A$  = area of the blasthole in square inches; and

$\mu$  = penetration rate in inches per minute.

Teale's specific energy equation quantifies the energy required to drill a unit volume of rock; including both the thrust and rotary components. Examining 6.9 it is apparent that all of the required inputs are available through the standard monitoring while drilling variables except for the area of the blasthole which is dictated by the diameter of the drill bit utilized. Peck then applied Teale's equation to an in-field rotary blasthole drill monitoring system to define the in-situ material properties based on the monitored drill performance variables to effectively quantify how easy or difficult the material was to blast.

It is proposed in this section that Teale's equation as applied by Peck could be used as a feedback to the smart pattern layout tool to refine the various blast pattern variables and tailor them to the in-situ material as observed through interpretation of the drill's performance. In this fashion fragmentation could be optimized, operational requirements of the production drill reduced, and production costs improved.

The initial blast pattern layout would be created using the forecasted specific energy of the in-situ material for the zone to be blasted. Then, as the drill works across the pattern the blast pattern variables that are influenced by in-situ properties would be adjusted – this would occur as the production drill executes the pattern or “on the fly”. The variables influenced by in-situ properties are discussed below.

Burden is influenced by the hardness of the in-situ material; the harder the in-situ material the smaller the burden value, the softer the in-situ material the larger the burden

value. In effect, for softer material blastholes can be further apart in the x-direction than for harder material. A minimum burden distance is required for all blasts. This relationship is illustrated in Figure 6-3.

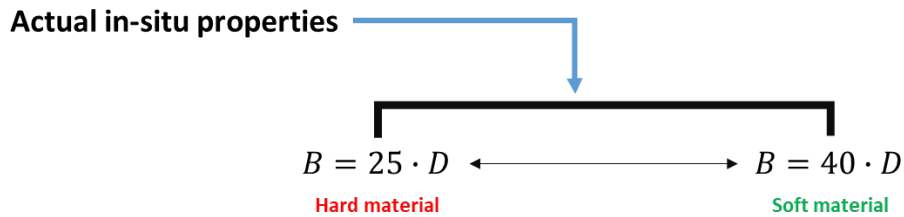


**Figure 6-3: Influence of in-situ material properties on burden**

Spacing is also influenced by the hardness of the in-situ material; the harder the in-situ material the smaller the spacing value, the softer the in-situ material the larger the spacing value. Similar to burden but for the y-direction, for softer material blastholes can be further apart than for harder material. A minimum spacing distance is required for all blasts. This relationship is illustrated in Figure 6-4.

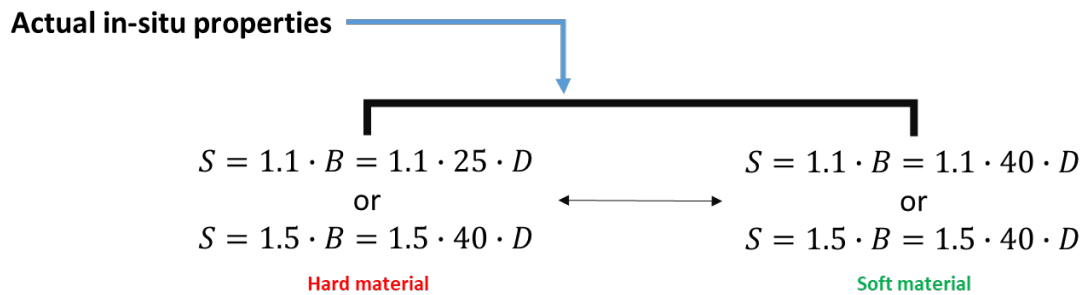


**Figure 6-4: Influence of in-situ material properties on spacing**

Subdrilling is influenced by both the hardness of the in-situ material and its toe zone as well as the intactness of the material. The harder the in-situ material (and its toe) the larger the depth of subdrilling and conversely the softer, the smaller the depth of subdrilling. Similarly, the more intact the material the more subdrilling and the more

fractured the less subdrilling. A minimum subdrilling length is required for all blastholes.

This relationship that determines required subdrilling is illustrated in Figure 6-5.

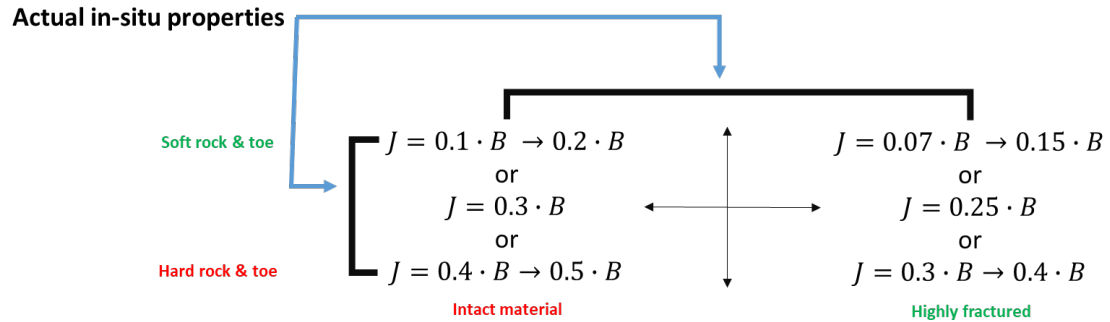


**Figure 6-5: Influence of in-situ material properties on subdrilling**

While this thesis only considers the drilling aspect of the drill and blast process, there are many blast-specific variables that are influenced by the in-situ material properties. These include, but are not limited to: hole loading parameters, explosive selection and detonation sequencing. Many additional potential on-the-fly adjustment gains could be made if blasting was considered in addition to blast pattern design.

## **Chapter 7**

### **Conclusion**

As human civilization continues to grow and evolve fewer high grade ore bodies will be available for development, mining and ultimate societal use. This will drive the need to develop low grade, surface deposits often in remote, inaccessible locations. The confluence of these factors will lead to extremely tight margins as mining companies attempt to optimize the Net Present Value of the deposit.

The economics of mining are driven by the physical constraints of mine design, capital expenditure constraints of the mining corporation, environmental constraints from the corporation and the nation state, societal constraints imposed by existing or traditional communities, regulatory constraints from government and labour bodies, technical risks due to required mineral processing techniques, economic risk due to market volatility or uncertainty, and potential regulatory risk due to changing government direction.

Of the above listed constraints which mining corporations are beholden to there is very little that can be controlled with the exception of human labour costs. These costs can be significant especially in developed countries and, even more so, when in remote locations within those countries. The economic need for lower cost leads to corporations' desire to reduce overall human labour costs through the introduction of equipment automation.

In a complimentary development, technology has been quickly improving and decreasing in cost as more and more of the world embraces and relies upon it for everyday life. The confluence of these two developments – scarcity of high grade deposits creating pressure for lower operating costs and widespread use of technology creating improved capability

---

and decreased costs – has made the appetite for equipment automation in surface mining a ripe one.

The typical work cycle of a blasthole drill in surface mining varies from the work cycles of the other mobile equipment employed. Unique operating requirements and constraints coupled with well-defined blast pattern design practices lead to key differences.

- Blast patterns are designed, reviewed and supplied by the drill and blast engineer well in advance of their execution by the blasthole drill.
  - Design hole locations are pre-defined and known.
  - Future drill movement is well understood and can be anticipated.
- A deposit is mined in parts and the preceding blasting is done in a corresponding fashion.
  - By design the blast pattern area is limited and contained.
  - The blast pattern area can be blocked off from access and bermed as necessary.
- The contained, restricted blast pattern area fosters a good work environment for robotic or autonomous vehicle operation.
  - Obstacle detection and avoidance systems can be added to autonomous vehicles however these systems come at both a capital cost and an increase in system complexity.
  - Many of the safety benefits from vision systems can be attained through the implementation of signage, barriers, worker training and properly drafted Safe Operating Procedure documentation – similar to a gated robot in a factory environment.

- 
- The blasthole drill is a very large, slow moving piece of mobile equipment that predominantly transits in a straight and predictable fashion.
    - Typically, blasthole drills are capable of two propel speeds: slow and normal. Slow is better suited for tight patterns or fine positioning with normal for longer distance movement. Example speeds for a commonly used drill model (Bucyrus 49HR) are a maximum drill velocity in slow speed of 0.12 m/s and a maximum drill velocity in normal speed of 0.40 m/s.
    - Blast patterns are made up of many design holes in a grid style distribution with distances between neighboring holes and neighboring rows in the 5 to 10 metre range. As a tracked vehicle the drill will leave the just drilled location in a straight line movement, slowly pivot to adjust its heading with the location of the to-be drilled hole, and then finish its movement in a straight line movement until at the to-be drilled hole. In this way the movement is always deliberate and predictable.
  - The majority of the blasthole drill's operating time is spent stationary and with its drill bit and steel in the ground drilling which further limits potential risk introduced by automation.
    - Research has shown that a minimum of 83% of a drill's operating time is spent stationary. This could be even higher if drilling through hard rock formations or employing multi-pass drilling.

When compared to other types of mobile equipment used in the mining process, these key differences in the work cycle of blasthole drills make them an attractive and logical

---

starting point for mobile equipment automation in mining. In addition, the prevalence of the requirement for drill and blasting in surface mining makes the market for blasthole drill automation and the corresponding payback through reduced human labour costs and increased asset utilization substantial. Research work for haul truck, shovel, grader and dozer automation are all actively pursuing autonomous solutions, however, none of these applications are as ready to work in an operational context as is the solution for autonomous surface rotary blasthole drilling.

### **7.1 Original Contributions of the Research**

The goals of this doctoral dissertation included the original contributions listed.

- Design, development and testing of a novel and advanced drill control system that incorporates advanced exceptions handling concepts. The exceptions handling allowed for the automatic drilling of complicated drilling scenarios as well as normal drilling conditions.
- Test the developed drill control system in a simulation environment and in a working mine site on an operating drill rig. Mine site testing demonstrated a notable production improvement and, when paired with drill cycle automation, a significant improved asset utilization.
- Design and test a novel adaptive collar module for a drill control system. Instead of basing the collar exit condition on depth it is based upon observed ground condition.

- 
- Define the relationship of bit design and efficient drilling with respect to the developed drill control system and explain the influence of bit wear. Explore the incorporation the output of a bit wear solution as an input to the drill control system.
  - Development of a proposed drill propel and positioning solution that incorporates HPGPS sensor information and crawler track motor speed sensor information. The provided positioning accuracy must meet or exceed mine operating requirements.
  - Test the developed drill propel and positioning system in a simulation environment and in a working mine site on an operating drill rig.
  - Discuss the requirements for an automatic levelling system and propose an improved solution compared to the present industry standard.
  - Development of a proposal for an intelligent drilling concept that would include automatic blast pattern generation and on-the-fly pattern variable adjustment based upon feedback of monitoring-while-drilling signals.
  - High-level, preliminary investigation into the incorporation of all the above concepts for a proposed autonomous surface rotary blasthole drill solution.

## **7.2 Research Scope**

The aim of this thesis was to propose and investigate a solution for an autonomous surface rotary blasthole drill system which was the first presentation in the public domain of such a concept. While the overall solution was presented at a high-level the individual

---

key elements or modules of the solution was explored in more detail and, where possible, tested both in a simulation environment and in a working mine site environment.

The scope of this research was somewhat limited by mine site and equipment access and availability. To expedite field testing and to minimize the time required only the most complicated aspects of the proposed solution were tested on machine and some concepts were only explored via data analysis on recorded machine operating data. However, where assumptions were made they are thought to be of a relatively minor nature and are heavily reinforced by the literature. The derived models for drill control, propel and positioning, and the proposed concept of intelligent drilling as well as the overall autonomous drill system concept proposed are novel and unique in the literature.

Of particular utility was the developed advanced drill controller which facilitated control of over 80% of drill operational time and incorporated novel exceptions handling. This resulted in a marked productivity improvement when compared to manual operation. In addition, the advanced drill controller resulted in fewer drill fault and jam conditions thus facilitating drill cycle automation. Building upon the advanced drill controller an autonomous drill solution has the potential to provide a large increase in overall drill capacity.

### **7.3 Recommendations for Future Work**

It is important to note that in most jurisdictions autonomous mobile equipment has not yet been addressed by existing legislation or regulations, this is presently the case for the province of Québec and other Canadian jurisdictions. As such, this research is presently ahead of the appropriate regulations. As regulatory bodies and government legislators

catch up to this research and similar work, restrictions or requirements may be imposed that could be addressed at a technical level with additional autonomous functionality or limitations. This is an important consideration that could lead to additional requirements for future work.

The research presented in this thesis has generated the following specific recommendations for future work.

### **1. Develop and field test an advanced drill control algorithm for hammer drills**

The developed, demonstrated and tested drill control system is designed for the most common type of drilling in surface mining – rotary drilling. The second most common type of drilling is hammer drilling which combines the elements of rotary drilling (rotary speed and feed force) with the additional input of percussive force which is applied at a selected and configurable frequency.

There would be interest from mines that employ hammer drilling for an advanced drill control solution. Although the overall blasthole drill machines that employ hammer drilling are physically similar to those that employ rotary drilling the performance metrics that would define what to regulate via feedback control differ. The depth of cut method which was the control strategy used for rotary drilling would not be used for hammer drilling. The likely control strategy that would best suit hammer drilling would be one built around drilling efficiency with some chosen penetration rate as one of several inputs.

### **2. Development of a bit wear monitoring method**

---

While the influence of bit wear on efficient drilling was explored during this research, previous literature has shown potential methods which with to quantify and monitor on-going drill bit wear. A large data set comprising field test data that encompasses the life of many drill bits should be collected. This dataset should then be utilized to develop and validate a drill bit wear monitoring solution that could then be used as an input to the developed advanced drill control solution.

### **3. Test adaptive control for propel and positioning module**

Presently the propel and positioning module has several gains applied at different steps of the movement process. These gains have been chosen based upon the machine studied and used for the field testing. The gains could be less than ideal for different drill model types or if the hydraulic track motor circuit substantially changes due to circuit pressure variations from maintenance or the replacement of the track motors themselves. While track motor speed sensor inputs help to compensate for this, adaptive gain tuning methods could provide a more robust propel and positioning algorithm. For this reason, adaptive control should be explored and tested on several different makes and models of drills.

### **4. Perform field test of intelligent drilling concept**

This research proposed the intelligent drilling concept but due to limitations on the extent of the research work the concept was not tested in a working mine site. An intelligent drilling system should be deployed at a working mine site in tandem with an autonomous drill system. The intelligent drill should be observed

and tested through several patterns and refined as necessary. Emphasis should be placed on the comparison between the intelligent drill system's operation and a manual drill or autonomous drill working from designs created by an average drill and blast engineer.

#### **5. Perform long-term validation testing of the proposed autonomous drill system**

The autonomous drill solution proposed in this thesis was only tested on a module by module basis but never as an entire system. Full and long-term validation testing and refinement of an autonomous drill solution should be conducted at a working mine site with comparison to a manually operated drill that is preferably of the same manufacturer and model. Attention should be paid not just on productivity and performance but also on component lives, maintenance costs, energy usage and quality of drilling.

#### **6. Based upon long-term validation testing collect performance data for ROI calculation**

While it is logical to make a case for payback to corporations by deploying autonomous drill systems and other forms of autonomy until systems are put into operations these ROI models are simply forecasts. A long-term validation program would provide hard data which could be used to derive a substantive ROI calculation. Research could then examine the data to determine at what price point autonomous drill systems make sense for mining corporations and if there is a benefit to fleet autonomy versus single machine autonomy.

---

### **7. Explore multiple row positioning algorithm and potential optimization**

Much of the research has focused on single row automation due to the restrictive operating nature of the electric drills used for the field testing. However, diesel powered drills are commonly used in the United States of America and other countries. These do not require an electric trailing cable and thus have no corresponding limit on orientation and movement.

For these machines, how a pattern is approached and drilled should be examined and optimized. Additional exploration on optimization of pattern execution for electric machines could also be of value.

### **8. Expand On-The-Fly Pattern Adjustment concept to blast loading and detonation sequencing**

The intelligent drilling concept of adjusting blast pattern variables based upon observed monitoring-while-drilling signals could be expanded to the blast loading and blast detonation steps of the mining process. The literature shows that many blast loading variables are influenced by in-situ material properties as are variables associated with blast timing and sequencing. The adjustment of these variables using acquired MWD signals could provide additional benefits to mine operators. The expansion of intelligent drilling into blast loading and detonation should be explored.

---

## Bibliography

- Aboujaoude, C. E. (1991). *Modeling, Simulation and Control of Rotary Blasthole Drills*.  
Montreal, QC: McGill University.
- Aboujaoude, C. E. (1997). *Feedback Control of Vibrations in Surface Rotary Blasthole Drilling*.  
Montreal, CA: McGill University.
- Anderson, R. J. (2012). *MECH-420 Course Notes, Winter 2012*. Kingston, CA: Queen's  
University.
- Astolfi, A. (1999). Exponential Stabilization of a Wheeled Mobile Robot Via Discontinuous  
Control. *Journal of Dynamic Systems, Measurement, and Control Volume 121*, 121-126.
- Atlas Copco Drilling Solutions LLC. (2012). *Blasthole Drilling in Open Pit Mining, Third  
edition*. Garland, USA: Ulf Linder, ulf.linder@us.atlascopco.com.
- Bailey, J. a. (1960). An Analytical Study of Drill-String Vibration. *ASME: Journal of  
Engineering for Industry*, 122-127.
- Baker Hughes Inc. (2009). *Hughes Christensen Drill Bit Catalog*. Retrieved from  
[www.bakerhughes.com](http://www.bakerhughes.com)
- Bar-Cohen, Y. a. (2009). *Drilling in Extreme Environments: Penetration and Sampling on Earth  
and other Planets*. Weinheim, Germany: Wiley-VCH.
- Besaisow, A. a. (1986, October). A study of Excitation Mechanisms and Resonance Inducing  
BHA Vibrations. *Proceedings of the Society of Petroleum Engineers*, p. Paper No. 15560.
- Branscombe, E. (2010). *Investigation of Vibration Related Signals for Monitoring of Large Open-  
Pit Rotary Electric Blasthole Drills*. Kingston, CA: Queen's University.
- Briggs, G. a. (2002). *Technical Challenges of Drilling on Mars*. American Institute of  
Aeronautics and Astronautics, Report No. 0469.

- 
- Bucyrus International, Inc. (2005). *49HR Blast Hole Drill Maintenance and Operation Manual*. South Milwaukee, USA: Bucyrus International, Inc.
- Clausing, D. (1959). Comparison of Griffith's Theory with Mohr's failure criteria. *Third Symposium on Rock Mechanics*. Colorado School of Mines.
- Cooper, G. (2002). A proposal for the real-time measurement of drill bit tooth wear. *Geothermal Resources Council Annual Meeting*. Reno, USA.
- Cooper, G. e. (1987). The Interpretation of Tricone Drill Bit Vibrations for Bit Wear and Rock Type. *RETC Proceedings*, (pp. 202-218).
- Cunningham, C. (2005). The Kuz-Ram fragmentation model - 20 years on. *Brighton Conference Proceedings 2005, R. Holmberg et al* (pp. 201-210). Brighton: 2005 European Federation of Explosives Engineers.
- Deily, F. D. (1968). Downhole Measurements of Drill String Forces and Motions. *ASME: Journal of Engineering for Industry*, 217-225.
- Drilltech Mission, LLC. (2005). *Introduction to Blasthole Drilling*. Alachua, USA: Drilltech Mission, LLC.
- Dudek, G. J. (2010). *Computational Principles of Mobile Robotics*. New York, USA: Cambridge University Press.
- Fairhurst, C. e. (1956). Some principles and developments in hard rock drilling techniques. *Annual Drilling and Blasting Symposium*. University of Minnesota.
- Franklin, G. (1980). *Digital control of dynamic systems*. Reading, USA: Addison-Wesley Publishing Company.
- Franklin, G. F., Powell, J. D., & Emami-Naeini, A. (2002). *Feedback control of dynamic systems, 4th edition*. Upper Saddle River, New Jersey, USA: Prentice Hall.
- Giancoli, D. (2000). *Physics for Scientists and Engineers, Third Edition*. Upper Saddle River, USA: Prentice Hall.

- 
- Gokhale, B. V. (2011). *Rotary Drilling and Blasting in Large Surface Mines*. London, UK: Taylor & Francis Group.
- Harnischfeger Corporation. (2006). *P&H 120A Mechanical Systems Manual*. Milwaukee, USA: Harnischfeger Corporation.
- Hartman, H. (1959). Basic Studies of Percussive Drilling. *Mining Engineering, Volume 11, No. 1*.
- Jardine, S. M. (1994, January). Putting a damper on drilling's bad vibrations. *Oilfield Review*, pp. 15-20.
- Lucifora, D. J. (2012). *Comparative Modeling, Simulation, and Control of Rotary Blasthole Drills for Surface Mining*. Kingston, CA: Queen's University.
- Maurer, W. (1959). *Impact Crater Formation in Sandstone and Granite*. Golden, USA: Colorado School of Mines.
- Maurer, W. (1962). The Perfect Cleaning Theory of Rotary Drilling. *Journal of Petroleum Technology*, 1270-1274.
- Mukherjee, S. e. (2006). Technologies for exploring the Martian subsurface. *Proceedings of the IEEE Aerospace Conference*. Big Sky, MT.
- Naganawa, S. (2012). Feasibility study on roller-cone bit wear detection from axial bit vibration. *Journal of Petroleum Science and Engineering* 82-83, 140-150.
- Peck, J. P. (1989). *Performance Monitoring of Production Drills*. Montreal, QC: McGill University.
- Pelletier, S. e. (1993). Characterization of wear and profile of diamond drill bit by optical profilometry. *Review of Scientific Instruments*, 65 (1).
- Schivley, J. G. (1995). *United States of America Patent No. 5,449,047*.
- Simon, R. (1953). Collected Reports. *Drilling Research Institute (1949-1953)*.
- Teale, R. (1965). The Concept of Specific Energy in Rock Drilling. *International Journal of Rock Mechanics and Mining Sciences*, 57-73.

---

Zacny, K. e. (2008). Drilling systems for extraterrestrial subsurface exploration. *Astrobiology*, 8 (3), 665-706.

Zink, C. (2005). Optimizing Drilling Productivity and Bit Life with "Depth of Cut" Studies. *WME Drilling & Blasting*.

Zink, C. (2007). *Total Drilling Cost Curve Analysis*. Grand Prarie, USA: Atlas Copco Secoroc.

---

## Appendix A: Feed Motor and Rotary Motor Response Testing, Modelling

When considering a production drilling application, there are five control inputs for the drilling component of the drill rig's duty cycle (with units):

- Weight-on-bit (kN);
- Rotary speed (rpm);
- Bailing air pressure (bar);
- Water flow (L/min); and,
- Hammer blow frequency (Hz).

Limiting the analysis to rotary production drilling eliminates the hammer blow frequency parameter and reduces the control inputs to four.

Water flow and bailing air pressure are supplied via a pump and a compressor, respectively. On many drill rigs the water flow and air pressure set-points are simplistic and can only be set to on or off. Some rigs offer more precise (albeit still coarse) control through the modulation of a flow control rheostat where several positions representing different levels of fluid flow (from off to full flow) can be selected. This process is relatively straightforward and well defined and the associated system dynamics will not be further explored.

Both weight-on-bit and rotary speed are provided via dedicated motors: the feed motor and the rotary motor. The rotary motor directly supplies rotation speed through the rotation of the drill string steel. The feed motor indirectly supplies weight-on-bit through attempting to attain a selected penetration rate (m/s). Typically, there are two operating thresholds that are selected by the drill operator or controller: penetration rate (m/s) and

---

weight-on-bit (kN). The drill rig will then attempt to attain the chosen penetration rate while also respecting the weight-on-bit threshold. In this fashion, drill rig feed performance is always governed by either weight-on-bit or penetration rate depending on the in-situ ground conditions encountered.

Since the developed advanced drill control algorithm is designed to control weight-on-bit and rotary speed the system dynamics for both the feed and rotary motors are of interest. If the system dynamics are understood and modelled, then a drill plant model can be created and simulated for laboratory development and testing of the drill control algorithm.

To facilitate modelling of the rotary and feed system dynamics, a drill rig built by one of the three industry leading OEMs (Caterpillar) was instrumented at a partner mine site. The partner mine site was a Canadian surface iron ore mine. Various signals relating to the rotary and feed motors were recorded. The acquired data was of a relatively high frequency at 909.1 Hz which was the upper limit of the utilized data acquisition unit. The list of recorded signals is provided below. All recorded signals were in volts.

- Rotary Motor Armature Voltage;
- Rotary Motor Armature Amps;
- Rotary Motor Field Current;
- Rotary Motor Speed Reference;
- Hoist Motor Armature Voltage;
- Hoist Motor Armature Amps;
- Hoist Motor Field Current;
- Hoist Motor Speed Reference; and,

- Hoist Motor Pulldown Current Limit.

System response testing was conducted on the drill rig for both the rotary motor and the feed motor. The response testing was accomplished through a series of input-output test that encompassed the full range of drill rig operational performance. The input-output steps were varied to observe (and eventually model) any present system characteristics. The unscaled rotary motor input-output data and the feed motor input-output data are provided in Figure A-1 and Figure A-2, respectively.

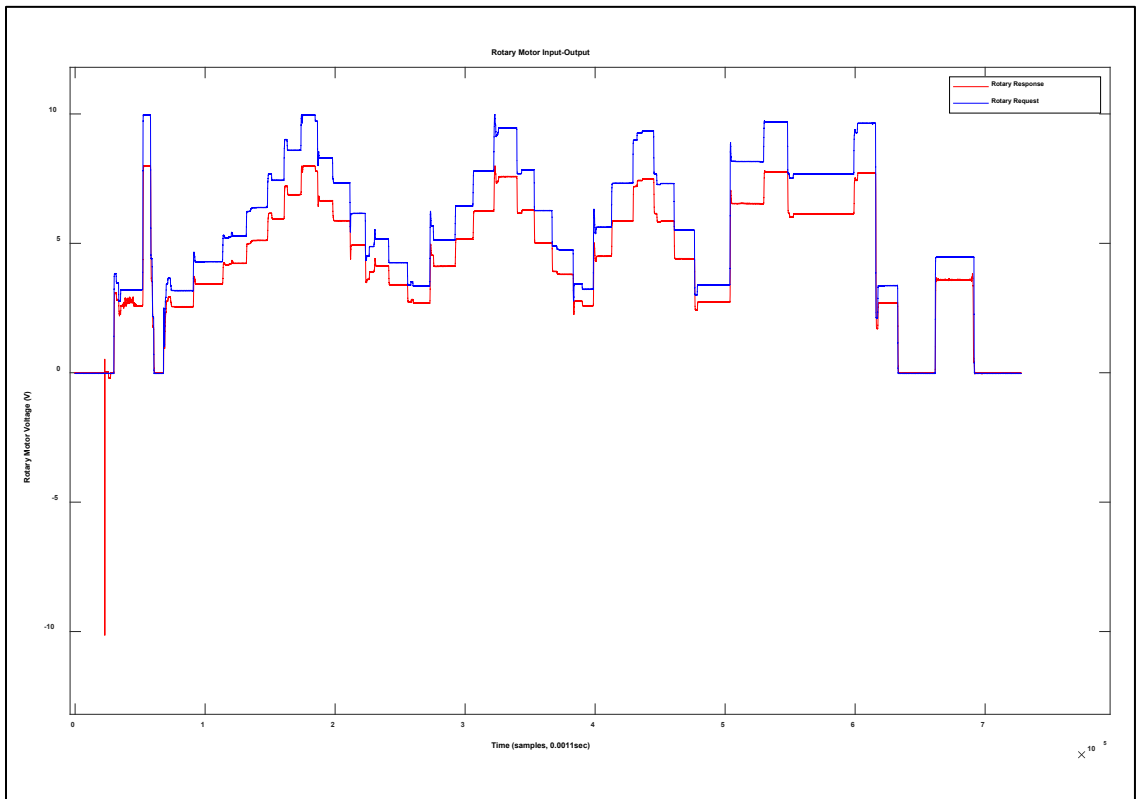


**Figure A-1: Rotary motor input-output data (unscaled)**

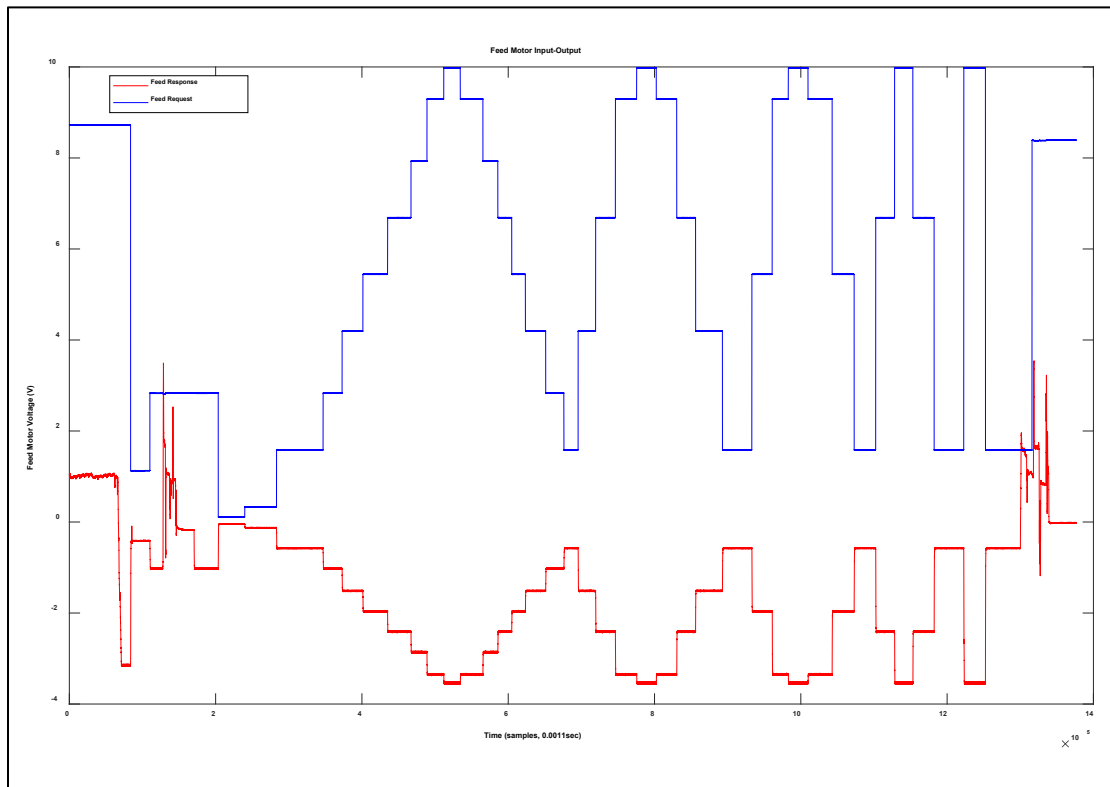


**Figure A-2: Feed motor input-output data (unscaled)**

The scaled rotary motor input-output data and the feed motor input-output data are provided in Figure A-3 and Figure A-4, respectively. The rotary motor plot shows both the request and response in rotation per minute. The feed motor plot shows both the request and response in kilonewtons.

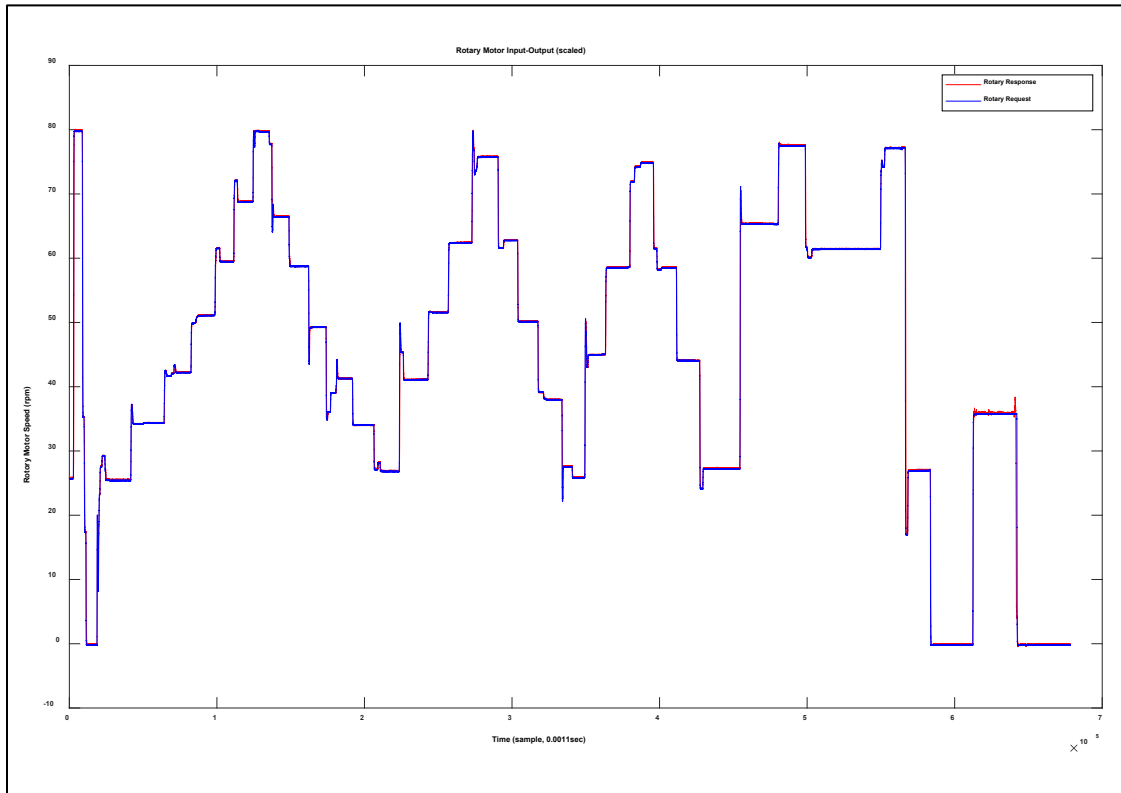


**Figure A-3: Rotary motor input-output data (scaled)**

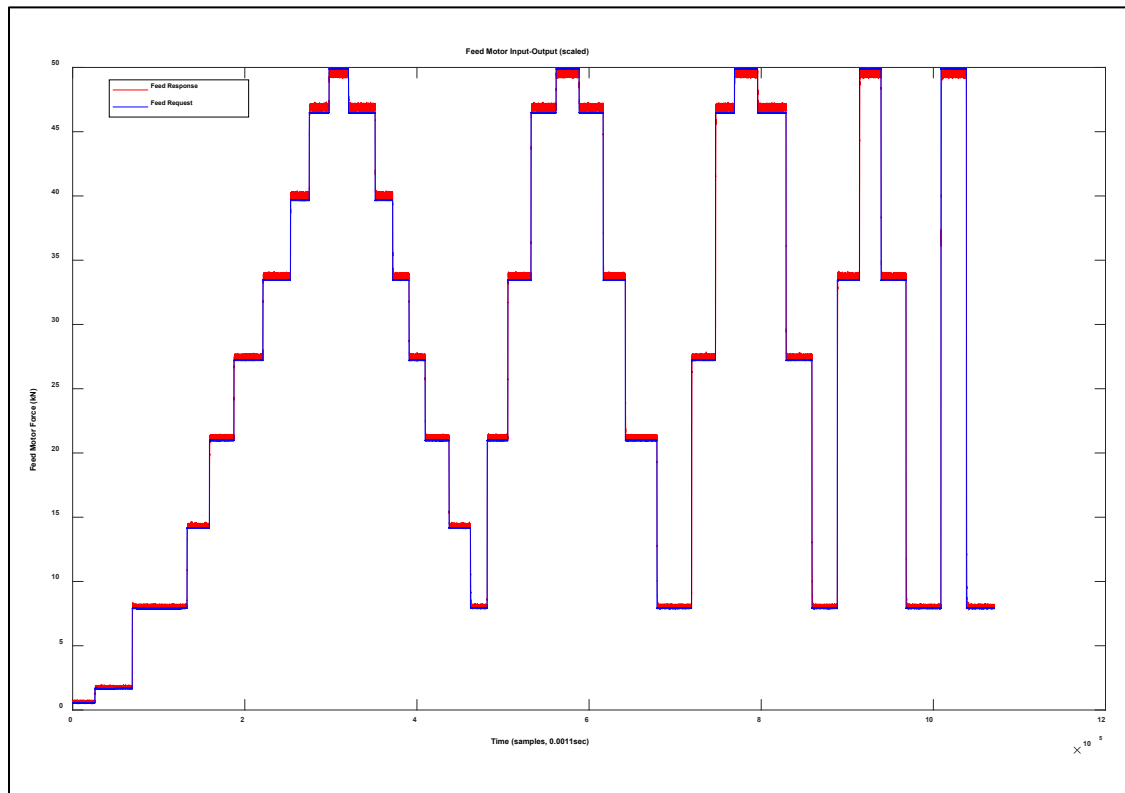


**Figure A-4: Feed motor input-output data (scaled)**

Once scaled, the acquired motor response data can be used in the creation of a dynamic model for the feed and rotary actuators. This was accomplished using the System Identification Toolbox in MATLAB. The toolbox takes input-output data as an input and produces a modelled transfer function that simulates the system responses captured in the data. Depending on the type of tests performed and how representative of the system the chosen model is, a model of varying fit can be attained. While the thoroughness of the performed testing and corresponding dataset is dependant on machine access and mine site cooperation, the choice of model is at the researcher's discretion.

To assist in the choice of system model type, it is useful to conduct a Newtonian analysis with the assistance of a free-body diagram of the system. The free-body diagram

produced can be seen in Figure A-5 below. Based upon the free-body diagram the expected order of poles and zeroes for the produced transfer function can be understood.

This forms the basis in the selection of the system model type.

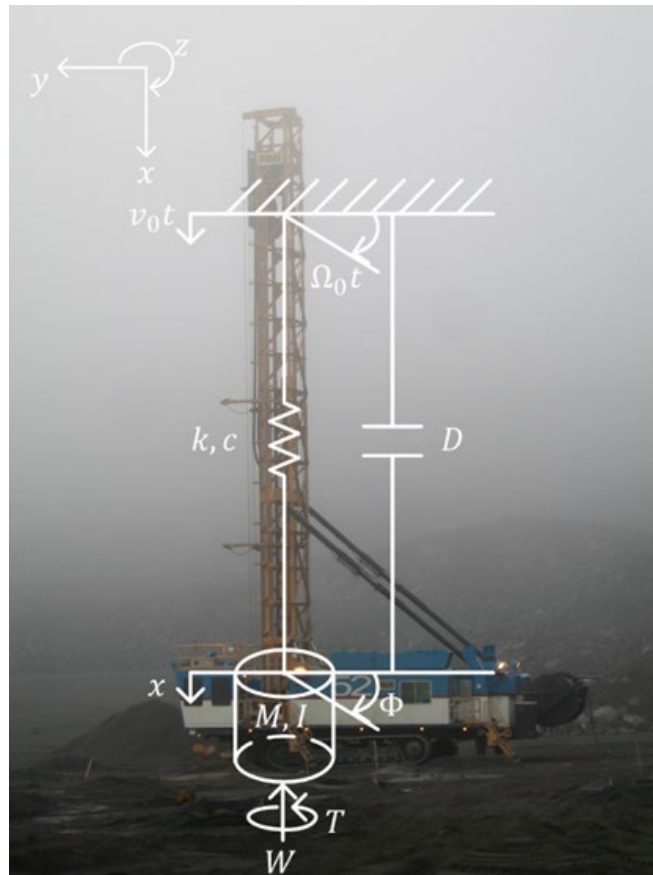


**Figure A-5: Drill model**

Where,

$\Omega_0$  = constant revolutions per minute; and,

$v_0$  = constant metres per minute.

From the above free body diagram of the system it is apparent that we are interested in the forces and torques about two axes of our coordinate system: in the x-direction and about the z-direction.

Further examining the free body diagram, a summation of the forces in the x-direction yields the following equation

$$\sum F_x: -W = M \frac{d^2x}{dt^2} + D \frac{dx}{dt} + k(x - v_0 t). \quad (\text{A.1})$$

Similarly, a summation of torques about the z-direction yields the following equation

$$\sum \tau_z: -T = I \frac{d^2\Phi}{dt^2} + R \frac{d\Phi}{dt} + c(\Phi - \Omega_0 t). \quad (\text{A.2})$$

From the summation of forces in the x-direction the following second order transfer function is found

$$T.F. = \frac{x}{U} = \frac{1}{Ms^2 + Ds + k}. \quad (\text{A.3})$$

The forces in the x-direction are contributed by the feed motor and therefore A.3 represents the format of a transfer function for the feed motor dynamics. Examining the transfer function, it can be noted that the transfer function for the feed motor dynamics has two poles and no zeroes. A similar type transfer function should be selected when using the System Identification Toolbox to model the feed motor input-output data.

From the summation of torques about the z-direction the following second order transfer function is found,

$$T.F. = \frac{\Phi}{U} = \frac{1}{Is^2 + Rs + c}. \quad (\text{A.4})$$

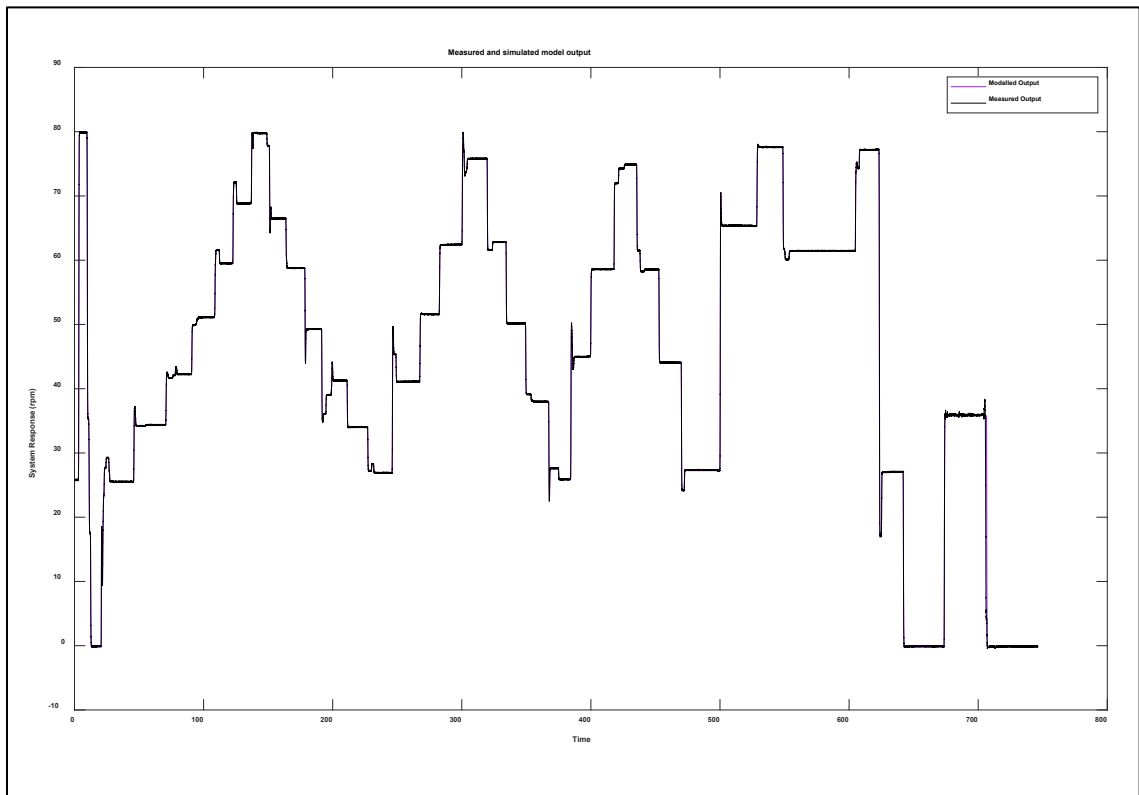
The torques about the z-direction are contributed by the rotary motor and therefore A.4 represents the format of a transfer function for the rotary motor dynamics. Examining the transfer function, it can be noted that the transfer function for the rotary motor dynamics has two poles and no zeroes. A similar type transfer function should be selected when using the System Identification Toolbox to model the rotary motor input-output data.

---

Using the response test input-output data and the MATLAB System Identification Toolbox, dynamic system models were created for the rotary and feed motors.

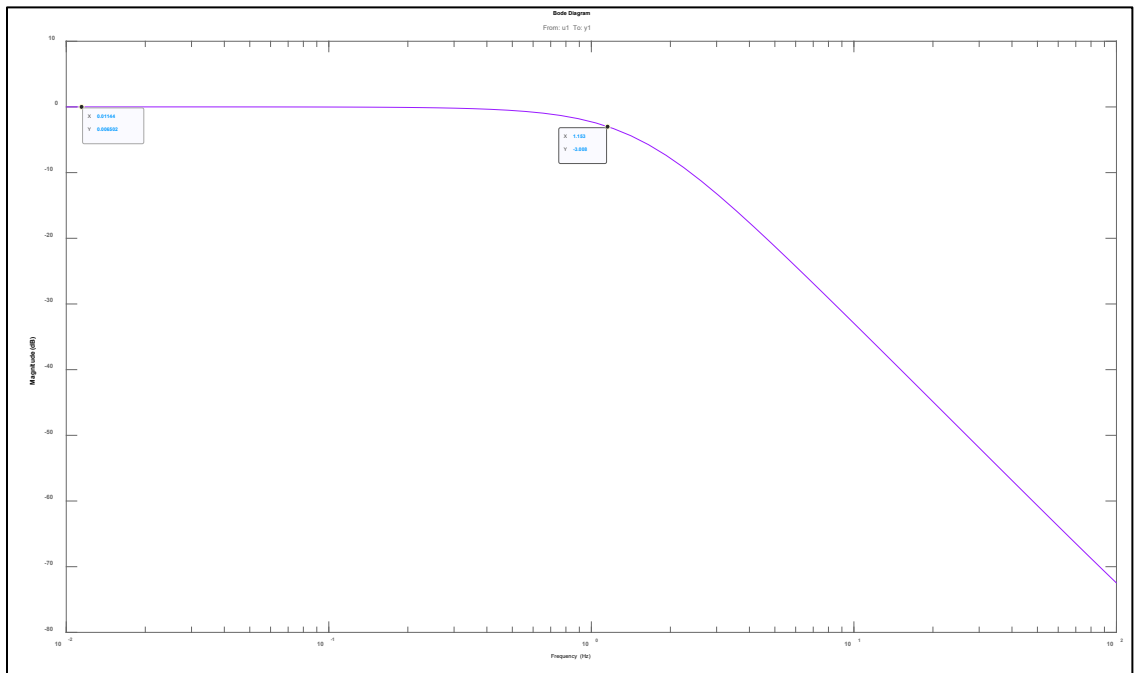
The rotary dynamic system model had a fit of 95.36. This fit is considered very good and reinforces the use of Newtonian analysis in the selection of model type. Figure A-6 and A.5 show a comparison of measured to simulated model output and the corresponding transfer function for the derived model, respectively. It should be noted that all the derived transfer functions are discrete-time as this was the format of the collected data. Figure A-7 shows the magnitude only Bode plot of the rotary dynamic system model defined by A.5. Highlighted on the plot is the -3 dB point relative to the d.c. gain, at a frequency of approximately 1.14 Hz. This is indicative of the natural frequency of the system. Note that the Bode plot is defined up to 100 Hz due to the magnification of the plot at which there is no practical limitation due to the Nyquist frequency since a 909 Hz sampling rate was used.

Figure A-8 shows the step response plot of the rotary dynamic system model defined by A.5. Highlighted on the plot are the rise time (0.296 seconds), settling time (0.474 seconds), and the steady state value (1.0). Examining Figure A-8, the system exhibits no overshoot and appears to be an overdamped system with no steady state error.



**Figure A-6: Rotary motor, measured and simulated model output**

$$H(z) = \frac{0.0001081}{z^2 - 1.982z + 0.9817} \quad (\text{A.5})$$



**Figure A-7: Bode magnitude plot – rotary motor**

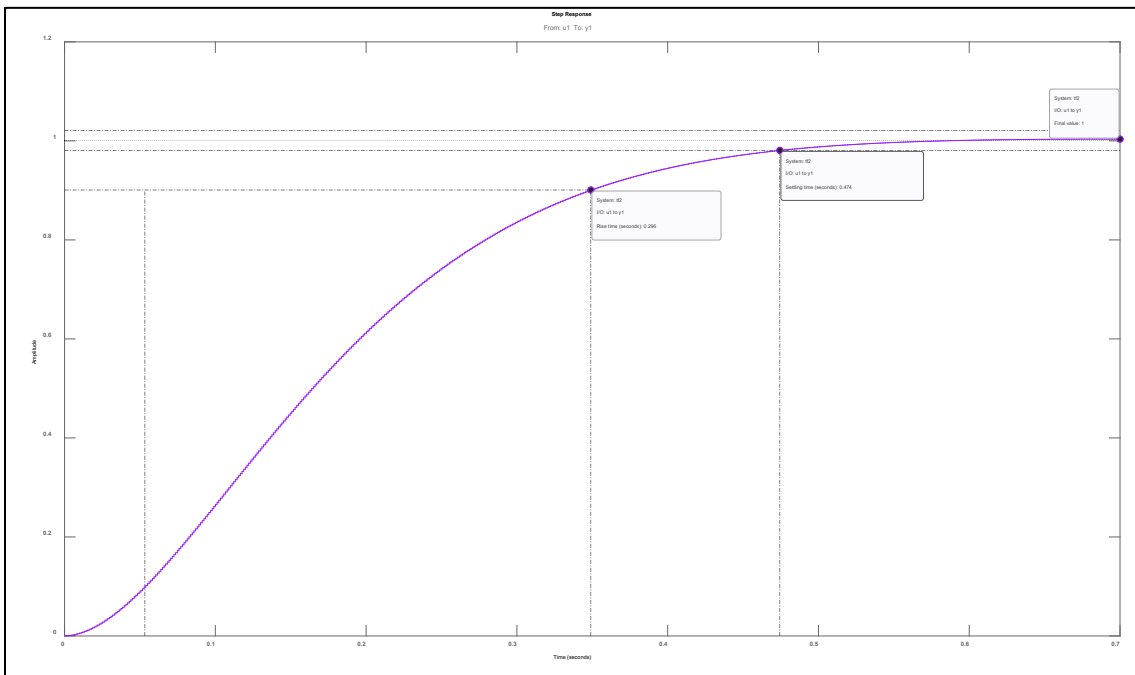


**Figure A-8: Step response plot – rotary motor**

---

The feed dynamic system model had a fit of 98.15. This fit is considered very good and reinforces the use of Newtonian analysis in the selection of model type. Figure A-9 and A.6 show a comparison of measured to simulated model output and the corresponding transfer function for the derived model, respectively.

Figure A-10 shows the magnitude only Bode plot of the feed dynamic system model defined by A.6. Highlighted on the plot is the -3 dB point relative to the d.c. gain, at a frequency of approximately 0.855 Hz. This is indicative of the natural frequency of the system. Note that the Bode plot is defined up to 450 Hz due to the Nyquist frequency for a 909 Hz sampling rate.

Figure A-11 shows the step response plot of the feed dynamic system model defined by A.6. Highlighted on the plot are the rise time (0.409 seconds), settling time (0.731 seconds), and the steady state value (1.0). Examining Figure A-11, the system exhibits no overshoot and appears to be an overdamped system with no steady state error.

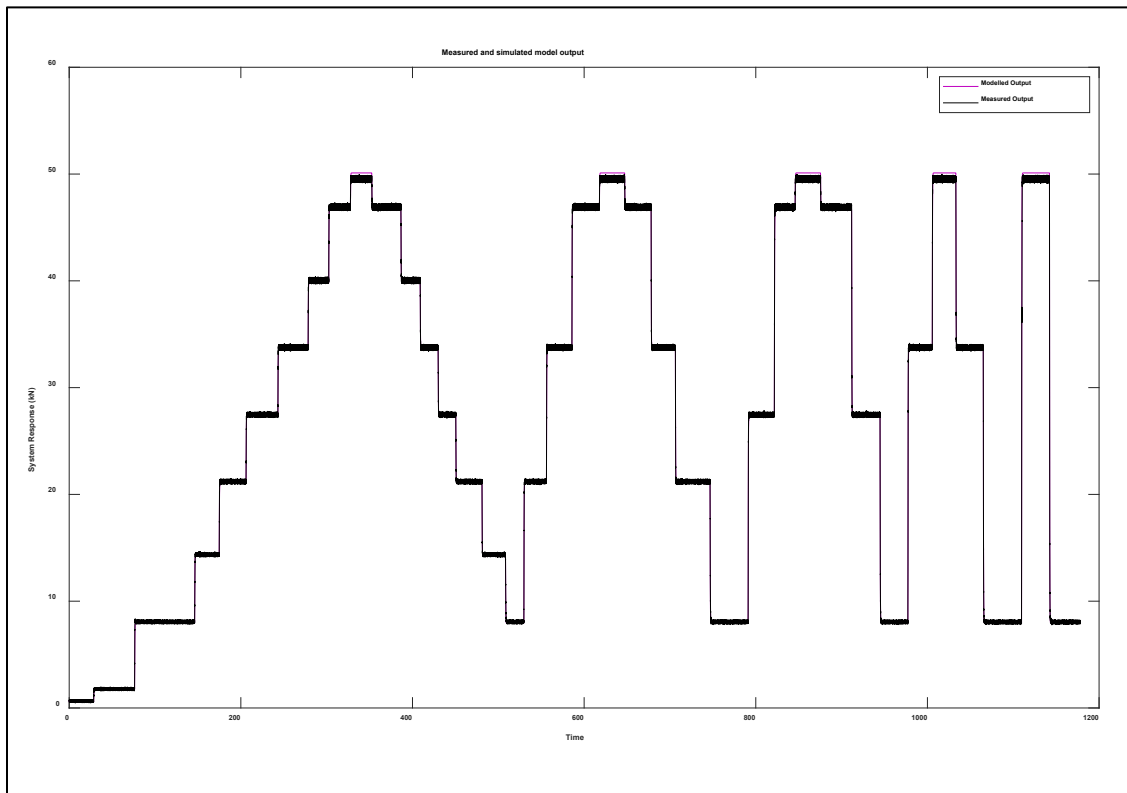


**Figure A-9: Feed motor, measured and simulated model output**

$$H(z) = \frac{0.000106}{z^2 - 1.977z + 0.9776} \quad (\text{A.6})$$

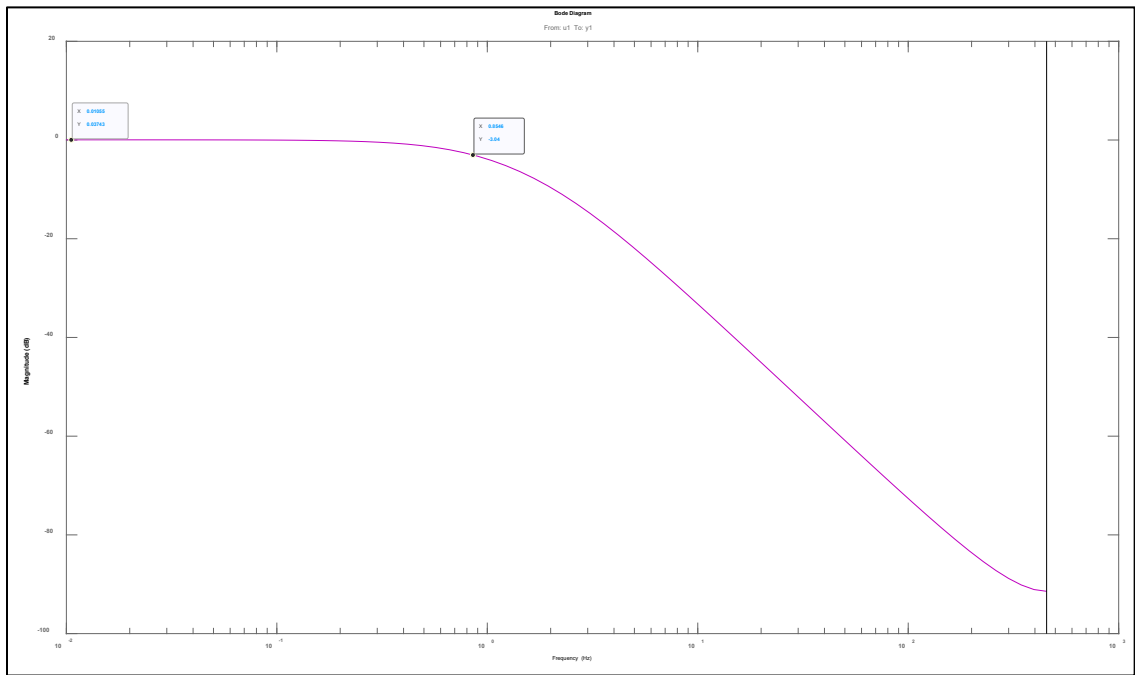


Figure A-10: Bode magnitude plot – feed motor

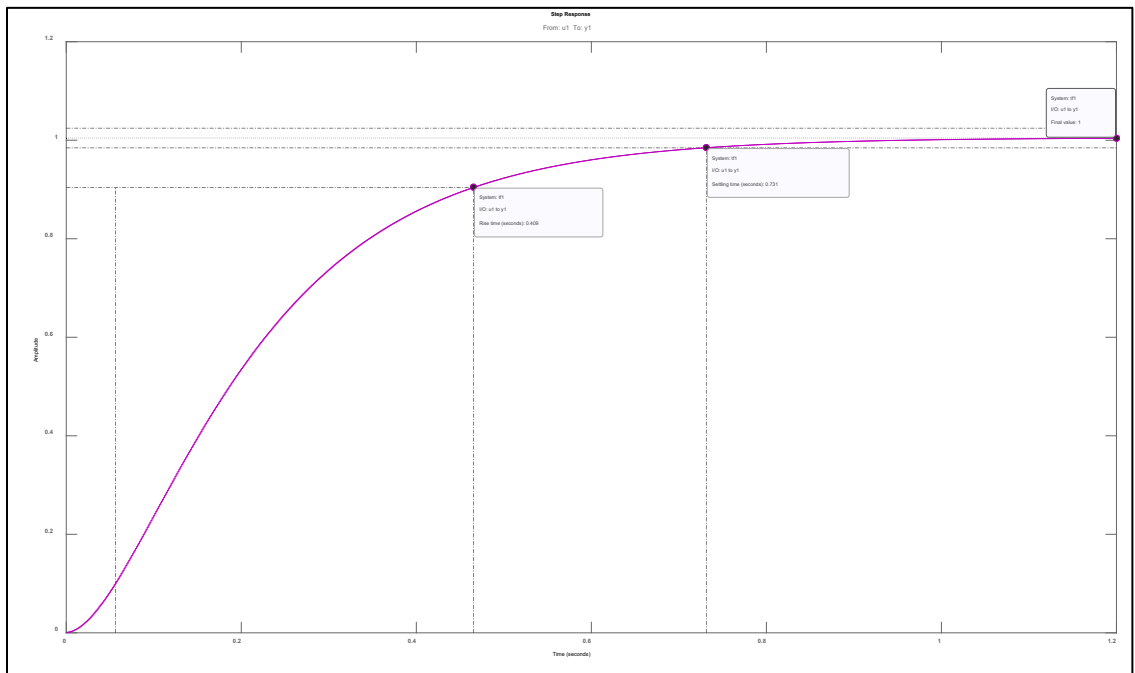


Figure A-11: Step response plot – feed motor